DRUG OVERDOSE TREATMENT WITH LIPOSOMES

By

BRETT A. HOWELL

A DISSERTATION PRESENTED TO THE GRADUATE SCHOOL
OF THE UNIVERSITY OF FLORIDA IN PARTIAL FULFILLMENT
OF THE REQUIREMENTS FOR THE DEGREE OF
DOCTOR OF PHILOSOPHY

UNIVERSITY OF FLORIDA

2010

To my lovely wife, Michele, and my parents, Dwight and Carla

ACKNOWLEDGMENTS

First and foremost, I would like to express my deepest gratitude to my doctoral advisor, Dr. Anuj Chauhan. Throughout my time at the University of Florida, Dr. Chauhan has challenged me on every level. He has directed me down the right path countless times, while also ensuring my growth as an independent scientist and engineer. He has been both an excellent advisor and friend, and I am deeply blessed to have spent my time as a doctoral student under his guidance.

I also wish to extend many thanks to my other doctoral committee members, Dr. Tanmay Lele, Dr. Yiider Tseng, and Dr. Sihong Song, for their insightful viewpoints and willingness to participate in my doctoral review process. In addition, I must thank Dr. Spyros Svoronos and Dr. Oscar Crisalle for the opportunity to serve as a teaching assistant under their leadership. They were both gracious and kind leaders. Dr. Crisalle was also instrumental in persuading me to choose the Department of Chemical Engineering at the University of Florida, for which I am extremely grateful.

As a graduate student in Dr. Chauhan's lab, I have had the privilege of working with many fine colleagues. Dr. Jinah Kim was especially helpful during my first days in the lab, as she taught me many important lab procedures and techniques, as well as the consequence of efficiency. Dr. Yash Kapoor was an excellent mentor and friend, with whom I had the opportunity to do collaborative research on assessing ocular toxicity. Not only was Yash exceptionally talented in the laboratory, but he also never failed to brighten everyone's day with his constant smile and positive attitude. Many others were also very helpful lab mates and good friends, including Dr. Chi-Chung Li, Dr. Heng Zhu, Chhavi Gupta, Cheng-Chun Peng, Hyun Jung Jung, and Lokendrakumar Bengani.

Many current and former staff members of the Department of Chemical Engineering were also very accommodating during my time in Gainesville. I would like to thank Shirley Kelly, Deborah Aldrich, Deborah Sandoval, Donna Roberts, Melissa Fox, and Sean Poole for their invaluable assistance.

Next, I must thank my wonderful parents, Dwight and Carla Howell, for a lifetime of support and encouragement. Without their constant uplifting words and trusted direction, I would certainly not have completed this work. They are and always will be precious people in my life. My grandparents, Jim and Carolyn Howell, and Bill and Rachel Gaskey, are also due many thanks for their love and support over the years. My father-in-law and mother-in-law, David and Linda Popple, have also done much to encourage Michele and me during our stay in Gainesville.

Although all the individuals listed above have done much to aid in my completion of my doctoral degree, none more so than my loving wife, Michele. She has been extremely understanding, patient, and helpful since the moment we decided to relocate to Gainesville. Words cannot express my affection and gratitude for her. She is an angel in my eyes, and has been by my side through both the good times and the bad. I am forever indebted to her for all her love and support.

TABLE OF CONTENTS

page

LIST OF TABLES

LIST OF FIGURES

LIST OF ABBREVIATIONS

AA	Acrylic Acid
AMI	Amitriptyline
APL	Acidic Phospholipids
AUC	Area Under the Drug Concentration Versus Time Curve
B:P	Blood to Plasma Drug Concentration Ratio
BSA	Bovine Serum Albumin
BUP	Bupivacaine
CH	Cholesterol
CI	Confidence Intervals
DI	Deionized
DMPC	1,2-dimyristoyl-sn-glycero-3-phosphocholine
DOPG	1,2-dioleoyl-sn-glycero-3-[phospho-rac-(1-glycerol)]
DOS	Dosulepin
DPPE	1,2-dipalmitoyl*sn*-glycero-3-phosphoethanolamine
EGDMA	Ethylene Glycol Dimethacrylate
F	Bioavailability
H	Hematocrit
IMI	Imipramine
IV	Intravenous
MAA	Methacrylic Acid
MLL	Multilamellar Liposomes
PBPK	Physiologically Based Pharmacokinetic
PBS	Phosphate Buffered Saline
PD	Pharmacodynamic

PEG	Polyethylene Glycol
PK	Pharmacokinetic
RBC	Red Blood Cell
RES	Reticuloendothelial System
SUV	Small Unilamellar Vesicles
TCA	Tricyclic Antidepressant
ULL	Unilamellar Liposomes
UV	Ultraviolet

Abstract of Dissertation Presented to the Graduate School
of the University of Florida in Partial Fulfillment of the
Requirements for the Degree of Doctor of Philosophy

DRUG OVERDOSE TREATMENT WITH LIPOSOMES

By

Brett A. Howell

May 2010

Chair: Anuj Chauhan
Major: Chemical Engineering

Many drugs such as tricyclic antidepressants and local anesthetics cause severe toxicity and/or death when taken at excessive and sometimes normal dosage levels. The subject of this work was the development of a drug overdose treatment to counteract toxicity. Liposomes were chosen as the primary vehicle for toxicity reversal.

The binding of the tricyclic antidepressants amitriptyline, nortriptyline, imipramine, dosulepin, and opipramol to several variations of liposomes was measured. The medium of measurement was also varied from buffer to serum to assess in vivo affects. The effects of lipid type and loading, liposome size, polyethylene glycol inclusion and chain length, protein interaction, and storage were considered. Pegylated, anionic liposomes exhibited high affinity binding to all of the tricyclic antidepressants studied, despite the presence of serum proteins. Liposome size and polyethylene glycol chain length were inconsequential, while the proportion of polyethylene glycol incorporated into liposomes was optimal at about 5%. Liposome-drug binding was also found to occur to a significant extent for the local amide anesthetic drug bupivacaine.

Additionally, interactions between cationic drugs and anionic liposomes were studied by measuring binding of drugs and the effect of binding on liposome

permeability. Experiments and modeling indicated that, although electrostatic interactions were important, the fraction of drug sequestered in the double-layer was negligible. The majority of the drug enters the bilayer with the charged regions interacting with the charged lipid head groups and the lipophilic regions associated with the bilayer. Bupivacaine binds significantly less compared to tricyclic antidepressants because its structure is such that the charged region has minimal interactions with the lipid heads once the bupivacaine molecule partitions inside the bilayer. Conversely, the tricyclic antidepressants are linear with distinct hydrophilic and lipophilic regions, allowing the lipophilic regions to lie inside the bilayer and the hydrophilic regions to protrude out. This conformation maximizes the permeability of the bilayer, which leads to an increased release of a hydrophilic fluorescent dye from liposomes.

Lastly, physiologically based pharmacokinetic models were developed for the design and optimization of liposome therapy for overdoses. The in vitro drug-binding data for pegylated, anionic liposomes and published mechanistic equations for partition coefficients were used to develop the models. The models were proven reliable through comparisons to intravenous data. Drug overdoses were simulated for various drug and liposome doses, elapsed time between drug intake and liposome treatment, and patient specific input parameters. The liposomes were predicted to be highly effective at treating amitriptyline overdoses. Although liposomes could potentially treat an anesthetic overdose, the drug redistribution was less effective. Published data on local cardiac function was used to relate the predicted concentrations in the body to local pharmacodynamic effects in the heart.

CHAPTER 1
INTRODUCTION

Over the past century, the development of new drugs and therapies has advanced at a rapid pace, providing those who struggle with sickness and disease exciting new treatment options. In many cases, however, the same drugs designed to improve the quality and/or length of life for individuals are accidentally or purposefully abused. Thus, prescription drug poisonings now represent a significant public health problem in the United States and around the world. A publication by Diane Wysowski from the Food and Drug Administration pointed to over 25,000 deaths in 2003 in the United States due to toxicity from prescription drugs [1]. Furthermore, the number of poisonings increased by 55% from 1999 to 2003, and Wysowski concluded, ‘‘deaths due to overdoses are the most prominent cause of drug related mortality in death certificate data,’’ and that ‘‘preventive strategies should be considered.’’

Tricyclic antidepressant (TCA) drugs are frequently the cause of many of those poisonings. TCA poisoning is a leading cause of self-poisoning in the world [2], causing extensive hospital stays [3,4] and many deaths [5,6]. In fact, deaths from such overdoses represent the third most reported to poison control centers in the United States [7], and approximately 268 people die from TCA overdoses every year in Britain [8]. The primary and typically lethal effect of TCA drugs is the impact on the cardiac system [9,10]. Tachycardia, vasodilation, myocardial depression, and cardiac conduction disturbances are some of the serious cardiovascular effects caused by TCA overdose [11]. As opposed to selective serotonin re-uptake inhibitors (SSRI), which are antidepressant medications developed in more recent years with milder side effects and higher toxic dosage levels, TCA’s are often toxic at low dosages. This is especially true

when taken by young children, where one or two pills can cause acute toxicity [2]. Furthermore, overdose cases involving TCA's can be fatal, and have been statistically shown to result in longer hospital stays than overdose cases with other antidepressant drugs [3]. Still, a large number of individuals continue to use TCA's to treat common depression disorders. Morgan et al. have recently reported a rise in overall TCA prescriptions in England from 1993 to 2002 [6].

Local anesthetics are less likely to be taken at elevated levels than TCA's, since they are administered at medical facilities, but adverse reactions during routine treatment remain a threat [12-15]. They present dangers to both the cardiac [16,17] and central nervous systems (CNS) [17]. Although most patients recover from such reactions as a result of being in medical facilities at the time of local anesthetic administration, many face extended recovery periods and long term injuries, while a select few do not survive. This is especially tragic since many patients arrive for routine surgeries requiring local anesthetics in fairly good health.

Traditional methods of treating drug or substance toxicity include specific antidotes, such as anti-venoms developed to counteract snake bites, gastric lavage, charcoal administration for toxin absorption, and pH manipulation through sodium bicarbonate administration. These and other similar methods of treatment are marked by key deficiencies. Specific antidotes are difficult to develop, produce, and store for every possible toxin. In addition, they often lack the ability to circulate in the blood compartment for adequate periods of time due to the immune system responses they invoke. Charcoal administration is aimed at removing the toxin from the victim's stomach prior to absorption, but is only effective if given shortly after overdose or for

toxins slowly absorbed. Other methods of treatment typically focus on restoring patient well-being while the toxin is naturally removed from the body. The major disadvantage to this approach is the extended period of time required for the clearance of some drugs or substances, resulting in days or even weeks of often painful and expensive recovery.

One possible method of drug overdose treatment is the use of small nano or micro carriers designed to sequester excess drug from the body. This idea was first proposed in 1973, but has recently garnered more attention due to burgeoning research in the general area of nanotechnology [18]. Nanoparticles can induce detoxification through a variety of mechanisms. Toxins may be redistributed from the site of toxicity, which often includes the heart and/or brain, into the blood compartment as a result of specific or non-specific drug-particle binding. The nanoparticles may also carry some antidote or deactivating enzyme, combining traditional treatment ideas of the past with improved delivery methods. Finally, the particles may be composed of a material or substance that acts directly on the injured area to rapidly improve the effected organ's functions, rather than interacting with the toxin or drug compound directly.

Several studies have been done in recent years involving drug detoxification with nano or microparticles. Varshney et al. used eight pluronic surfactants in combination with ethyl butyrate to find the best surfactant for drug binding to microemulsions [19]. Pluronic F-127 was deemed the most promising surfactant, and an optimized microemulsion formulation was capable of extracting 60% of the local anesthetic bupivacaine (BUP) from a buffered solution at an oil content of 1 mg oil/mL across a wide range of drug concentrations. In an effort to understand the binding process between the TCA amitriptyline (AMI) and similar emulsions, James-Smith et al. used

turbidity analysis to determine that approximately 12 AMI molecules were bound per F-127 molecule [20]. The importance of the oil phase in their systems was also demonstrated based on its ability to induce a surface charge and attract AMI. Underhill et al. studied oil-filled nanocapsules stabilized by Brij 97 surfactant and thereafter coated with polysilicate/polysiloxane shells [21]. Their presumed mechanism for drug affinity was hydrophobic interactions between lipophilic drugs and oil phases. They were able to remove greater than 99% of BUP from drug solutions at concentrations below 200 μM. Quinoline was also studied for proof of concept purposes, and 97% was removed from solutions after 15 minutes with 1.4% w/v oil content nanocapsules. Lee and Baney studied yet another type of detoxification system where a different attraction mechanism was proposed [22]. They reacted chitosan polymers with dinitro-fluorobenzene to form dinitrophenyl chitosans. The resulting chitosans were only partially soluble in water, attributed to the reduced protonation of amino groups [22]. The insoluble chitosans were used for drug uptake studies and removed 90% of AMI from saline solutions at a relatively high polymer concentration of 0.4%. Chakraborty and Somasundaran used poly(acrylic acid) microparticles to sequester AMI and BUP from normal saline [23].

Perhaps the most relevant work to the research presented herein was done by Dhanikula et al. They reported results from experiments using nanoparticles for the sequestration of AMI and other drugs [24,25]. In one study, they use oil-filled lipid nanocapsules for haloperidol, docetaxel, and paclitaxel sequestration [24]. They hypothesized that the oil-filled nanocapsules bind to drug based on oil-drug affinities. In a second study, they used spherulites and nanocapsules to do in vitro experiments

involving AMI, as well as ex vivo experiments using amitriptyline-intoxicated rat hearts [25]. Spherulites are similar to nanocapsules and liposomes, with one key difference. They have numerous concentric bilayers surrounding their core, rather than a single layer. The work of these and other researchers on drug binding to nanoparticles is further discussed throughout Chapters 2-7. Despite the numerous studies conducted on developing nanoparticles for drug detoxification, no effective, widely useful solution has been introduced into the market.

Accordingly, the overall goal of the present work was to design nanoparticles capable of treating TCA and BUP overdoses. Liposomes were chosen as the platform for development. Liposomes are spherical nanoparticles composed of a bilayer of phospholipids encapsulating an aqueous core. Their unique structures make it possible for them to carry water soluble compounds, which has led to applications in drug delivery [26]. Unlike micelles, liposomes rarely form spontaneously and typically require some form of energy for complete formation [26]. This is especially true if unilamellar, uniformly sized liposomes are desired. Common methods of making liposomes include the reverse phase evaporation (RES) method [27], probe or bath sonication [27], and hydration followed by extrusion [28]. One major advantage of using liposomes is their proven biocompatibility for many phospholipids used. To accomplish the goal of designing liposomes for the treatment of TCA or BUP overdose, liposomes were optimized (Chapters 2-5), the binding process was characterized (Chapter 6), and physiologically based pharmacokinetic (PBPK) models were used to predict in vivo efficacy based on the in vitro data (Chapter 7).

AMI is a primary TCA of concern. In Chapter 2, we tested the AMI binding ability of charged liposomes in the presence of serum proteins. Serum proteins are present throughout the blood stream and could therefore interact with liposomes during the drug sequestration process, rendering the liposomes less effective. The primary goal of Chapter 2 was to quantify the protein effects on liposome treatment, both from a competition and interference stand point. Liposome charge and loading were varied, drug binding was measured to serum proteins individually and via human serum samples, and the primary metabolite of AMI, nortriptyline, was also tested. A two-site binding model was proposed and fit to the drug-protein binding data. The low drug concentration regimes in which most of the data was measured allowed protein-drug binding to be uniquely characterized.

Based on the results from Chapter 2, where proteins were shown to interact with charged liposomes, lipids altered to include covalently attached polyethylene glycol (PEG) were added to the liposome formulations. Coverage with surface polymers such as PEG is the most widely known method of counteracting opsonization and protein binding. The resulting liposomes have a surface layer of PEG that is approximately 5 nm thick [29]. Using this technique, Awasthi et al. have shown significant increases in circulation times for pegylated versus conventional liposomes, with less accumulation in the liver as well [30]. This phenomenon has also been observed for nanocapsules fabricated with and without PEG [31]. The degree of surface coverage, achieved through polymer chain length and percent inclusion, is also noteworthy, as liver and spleen accumulation are minimal at PEG inclusions of around 10% by mole, but increase beyond such concentrations [31,32]. By choosing an optimum proportion of

PEG, the correct chain length, and the best preparation technique, one can greatly enhance the pharmacokinetic properties of most nanoparticles. AMI binding to the PEG-altered liposomes was reported in Chapter 3. Additionally, the effect of increased lipid loading and various liposome sizes on AMI binding was investigated. To simulate the packaging effects that liposomes would undergo during clinical situations, liposomes stored for a period of one month were tested for their drug binding ability.

In Chapters 2 and 3, liposomes were optimized for maximum AMI uptake. A system capable of treating multiple overdoses is significantly superior to a therapy targeted at only one drug. AMI is one of three key antidepressants related to overdose fatalities, along with imipramine (IMI) and dosulepin (DOS), which is also known as dothiepin. Henry et al. [5] and Morgan et al. [6] reported that these three drugs produce the highest death rates among all antidepressants used in the United Kingdom. The first goal of Chapter 4 was to therefore extend the use of liposomes to IMI and DOS. In addition, opipramol is a drug similar in structure to tricyclic antidepressants but used for the treatment of anxiety disorders. It has also been cited as heavily involved in drug overdose cases in Germany and Turkey, where it is primarily used [3]. Including opipramol into the study allowed us to test liposome-drug binding for an important drug, and the effect of drug charge on binding, as opipramol is only 83% protonated compared to 99% for the TCA's. Chapter 4 also included experiments aimed at quantifying the effect of changing the PEG chain length, if any, on the drug-liposome interactions. PEG length is an important parameter for liposome in vivo circulation time.

Local anesthetic drugs are useful for providing regional anesthesia or analgesia with limited systemic exposure. However, their ability to cause toxicity has been pointed

out above. Such instances can occur without warning and require rapid action to ensure patient survival [17]. A rapid treatment protocol for toxicity reversal would drastically reduce the risks of using such drugs. Several in vivo animal models and emerging case studies show that lipid emulsions, such as Intralipid® 20%, composed of 20% soybean oil, 1.2% egg yolk phospholipids, 2.25% glycerin, and water, through rapid drug binding or improved oxidative metabolism, may be one useful modality for treating overdoses [12-14,17,33-40]. Such emulsions have traditionally been used to supply patients with calories and essential fatty acids during illness and other times when consuming adequate amounts of fat is difficult. Weinberg et al. first studied the pre-treatment effects of lipid emulsions on rat toxicity induced with BUP [41]. They showed an in vitro sequestration in plasma of 75.3% of BUP at final lipid concentrations of 15%. More significantly, they showed median lethal doses of 82 mg/kg for rats treated with lipid emulsions prior to drug exposure, which was about 5 fold higher than the dose of 17.8 mg/kg in the control, untreated group. Their study was followed by additional work by Weinberg et al., where dogs were treated with lipid emulsions 10 minutes after drug induced toxicity [42]. Six treated dogs survived, while the six untreated dogs did not. Furthermore, they reported recovery of myocardial tissue pH and oxygen pressure for lipid emulsion treatment versus the control. Since the results of their studies were published, several cases of successful detoxification with similar lipid emulsions have been reported [12-14,33,34]. Thus, lipid emulsions have been shown to be an effective detoxification therapy under critical conditions in clinical settings.

Still, questions remain about the use of lipid emulsions for detoxification. First, the mechanism of toxicity reversal is still unclear, as Weinberg et al. and many others suggest [41-46]. Possible mechanisms include the redistribution mechanism, where drug is relocated to the blood compartment, as well as restored energy production in the myocardium. BUP is known to hinder fatty acid transport at the mitochondrial membrane, causing disruption to energy demanding processes. The possibility of lipid emulsions improving fatty acid oxidation and subsequent improved adenosine triphosphate production has been widely suggested and even supported through clinical results [14]. Yet another mechanism has also been mentioned, in which increased nitric oxide production induced by lipid emulsions could reduce bupivacaine toxicity [41]. The mode of toxicity reversal is not the only issue surrounding the use of lipid macroemulsions for detoxification therapy. Concerns over the abandonment of fervent toxicity prevention efforts and the possible side effects of administering such large amounts of lipids to patients have also been raised [45,46].

Chapter 5 represents our attempts to both improve the current treatment protocol for local anesthetic adverse reactions through superior liposome therapies, and better understand the mode of action of emulsions currently being used. Liposomes have already been explored as drug delivery vehicles for local anesthetics, which suggest high-affinity binding between liposomes and local anesthetics [47-53]. The PEG coated, anionic liposomes explored in Chapters 2-4 were used to measure BUP binding in Chapter 5. Multilamellar liposomes were also utilized in drug binding experiments, which led to some very interesting observations about multilamellar versus unilamellar liposomes in the context of charged liposome-drug interactions. Data reported for BUP

binding to macroemulsions in literature was compared to in vitro data for liposomes to determine which formulation had the higher drug affinity.

In Chapter 6, we move from the optimization phase to a more fundamental look at liposome-drug interactions. The association of small molecules with lipid and/or cell membranes has been a subject of several studies, primarily due to the pivotal role such interactions play in determining how drugs, nutrients, and other xenobiotics introduced into the body affect the function and vitality of the cell membrane [54-61]. These interactions have also been explored due to their relevance in applications, such as drug loading and release from liposomes [62-68] and, within the context of this work, drug overdose treatment with liposomes [24,25,69-72]. The interactions of molecules with liposomes and lipid bilayers in general impact drug delivery and drug overdose treatment through several mechanisms. First, the equilibrium binding of drugs to bilayers controls the release rate when the release is limited by equilibrium partitioning, which is true for drugs that exhibit a high binding affinity for liposomes. Second, the bilayer permeability of water-soluble drugs loaded into liposomes has a profound effect on their rate of release unless liposome destruction is triggered by some alternative mechanism. Finally, the interaction of drugs with lipid bilayers of the endothelial cells lining the capillaries can impact the transport of drugs and other solutes into tissues. Chapter 6 involves additional liposome-drug binding studies where various parameters such as surface charge, bilayer fluidity, number of lamellae, and ionic strength were altered. Moreover, leakage of a water soluble fluorescent dye from the core of liposomes was studied to give some insights into differences in drug-bilayer interactions

for TCA's and BUP. A continuum model incorporating electrostatics and a Langmuir binding isotherm was used to help analyze the experimental results.

In Chapters 2-6, we identified anionic, pegylated liposomes capable of sequestering TCA's and BUP from human serum solutions with the goal of using liposome therapy to reduce toxicity through drug redistribution from vital organs to the blood compartment. While our in vitro drug binding data suggested great potential for liposome based overdose therapy, the in vivo efficacy could not be directly assessed. As a next step in our efforts to prove the effectiveness of the liposomal systems, we attempted to utilize physiologically based pharmacokinetic (PBPK) models and our in vitro data to predict the in vivo behavior.

Predictions of in vivo behavior based on in vitro data represent an exciting and growing research area that can lead to reductions in time and costs associated with developing new drug therapies, as well as the amount of animal testing required. PBPK models are exceptional tools for this purpose [73-76], offering a versatile method for predicting the pharmacokinetic profiles, optimal doses, and pharmacodynamic (PD) effects of new therapies early in the drug discovery process. PBPK models are essentially block compartment models more closely representing physiology than traditional pharmacokinetic models [77], and have been utilized for a wide array of purposes [78-82]. We combined partition coefficients calculated from published mechanistic equations with our in vitro data for protein and liposome binding to estimate drug distribution throughout the human body. The models were validated for reliability using published intravenous data. The models allowed for variations in drug dose, liposome dose, time lapse between drug and liposome dose, hepatic clearance,

absorption times, partition coefficients, and liposome clearance to be simulated without any additional in vivo experiments. Lastly, reported local pharmacodynamic changes in cardiac tissue and cell components as a function of AMI or BUP concentration were correlated to concentration versus time profiles generated by our models to allow for an estimate of the extent to which liposomes would ultimately induce cardiac tissue recovery to basal levels.

CHAPTER 2
UPTAKE OF AMITRIPTYLINE AND NORTRIPTYLINE WITH LIPOSOMES, PROTEINS, AND SERUM

2.1 Introduction

The goal of this chapter was to test the suitability of charged liposomal systems at treating amitriptyline (AMI) overdose under physiological conditions. The major difference between PBS and the blood is the presence of plasma proteins, which also bind a significant amount of drug. Thus, in this chapter we focused on the effect of plasma proteins on the sequestration, or temporary removal from solution by complexation, of AMI by liposomes.

Additionally, we sought to understand the role of liposome-protein interactions in drug overdose treatment, and to apply that knowledge to further optimize our liposomal systems. Uptake of nortriptyline, the major metabolite of AMI, was also investigated with similar liposomal suspensions. A primary characteristic of each species considered in this study was net charge. At the physiological pH of 7.4, both AMI and nortriptyline exist predominantly in their positively charged forms. DMPC has no net charge, whereas DOPG bears a negative charge. Previous studies showed that liposomes composed of more negatively charged lipids sequestered more AMI than those with neutral lipids [71]. Accordingly, we studied liposomes composed of a 50:50 molar ratio of DMPC and DOPG, as well as pure DOPG lipids. The structures of both drugs and both lipids are shown in Figure 2-1. In addition to investigating the suitability of liposomes for overdose treatment, we have investigated binding isotherms for AMI with albumin, fibrinogen, and globulins. These studies have revealed some very interesting behavior which is particularly evident at low drug concentrations, a regime which has not been explored in detail by previous investigators.

2.2 Materials and Methods

2.2.1 Materials

Methanol, chloroform, Dulbecco's phosphate buffered saline (PBS) without calcium chloride and magnesium chloride, bovine serum albumin (BSA), fibrinogen from bovine plasma, *γ*-globulins from human blood, human serum from male plasma, nortriptyline hydrochloride, and amitriptyline hydrochloride were purchased from Sigma Aldrich. 0.45 μm nylon syringe filters, YM30 centrifugation filters (30,000 molecular weight cut-off), and YM10 centrifugation filters (10,000 molecular weight cut-off) were purchased from Fisher Scientific. The lipids 1,2-dimyristoyl-*sn*-glycero-3-phosphocholine (DMPC), in powder form, and 1,2-dioleoyl-*sn*-glycero-3-[phospho-*rac*-(1-glycerol)] (sodium salt) (DOPG), in powder form, were purchased from Avanti Polar Lipids, Inc.

2.2.2 Liposome Preparation

Liposomes containing a mixture of DMPC and DOPG lipids as well as liposomes containing DOPG lipids were prepared using an ultrasonication procedure. For preparing DOPG liposomes, 20 mg of lipid was dissolved in a 9:1 mixture (by volume) of chloroform:methanol such that a 10 mg/mL concentration of lipids was obtained. The organic solvent was then evaporated under a stream of nitrogen. After an even and uniformly dried lipid film was obtained, the dried lipid layer was hydrated with PBS, such that the lipid concentration was 40 mg/mL, and the hydrated lipid was sonicated in a bath sonicator (G112SP1 Special Ultrasonic Cleaner, Avanti Polar Lipids, Inc.) at room temperature for 20 minutes to form lipid vesicles. More PBS was then added, such that the lipid concentration became 4 mg/mL, and the lipid suspension was sonicated using a probe sonicator (Fisher Scientific Sonic Dismembrator Model 100) for 40 minutes at

room temperature to reduce the vesicle size. The suspension was surrounded by a cool water bath during the sonication to avoid excessive heat buildup. The liposomal dispersion was filtered using a 0.45 μm filter. Effective diameter was previously determined to be 40-45 nm using a Brookhaven particle size analyzer [71]. Liposomes containing both DMPC and DOPG lipids in 50:50 molar ratios were prepared by following the same procedure as described above, except that the two lipids were mixed in a 50:50 molar ratio before dissolving the lipids in the organic liquid. In some experiments the lipid loading was doubled at the dissolution step, and this resulted in a loading of 8 mg/mL in the final liposomal suspension.

2.2.3 Amitriptyline Uptake Experiments

To quantify AMI uptake by liposomes, proteins, and mixtures of both liposomes and proteins, filtration and HPLC analysis were used. Percentage of drug uptake was calculated by subtracting the final drug concentration from the initial drug concentration measured from control solutions and dividing by the initial drug concentration. This method could measure the binding of AMI, but it provided no information regarding the time scale on which binding occurred, due to the long time required for filtration. The time scale for binding between AMI and liposomes was previously investigated, however, and found to be extremely rapid [71]. To determine the initial drug concentrations used for the percent uptake calculations, control drug solutions were made and a volume of PBS equal to the volume of the liposome dispersion added to the samples was added to the control solutions to eliminate error due to dilution.

2.2.4 Amitriptyline Uptake with Liposomes

AMI uptake was expected to depend on lipid and drug loading. The initial AMI concentration was varied from around 1 to 100 μM, and two different lipid loadings, 0.36 and 0.72 mg lipid/mL were used in the experiments described below.

Liposomes were added to solutions of AMI, which were all made with PBS (pH 7.4), such that the volume of the liposomal dispersion (containing 4 or 8 mg lipid/mL) was 9% of the total solution volume giving a final lipid concentration of 0.36 or 0.72 mg lipid/mL. After being stirred for 10 minutes, the solutions were ultracentrifuged at 3000 rpm for 15-20 minutes in a vial that contained a YM30 filter (30,000 molecular weight cut-off). Filter sizes were chosen to ensure that most of the drug that was not bound passed through the filters, while liposome-drug complexes and liposomes did not pass through the filters, as verified in [71]. To ensure that all unbound AMI was accounted for, solutions of AMI at various concentrations were passed through YM30 and YM10 filters in a separate test. Small amounts of AMI were taken up by the filters, and a linear correction curve was made and used to correct for AMI adsorbed by the membranes. To minimize the effect of any leaching components from the filter, the filters were rinsed with de-ionized water and then PBS at 3000 rpm for 20 minutes prior to their use in these experiments. The concentration of AMI in the filtrate (free drug concentration) was measured using HPLC analysis. AMI was detected at an absorbance of 215 nm after passing through a C18 column (Waters) using an acetonitrile/50 mM $NH_4H_2PO_4$ solvent mixture in a 35/65 ratio. The calibration curve for concentration versus area under the curve was linear with $R^2 > 0.99$.

2.2.5 Amitriptyline Uptake with Proteins

Albumin from bovine serum, fibrinogen from bovine plasma, and globulins from human blood were each tested separately for their ability to bind AMI. Human blood is made up of approximately 7% protein, with 4.5% albumin, 0.3% fibrinogen, and 2.5% globulins [83]. We conducted experiments with 2% and 4% (w/w) albumin, 2% (w/w) fibrinogen, and 1% (w/w) globulins. Also, a mixture of 4% albumin, 2% fibrinogen, and 1% globulins was tested for AMI uptake. Each protein was weighed and AMI solutions were then added to the proteins. The procedure described above for uptake with liposomes was then followed, with the exception of filtration times, which were increased to a period ranging from 45 minutes to 5 hours.

2.2.6 Amitriptyline Uptake with Mixtures of Liposomes and Proteins

For the mixtures tested, the proteins were first weighed and combined with AMI solutions. Liposomes were then added to the solutions such that the volume of the liposomal dispersion (containing 4 or 8 mg lipid/mL) was 9% of the total solution volume (giving a final concentration of 0.36 or 0.72 mg lipid/mL). Mixtures with protein concentrations of 4% albumin (w/w), 2% fibrinogen (w/w), and 1% globulins (w/w) were tested individually. To simulate more realistic serum conditions, a mixture of 4% albumin (w/w), 2% fibrinogen (w/w), and 1% globulins (w/w) was tested.

2.2.7 Amitriptyline Uptake with Human Serum

50:50 DMPC:DOPG liposomes were added to solutions of AMI in human serum from male plasma, such that the volume of the liposomal dispersion was 9% of the total solution volume, giving a final lipid concentration of 0.72 mg lipid/mL. Control solutions of AMI in PBS and AMI in serum without liposomes were also made to allow for uptake quantification and comparison. After being stirred, the solutions were ultracentrifuged at

5000 rpm for 15 minutes in a vial that contained a YM10 filter (10,000 molecular weight cut-off). YM10 filters were used for serum, rather than YM30 filters, due to the presence of many components present in serum that could pass through the membrane. To minimize the effect of any leaching components from the filter, the filters were rinsed first with DI water and then with PBS at 5000 rpm for 10 minutes prior to their use in these experiments.

2.2.8 Reversibility of Binding (Dilution Method)

To ensure that the drug binding to liposomes and proteins is reversible, two different paths were followed to obtain the same final composition, and uptake was measured for both cases. Specifically, two samples were tested with identical AMI concentrations at a 4% albumin (w/w) concentration. The drug and albumin were combined as described above for the control sample, and then 50:50 DMPC:DOPG liposomes were added to produce a final lipid concentration of 0.72 mg lipid/mL. For the second sample, a more concentrated drug solution was first combined with the proteins, followed by the 50:50 DMPC:DOPG liposomes. After 10 minutes, the second sample was diluted to the same final AMI and liposome concentrations as the control sample. Both samples were filtered and the AMI concentrations were measured via HPLC.

2.2.9 Time Dependency of Amitriptyline Uptake

To gain insight into the effects of time on the liposome-drug binding and the liposome-drug-protein interactions, experiments were conducted in which liposomes were added to AMI solutions as described in Section 2.2.4 and uptake was measured after approximately 24 and 48 hours. This experiment was carried out for mixtures with

2% fibrinogen (w/w) and 50:50 DMPC:DOPG liposomes. The final lipid concentration was again 0.72 mg lipid/mL.

2.2.10 Nortriptyline Uptake with Liposomes and Albumin

Once inside the body, the major metabolite of AMI is nortriptyline. Since an overdose of nortriptyline may also cause toxicity, we have measured the uptake of nortriptyline with pure DOPG and 50:50 DMPC:DOPG liposomal systems [84]. Uptake measurements were done in PBS and in the presence of 4% albumin. The procedures were the same as described in Sections 2.2.4, 2.2.5, and 2.2.6, with the exception of the protocols for HPLC analysis. A solvent mixture of acetonitrile/50 mM $NH_4H_2PO_4$ at a ratio of 32.5/67.5 was used for nortriptyline detection. Nortriptyline was detected by measuring absorbance at 215 nm. The calibration curve for concentration versus area under the curve was linear with $R^2 > 0.99$.

2.3 Results and Discussion

2.3.1 Amitriptyline Uptake with Liposomes

In all of the results reported below, the percentage of drug uptake was determined by measuring both the AMI sample and a control AMI solution. The control solution was diluted with PBS to match the dilution effect from the liposome solution added to the AMI sample. Percentage of AMI uptake was plotted as a function of final AMI concentration. Typically, two experiments were done with the same starting drug concentration, and results from each of these are included in the figures. The close proximity of the results from the repeat runs indicates the reproducibility of AMI uptake with liposomes.

2.3.1.1 Effect of lipid loading

The effect of lipid loading was investigated for both the 50:50 DMPC:DOPG system and the pure DOPG system. Figure 2-2 shows the AMI uptake as a function of final AMI concentration for lipid loading levels of 0.36 and 0.72 mg lipid/mL for both systems. For pure DOPG, uptake values varied from around 95% at 0.36 mg lipid/mL and final AMI concentrations of around 2.5 μM, to nearly 100% at 0.72 mg lipid/mL and final AMI concentrations on the order of 0.01 μM. The 50:50 DMPC:DOPG system seemed to be more sensitive to loading, with uptake values ranging from 90 to 99% in the same concentration range. In both cases, uptake increased as lipid loading increased, which was expected. The fractional uptake decreases on increasing the concentration, which is expected because there are only a limited number of binding sites on liposomes, and as the bulk drug concentration gets larger, a majority of these sites are occupied (saturated) leading to a reduction in fractional drug uptake on further increase in concentration. Both lipid loading levels produced relatively high uptake values for both the 50:50 DMPC:DOPG system and the pure DOPG system. Also important to note is that the maximum lipid loading level used in this study of 0.72 mg lipid/mL is still low compared to lipid loading levels in other studies [25]. Thus, the results presented here are the lower bounds of the uptake capabilities of these systems and may be improved with higher lipid loading.

If one neglects interaction between liposomes, the uptake data for the system in which the lipid loading is doubled (Φ_{double}) can be predicted by scaling up the uptake data at the original lipid loading (Φ). Here Φ refers to the fraction of drug bound to liposomes divided by the total amount of drug initially in solution, and so the ratio of drug on liposomes to free drug is as follows:

$$\frac{\phi}{1-\phi}. \tag{2-1}$$

This ratio depends only on the drug concentration and the amount of lipids added to the system. At a given free drug concentration, the amount of bound drug should double on doubling the loading, and so the ratio of bound to free drug should also double, i.e.,

$$\frac{\phi_{\text{double}}}{1-\phi_{\text{double}}} = \frac{\phi}{1-\phi} + \frac{\phi}{1-\phi}. \tag{2-2}$$

The above equation can be simplified to give

$$\phi_{\text{double}} = \frac{2\phi}{1+\phi}. \tag{2-3}$$

However, one has to ensure that Φ and Φ_{double} correspond to the same final drug concentration. The solid and dashed lines in Figure 2-2 are trend lines from the predicted data based on the above equation. A good match between the predictions and the experimental data suggests that the system is dilute in lipid and so inter-liposome interaction is negligible. If such interaction were present, liposomes could possibly fuse, which may reduce the number of sites available for drug adsorption.

2.3.1.2 Effect of charge

At a pH of 7.4, DMPC has a net neutral charge, DOPG carries a (−1) charge, and AMI is predominately present in its charged form (AH^+). To clearly illustrate the effect of charge on uptake, DOPG and 50:50 DOPG:DMPC should be compared at equal lipid loadings of 0.72 mg/mL. The data plotted in Figure 2-2 confirms that charge, and hence electrostatic interactions, play an important role in sequestration. Both systems sequestered AMI extremely well, but the pure DOPG system, which carried twice as much net charge as the 50:50 system, approached 99.99% uptake at very low AMI

concentrations. The DOPG lipids form an exterior bilayer surface that is negatively charged, which attracts the positively charged drug. Although the DMPC lipid also contains a negative charge, its positively charged group repels the positively charged drug and likely also causes inter-lipid interaction, which further reduces the available negative charges for binding. Also, it is interesting to note that pure DOPG liposomes at 0.36 mg/mL sequestered more drug than the 50:50 DMPC:DOPG liposomes at 0.72 mg/mL. This suggests that the dependence of uptake on charge is non-linear, and probably depends on other factors, such as bilayer structure and the presence of positive charge on DMPC lipids.

2.3.2 Amitriptyline Uptake with Proteins

The amount of AMI bound to albumin from bovine serum, fibrinogen from bovine plasma, and γ-globulins from human blood was measured, because it is well known that AMI is approximately 95% bound to serum proteins while inside the blood stream [85]. Any particles developed for overdose treatment will be competing with proteins for AMI, as well as interacting with proteins themselves. Our goal was to quantify the in vitro binding between AMI and proteins without liposomes using our uptake procedures, and then compare this data with AMI uptake from mixtures of proteins and liposomes to determine if significant interactions between liposomes and proteins occurred.

2.3.2.1 Uptake with albumin

AMI uptake by albumin at 2% and 4% (w/w) is plotted as a function of final AMI concentration in Figure 2-3. Similarly to lipid loading, increased protein loading resulted in increased uptake. The fractional uptake also decreased as the concentration was increased, which was probably due to saturation effects. However, the fractional uptake leveled off above an equilibrium concentration of about 20 μM. This behavior was also

evident in other results shown below. The 4% albumin data, which is approximately equal to the amount of albumin in blood, shows binding levels of around 90% at low concentrations. This data shows that on a weight basis, albumin has a much lower affinity for AMI compared to the liposomes because liposomes have a maximum AMI uptake of 99.9% at concentrations of 0.072% (w/w). The solid line in Figure 2-3 is the trend line predicted by Equation 2-3 for 4% albumin based on the uptake data for 2% albumin, assuming no protein-protein interaction. Again, a good match between the prediction and the experimental data suggests that the system is dilute in protein and so inter-protein interaction is negligible.

While inter-protein interaction appeared to be negligible, the AMI binding curve for albumin showed an unexpected behavior. The albumin concentrations of 4% and 2% (w/w) were equivalent to around 600 and 300 μM, respectively. At AMI concentrations below 20 μM, one would expect AMI uptake to be constant across a range of drug concentrations because the binding sites on proteins are far more numerous than the number of drug molecules in solution. However, the data shows that the fractional uptake decreases significantly, even at very low concentrations. To ensure that time dependent kinetic effects were not responsible for this behavior, the fractional uptake was measured for an initial AMI concentration of 25 μM after allowing the system to equilibrate for a period of time varying from one to three days. These results in Figure 2-3 show that the uptake values after days one, two, and three were consistent with the previous data. This suggests that the uptake values reported here represent equilibrium uptake.

The sharp decay in fractional uptake followed by leveling off at concentrations above 20 μm suggests that there are two different binding sites on the proteins. Below, we propose a simple two site binding model to quantitatively understand the drug binding. The detailed interactions at these binding sites cannot be explored by the techniques used in this paper, but the model still sheds light on the mechanisms of uptake.

We propose that the drug can bind to two different sites on the protein to form complexes denoted by DP and DP$*$:

$$D + P \underset{}{\overset{\frac{1}{K_1}}{\rightleftharpoons}} DP\,, \tag{2-4}$$

$$D + P \underset{}{\overset{K_2}{\rightleftharpoons}} DP^{*}\,, \tag{2-5}$$

where D is unbound AMI, P is unbound protein, DP is the drug-protein complex resulting from one mechanism, and DP$*$ is the drug-protein complex resulting from a second mechanism. We have further assumed that the number of $*$ sites are much larger than the number of drug molecules and so the reaction resulting in DP$*$ is zero order with respect to drug concentration. This assumption is based on the fact that the fractional uptake levels off beyond the 20 μm drug concentration. Accordingly, the equilibrium for the $*$ binding can be represented by the following equation:

$$DP^{*} = \beta D\,, \tag{2-6}$$

where β is the equilibrium constant for the $*$ binding under the assumption of very large protein concentration. A mass balance for the drug yields

$$(\beta \times D) + D + DP = D_{total}, \quad (2\text{-}7)$$

where D and D_{total} are the free and total AMI concentrations, respectively, and DP is the concentration of the DP complex. A mass balance on the protein yields

$$DP + P = P_{total}, \quad (2\text{-}8)$$

where P and P_{total} are the free and total concentrations of the protein that contains a site that could be used for formation of the DP complex. The binding sites for the two mechanisms are assumed to be completely independent, and so the mass balance for DP is unaffected by DP*. Based on Equations 2-4 through 2-8, Equation 2-9 was derived for the drug-protein complex DP,

$$DP = \frac{(K_1 + \beta \cdot K_1 + D_{total} + P_{total}) - \sqrt{(K_1 + \beta \cdot K_1 + D_{total} + P_{total})^2 - (4 \cdot D_{total} \cdot P_{total})}}{2}, \quad (2\text{-}9)$$

which was then used in Equation 2-10 to solve for the fraction of AMI bound (f):

$$f = \frac{DP + \frac{\beta}{1+\beta}(D_{total} - DP)}{D_{total}}. \quad (2\text{-}10)$$

The model was used to find the values of K_1 and P_{total} that best described the experimental data. The value of β was determined by equating the fractional uptake value in the plateau region to β/(1+β). For the case of 2% albumin where a β value of 1.78 was used, the best fit K_1 value was 2.78 μM^{-1}, and the effective P_{total} for albumin was 5.13 μM. For 4% albumin (β = 3.35), the best fit values of K_1 and P_{total} were 1.83 μM^{-1} and 9.24 μM, respectively. The fitted values of P_{total} were much smaller than the total protein concentration, which were 600 and 300 μM for the 4 and 2% protein solutions, respectively. Thus, the data suggest that a significant number of albumin molecules were unavailable for binding. This could be due to inhibition of one

mechanism by the other or conformational changes upon binding. Aggregation was unlikely, as lyophilized protein in the presence of salt was used to ensure solubility. Additionally, the close correlation between the predictions from Equation 2-3 and the 4% albumin data further support the lack of aggregation. Another potential reason for the difference between the fitted and the true value of P_{total} could be that the binding site is not available in the native state of the protein, but slight conformational fluctuations around the native state allow the binding. In this case, the fitted P_{total} would be the concentration of the protein molecules that possess the conformations that allow binding. These results suggest that the concentration dependent nature of AMI binding to serum proteins at therapeutic concentrations could be important considerations for physicians, particularly in the case of overdose treatment.

2.3.2.2 Uptake with fibrinogen

Figure 2-4 shows AMI uptake with 2% fibrinogen (w/w), which is about double the fibrinogen concentration in plasma. Since the system is dilute for 4% albumin, it can be assumed that 2% fibrinogen is also dilute, and so Equation 2-3 can be used to predict the uptake data for 1% fibrinogen (w/w). Fibrinogen at 2% (w/w) binds about the same amount of drug as 2% (w/w) albumin, and so the model presented in Section 2.3.2.1 was used to predict K_1 and the effective P_{total} value. A value of 0.67 was used for β in these calculations. A K_1 value of 2.90 μM^{-1} suggested a similar affinity for AMI as albumin, while a P_{total} value of 1.68 μM versus an actual fibrinogen concentration of around 60 μM again pointed to a small percentage of protein molecules available for binding.

2.3.2.3 Uptake with globulins

Figure 2-4 also shows the drug uptake data for globulins at a concentration of 1% (w/w), and the scaled up prediction for uptake by 2% (w/w). The scaled up data shows that at the same loading, the globulins take up slightly less drug than albumin or fibrinogen. Again, Equation 2-10 was applied to the globulin case to examine the affinity and availability of the protein. The P_{total} of 2.08 μM versus an actual globulin concentration of 67 μM was consistent with albumin and fibrinogen, once more pointing to a lack of available protein molecules for AMI binding. The K_1 value of 7.10 μM^{-1} confirmed the lower affinity of globulins for AMI than albumin or fibrinogen. A value of 0.025 was used for β in these calculations.

2.3.3 Amitriptyline Uptake with Mixtures of Liposomes and Proteins

The results from Sections 2.3.1 and 2.3.2 provided information on the AMI binding properties of liposomes and proteins independently. The liposomes were shown to sequester large amounts of AMI in PBS, while the proteins also bound to the drug, although to a lesser extent. Below we report the drug uptake in the presence of both liposomes and proteins. These experiments were conducted to better simulate in vivo conditions and also to determine whether the proteins bind to the liposomes. To accomplish the latter objective, a simple mass balance was utilized to predict the drug uptake by a mixture of liposomes and proteins, based on the assumption that these components do not interact with each other, i.e., proteins do not bind to liposomes. The mass balance leads to the following equation:

$$\phi_{\text{mix}} = \frac{\sum_{\text{n}} \frac{\phi_i}{1-\phi_i}}{1+\sum_{\text{n}} \frac{\phi_i}{1-\phi_i}}, \qquad \text{(2-11)}$$

where Φ_i and Φ_{mix} are the uptakes in the i^{th} component and the mixture, respectively. If the measured uptake for the mixture is less than that predicted by the above equation, one may expect that the proteins are adsorbing on the liposomes, leading to a reduction in the number of available sites on liposomes for drug adsorption.

2.3.3.1 Albumin and liposomes

In the experiments described below, 4% albumin was combined with 50:50 DMPC:DOPG liposomes at lipid concentrations of 0.36 and 0.72 mg lipid/mL, as well as pure DOPG liposomes at a lipid concentration of 0.36 mg lipid/mL.

Figure 2-5 shows the AMI uptake predictions and experimental results for 50:50 DMPC:DOPG liposomes and 4% albumin as a function of final AMI concentration. At the lower lipid loading level of 0.36 mg lipid/mL, the system behaved as if no interaction took place between the liposomes and albumin. The experimental values closely corresponded to the trend line predicted by the mass balance. This would seem to suggest that the effectiveness of the liposomes at sequestering AMI is uninhibited by the presence of albumin. However, at the higher lipid loading level of 0.72 mg lipid/mL, the experimental values were consistently lower than the predicted values. Increasing the lipid loading level seemed to increase binding between the liposomes and proteins, causing the overall system uptake of AMI to be reduced. At the lowest final AMI concentrations of around 0.1 μM, the uptake values were around 97%, as opposed to predictions approaching 99%. The system of liposomes and albumin was still a marked improvement over the 4% albumin (w/w) system alone, which only bound around 90% of the drug at similar concentrations. Doubling the amount of lipid in the system did increase the uptake in the low concentration regime from around 94-95% to around 97%. Thus, increasing lipid loading appears to increase uptake, but the effect is less

than expected in the presence of albumin due to competing interactions with the proteins.

AMI uptake values for mixtures of pure DOPG liposomes and 4% albumin at a lipid loading level of 0.36 mg lipid/mL are also plotted in Figure 2-5. The data shows that significantly less AMI was bound in the mixture of liposomes and proteins than the predicted values. This was particularly true in the low concentration region. Additionally, the measurements have more variation compared to that in results reported earlier. There also seems to be a minimum in the drug uptake that occurs at a concentration of 0.35 μM. The drug uptake by the mixture of 4% albumin and pure DOPG liposomes at 0.36 mg/mL was comparable to the uptake by the mixture of 4% albumin and 50:50 DOPG:DMPC liposomes at 0.36 mg lipid/mL. This is in contrast to the performance of the liposomes in the absence of albumin, where the pure DOPG liposomes sequestered significantly more AMI than the 50:50 liposomes. The pure DOPG liposomes carry twice as much charge as the 50:50 DMPC:DOPG system, and this may be leading to increased protein binding, causing a greater reduction in uptake than for the 50:50 DMPC:DOPG system. These results suggest that pure DOPG liposomes may not be the optimal system to use for drug detoxification due to high levels of protein interaction. Due to this reason, the 50:50 DMPC:DOPG system at a lipid concentration of 0.72 mg lipid/mL was used for subsequent mixture experiments involving fibrinogen and globulins, rather than pure DOPG liposomes.

2.3.3.2 Fibrinogen and liposomes

Mixtures of 2% fibrinogen and 50:50 DMPC:DOPG liposomes at lipid concentrations of 0.36 and 0.72 mg lipid/mL were tested for AMI uptake, and the measured and predicted uptake values are plotted in Figure 2-6. For the lower lipid

loading of 0.36 mg lipid/mL, the measured uptake values were around 88 to 89%, falling significantly below the predicted values. This was especially true in the lowest concentration regime, where the uptake was roughly 5% less than expected at a final concentration of around 0.1 μM. A lipid loading of 0.72 mg lipid/mL produced a mixture with similar behavior. Maximum uptakes were between 95% and 96%. The largest deviation from the predicted values was again in the low concentration area of the plot, with the measured uptake falling almost 4% below the prediction.

These results show that 50:50 DMPC:DOPG liposomes sequester significantly more AMI than 2% fibrinogen alone. 2% fibrinogen only bound 75% of the AMI in solution at a final AMI concentration of nearly 0.10 μM. The mixture of both liposomes and fibrinogen bound 95-96% in the same concentration region. However, the results also point to interactions between liposomes and fibrinogen that hinder the ability of liposomes to sequester free AMI from solution, similar to the effect observed with albumin and pure DOPG liposomes. The albumin also affected the 50:50 DMPC:DOPG system, but to a lesser extent. It is important to note that fibrinogen has an inhibitory effect on drug uptake by liposomes at 2% (w/w), which is half the concentration of albumin (4% (w/w)). Therefore, it seems that fibrinogen has a higher inhibitory effect, presumably due to a larger binding to the liposomes. With the approximate protein concentration of 7% (w/w) in plasma, it is apparent that liposome-protein interactions will play an important role in overdose treatment, and that fibrinogen is one of the key proteins to consider when studying those interactions.

2.3.3.3 Globulins and liposomes

Figure 2-7 shows the predicted trend line and the measured values for AMI uptake behavior for a mixture of 1% globulins (w/w) and 50:50 DMPC:DOPG liposomes at a

lipid loading of 0.72 mg lipid/mL. The uptake values for the system were around 95-96%, as compared to 30-40% in the same drug concentration range for pure 1% globulins. Thus, the liposome-protein mixture sequestered a substantially larger amount of AMI from solutions than globulins alone. An inhibition was once again observed at low concentrations as the uptake seemed to level off at 95-96%, rather than approaching 99%. Based solely on these preliminary results, it seems that all three proteins reduce the uptake of AMI by liposomes at low AMI concentrations, with fibrinogen and globulins having more drastic effects than albumin. To check for additional effects arising from interactions between the proteins themselves, experiments were conducted where mixtures of all three proteins were used. These results are presented below.

2.3.3.4 Albumin, fibrinogen, globulins, and liposomes

AMI uptake was first measured for the 7% (4% albumin (w/w), 2% fibrinogen (w/w), 1% globulins (w/w)) protein mixture without the addition of liposomes. The data from measurements of protein binding for each individual protein were used to predict the uptake for the mixture by using Equation 2-11. Next, mixtures containing 4% albumin (w/w), 2% fibrinogen, 1% globulins (w/w), and 50:50 DMPC:DOPG liposomes with a lipid loading of 0.72 mg lipid/mL were tested. The predicted trend line of AMI binding in the presence of 7% proteins plus liposomes, measurements from 7% proteins, and measurements from 7% proteins plus liposomes are plotted in Figure 2-8.

Several noteworthy observations can be made from the experimental results. As previously observed, the protein-liposome mixture did not sequester as much AMI as the simple mass balance equation predicted. Rather than approaching 98-99% uptake at low concentrations, the system only bound around 96% of the drug. This result again

suggests that under the experimental conditions, proteins are interacting with liposomes, and are perhaps adsorbing on the surface. However the presence of liposomes results in a significant reduction in the free drug concentration. For instance, at an initial AMI concentration of nearly 1.70 μM, the proteins bound around 90% of the AMI, bringing the final concentration to roughly 0.17 μM. With an almost identical initial drug concentration, the protein-liposome mixture bound around 96% of the drug, resulting in a final AMI concentration of around 0.07 μM. Therefore, we have succeeded in reducing the free AMI concentration by nearly 60% in the presence of 7% proteins with 50:50 DMPC:DOPG liposomes at a lipid loading of 0.72 mg lipid/mL.

The initial AMI concentration of 1.70 μM was tested based on the reported relevant values for overdose treatment of 1-3 μM [9]. Other groups, including Dhanikula et al. [25], have tested in vitro AMI uptake at even lower concentrations. Uptake increases with decreasing concentration, and the reported therapeutic dose range for AMI is 0.3 to 0.8 μM [9]. Thus, any uptake values found in or below this concentration range may not be as relevant to overdose treatment. While the 7% protein mixture does not contain all the components found in human plasma, the experimental uptake values found in this study still highlight the potential for DMPC:DOPG liposome systems to be used for AMI overdose treatment.

2.3.3.5 Effects of liposome-protein binding

All of the results presented thus far suggest that proteins interact with liposomes and perhaps adsorb on the surface. This hypothesis is supported by extensive literature in this field. Chonn, Semple, and Cullis [86,87] have done numerous studies and concluded that significant amounts of proteins bind to liposomes. The amount of protein bound depends largely on the composition and charge of the liposomes. They

have also found that in vivo half-lives of liposomes tend to be longer for those that bind less protein. One of their studies involved the use of 35:45:20 phosphatidylcholine (PC):cholesterol (CH):phosphatidylglycerol (PG) liposomes [86]. While these liposomes were slightly different than the ones used in our experiments, they did contain both the PC and PG components. Protein binding data taken from that study suggested that roughly 6×10^{-7} moles of protein were bound to liposomes per gram of lipid. Assuming an AMI uptake of 98% at 1 μM, 1.40×10^{-6} moles of AMI would be bound to liposomes per gram of lipid. These rough estimates show that at small drug concentrations, the number of drug molecules that bind to the liposome surface is comparable to the number of bound protein molecules, and so it is expected that the fractional drug uptake will decrease. However at higher drug concentrations, the bound drug molecules are significantly more numerous than the bound protein molecules leading to a small change in fractional uptake.

In spite of the detrimental effect of protein binding, the liposomes were able to reduce the free AMI concentration by 50-60%. While encouraging, this in vitro result failed to account for possible in vivo effects. One of the most important effects to consider is the response by the body's immune system and its effect on the lifetime of liposomes in the circulatory system. While we cannot make any assumptions about the potential half-life of our liposomes without in vivo experiments or pharmacokinetic modeling, we can review the reported values from Chonn, Semple, and Cullis. In their studies, they report 50% of the 35:45:20 PC:CH:PG liposomes to be recovered from mice after 30 minutes, and around 30% to be recovered after 120 minutes [86]. For some applications, including drug delivery, these circulation times may be completely

unacceptable. However, these may be adequate for drug detoxification as AMI uptake has been shown to be rapid. A quick removal of the liposomes by the immune system from the blood stream to the liver may even be desirable in the case of overdose treatment. But, if increasing residence time in the circulatory system is necessary, it can be done by increasing the lipid loading [87]. As the lipid loading used in our study was very low compared to other studies, we could increase our lipid loading, and this may have the dual benefits of increases in drug uptake and circulatory half lives. Cholesterol addition is another possibility, as it adds stability to liposomes and increases in vivo circulation times in some cases [87].

2.3.4 Uptake of Amitriptyline with Liposomes in Human Serum

The results presented above show that the three main proteins present in blood bind to liposomes, leading to a reduction in drug uptake efficiencies. In reality, human blood also contains other proteins which are present in trace amounts and are difficult to isolate. Thus, to better gauge the effectiveness of liposomes at sequestering drug under in vivo conditions, drug uptake experiments were conducted in human serum. AMI uptake in human serum is plotted as a function of final AMI concentration in Figure 2-9. In serum, AMI was roughly 90-92% bound without liposomes, which is comparable to the experimental results found in 7% proteins. When liposomes were added, the uptake rose to 94-98%. Thus, AMI uptake values with liposomes fell from 99% in PBS to 96 in 7% proteins, and increased to 98% in human serum. As opposed to the 50-60% free drug concentration reduction seen in the presence of 7% proteins, the 50:50 DMPC:DOPG liposomes produced a 35-70% reduction in serum. Clearly, the protein-liposome interactions have increased the variability in drug uptake by liposomes, while the overall effectiveness of the liposomes in serum with respect to AMI detoxification

appears to be comparable to 7% protein mixtures. A reduction of free drug concentration by about 35-70% could have a significant beneficial effect in cases of drug overdose [88]. Furthermore, it may be possible to give the overdose patient multiple doses of liposomes, which could lead to a larger reduction. It may also be possible to increase the lipid loading, which could lead to higher drug uptake values and longer circulation times in the bloodstream.

2.3.5 System Characterization

The results presented in the previous section inherently assume that the binding of AMI to proteins and liposomes is reversible, and that the measured values correspond to thermodynamic equilibrium. To test these hypotheses, the experiments described below were conducted.

2.3.5.1 Reversibility of binding

Albumin and 50:50 DMPC:DOPG liposomes with a final lipid concentration of 0.72 mg lipid/mL were used to test for binding reversibility. As described in Section 2.2.8, two samples with the same final composition were prepared by following two different paths, and the drug uptake was measured for each case. If the AMI was bound to the albumin or liposomes irreversibly, the uptake for the two samples would not match, as they were allowed to reach an initial equilibrium at different concentrations. The results of the experiment are shown in Figure 2-10.

At a final AMI concentration of 0.50 μM, the uptake values for both the diluted sample and standard sample were around 96.4%. At a final concentration closer to 0.12 μM, the uptake values for the two samples differed by less than 1%, which is within the range of experimental error. It is noted that the experimental error is likely to be larger at smaller concentrations because a small amount of mass loss from the systems

could cause appreciable errors in the fractional uptake. Based on this data, the binding of AMI appears to be reversible.

2.3.5.2 Time dependency of amitriptyline uptake

To determine whether the measurements reported above correspond to equilibrium, it was decided to conduct uptake measurements at various times. A system with 2% fibrinogen (w/w) and 50:50 DMPC:DOPG liposomes with a lipid loading of 0.72 mg lipid/mL was used for these experiments. AMI uptake was measured 24 and 48 hours after mixing all the components, and these results, along with those measured immediately after mixing, are plotted in Figure 2-11. The uptake values of AMI after 24 and 48 hours were very similar to the sample filtered shortly after mixing. This result suggests that the binding is quick and that the measured values correspond to equilibrium binding.

2.3.6 Nortriptyline Uptake

Based on the fact that nortriptyline is the well-known primary metabolite of AMI, it can be anticipated that nortriptyline may be important in AMI overdose cases [89]. This is supported by the results of a case study by Franssen et al. [89], which showed an initial concentration of nortriptyline of around 700 µg/L for a patient who had overdosed on AMI. Nortriptyline could be of concern for AMI overdose patients, as many people who overdose on AMI have been using the drug for depression related illnesses prior to overdosing. Thus, nortriptyline will undoubtedly be present in their system at the time of overdose if they have recently taken AMI regularly. The study conducted by Franssen et al. also demonstrated that nortriptyline can cause many of the same serious health problems associated with AMI. For this reason, nortriptyline uptake was investigated

with 50:50 DMPC:DOPG liposomes at lipid loading levels of 0.36 and 0.72 mg lipid/mL and DOPG at lipid loading levels of 0.36 and 0.72 mg lipid/mL.

2.3.6.1 Nortriptyline uptake with 50:50 DMPC:DOPG liposomes

Figure 2-12 shows nortriptyline and AMI uptake by 50:50 DMPC:DOPG liposomes versus final drug concentration. At final nortriptyline concentrations of nearly 0.025 μM, the maximum uptake was slightly higher than 96% at a lipid loading of 0.36 mg lipid/mL. For a lipid loading of 0.72 mg lipid/mL, the nortriptyline uptake reached values slightly greater than 99%. The AMI data plotted in the same figure shows that the liposomes sequester nortriptyline more efficiently compared to AMI. These results show that any system designed for the treatment of AMI overdose will likely result in reduction of free drug concentration of nortriptyline as well. This was expected, as both compounds are predominantly charged at pH 7.4 and have similar structures.

2.3.6.2 Nortriptyline uptake with DOPG liposomes

Nortriptyline uptake with pure DOPG liposomes is plotted as a function of final concentration in Figure 2-13. Both lipid loadings for both compounds showed uptakes greater than 99%. As is the case for AMI, the pure DOPG liposomes sequester more nortriptyline than the 50:50 DMPC:DOPG liposomes. Again, this was expected because the binding of nortriptyline to liposomes is also driven by electrostatic interactions.

2.3.6.3 Nortriptyline uptake with albumin

To determine the effect of protein-liposome interaction on nortriptyline binding, the uptake of nortriptyline with 50:50 DMPC:DOPG liposomes at a lipid concentration of 0.72 mg lipid/mL was tested in the presence of 4% albumin. In the presence of liposomes and albumin, around 98% of the nortriptyline was bound. Without liposomes,

the albumin bound only 85% to 86% of the drug. Both of these results were comparable to the binding seen by AMI in the presence of albumin and mixtures of albumin and liposomes. Overall, the results provide additional evidence for the possible dual effectiveness of liposomes at sequestering both AMI and nortriptyline.

2.4 Conclusions

Liposomes composed of DOPG and 50:50 DMPC:DOPG were tested for their ability to sequester AMI in PBS, in the presence of albumin, fibrinogen, and globulins, as well as in the presence of human serum. Experiments were conducted using filtration procedures where free AMI was allowed to pass through filters, while liposomes and proteins were largely removed. In PBS at a pH of 7.4, both the DOPG liposomes and the 50:50 DMPC:DOPG liposomes sequestered at least 99% of the AMI at low concentrations. In the presence of albumin, pure DOPG liposomes were shown to be greatly inhibited by the proteins. In the presence of 7% proteins (w/w) composed of 4% albumin, 2% fibrinogen, and 1% globulins, the 50:50 DMPC:DOPG liposomes at a lipid loading of 0.72 mg lipid/mL sequestered 95-96% of the free drug, as opposed to a predicted 99%. The free AMI concentration was still reduced by 50-60%, however. In human serum, the 50:50 DMPC:DOPG liposomes took up about 94-98% of the drug and reduced the free drug concentration by 35-70%. These results suggest that liposome-protein interactions reduce the effectiveness of 50:50 DMPC:DOPG liposomes to sequester AMI. This is probably due to protein adsorption to the surface of liposomes, reducing the number of available charged sites for drug binding.

Other aspects of liposome dispersions for drug detoxification were examined as well. Filtration techniques were again used to determine that AMI binding to liposomes in the presence of proteins is quick and reversible. Finally, uptake studies conducted

with nortriptyline, the major metabolite of AMI, suggests that systems developed for AMI overdose treatment may also be useful for reducing the free concentration of nortriptyline.

While the presence of serum proteins reduces the drug binding capacity of liposomes, a 35-70% reduction in drug concentration, which is attainable by the systems explored in this chapter, may have significant benefits for overdosed patients [88]. Additionally, even the highest lipid loading used in this chapter is below the lipid loadings used in other related studies, and so it may be feasible to increase the lipid loading or give multiple liposome injections to the overdosed patients. Still, the study demonstrates the ability of liposomes to remove free AMI from solutions in the presence of proteins and human serum, and supports the idea of using a single detoxification treatment for both AMI and nortriptyline.

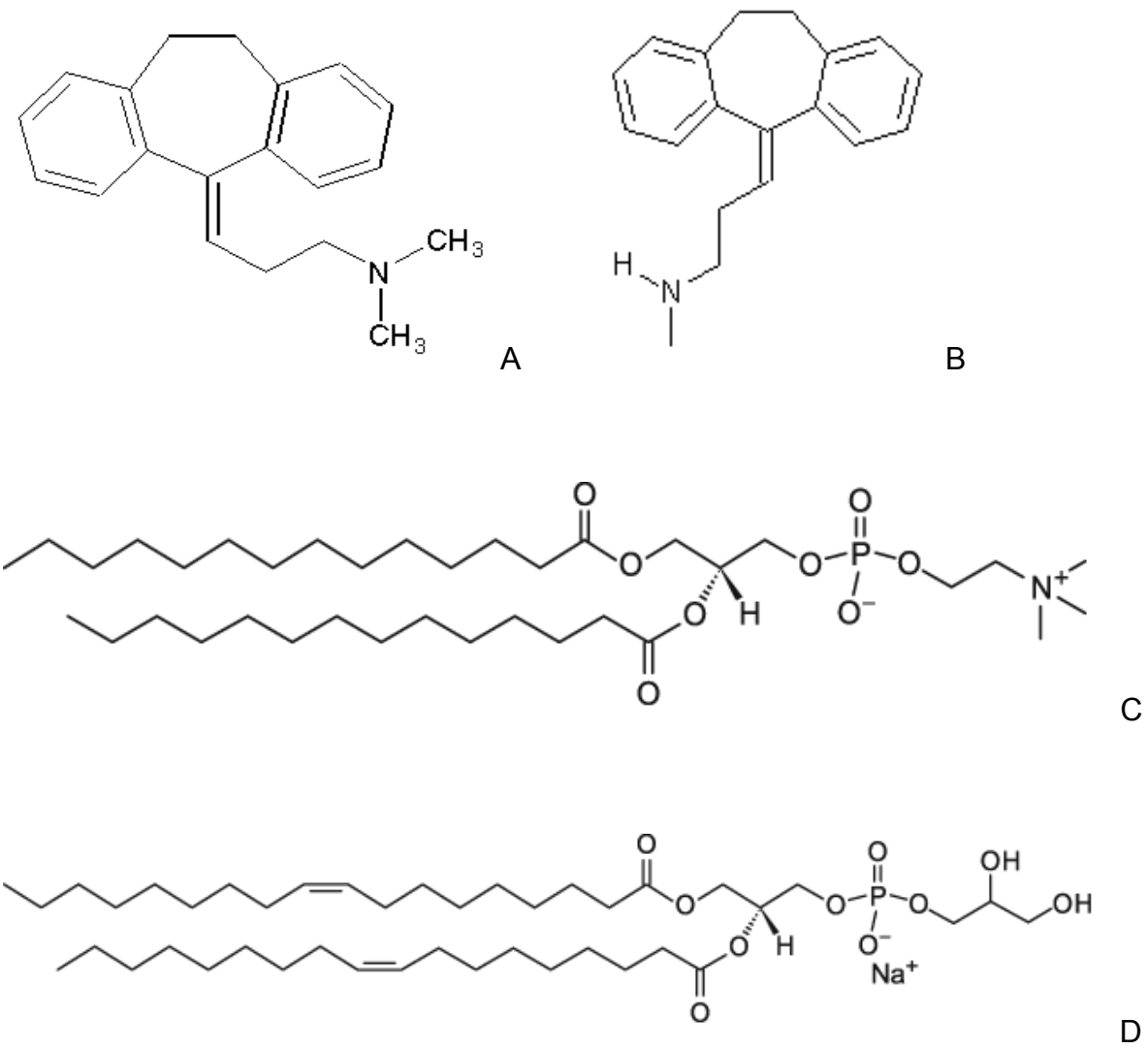

A B C D

Figure 2-1. Structures of drugs and lipids used for drug uptake studies with liposomes: (a) amitriptyline; (b) nortriptyline; (c) 1,2-dimyristoyl-sn-glycero-3-phosphocholine (DMPC) lipid; (d) 1,2-dioleoyl-sn-glycero-3-[phospho-rac-(1-glycerol)] (DOPG) lipid.

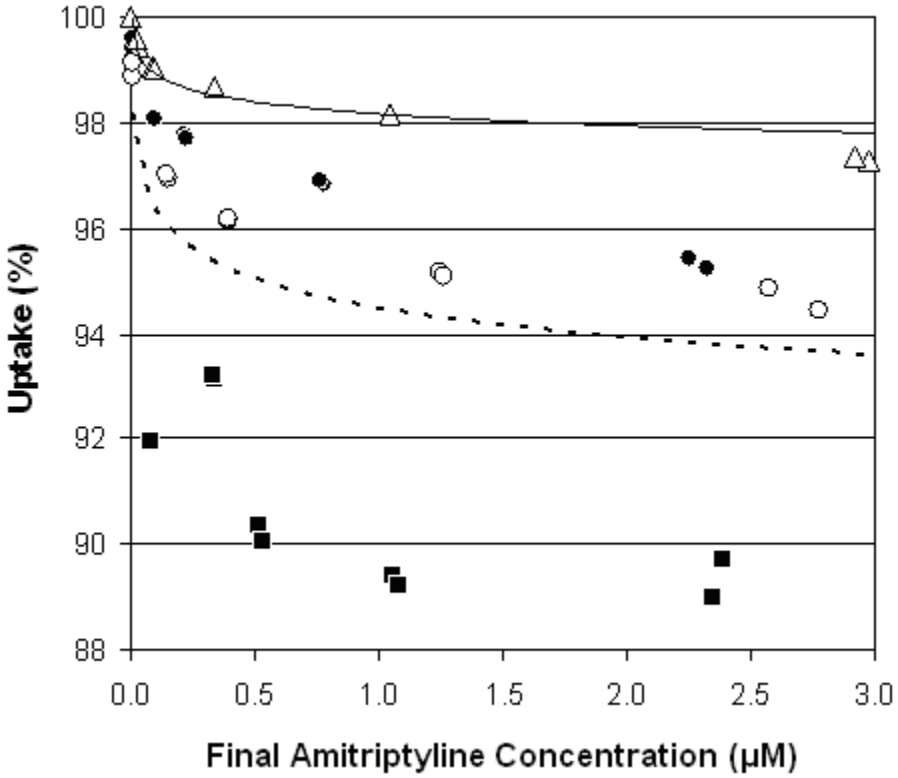

Figure 2-2. Measured and predicted (Equation 2-3) percent amitriptyline uptake for pure DOPG liposomes and 50:50 DMPC:DOPG liposomes in pH 7.4 buffer at final lipid concentrations of 0.36 and 0.72 mg lipid/mL versus final amitriptyline concentration. Key: DOPG at 0.72 mg/mL (Δ); DOPG at 0.36 mg/mL (●); DOPG at 0.72 mg/mL prediction (solid line); 50:50 DMPC:DOPG at 0.72 mg/mL (○); 50:50 DMPC:DOPG at 0.36 mg/mL (■); 50:50 DMPC:DOPG at 0.72 mg/mL prediction (- - -).

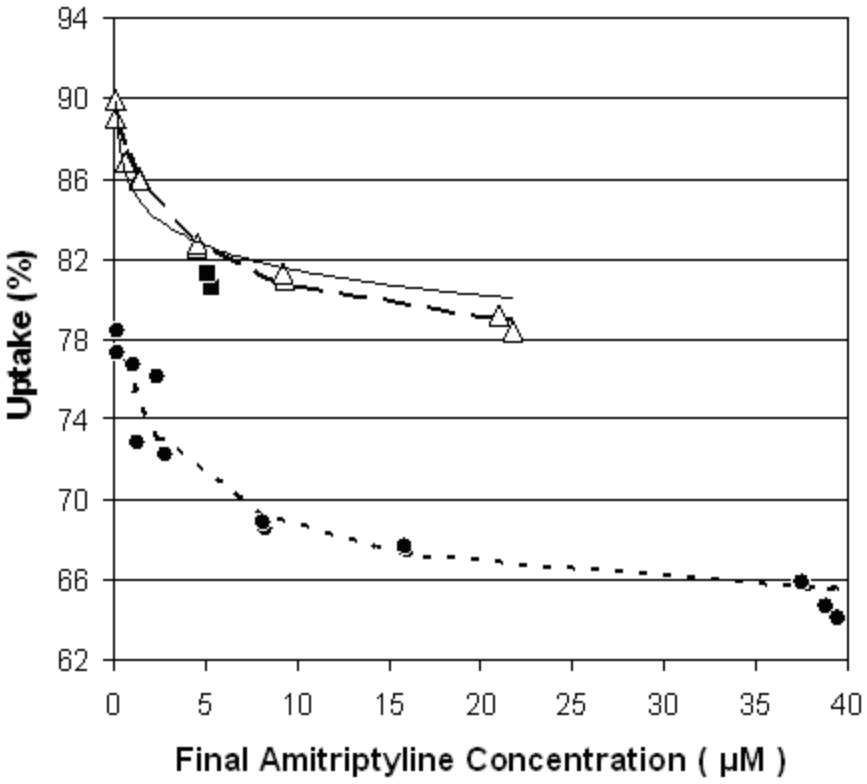

Figure 2-3. Measured and modeled (Equation 2-10) percent amitriptyline uptake for 2% albumin (w/w) in pH 7.4 buffer versus final amitriptyline concentration. Measured, modeled (Equation 2-11), and predicted (Equation 2-3) percent amitriptyline uptake for 4% albumin (w/w) in pH 7.4 buffer versus final amitriptyline concentration. Key: 4% albumin (Δ); 4% albumin extended mixing time (■); 4% albumin prediction (solid line); 4% albumin model (— —); 2% albumin (●); 2% albumin model (- - -).

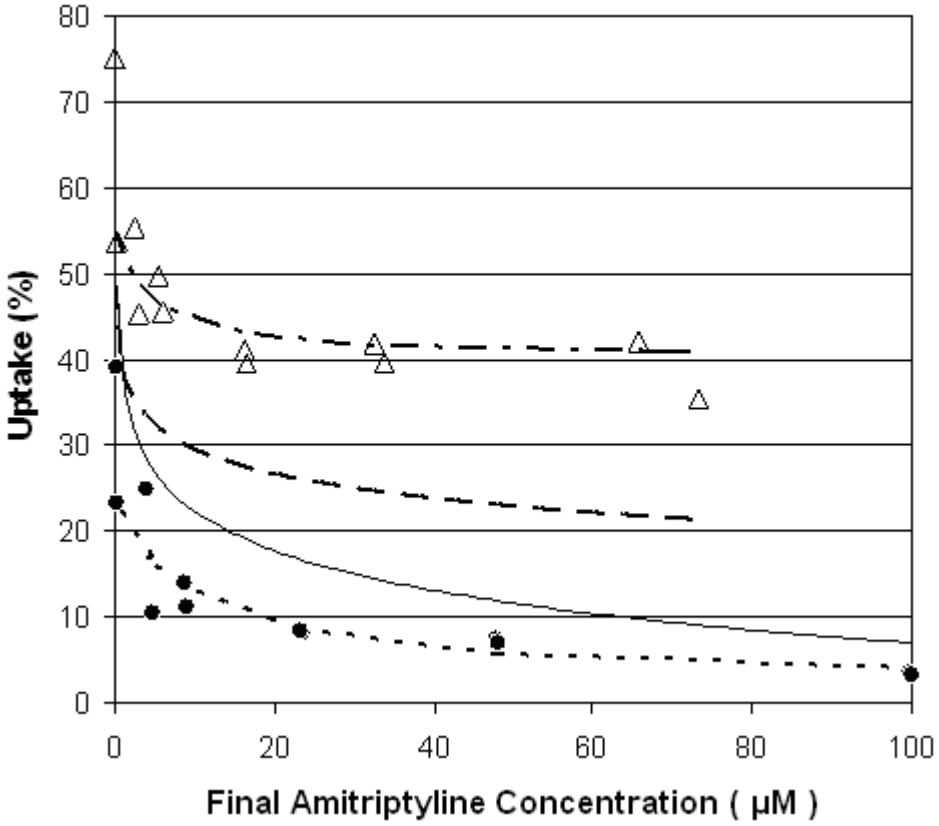

Figure 2-4. Measured and modeled (Equation 2-10) percent amitriptyline uptake for 2% fibrinogen and 1% globulins (w/w) in pH 7.4 buffer versus final amitriptyline concentration; predicted (Equation 2-3) percent amitriptyline uptake for 1% fibrinogen and 2% globulins (w/w) in pH 7.4 buffer versus final amitriptyline concentration. Key: 2% fibrinogen (Δ); 2% fibrinogen modeled (— - —); 1% fibrinogen prediction (— —); 1% globulins (●); 1% globulins modeled (- - -); 2% globulins prediction (solid line).

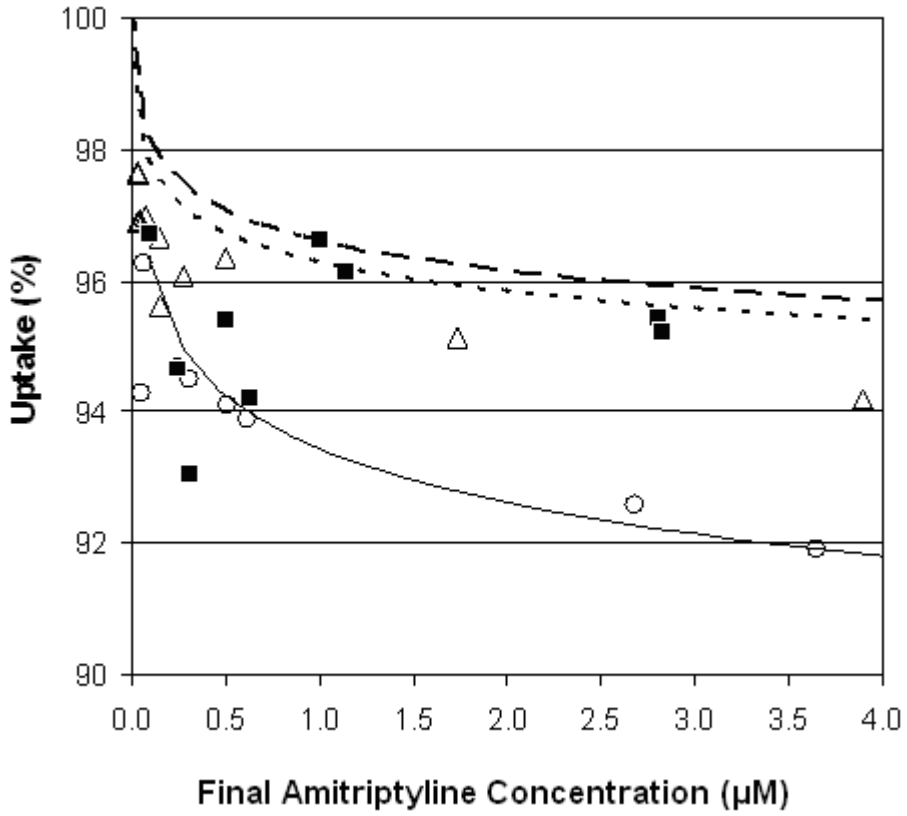

Figure 2-5. Measured and predicted (Equation 2-11) percent amitriptyline uptake for mixtures of 4% albumin (w/w) and 50:50 DMPC:DOPG liposomes with lipid concentrations of 0.72 and 0.36 mg lipid/mL and mixtures of 4% albumin and DOPG liposomes with lipid concentrations of 0.36 mg lipid/mL in pH 7.4 buffer versus final amitriptyline concentration. Key: 4% albumin + 50:50 DMPC:DOPG at 0.36 mg lipid/mL (○); 4% albumin + 50:50 DMPC:DOPG at 0.36 mg lipid/mL prediction (solid line); 4% albumin + 50:50 DMPC:DOPG at 0.72 mg lipid/mL (Δ); 4% albumin + 50:50 DMPC:DOPG at 0.72 mg lipid/mL prediction (- - -); 4% albumin + DOPG at 0.36 mg lipid/mL (■); 4% albumin + DOPG at 0.36 mg lipid/mL prediction (— —).

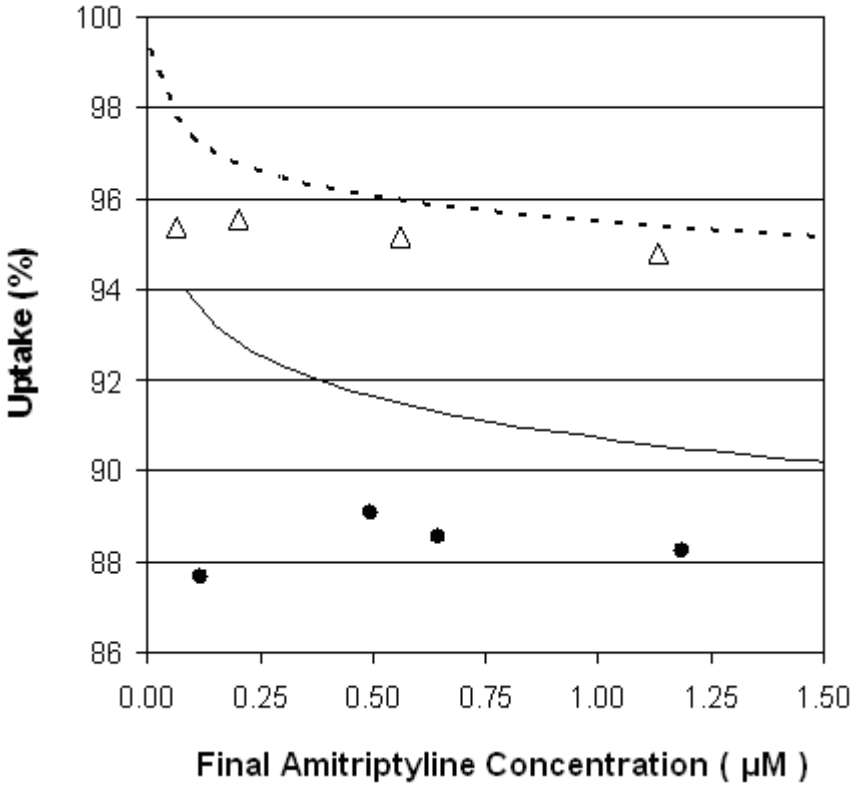

Figure 2-6. Measured and predicted (Equation 2-11) percent amitriptyline uptake for mixtures of 2% fibrinogen (w/w) and 50:50 DMPC:DOPG liposomes with lipid concentrations of 0.36 and 0.72 mg lipid/mL in pH 7.4 buffer versus final amitriptyline concentration. Key: 2% fibrinogen + 50:50 DMPC:DOPG at 0.36 mg lipid/mL (●); 2% fibrinogen + 50:50 DMPC:DOPG at 0.36 mg lipid/mL prediction (solid line); 2% fibrinogen + 50:50 DMPC:DOPG at 0.72 mg lipid/mL (Δ); 2% fibrinogen + 50:50 DMPC:DOPG at 0.72 mg lipid/mL prediction (- - -).

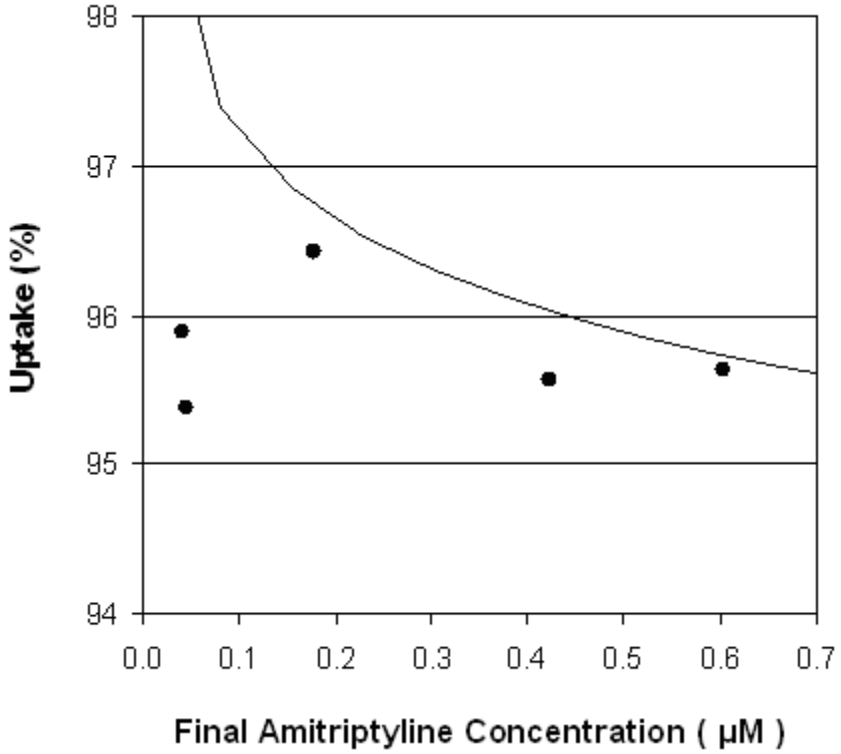

Figure 2-7. Measured and predicted (Equation 2-11) percent amitriptyline uptake for mixtures of 1% globulins (w/w) and 50:50 DMPC:DOPG liposomes with lipid concentrations of 0.72 mg lipid/mL in pH 7.4 buffer versus final amitriptyline concentration. Key: 1% globulins + 50:50 DMPC:DOPG at 0.72 mg lipid/mL (●); 1% globulins + 50:50 DMPC:DOPG at 0.72 mg lipid/mL prediction (solid line).

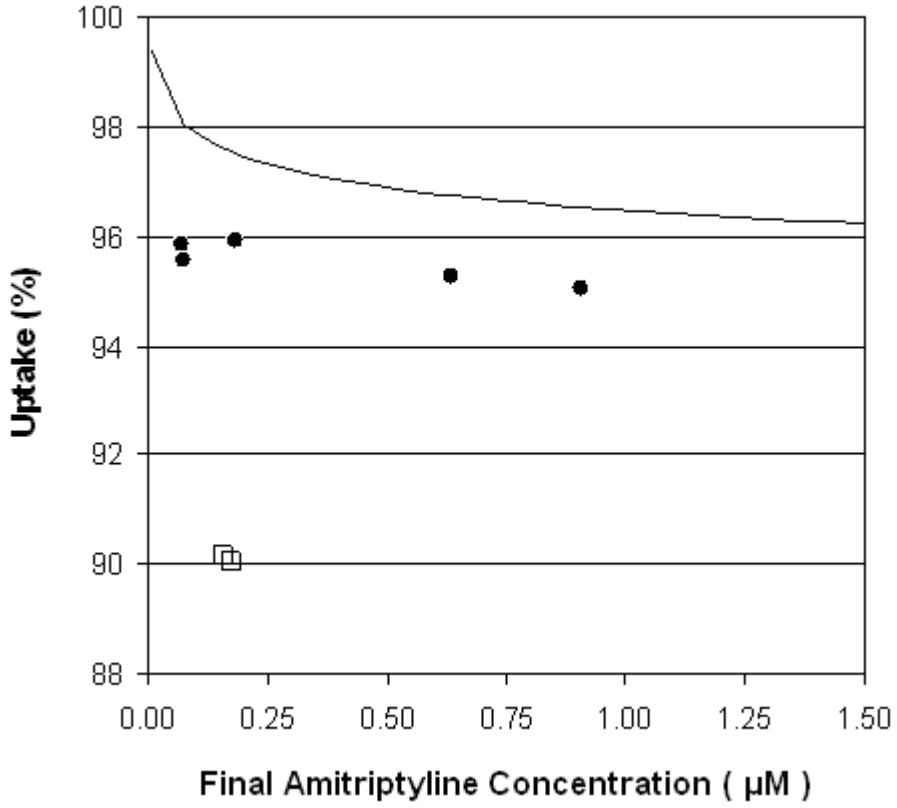

Figure 2-8. Measured and predicted (Equation 2-11) uptake of amitriptyline with 7% proteins (4% albumin, 2% fibrinogen, 1% globulins) and 50:50 DMPC:DOPG liposomes (0.72 mg lipid/mL) versus final amitriptyline concentration; measured uptake of amitriptyline with 7% proteins versus final amitriptyline concentration. Key: 7% proteins + 50:50 DMPC:DOPG at 0.72 mg lipid/mL (●); 7% proteins + 50:50 DMPC:DOPG at 0.72 mg lipid/mL prediction (solid line); 7% proteins (□).

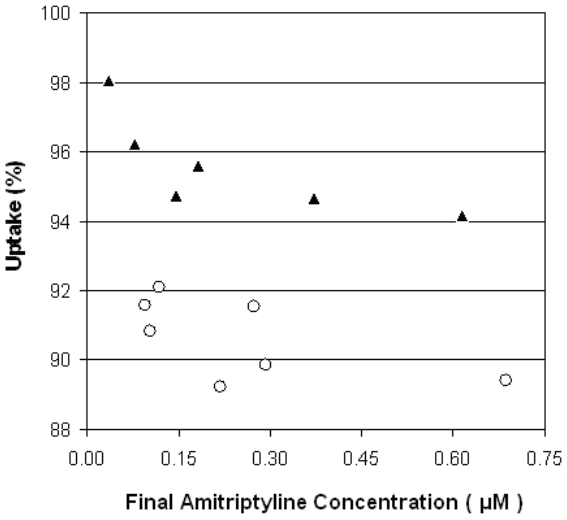

Figure 2-9. Measured uptake of amitriptyline in human serum with and without 50:50 DMPC:DOPG liposomes (0.72 mg lipid/mL) versus final amitriptyline concentration (the data corresponding to 98% uptake is two overlapping points). Key: human serum + 50:50 DMPC:DOPG at 0.72 mg lipid/mL (▲); human serum (○).

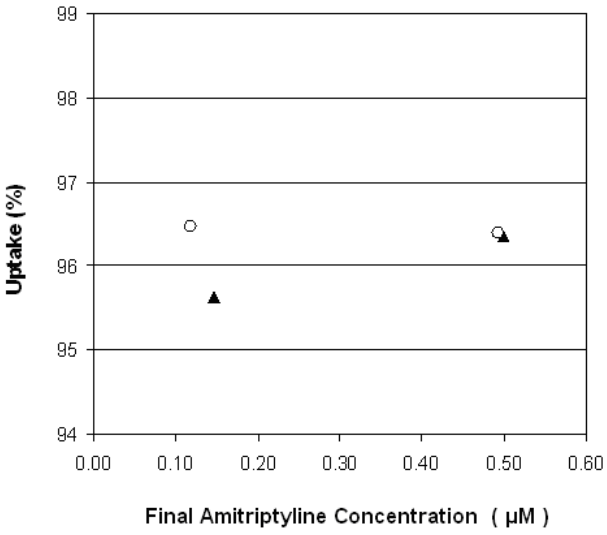

Figure 2-10. Percent amitriptyline uptake for mixtures of 4% albumin (w/w) and 50:50 DMPC:DOPG liposomes in pH 7.4 buffer versus final amitriptyline concentration where standard and dilution test methods were used to test for reversible binding. Key: standard test method (▲); dilution test method (○).

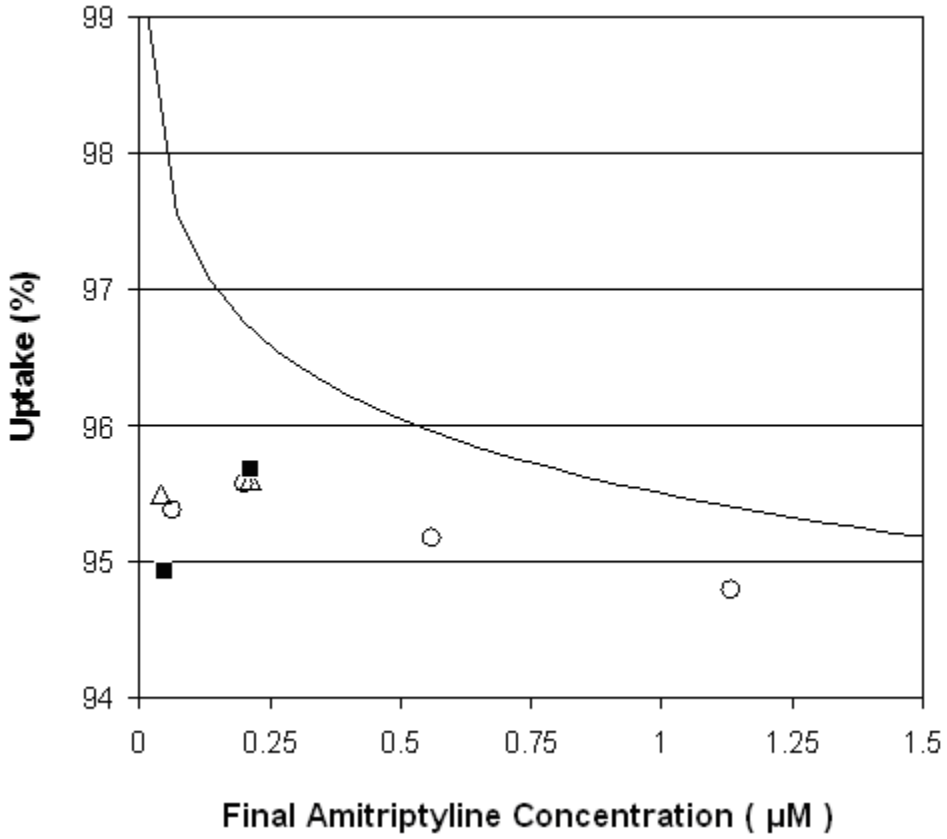

Figure 2-11. Measured and predicted (Equation 2-11) percent amitriptyline uptake for mixtures of 2% fibrinogen (w/w) and 50:50 DMPC:DOPG liposomes with lipid concentrations of 0.72 mg lipid/mL in pH 7.4 buffer versus final amitriptyline concentration filtered shortly after mixing, 24 hours later, and 48 hours later. Key: shortly after mixing (○); prediction (solid line); 24 hours later (Δ); 48 hours later (■).

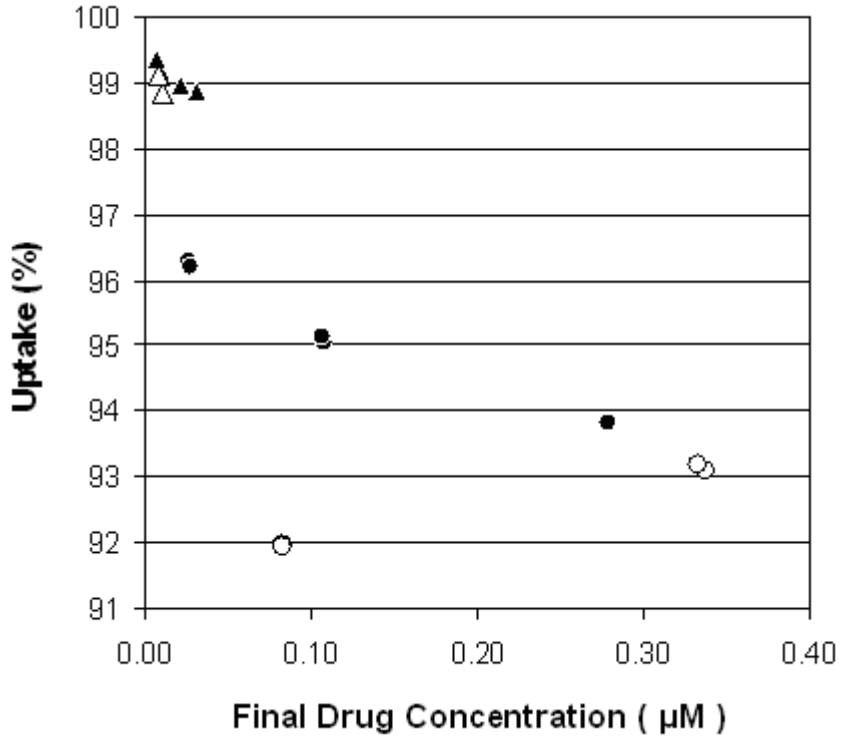

Figure 2-12. Percent amitriptyline and nortriptyline uptake for 50:50 DMPC:DOPG liposomes in pH 7.4 buffer at final lipid concentrations of 0.36 and 0.72 mg lipid/mL versus final drug concentration. Key: amitriptyline with 50:50 DMPC:DOPG at 0.36 mg/mL (○); nortriptyline with 50:50 DMPC:DOPG at 0.36 mg/mL (●); amitriptyline with 50:50 DMPC:DOPG at 0.72 mg/mL (Δ); nortriptyline with 50:50 DMPC:DOPG at 0.72 mg/mL (▲).

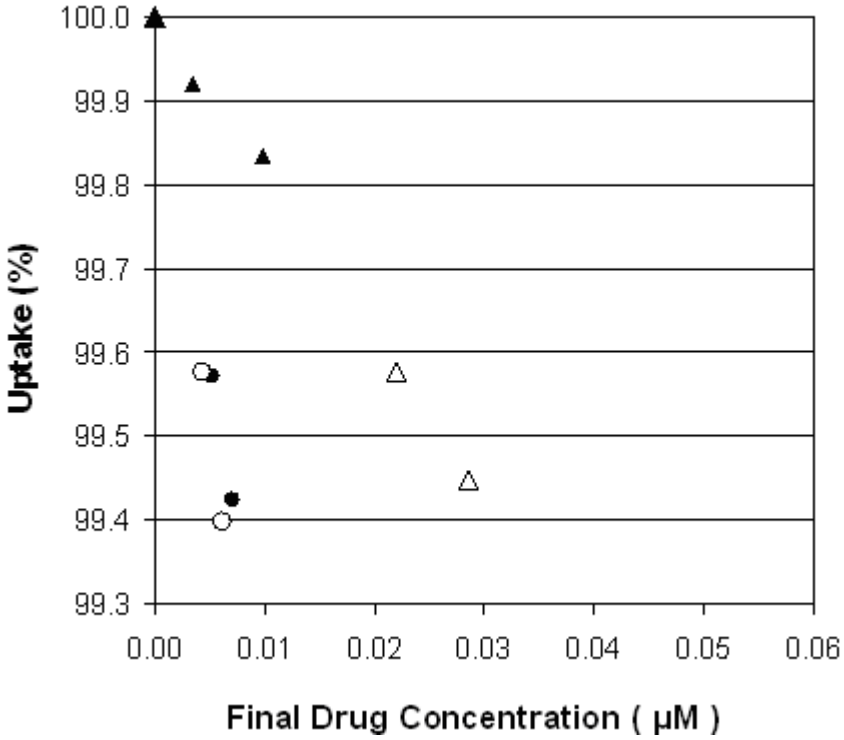

Figure 2-13. Percent amitriptyline and nortriptyline uptake for pure DOPG liposomes in pH 7.4 buffer at final lipid concentrations of 0.36 and 0.72 mg lipid/mL versus final drug concentration. Key: amitriptyline with DOPG at 0.36 mg/mL (○); nortriptyline with DOPG at 0.36 mg/mL (●); amitriptyline with DOPG at 0.72 mg/mL (Δ); nortriptyline with DOPG at 0.72 mg/mL (▲).

CHAPTER 3
AMITRIPTYLINE BINDING TO PEGYLATED, ANIONIC LIPOSOMES

3.1 Introduction

In Chapter 2, we showed that although negatively charged liposomes are good candidates for amitriptyline (AMI) overdose treatment, their effect is reduced due to interactions between liposomes and proteins present in human blood. The current chapter intends to prove that the inclusion of polyethylene glycol (PEG) chains on the liposomes could significantly improve the drug sequestration by liposomes. In addition to improving drug uptake characteristics, inclusion of polyethylene glycol (PEG) into the liposomes will presumably lead to longer in vivo circulation times of the vesicles, which is desirable. Additionally, we report the effect of increased lipid loading on drug uptake, as the loading of 0.72 mg lipid/mL explored in Chapter 2 was considerably lower than reported values in other studies [25]. Furthermore, we report the effects of liposome size on the drug binding characteristics, which to our knowledge has not been considered before. During storage, pharmaceutical products such as liposomes can undergo changes resulting in a lack of potency or undesired side effects. As a preliminary screening for packing effects, liposomes were also stored and checked periodically for their drug uptake properties.

3.2 Materials and Methods

3.2.1 Materials

Human serum from male plasma, methanol, chloroform, Dulbecco's phosphate buffered saline (PBS) without calcium chloride and magnesium chloride, cholesterol (CH), and amitriptyline hydrochloride were purchased from Sigma-Aldrich. 0.45 μm nylon syringe filters and Centriprep YM10 centrifugation filters (10,000 molecular weight

cut-off) were purchased from Fisher Scientific. The lipids 1,2-dimyristoyl-*sn*-glycero-3-phosphocholine (DMPC), in powder form, 1,2-dioleoyl-*sn*-glycero-3-[phospho-rac-(1-glycerol)] (sodium salt) (DOPG), dissolved in chloroform, and 1,2-dipalmitoyl*sn*-glycero-3-phosphoethanolamine-*N*-[methoxy(polyethylene glycol)-2000] (ammonium salt) (DPPE-mPEG-2000), in powder form, were purchased from Avanti Polar Lipids, Inc. A Mini-Extruder kit for liposome preparation was also purchased from Avanti Polar Lipids, Inc.

3.2.2 Liposome Preparation via Sonication

Liposomes composed of a molar ratio of 50:50 DMPC:DOPG, 55:15:30 DMPC:DPPE-mPEG-2000:CH, 95:5 DOPG:DPPE-mPEG-2000, 85:15 DOPG:DPPE-mPEG-2000, and pure DOPG lipids were prepared using an ultrasonication procedure. Lipids were combined in their respective molar ratios and then dissolved in a 9:1 mixture (by volume) of chloroform:methanol such that a 20 mg/mL concentration of lipids was obtained. The organic solvent was then evaporated under a stream of nitrogen. After an even and uniformly dried lipid film was obtained, the dried lipid layer was hydrated with PBS, such that the lipid concentration was 80 mg/mL, and the mixture was sonicated in a bath sonicator (G112SP1 Special Ultrasonic Cleaner, Avanti Polar Lipids, Inc.) at room temperature for 20 minutes to form lipid vesicles. More PBS was then added, such that the lipid concentration became 8 mg/mL, and the lipid suspension was sonicated using a probe sonicator (Fisher Scientific Sonic Dismembrator Model 100) for 40 minutes at room temperature to reduce the vesicle size. The suspension was surrounded by a cool water bath during the sonication to avoid excessive heat buildup. The liposome dispersion was filtered using a 0.45 μm

filter. In some experiments, the lipid loading was doubled at the dissolution step, and this resulted in a loading of 16 mg lipid/mL in the final liposome suspension.

3.2.3 Liposome Preparation via Extrusion

It has been reported that liposome diameters of around 100-200 nm are best for extending in vivo circulation time [26,90]. Accordingly, it was decided to explore the effect of liposome size on drug binding by preparing liposomes of controlled size by using the extrusion process. Specifically, liposomes composed of a molar ratio of 50:50 DMPC:DOPG, 95:5 DOPG:DPPE-mPEG-2000, and pure DOPG lipids were prepared via extrusion. An even and uniformly dried lipid film was obtained with the appropriate lipid composition by following the same procedures as described above. Next, the dried lipid layer was hydrated with PBS, such that the lipid concentration was 8 mg/mL. The lipid suspension was then heated to 30°C and stirred for 45 minutes. After stirring, the lipid dispersion was extruded through a 100 nm membrane 13 times. The same procedures were used to prepare larger liposomes by using a membrane with a pore size of 400 nm.

3.2.4 Liposome Characterization

The mean diameters and size distributions of the liposomes were analyzed using a Precision Detectors PDDLS/CoolBatch + 90T instrument. The data was analyzed with the Precision Deconvolve32 Program. The measurements were taken at 20°C with a scattering angle of 90° using a 683 nm laser source.

3.2.5 Measurement of Amitriptyline Uptake by Liposomes in Buffer and Human Serum

Liposomes were added to solutions of AMI in PBS or human serum from male plasma, such that the volume of the liposome dispersion was 9% of the total solution

volume, giving a final lipid concentration of 0.72 mg lipid/mL. In some cases the final lipid concentration in the drug-liposome mixture was doubled to 1.44 mg lipid/mL by either preparing liposomes with a higher lipid loading of 16 mg lipid/mL or by mixing a larger volume of liposomes with 8 mg/mL lipid loading. The initial AMI concentration varied from about 1 to 10 μM, and in some cases 1 to 20 μM, which is a physiologically relevant range for toxic plasma drug levels [9,91,92]. Control solutions of AMI in PBS and AMI in serum without liposomes were also made to allow for uptake quantification and comparison. After being stirred, the solutions were ultracentrifuged at 5000 rpm for 15 minutes in a vial that contained a YM10 filter (10,000 molecular weight cutoff). To minimize the effect of any leaching of components from the filter, the filters were rinsed first with DI water and then with PBS at 5000 rpm for 10 minutes prior to their use in these experiments. The concentration of AMI in the filtrate (free drug concentration) and the control solution was detected by measuring UV absorbance at 215 nm after passing the samples through a C18 column using an acetonitrile/50 mM $NH_4H_2PO_4$ solvent mixture in a 35/65 ratio. The calibration curve for concentration versus area under the curve was linear with $R^2 > 0.99$. To ensure that all unbound AMI was accounted for, solutions of AMI at various concentrations were passed through YM10 filters in a separate test. Small amounts of AMI were taken up by the filter, and a linear correction curve was made and used to correct for AMI adsorbed by the membranes in subsequent tests.

3.2.6 Storage Tests

The stability and effectiveness of any pharmaceutical product after storage is an important issue, especially for complex dosage forms such as liposome suspensions. Experiments were therefore carried out to study the effects of storage on liposomes in

the context of drug overdose treatment. The liposomes chosen for this portion of the study, based on results from experiments discussed in Section 3.2.5, were pure DOPG liposomes and 95:5 DOPG:DPPE-mPEG-2000 liposomes. Lipid dispersions were extruded through 100 nm membranes as described in Section 3.2.3, with a lipid loading of 8 mg/mL. The liposomes were stored in the refrigerator at temperatures of 2-8°C for 34 days. Periodically, liposome samples were withdrawn and tested to measure the drug binding characteristics at an AMI concentration of 2.7 μM. This method of storage was chosen based on similar reported storage methods for commercial drug loaded liposome based therapies such as CAELYX™ and DOXIL™.

3.2.7 Data Analysis

The data was analyzed using JMP software developed by SAS. Regression lines were fitted to the concentration dependent uptake data, and 95% confidence intervals (CI) are displayed to allow for both experimental error analysis and comparison between two or more data sets. The confidence intervals were calculated for mean uptake values using the Student *t* distribution. For the time dependent storage data, data points were replicated and error bars are shown.

3.3 Results and Discussion

3.3.1 Liposome Characterization

Sonication and extrusion methods were used in the present study to form liposomes. Sonication was one of the first methods commonly used to form lipid vesicles and has been used by a number of researchers for preparing small unilamellar vesicles (SUV) [27,93,94]. The mean diameters and size distributions of several of the liposomes explored here are shown in Figure 3-1. The 85:15 DOPG:DPPE-mPEG-2000 liposomes and pure DOPG liposomes, which were both sonicated, showed similar

size distributions with primary modes containing liposomes with mean diameters of 41.5 ± 5 and 39.2 ± 4.5 nm, respectively. In both cases, and particularly for the PEG-lipids, a small percentage of the liposomes had diameters in the range of about 400 nm. The 55:15:30 DMPC:DPPE-mPEG-2000:CH liposomes, which were also sonicated, were much larger with diameters of 77.7 ± 10.4 nm. This trend of increasing vesicle size upon inclusion of CH was also observed by Lapinski et al. with DOPC lipids [94]. Extrusion, a more recently developed method of forming lipid vesicles, has become a widely accepted technique due to the ability to control vesicle size [94,95]. The 95:5 DOPG:DPPE-mPEG-2000 liposomes extruded with 100 nm membranes had a mean diameter of 118 ± 15 nm. The 50:50 DMPC:DOPG liposomes made with 400 nm membranes had a vesicle size of 284 ± 36 nm.

3.3.2 Increased Lipid Loading for 50:50 DMPC:DOPG Liposomes

In Chapter 2, a concentration dependent free AMI reduction of 35-70% by 50:50 DMPC:DOPG liposomes was reported in human serum samples. While the magnitude of this reduction is clinically significant, the concentration dependence of the uptake is undesirable. The decrease in fractional uptake with increasing concentration likely arises due to saturation of the binding sites on liposomes, and so it may be speculated that an increased lipid loading would reduce this effect. Increasing the lipid loading in the drug-liposome mixtures can be accomplished either by increasing the volume of liposome dispersions added to drug solutions, or by increasing the lipid loading in the liposome formulation. Both of these approaches were utilized to increase the lipid loadings. Figure 3-2 shows AMI uptake values as a function of final drug concentration for the 50:50 DMPC:DOPG liposomes at 0.72 mg lipid/mL and data for loadings of 1.44 mg lipid/mL obtained by adding the liposome dispersion at either 9% by volume at 8

mg/mL lipid loading or at 18% by volume with 16 mg/mL lipid loading. The data shows minimal improvement in drug removal in both cases despite doubling of lipid loading. A simple mass balance can be used to facilitate quantitative comparisons between the expected increase due to double lipid loading and the observed behavior. For any mixture of colloids in equilibrium with free drug, the partition coefficients between the bound and the free concentration can be obtained from uptake data for each colloid separately, and the uptake for the mixture can then be obtained, assuming that no interactions are taking place within the system (discussed in Chapter 2). The uptake in the mixture is given by

$$\frac{\phi_{\mathrm{mix}}}{1-\phi_{\mathrm{mix}}} = \frac{\phi_1}{1-\phi_1} + \frac{\phi_2}{1-\phi_2} + \ldots + \frac{\phi_n}{1-\phi_n}, \tag{3-1}$$

where Φ_{mix} is the fraction of drug bound in the mixture and Φ_1, Φ_2, etc., are the fractions of drug bound in the components of the mixture measured separately. It must be ensured that all the uptakes in the above equation correspond to identical free drug concentration. This equation was solved to obtain the fraction of drug bound for 50:50 DMPC:DOPG liposomes at 0.72 mg lipid/mL in human serum samples, and the results are also shown in Figure 3-2. The disparity between the predicted behavior in a system lacking protein-liposome interactions and the experimental data is most likely due to saturation of binding sites on liposomes by proteins, which implies a need for shielding of those sites by inclusion of PEG into the liposomes.

3.3.3 Effect of Vesicle Size on Amitriptyline Sequestration

Any foreign particle introduced into the body will be naturally removed by the reticuloendothelial system (RES). For a most effective drug detoxification system, blood

stream circulation times should be maximized. A number of factors impact liposome circulation time, including liposome size, lipid type and composition, and modifications such as PEG incorporation. Literature indicates that liposomes with sizes ranging from roughly 100-200 nm may be best for in vivo applications [26,90]. In addition, commercial liposome formulations such as CAELYX and DOXIL report average vesicle sizes of 100 nm. In view of the importance of the liposome size on circulation times, we chose to investigate the uptake dependency on size using 50:50 DMPC:DOPG liposomes in PBS solutions of AMI. Drug uptake values for sonicated (40-45 nm) and extruded (100 and 284 nm) liposomes are shown in Figure 3-3. All three liposome sizes showed maximum uptake values of approximately 99%, and the drug uptake seems to be independent of liposome size. This result shows that the curvature of the lipid bilayers does not impact drug sequestration. In the results reported below, both 100 nm and 40-45 nm liposomes were used.

3.3.4 Liposomes Incorporated with Polyethylene Glycol (PEG)

A common method used to overcome the effect of protein-liposome interactions and liposome scavenging by the RES is incorporation of PEG into the lipid membrane. Such liposomes have been used for a variety of applications and are currently incorporated into commercial drug delivery formulations such as CAELYX and DOXIL. Dhanikula et al. have used PEG coated nanocapsules composed of triglycerides for detoxification purposes, although their proposed methods of drug-particle interaction were pH and concentration gradients rather than charge-charge interactions, as in our case [24].

Pegylation of liposomes can be achieved by mixing lipids that have covalently attached PEG chains into the lipid mixture. Here, lipids modified with PEG were

incorporated into neutral and predominantly anionic liposomes at various molar ratios to assess the affect of PEG on in vitro drug removal. Cholesterol (CH) was also included in the neutral liposome formulation for a screening of its potential effects on drug removal. To achieve incorporation of PEG, DPPE-mPEG-2000 was chosen due to its negative charge and PEG chain length. It was hypothesized that lipids containing PEG chains of 2000 units would minimize protein interactions with the liposomes without impacting drug binding. DPPE-mPEG-2000 was added at 5% by mole based on results from several studies indicating long circulating properties for similar formulations [24,87,96-98]. In addition, 15% by mole incorporation was also tested to explore the effect of larger proportions of polymer in the liposome bilayer.

A number of researchers have explored the configuration of the surface of pegylated liposomes. The approximate thickness of the surface coating for PEG chains of 2000 kD is 5 nm, which is much less than typical liposome diameters observed here [29]. The area of coverage for one PEG-2000 chain on the surface of a liposome was approximated to be 2.6 nm^2 by Rex et al. [99]. Additionally, they performed Monte-Carlo simulations which suggested that a large portion of the liposome surface was uncovered by PEG-2000 polymers at 2-10% addition of PEG modified lipid (molar basis). Yoshida et al. also conducted simulations to estimate surface coverage and concluded that approximately 45% of the surface would be covered at 5% addition of PEG-2000 [95]. As far as the conformation of the PEG chains is concerned, Moghimi and Szebeni suggest that at very low coverages (below 5%), the polymers exhibit a mushroom-like behavior with a lack of extension into the aqueous bulk phase [100]. At moderate to high coverages (5% or more), a brush-like configuration is assumed.

Gbadamosi et al. showed that liposomes with polymers in the brush-like configuration were much less susceptible to phagocytosis by macrophage type cells than liposomes with polymers in the less extended mushroom configuration [101]. Thus, the inhibition of phagocytosis by the addition of PEG is not simply a function of the surface coverage, but is more directly affected by the PEG configuration, which in turn is directly affected by surface coverage. The studies cited above clearly prove that 5-15% pegylation significantly reduces protein binding, but the effect of the pegylation on drug binding needs investigation, and this issue is discussed below.

In addition to DPPE-mPEG-2000, DOPG was used as the primary component in the 95:5 and 85:15 DOPG:DPPE-mPEG-2000 liposome suspensions in view of its affinity for AMI due to electrostatic interactions (see Chapter 2 and [71]). Also, drug uptakes were measured for pure DOPG liposomes to gauge the effect of polymer inclusion on drug binding. Additionally, predominantly neutral pegylated liposomes were prepared (55:15:30 DMPC:DPPE-mPEG-2000:CH) to demonstrate the effect of lack of charge on drug binding properties. All reported final lipid concentrations refer to phospholipid concentrations and do not include CH.

3.3.4.1 Amitriptyline removal from human serum by various liposome formulations

To compare the drug uptake performance of several liposome formulations in human serum, liposomes were made via sonication (see Section 3.2.2) with lipid concentrations of 0.72 mg lipid/mL. AMI uptake for pure human serum without liposomes, 95:5 and 85:15 DOPG:DPPE-mPEG-2000 liposomes, 50:50 DMPC:DOPG liposomes, and 55:15:30 DMPC:DPPE-mPEG-2000:CH liposomes is plotted as a function of final AMI concentration in Figure 3-4. Clearly, the liposomes including

DMPC and CH have a much lower binding capacity than the other three formulations. By comparing the binding capacity of a mixture of the 55:15:30 DMPC:DPPE-mPEG-2000:CH liposomes and serum proteins with serum proteins alone, it is clear that they fail to reduce the free drug concentration by any appreciable amount. The results also suggest that the 95:5 liposomes are slightly superior to the other two types. Figures 3-5 and 3-6 show the 50:50 DMPC:DOPG and the 85:15 DOPG:DPPE-mPEG-2000 liposome uptake values, respectively, compared to the 95:5 DOPG:DPPE-mPEG-2000 values, along with the 95% CI for each data set. Based on the CI, the 95:5 and 50:50 liposomes have significantly different uptake behaviors at most AMI concentrations, but behave similarly for final concentrations of less than 0.10 μM. The fractional uptake reduces with increasing concentration for both 50:50 and the 95:5 liposomes, but the reduction is less for the 95:5 liposomes. The most plausible explanation for this behavior is protein-liposome interactions in both cases, which saturate the liposome surface and limit the number of adsorption sites available to the drug. The PEG modification seems to decrease this effect, however, causing a more gradual decrease in drug binding in the case of the 95:5 liposomes.

In the case of the 85:15 liposomes, a less drastic decrease in drug affinity is again seen, but the uptake values as a whole are lower than the 95:5 liposomes. The polymer inclusion has decreased the protein-liposome interactions as hoped, but has also affected the drug-liposome affinity. The extra 10% by mole of DPPE-mPEG-2000 is actually a much larger increase by weight, as the ratio of formula weights for DOPG and DPPE-mPEG-2000 is roughly 4:1. The amount of negative charge in the system has therefore been decreased substantially when comparing the 95:5 and 85:15

DOPG:DPPE-mPEG-2000 liposomes. Clearly, the increase in negative charge for the 95:5 liposomes has led to an increase in drug uptake. It is, however, unclear whether the presence of the PEG affects the drug uptake directly in any manner. To address this issue, AMI uptake was also measured for 95:5 and 85:15 DOPG:DPPE-mPEG-2000 liposomes at 0.72 mg lipid/mL in buffer solutions without proteins present. The goal was to use the uptake values for one system to scale up to the other system, as discussed in Section 3.3.2. In this case, the method was slightly adapted to probe for the effect of changing the net charge of the system. The ratio of net charge for 95:5 liposomes compared to the 85:15 liposomes (also the ratio of the total moles of lipid in the systems) is 1.217. Based on the assumptions that increased drug uptake would be directly proportional to increased charge and that no other factors played a role in binding, the following equation was derived for the partition coefficient for the drug in liposomes with increased charge:

$$\frac{\phi_{95:5}}{1-\phi_{95:5}} = 1.217 \times \frac{\phi_{85:15}}{1-\phi_{85:15}} . \qquad (3\text{-}2)$$

The fraction of drug bound to the 95:5 liposomes was obtained from the above equation, and the results, along with the uptake data for both types of liposomes in buffer, are shown in Figure 3-7. The 95:5 DOPG:DPPE-mPEG-2000 liposomes took up more drug than the scale up equation predicted, suggesting a direct effect of PEG on drug binding. The 5% PEG liposomes sequestered more drug than predicted, suggesting a negative correlation between increased PEG-lipid percentage and drug binding. This effect could be due to steric interactions which limit the number of sites on liposomes that are available for drug binding. Alternatively, the high PEG percentage

could be impacting the structure of the lipid bilayer leading to a reduction in drug sequestration in the bilayer, which is another potential mechanism for drug uptake by liposomes. In either case, a factor other than electrostatics seems to be affecting the binding between the liposomes and the drug, and a 5% inclusion of lipids modified with PEG was nearly optimal for minimization of liposome-protein interactions while maximizing drug-liposome affinity.

The average difference in fractional drug uptake between the 85:15 and 95:5 DOPG:DPPE-mPEG-2000 formulations in Figure 3-6 is roughly 2-3%, which may seem insignificant. However, it is important to note that the goal of liposome injections will be to reduce the free drug concentration as much as possible because the free drug will bind to the receptors in the body (sodium ion channels for AMI) leading to toxic effects. Since the fractional uptake values are very close to 100%, a difference in 2-3% in fractional uptake could lead to a very large percentage decrease in the free drug concentration. To better illustrate the effect of liposomes on overdose treatment, the fractional drug uptake by serum is compared with that for 95:5 DOPG:DPPE-mPEG-2000 liposomes in serum in Figure 3-8. Serum binds to about 92% of the drug, leading to 8% free drug, while liposomes and serum together bind to about 98% of the drug, leading to 2% free drug. Thus, liposome addition reduces the free drug from 8 to 2%, which represents a 75% reduction. Similarly, the reduction in total uptake by 2-3% for the 85:15 liposomes results in a free drug reduction of around 30-50%, as opposed to 75%. The AMI uptake by 95:5 DOPG:DPPE-mPEG-2000 liposomes is thus significantly superior to the other systems studied here and all previously published data. More importantly, the variability over the relevant initial concentration range of 1-10 μM has

been drastically reduced with the inclusion of PEG chains, making these treatments more suitable clinically. Predicted uptake values for 95:5 DOPG:DPPE-mPEG-2000 liposomes in human serum were again calculated using Equation 3-1, and are also shown in Figure 3-8. Although the drug concentration dependency of the uptake values has been reduced, the failure to reach the predicted values still shows evidence for site occupation by proteins. However, the difference between the predictions for the pegylated liposomes is much less than the difference for the unpegylated liposomes seen in Figure 3-2.

Clearly, strong evidence exist to conclude that the 95:5 DOPG:DPPE-mPEG-2000 vesicles are superior to the 50:50 DMPC:DOPG, 85:15 DOPG:DPPE-mPEG-2000, and 55:15:30 DMPC:DPPE-mPEG-2000:CH vesicles. To determine if the effect was actually a function of polymer inclusion and increased charge or simply increased charge, pure DOPG liposomes were tested and compared to 95:5 DOPG:DPPE-mPEG-2000 liposomes in Figure 3-9. As shown in the figure, the uptake values for both systems in human serum were almost equal. This shows that perhaps the reduction in protein binding is balanced by the reduction in charge leading to similar drug uptake by these systems. To determine the effect of pegylation, additional experiments were conducted to measure drug uptakes by both pure DOPG and 95:5 DOPG:DPPE-mPEG-2000 liposomes in PBS (without any proteins) and results were compared to those reported in Figure 3-9 for uptake in serum (with proteins) in the following section.

3.3.4.2 Assessment of protein-liposome interactions

To assess the affect of proteins on drug binding to liposomes with and without PEG, the summing of partition coefficients was again used (Equation 3-1). The predictions were made for drug uptake in mixtures of proteins and liposomes, and were

based on uptake experiments done with each component. Figure 3-10 shows the drug uptake for 95:5 DOPG:DPPE-mPEG-2000 liposomes in serum and PBS, along with the predictions for a mixture of liposomes and serum. Figure 3-11 shows the same for pure DOPG liposomes. Both liposome types were made via sonication (Section 3.2.2). For both liposomes, the drug uptake was lower than the predicted values. The fact that the fractional uptake was lower in mixtures of liposomes and serum than predicted suggests that proteins must be binding directly to the liposomes leading to a reduction in drug binding in serum. To determine the effect of pegylation on protein binding, it is instructive to compare the magnitude of differences between the predictions and the experimental results for both pegylated and unpegylated liposomes. This difference is smaller for the pegylated liposomes (Figure 3-10), with overlapping behavior at small concentrations. Interestingly, the drug uptake by the pegylated liposomes in PBS is almost concentration independent, whereas the pure DOPG liposomes show a clear reduction in drug uptake with increasing concentration. It is possible that the PEG chains provide additional sites for drug binding through non specific adsorption and this eliminates the saturation effects responsible for the decrease in fractional uptake with increasing concentration evident in all unpegylated systems. Regardless, this effect sharply contrasts the results in Section 3.3.4.1, which suggest a negative effect of PEG on drug uptake. We speculate that the presence of PEG does provide additional binding sites but 15% PEG reduces binding of the drug to liposomes due to effects discussed above, as well as to possible bilayer disruptions, and this reduction offsets the binding of the drug to the PEG. Again, this is a speculation and more investigations are needed to validate this hypothesis.

Based on the in vitro drug binding data reported above, the 95:5 DOPG:DPPE-mPEG-2000 liposomes seem best suited for overdose treatment but the pure DOPG systems are almost equally effective. Consequently, it is vital to consider in vivo effects as well, as they may be much more important in determining whether or not polymer inclusion is necessary. Studies in literature suggest that liposome removal by the RES to the liver is imminent without polymer shielding of proteins [30]. In the absence of pegylation, the liposomes along with the bound drug may enter the liver and spleen very quickly and fragment, leading to the possible release of the drug back into circulation. It is necessary to ensure that the drug is released back into the circulatory system at a rate that does not cause toxicity, and so the addition of PEG will most likely be necessary for in vivo applications.

3.3.4.3 Increased lipid loading for 95:5 DOPG:DPPE-mPEG-2000 liposomes

In Section 3.3.2, data was presented to show that increased lipid concentrations were ineffective at substantially increasing drug sequestration for 50:50 DMPC:DOPG liposomes in human serum. The 50:50 liposomes quickly became ineffective as the AMI concentration increased, making it very difficult to increase drug binding over a wide range of AMI concentrations. On the contrary, 95:5 DOPG:DPPE-mPEG-2000 liposomes appear to be less affected by protein interactions, and were subsequently tested for AMI binding at double the original lipid loading of 0.72 mg/mL. The liposomes were made via extrusion with 100 nm membranes. Figure 3-12 shows drug uptake as a function of final AMI concentration for human serum without liposomes and for 95:5 DOPG:DPPE-mPEG-2000 liposomes loaded at 1.44 mg lipid/mL in human serum. The lipid concentration in the liposome dispersion was 8 mg lipid/mL, and the dispersion was then added to the serum samples at 18% of the final solution volume. Also shown are

the predicted values for the liposome-serum mixture based on Equation 3-1. The higher loading resulted in consistent uptake values of nearly 99% across the drug concentrations tested. Additionally, the uptake values were nearly equal to the predicted values, pointing to a lack of binding inhibition by the proteins. By comparing Figures 3-2, 3-8, and 3-12, one can clearly see that the pegylated liposomes at higher lipid loadings are binding to the drug as effectively as they do in buffer solutions with no proteins present. Protein binding to the liposome surface has therefore been reduced to a level that is insignificant with respect to drug removal. Although the data appears to suggest that a small drug concentration range was tested, the actual initial AMI concentrations ranged from 1 to 20 μM. The liposomes sequestered high proportions of the drug and made the final drug concentration range exceptionally small.

The results are encouraging when considering the percentage reduction in free drug concentration. Figure 3-13 compares the percentage reduction achieved with three liposomal systems at initial AMI concentrations of 3, 6, and 9 μM. The magnitude of the free drug reduction has risen to almost 90% with 95:5 DOPG:DPPE-mPEG-2000 liposomes at 1.44 mg lipid/mL for total concentrations as high as 9 μM. To achieve a comparable lipid concentration in the bloodstream, roughly 5 g of lipid would need to be administered to a patient, which is half of the amount of spherulites composed of similar materials that are claimed to be safe for intravenous administration [25]. A 90% free drug reduction implies a substantial drug-liposome affinity and a high degree of binding selectivity despite the presence of serum proteins. While these values may not correlate directly to in vivo applications due to the presence of the immune system and other factors, a free drug reduction in the blood stream of even 20% could be significant

[88]. Thus, the systems tested here have a high likelihood of reducing toxicity in an overdosed patient.

The magnitude of the free drug reduction is not the only factor that should be considered from Figure 3-13. The free drug reduction dropped from 55% to 45% for the 50:50 DMPC:DOPG liposomes, and from 75% to 68% for the 95:5 DOPG:DPPE-mPEG-2000 liposomes at 0.72 mg lipid/mL. Such declines in reduction show evidence for site saturation at physiologically relevant concentrations. The 95:5 liposomes with more lipid showed no decline over the entire range tested. For the purposes of drug overdose treatment, the concentration independent behavior is enormously beneficial in clinical applications so that the same treatment would be equally effective in all overdosed patients.

The 95:5 DOPG:DPPE-mPEG-2000 liposomes at 1.44 mg lipid/mL show promise as a detoxifying agent. In addition to high binding efficacy, these systems are likely to circulate in the body for an extended period of at least a day. The liposomes will then accumulate in the liver, spleen, lungs, and other organs, and be eventually broken down by the liver into their phospholipid components. The breakdown of the liposomes will possibly release some drug back into the circulation but this amount will likely be significantly less than that during overdose because of the metabolization of the drug during the 24 hour period in which the liposomes circulate in the body. These issues are explored through pharmacokinetic modeling in Chapter 7.

3.3.5 Drug Uptake by Stored Liposomes

AmBisome™ is an anti-fungal liposome formulation supplied as lyophilized powder, which is reconstituted with sterile water prior to injection. Although this method increases storage time and could possibly be used with the liposomes tested here for

drug overdose treatment, a significant amount of lag time would be necessary for pharmacy reconstitution. Time is a key issue during drug overdose, and so the storage method for CAELYX and DOXIL seemed to be the most promising method to test. Both are liposomes for drug delivery to tumors, and both include PEG in their formulations for increased circulation time, as do the liposomes tested in the present study. They are stored as concentrated liposome dispersions at temperatures of 2-8°C for extended periods of time (greater than one month), although their exact shelf lives are unknown. Just prior to injection, both products are diluted with 5% dextrose solutions. To explore the effect of shelf life on the binding capacity of liposomes, 95:5 DOPG:DPPE-mPEG-2000 and pure DOPG liposomes were prepared via extrusion through 100 nm membranes at concentrations of 0.72 mg lipid/mL. AMI uptake by the liposomes was measured from the day of preparation to day 34. Most readings were taken in 7 day increments.

Figures 3-14 and 3-15 show drug uptake as a function of time for pure DOPG and 95:5 DOPG:DPPE-mPEG-2000 liposomes, respectively. The results show that liposome dispersions, especially those including PEG, continued to effectively remove AMI from human serum after being stored for several weeks. Although these experiments differed from actual clinical conditions and provided only a small sample, the preliminary assumption is that these liposome dispersions could be prepared and stored at 2-8°C for at least one month for drug overdose treatment.

3.4 Conclusions

In this chapter, liposomes composed of DOPG, 50:50 DMPC:DOPG, 95:5 and 85:15 DOPG:DPPE-mPEG-2000, and 55:15:30 DMPC:DPPE-mPEG-2000:CH were tested for their ability to sequester AMI in PBS and in the presence of human serum.

Factors such as liposome size, lipid loading, PEG inclusion, and storage were analyzed for their effects on drug binding. Uptake of drug by 50:50 DMPC:DOPG liposomes was not enhanced by increased lipid loading and remained at 35-70% in human serum. Liposome size was shown to have no effect on drug-liposome affinity, which implies that size can be chosen solely for in vivo considerations.

When considering liposomes incorporated with PEG, those composed of predominantly anionic lipids with a small amount of PEG-modified lipids were shown to sequester the drug from human serum most effectively. 95:5 DOPG:DPPE-mPEG-2000 liposomes at 0.72 mg lipid/mL reduced the free drug concentration of AMI in human serum by 65-75%. 85:15 DOPG:DPPEmPEG-2000 liposomes at 0.72 mg lipid/mL appeared to have too much PEG shielding and not enough negative charge, as they reduced the free drug concentration by only 30-50%. Thus, the optimal amount of PEG-modified lipid to be incorporated into liposomes to effectively shield proteins while also allowing diffusion and binding of the drug to the charged lipid membrane appeared to be 5%.

The best results were obtained for 95:5 DOPG:DPPE-mPEG-2000 liposomes loaded at 1.44 mg lipid/mL, which reduced the free AMI concentration in human serum by nearly 90% across a wide range of initial drug concentrations. Stability and continued effectiveness during storage are also important considerations for clinical applications, and preliminary storage tests performed on pure DOPG and 95:5 DOPG:DPPE-mPEG-2000 liposomes at 0.72 mg lipid/mL provided evidence for sustained drug binding effectiveness after being stored at 2-8°C for at least 34 days.

Overall, the results of this chapter indicate that liposomes composed of 95:5 DOPG:DPPE-mPEG-2000 lipids at a concentration of 1.44 mg lipid/mL sequester extremely large amounts of free AMI from human serum. Furthermore, these systems may be stored at 2-8°C for extended periods of time with little to no effect on drug uptake properties. Thus, these systems seem highly suitable for conducting animal and human trials for overdose treatment of AMI.

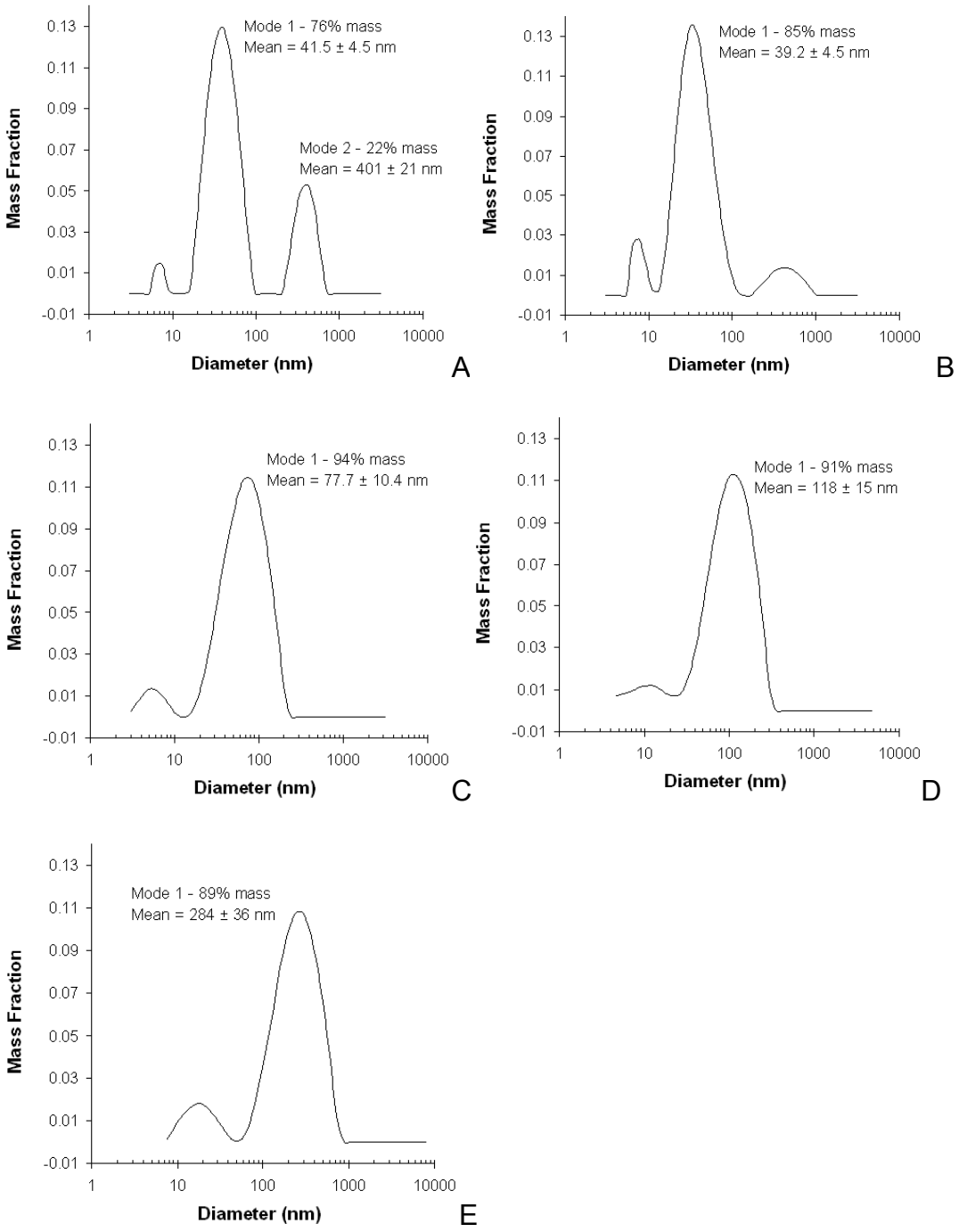

Figure 3-1. Size distributions of liposomes from dynamic light scattering for (a) sonicated 85:15 DOPG:DPPE-mPEG-2000, (b) sonicated DOPG, (c) sonicated 55:15:30 DMPC:DPPE-mPEG-2000:CH, (d) extruded 95:5 DOPG:DPPE-mPEG-2000, and (e) extruded 50:50 DMPC:DOPG.

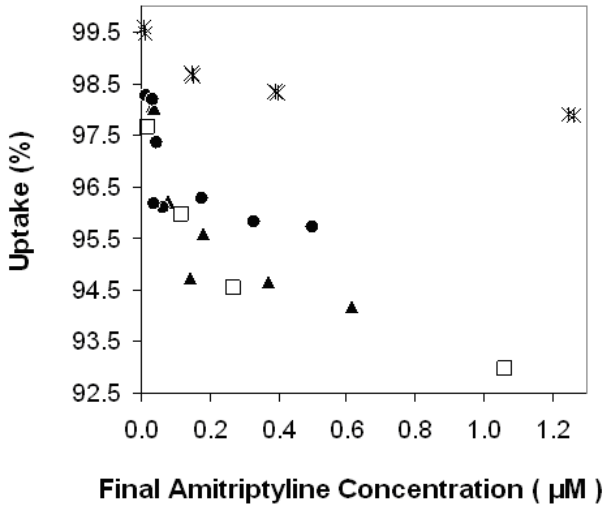

Figure 3-2. Percent amitriptyline uptake from human serum by 50:50 DMPC:DOPG liposomes at lipid loadings of 0.72 mg lipid/mL and 1.44 mg lipid/mL; prediction for 50:50 liposomes in human serum based on 50:50 uptake in buffer and serum uptake using Equation 3-1. Key: 50:50 DMPC:DOPG at 0.72 mg/mL (▲); 50:50 DMPC:DOPG at 1.44 mg/mL added at 9% by volume (●); 50:50 DMPC:DOPG at 1.44 mg/mL added at 18% by volume (□); prediction for 50:50 DMPC:DOPG at 1.44 mg lipid/mL in human serum (✳).

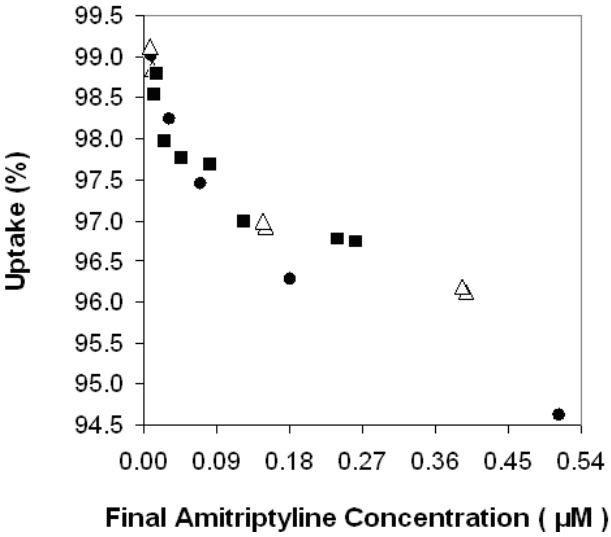

Figure 3-3. Percent amitriptyline uptake from buffer by 50:50 DMPC:DOPG liposomes of various sizes (40-45 nm, 100 nm, 284 nm) at a lipid loading of 0.72 mg lipid/mL. Key: 284 nm (●); 100 nm (■); 40-45 nm (Δ).

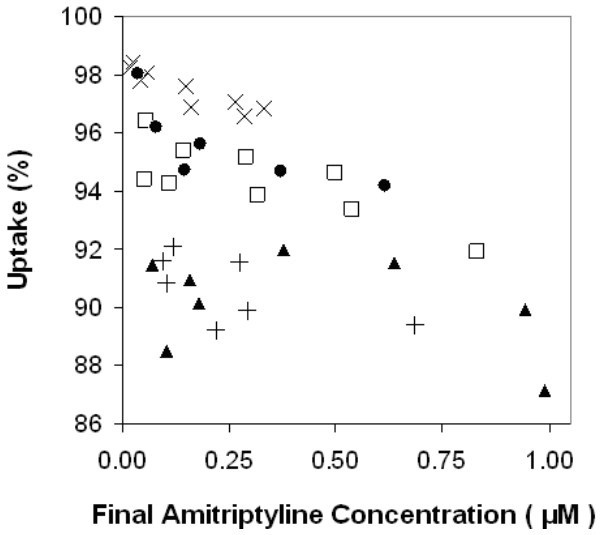

Figure 3-4. Percent amitriptyline uptake from human serum samples without liposomes and from human serum samples with 95:5 and 85:15 DOPG:DPPE-mPEG-2000 liposomes, 50:50 DMPC:DOPG liposomes, and 55:15:30 DMPC:DPPE-mPEG-2000:CH liposomes at lipid loadings of 0.72 mg lipid/mL as a function of final amitriptyline concentration. Key: human serum (+); 95:5 DOPG:DPPE-mPEG-2000 (X); 85:15 DOPG:DPPE-mPEG-2000 (□); 50:50 DMPC:DOPG (●); 55:15:30 DMPC:DPPE-mPEG-2000:CH (▲).

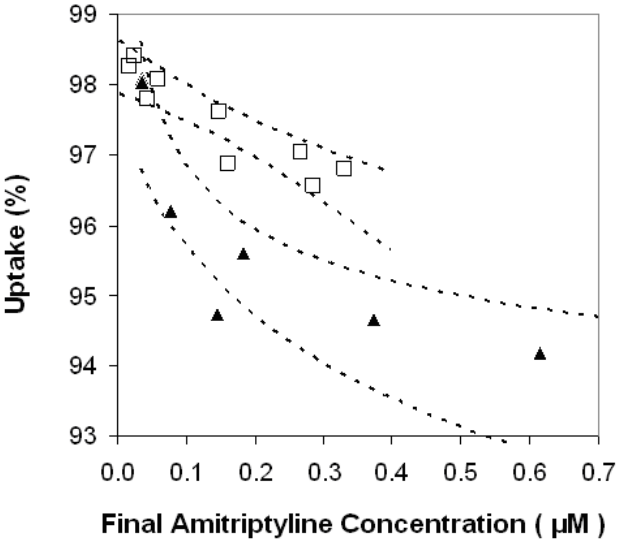

Figure 3-5. Percent amitriptyline uptake from human serum by 95:5 DOPG:DPPE-mPEG-2000 liposomes (□) and 50:50 DMPC:DOPG liposomes (▲) at lipid loadings of 0.72 mg lipid/mL versus final amitriptyline concentration with 95% CI (dashed lines).

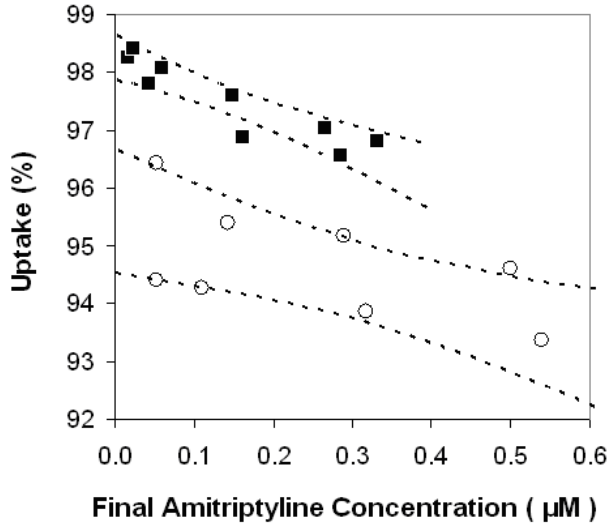

Figure 3-6. Percent amitriptyline uptake from human serum by 95:5 and 85:15 DOPG:DPPE-mPEG-2000 liposomes at lipid loadings of 0.72 mg lipid/mL versus final amitriptyline concentration with 95% CI (dashed lines). Key: 95:5 DOPG:DPPE-mPEG-2000 (■); 85:15 DOPG:DPPE-mPEG-2000 (○).

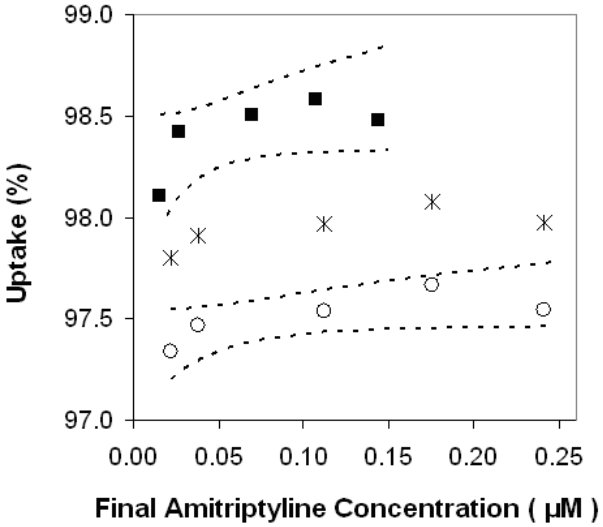

Figure 3-7. Percent amitriptyline uptake from buffer by 95:5 and 85:15 DOPG:DPPE-mPEG-2000 liposomes at lipid loadings of 0.72 mg lipid/mL versus final amitriptyline concentration with 95% CI (dashed lines); prediction for 95:5 uptake based on 85:15 uptake using Equation 3-2. Key: 95:5 DOPG:DPPE-mPEG-2000 (■); 85:15 DOPG:DPPE-mPEG-2000 (○); prediction for 95:5 DOPG:DPPE-mPEG-2000 (✳).

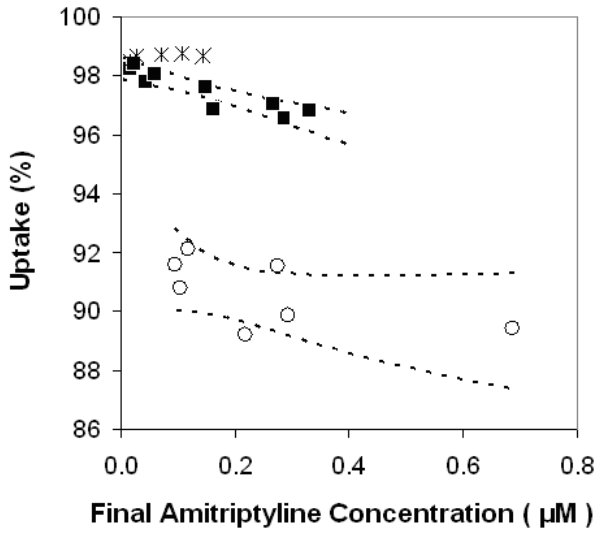

Figure 3-8. Percent amitriptyline uptake by human serum and by mixtures of human serum and 95:5 DOPG:DPPE-mPEG-2000 liposomes at a lipid loading of 0.72 mg lipid/mL versus final amitriptyline concentration with 95% CI (dashed lines); prediction for 95:5 uptake in serum based on 95:5 uptake in buffer and serum uptake using Equation 3-1. Key: 95:5 DOPG:DPPE-mPEG-2000 (■); human serum (○); prediction for 95:5 DOPG:DPPE-mPEG-2000 (✳).

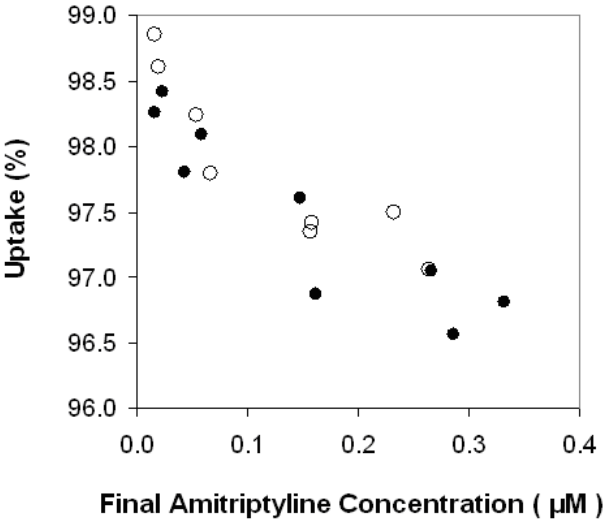

Figure 3-9. Percent amitriptyline uptake from human serum by 95:5 DOPG:DPPE-mPEG-2000 liposomes and pure DOPG liposomes at lipid loadings of 0.72 mg lipid/mL versus final amitriptyline concentration. Key: 95:5 DOPG:DPPE-mPEG-2000 (●); DOPG (○).

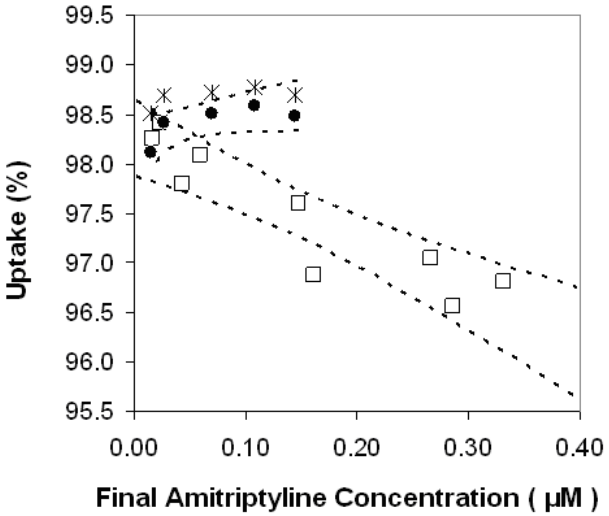

Figure 3-10. Percent amitriptyline uptake from human serum and buffer by 95:5 DOPG:DPPE-mPEG-2000 liposomes at lipid loadings of 0.72 mg lipid/mL versus final amitriptyline concentration with 95% CI (dashed lines); prediction for 95:5 uptake in serum based on 95:5 uptake in buffer and serum uptake using Equation 3-1. Key: human serum (□); buffer (●); prediction for 95:5 DOPG:DPPE-mPEG-2000 in serum (✳).

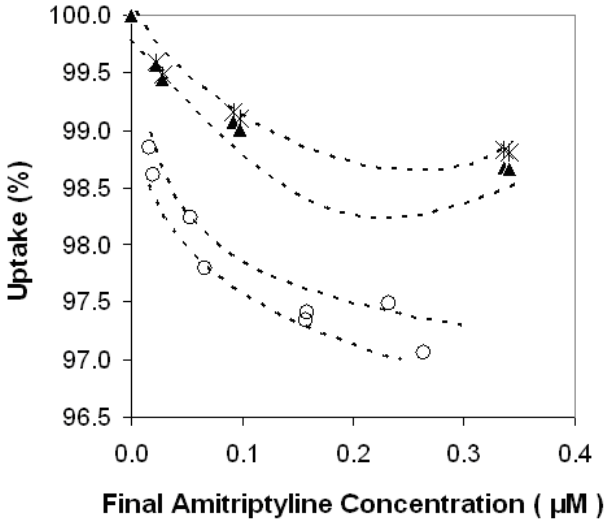

Figure 3-11. Percent amitriptyline uptake from human serum and buffer by pure DOPG liposomes at lipid loadings of 0.72 mg lipid/mL versus final amitriptyline concentration with 95% CI (dashed lines); prediction for DOPG uptake in serum based on DOPG uptake in buffer and serum uptake using Equation 3-1. Key: human serum (○); buffer (▲); prediction for DOPG in serum (✳).

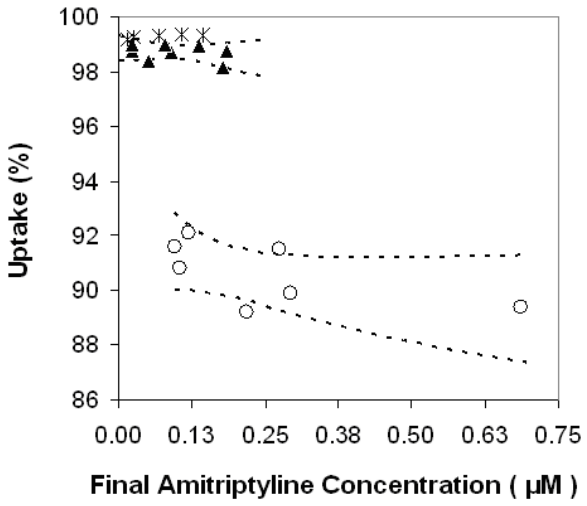

Figure 3-12. Percent amitriptyline uptake by human serum and by mixtures of human serum and 95:5 DOPG:DPPE-mPEG-2000 liposomes at a lipid loading of 1.44 mg lipid/mL versus final amitriptyline concentration with 95% CI (dashed lines); prediction for 95:5 uptake in serum based on 95:5 uptake in buffer and serum uptake using Equation 3-1. Key: 95:5 DOPG:DPPE-mPEG-2000 (▲); human serum (○); prediction for 95:5 DOPG:DPPE-mPEG-2000 (✳).

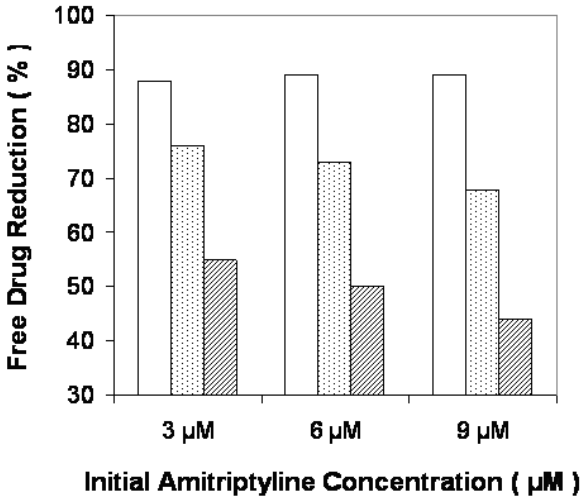

Figure 3-13. Free drug concentration reduction of amitriptyline in human serum by 95:5 DOPG:DPPE-mPEG-2000 liposomes at loadings of 1.44 (□) and 0.72 mg lipid/mL (⬚) and 50:50 DMPC:DOPG liposomes at 0.72 mg lipid/mL (▨). Free drug reduction was calculated based on the difference between free drug in human serum samples and free drug in human serum samples mixed with liposomes.

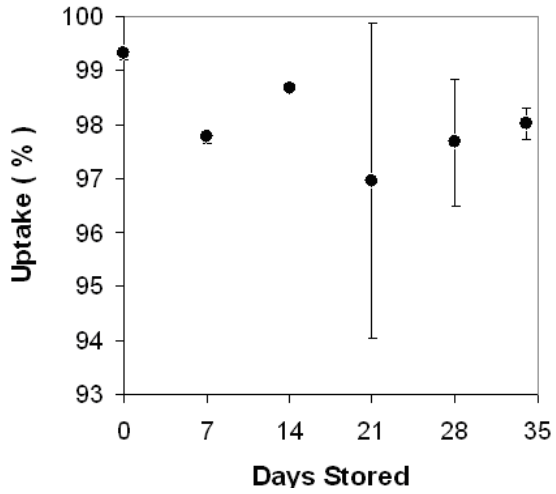

Figure 3-14. Percent amitriptyline uptake from human serum by pure DOPG liposomes at a lipid concentration of 0.72 mg lipid/mL and an initial drug concentration of around 2.7 μM (corrected for dilution) versus days stored. Data are reported as mean ± SD with n = 2.

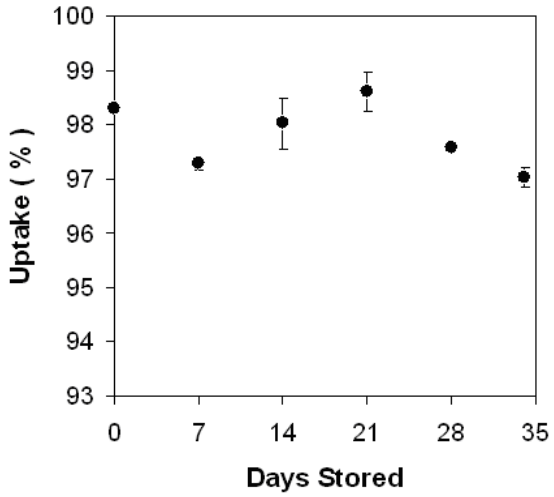

Figure 3-15. Percent amitriptyline uptake from human serum by 95:5 DOPG:DPPE-mPEG-2000 liposomes at a lipid concentration of 0.72 mg lipid/mL and an initial drug concentration of around 2.7 μM (corrected for dilution) versus days stored. Data are reported as mean ± SD with n = 2.

CHAPTER 4
BINDING OF IMIPRAMINE, DOSULEPIN, AND OPIPRAMOL TO LIPOSOMES FOR OVERDOSE TREATMENT

4.1 Introduction

In Chapters 2 and 3, pegylated, anionic liposomes were proven to be effective binding agents for amitriptyline (AMI) and nortriptyline. Three main goals were addressed in this chapter. First, we explored binding of other tricyclic antidepressants commonly involved in overdoses to determine whether pegylated liposomes could be useful as a general treatment strategy for drug overdose. Imipramine (IMI) and dosulepin (DOS), both weak bases existing in the predominantly charged state at the physiological pH of 7.4, were studied. Opipramol, a diprotic compound with pK_a values of around 4 and 8.1 [102-104], was also studied. At a pH of 7.4, one opiprmaol protonation site is 83% protonated while the other site is uncharged. Opipramol thus gave us the opportunity to test the effectiveness of liposomes at binding an important overdose drug and the chance to confirm the importance of electrostatic effects for drug binding to pegylated, charged liposomes.

Next, we explored the mechanisms of binding, particularly focusing on the importance of electrostatic effects, and also investigating the role of the PEG chain length on drug binding. It is important to understand the role of electrostatic interactions in drug binding because several overdose drugs are charged at physiological conditions. Electrostatics were studied using opipramol, as mentioned above. The role of PEG chain length is also very important because PEG chain lengths have been shown to affect the biodistribution and circulation time of polymer coated liposomes [31]. Thus, it was important to determine whether PEG chain length impacted drug binding so

that an optimum PEG chain length based on both pharmacokinetics (circulating times) and equilibrium drug binding could be determined.

Finally, we wished to compare the binding efficacy of liposomes to other targets inside the body to determine the binding potential of the liposomes in vivo. It is common knowledge that most tricyclic antidepressant drugs are highly bound to proteins once inside the blood stream [25,85], and in our prior work, we have shown that liposomes can compete favorably with plasma proteins for drug uptake ([71] and Chapters 2 and 3). However, there are acidic lipids in the body similar in structure to lipids considered here and so it is extremely important to compare the binding affinity of liposomes with other acidic lipid containing targets inside the human body. A brief discussion on the time scales relevant for drug redistribution from the organs to the blood compartment is also presented as evidence for the clinical feasibility of overdose treatment with liposomes. A more detailed pharmacokinetic analysis is presented in Chapter 7.

All of the binding experiments performed in this chapter were done in vitro in human serum samples or PBS at a pH of 7.4. It is misleading to measure the absolute binding of drug molecules to liposomes in the presence of proteins and assume the effective free drug concentration has been reduced by the same margin as in PBS (without proteins). For that reason, we have measured the binding of drugs to serum proteins in human serum, followed by mixtures of human serum and liposomes. Protein binding has already been accounted for when free drug concentration reductions are reported.

4.2 Materials and Methods

4.2.1 Materials

Methanol, chloroform, Dulbecco's Phosphate Buffered Saline (PBS) without calcium chloride and magnesium chloride, amitriptyline hydrochloride, imipramine hydrochloride, and opipramol dihydrochloride were purchased from Sigma Aldrich (St. Louis, MO). Dosulepin (dothiepin) hydrochloride was purchased from LGC Promochem (Teddington, UK). Human serum from male plasma and Centriprep YM10 centrifugation filters (10,000 molecular weight cut-off) were purchased from Fisher Scientific (Pittsburg, PA). The lipids 1,2-dioleoyl-sn-glycero-3-[phospho-rac-(1-glycerol)] (sodium salt) (DOPG), dissolved in chloroform, 1,2-dipalmitoyl-sn-glycero-3-phosphoethanolamine-N-[methoxy(polyethyleneglycol)-2000] (ammonium salt) (DPPE-mPEG-2000), in powder form, and 1,2-dipalmitoylsn-glycero-3-phosphoethanolamine-N-[methoxy-(polyethylene glycol)-5000] (ammonium salt) (DPPE-mPEG-5000), in powder form, were purchased from Avanti Polar Lipids, Inc. (Alabaster, AL). A Mini-Extruder kit for liposome preparation was also purchased from Avanti Polar Lipids, Inc.

4.2.2 Liposome Preparation via Extrusion

Liposomes composed of a molar ratio of 95:5 DOPG/DPPE-mPEG-2000 and 95:5 DOPG/DPPEmPEG-5000 were prepared via extrusion. Lipids were combined in their respective molar ratios and then dissolved in a 9:1 mixture (by volume) of chloroform/methanol such that a 12 mg/mL concentration of lipids was obtained. The organic solvent was then evaporated under a stream of nitrogen. After an even and uniformly dried lipid film was obtained, the dried lipid layer was hydrated with PBS. The lipid concentration after hydration was 8 mg lipid/mL PBS for 95:5 DOPG/DPPE-mPEG-2000 liposomes or 9.33 mg lipid/mL PBS for 95:5 DOPG/DPPE-mPEG-5000 liposomes.

The mass loading was slightly higher for the PEG-5000 liposomes so that the DOPG content would be identical for both types of liposomes. The lipid suspension was then heated to 30°C and stirred for 45 minutes. After stirring, the liposome solution was extruded through a 100 nm membrane 13 times.

4.2.3 Liposome Characterization

The mean diameters and size distributions of the liposomes were analyzed using a Precision Detectors PDDLS/CoolBatch+90T instrument. The data were analyzed with the Precision Deconvolve32 Program. The measurements were taken at 20°C with a scattering angle of 90° using a 683 nm laser source.

4.2.4 Drug Uptake With Liposomes in Human Serum or PBS

95:5 DOPG/DPPE-mPEG-2000 liposomes were added to solutions of IMI, DOS, or opipramol in human serum such that the volume of the liposome dispersion was 9% or 18% of the total solution volume, giving a final lipid concentration of 0.72 or 1.44 mg lipid/mL. 95:5 DOPG/DPPE-mPEG-5000 liposomes were added to solutions of IMI, DOS, or opipramol in human serum or PBS such that the volume of the liposome dispersion was 18% of the total solution volume, giving a final lipid concentration of 1.68 mg lipid/mL. The initial drug concentrations for all three drugs varied from around 3-25 μM, due to the significance of this range for serum drug concentrations during drug overdose [105]. Control solutions of drug in PBS and drug in serum without liposomes were also made to allow for uptake quantification and comparison. After being stirred for 15 minutes, the solutions were ultracentrifuged at 5000 rpm for 15 minutes in a vial that contained a YM10 filter (10,000 molecular weight cut-off). Experiments were done in Chapter 2 to ensure that the systems were at equilibrium before filtration. To minimize the effect of any leaching components from the filter, the filters were rinsed

first with DI water and then with PBS at 5000 rpm for 10 minutes prior to their use in these experiments. The concentration of the drugs in the filtrate (free drug concentration) and the control solution was detected by measuring UV absorbance at 215 nm after passing the samples through a C18 column (Waters Corp., Milford, MA) using an acetonitrile/50 mM $NH_4H_2PO_4$ solvent mixture in a 35/65 ratio for IMI and DOS and a 30/70 ratio for opipramol. The calibration curves for concentration versus area under the curve were linear with R^2>0.99. To ensure that all unbound drug was accounted for, solutions of the drugs at various concentrations were passed through YM10 filters in a separate test. Small amounts of drug were taken up by the filter, and a linear correction curve was made and used to correct for drug adsorbed to the membranes in subsequent tests.

4.2.5 Data Analysis

The data were analyzed using JMP software developed by SAS. Best fit regression lines were fit to the concentration-dependent uptake data, and 95% confidence intervals (CIs) were displayed to allow for both experimental error analysis and comparison between two or more data sets. The CI's were calculated for mean uptake values using the Student's *t* distribution.

4.3 Results and Discussion

4.3.1 Liposome Characterization

The 95:5 DOPG/DPPE-mPEG-2000 and DOPG/DPPE-mPEG-5000 liposomes extruded with 100 nm membranes had mean diameters of 118 ± 15 and 112 ± 15 nm, respectively.

4.3.2 Imipramine Uptake

The binding of IMI to liposomes was explored for initial drug concentrations ranging from 3 to 22 μM, which are relevant to overdose cases. Musshoff et al. [105] reported toxic values in human plasma to be 1.58 to 4.73 μM, but observed levels in dead victims from 1.58 to 79 μM. IMI percent uptake values for human serum and mixtures of human serum and liposomes are plotted as a function of final drug concentration in Figure 4-1. In Figures 4-1 through 4-3, the y-axis represents Φ x 100%, where $\Phi \equiv (C_T-C_F)/C_T$, C_T is the total drug concentration, and C_F is the free concentration assayed by HPLC. The final, or equilibrium, drug concentrations (C_F) were used on the x-axis rather than the initial drug concentrations so that the curves would represent equilibrium binding isotherms.

IMI binding to proteins in serum samples was roughly 80-84%, or equivalently, 16-20% of the IMI remained unbound in the solution. These values agree well with the free fractions of 24% and 8-15% reported by Rodgers et al. [106] and Kristensen [107], respectively. The total drug binding in the presence of liposomes and proteins rose to 96-98% for 95:5 DOPG/DPPE-mPEG-2000 liposomes at 0.72 mg lipid/mL. Doubling the lipid loading to 1.44 mg lipid/mL caused the drug uptake values to increase to around 98%, while also eliminating the uptake reduction with increasing drug concentration.

The lack of overlap in the CI's for uptakes for the 0.72 and 1.44 mg/mL lipid loadings demonstrates the significance of the reduction. The 95:5 DOPG/DPPE-mPEG-5000 liposomes at 1.68 mg lipid/mL also reduced the overall drug concentration by 98%. Other than a slight drop in drug uptake at low drug concentrations, the PEG-5000 liposomes behaved similarly to the PEG-2000 liposomes (CI overlap). This may

be an important result when final formulations are developed for in vivo use, as formulators could choose polymer chain lengths based on pharmacokinetic considerations without the risk of affecting the drug uptake capacity of the system.

To analyze the suitability of liposomes for overdose treatment, it is instructive to calculate the percentage change in the free drug concentration after liposomes are added to serum. The free drug concentration in serum is about 16-20%, and it reduces to 2% after liposome addition. This implies that liposomes reduce the free drug concentration in serum by about 88%. Poisonings occur due to partitioning of the drug into the cardiovascular tissue and central nervous system, which induces ion channel disruption and other effects [2]. Thus, a reduction in the free drug concentration could shift equilibrium towards the blood stream, driving some of the drug out of the most vital tissues and into the bloodstream and/or other less vital tissues. This is discussed in more detail in Section 4.3.5 and Chapter 7.

Pegylated liposomes are likely to be more suitable for overdose treatment because of a reduction in protein binding due to pegylation. The degree of protein binding to liposomes can be indirectly estimated by combining the uptake data from serum with the data from liposomes in buffer, and comparing the result with the case in which liposomes and serum are mixed. If a mixture contains several types of binding targets, the following mass balance can be used to obtain uptake values in mixtures if the uptakes are known for individual components,

$$\frac{\phi_{\mathrm{mix}}}{1-\phi_{\mathrm{mix}}} = \frac{\phi_{1}}{1-\phi_{1}} + \frac{\phi_{2}}{1-\phi_{2}} + \ldots + \frac{\phi_{\mathrm{n}}}{1-\phi_{\mathrm{n}}}, \tag{4-1}$$

where Φ_{mix} is the fraction of drug bound in the mixture and Φ_1, Φ_2, etc., are the fractions of drug bound in the components of the mixture measured separately, with each being measured at the same final (equilibrium) concentration (see Chapters 2 and 3). For instance, Φ_1 and Φ_2 could be the bindings in serum (without liposomes) and liposomes in PBS, respectively, and the above equation could be used to predict the uptake in serum after the addition of liposomes, Φ_{mix}. Figure 4-1 shows the projected uptake values for a 1.44 mg/mL loading of 95:5 DOPG/DPPE-mPEG-2000 liposomes in serum along with the measured values in the magnified region of the figure. The predicted values are higher than those obtained experimentally, although only slightly. This difference is likely due to protein binding to liposomes, and its magnitude is much less than that for unpegylated liposomes, which is expected as pegylation was shown to reduce protein binding to liposomes in Chapter 3.

4.3.3 Dosulepin Uptake

DOS uptake versus final DOS concentration is shown in Figure 4-2. Again, the initial drug concentrations tested ranged from 3 to 25 μM, which is the physiologically relevant range. The results in Figure 4-2 show that the serum proteins sequester 88-92% of the drug. These values are similar to those for AMI and slightly higher than the values observed for IMI. This is reasonable as DOS and AMI are more similar in structure than AMI and IMI. At a lipid loading of 0.72 mg lipid/mL, the 95:5 DOPG/DPPE- mPEG-2000 formulation sequestered almost all of the drug at low concentrations and just above 96% at higher concentrations. When the lipid loading was doubled, the values ranged from almost 100% to about 98.5%. The lack of overlap between the CI's for serum, serum and a 0.72 mg/mL loading of lipids, and serum with 1.44 mg/mL lipids points to a significant effect of liposomes on drug uptake. The free

drug concentration reduction from 8-12% to about 1.5% after addition of liposomes at 1.44 mg lipid/mL to serum implies an average free drug reduction of about 93%. The 95:5 DOPG/DPPE-mPEG-5000 liposomes at 1.68 mg lipid/mL behaved exactly as the PEG-2000 liposomes, as was observed for IMI. These results for binding of DOS again point to the effectiveness of the polymer coated liposomes made of a predominantly anionic lipid for minimizing protein-liposome interactions and sequestering multiple weak bases from serum samples. These results also show a lack of impact of the PEG chain length on drug uptake, as the uptakes are similar for the PEG chain lengths of 2000 and 5000 tested here.

By again using the uptake data from serum and liposomes in PBS in combination with Equation 4-1, we predicted the uptake values for 95:5 DOPG/DPPE-mPEG-2000 liposomes at 1.44 mg/mL in serum, and the results are shown in the magnified portion of Figure 4-2. The measured values are slightly less than the predicted ones, again demonstrating that while pegylation reduces protein binding to liposomes, it does not completely eliminate the binding.

4.3.4 Opipramol Uptake and the Importance of Electrostatic Interactions

Unlike IMI and DOS, opipramol is a diprotic drug with pK_a values of around 8 and 4, and thus, about 80% of the drug molecules have one site protonated at a pH of 7.4 [102-104]. A comparison between the uptake of opipramol with the uptakes of IMI and DOS illustrate the importance of the electrostatic interactions in drug binding to the anionic, pegylated liposomes. An earlier study by Austin et al. [55] involving the net neutral, zwitterionic lipid DMPC pointed to a more favorable thermodynamic interaction between the lipid bilayer and charged drugs versus neutral ones. Here, changes in

partitioning are compared for charged versus partially uncharged drugs for liposomes composed of a net negative lipid, DOPG.

Opipramol uptake as a function of final drug concentration is displayed in Figure 4-3. The total drug concentrations in these experiments ranged from 3 to 23 μM. The serum proteins sequestered about 76-82% of the drug from solution, which is lower in comparison to binding for IMI and DOS to serum proteins. This difference is likely due to reduced electrostatic interactions between the drug and albumin and other serum proteins that possess multiple charged sites. The 95:5 DOPG/DPPE-mPEG-2000 liposomes added to the serum at 0.72 and 1.44 mg lipid/mL increased uptakes to approximately 88-92% and 92.5-95.5%, respectively. The CI's show that the liposomes significantly increase the amount of drug bound in the system. Again, the CI's for both PEG-2000 and PEG-5000 liposomes overlap and imply no drug binding differences between the different PEG chain lengths.

The uptake values for the serum and mixtures of serum and liposomes were all lower than those observed for IMI and DOS, where over 99% of the drug molecules were in the protonated form. This confirmed the hypothesis that charge was playing a role in drug binding. The change in free drug concentration remained relatively high at about 76%. A reduced presence of charge-charge interactions in the system by 20% reduced the free drug concentration reduction by 12% compared to the values seen for IMI and DOS. This proves that electrostatic interactions play an important role in drug sequestration. Furthermore, the results show that the 95:5 DOPG/DPPE-mPEG-2000/5000 liposomes are capable of sequestering drugs that are only partially charged.

4.3.5 In Vivo Considerations: Competition and Pharmacokinetics

A nanoparticulate system can only reduce toxic effects from a drug overdose if it has a higher affinity for the drug in comparison to other target sites in the body. Two major binding targets in the body for drugs considered here are the acidic phospholipids and serum proteins. Our data reported above show that the partition coefficient for drug binding to liposomes is significantly higher than that for drug-protein binding, as evidenced by the fact that a liposome addition of 1.44 mg/mL reduces the free drug concentration in serum, which contains about 7% protein by weight, by as much as 90%. Below, we compare the binding capacity of the liposomes with another important binding target in the body, acidic phospholipids.

Acidic phospholipids (APL) are present inside red blood cells and within the cells of all major tissues. Here, we utilize the approach developed by Rodgers et al. [106] to estimate the equilibrium constant (K_a) for drug-APL binding inside red blood cells. The estimated K_a for drug-APL binding inside red blood cells is representative of equilibrium constants for drug-APL binding for all other tissues in the body [106]. The K_a value for IMI binding to APL in red blood cells can be calculated from the following equation (Equation 20 in [106]),

$$K_{\mathrm{aBC}} = \left(\begin{array}{l} \mathrm{Kpu}_{\mathrm{BC}} - \left(\dfrac{1 + 10^{\mathrm{p}K_{\mathrm{a}} - \mathrm{pH}_{\mathrm{BC}}}}{1 + 10^{\mathrm{p}K_{\mathrm{a}} - \mathrm{pHp}}} \cdot f_{\mathrm{IW,BC}} \right) \\ - \left(\dfrac{\left(P \cdot f_{\mathrm{NL,BC}} + (0.3P + 0.7) \cdot f_{\mathrm{NP,BC}} \right)}{1 + 10^{\mathrm{p}K_{\mathrm{a}} - \mathrm{pH}_{\mathrm{p}}}} \right) \end{array} \right) \cdot \left(\frac{1 + 10^{\mathrm{p}K_{\mathrm{a}} - \mathrm{pH}_{\mathrm{p}}}}{[\mathrm{AP}^-]_{\mathrm{BC}} \cdot 10^{\mathrm{p}K_{\mathrm{a}} - \mathrm{pH}_{\mathrm{BC}}}} \right) . \quad (4\text{-}2)$$

This equation is based on using the known partition coefficient for the drug in the RBC and the known composition of the RBC to estimate the partition coefficient for binding to the APL. For details on the equation and the parameters used for the calculation, see [106], although it should be noted that a blood to plasma ratio of 1.1 was used here for IMI [108], rather than the value of 1.67 used by Rodgers et al. [106]. The resulting K_a value for IMI is 3.9 g/mg. The association constant between liposomes and IMI can be calculated based on the data reported for drug binding to liposomes in PBS at 0.72 mg lipid/mL by using the following equation (Equation 10 from [106]),

$$K_a = \frac{f_b}{f_u[P]}, \tag{4-3}$$

where f_b is the fraction of bound drug, f_u the fraction of unbound drug, and [P] the concentration of APL in mg/g. The results for K_a are shown as a function of concentration in Table 4-1. The mean K_a value for IMI-liposome binding is about 77 g/mg over the relevant therapeutic concentration range, which is about 20 times larger than the value of 3.9 g/mg for APL in the red blood cells. As the approximate amount of lipids added to an overdosed patient could approach 10 g without toxic effects, the amount of lipids added via liposomes would substantially increase the total APL concentration in the blood compartment, which has about 1.2 g of APL [25,106]. A human body contains about 90 g of APL, and thus the total drug bound to 10 g of liposomes would far exceed the drug bound to all the APL in the body [106]. It should also be noted that a large fraction of the APL in the body are present in organs with low blood flow and so these APL are not truly available for binding within the time frame relevant to overdoses.

Based on the above data, it is clear that liposome administration into the blood can reduce the free drug concentration in the blood by a factor of about 8. However, overdose treatment requires a substantial reduction in drug concentration in vital organs such as the heart and central nervous system. If the overdose occurred a long period of time prior to treatment, all tissues would be in equilibrium at the instance of liposome administration. In this scenario, the total change in drug concentration in any tissue would be negligible after the body achieved the new steady state concentrations due to the large volume of distributions for the drugs of interest. However, most overdose cases do not correspond to this scenario. As shown in Table 4-2, the average times between ingestion and treatment observed in several overdose cases was typically between 2 and 4 hours. The drugs considered in this chapter are consumed orally, in which case the maximum blood levels are reached about 2-8 hours after ingestion [2,109]. During overdose, this time will increase substantially [2,8]. Additionally, several tissues in the body equilibrate rather slowly with the blood compartment. A good first approximation for equilibration times is the product of the partition coefficient of an organ and its volume, divided by the blood flow rate to the organ. In Table 4-3, these quantities have been estimated for many of the vital organs of the body. Many of the organs equilibrate within an hour or so of an IV dose. The muscle, skin, and adipose tissues, which account for almost 80% of the volume of distribution, equilibrate on a slower time scale than most other organs, requiring 4-10 times longer. If the time required for significant oral absorption and for the ‘‘slow’’ tissues to reach equilibrium are roughly combined, these large tissues will have little drug in them at the time of liposome administration, assuming that time lapses between overdose and treatment

are similar to those reported elsewhere [7,110-112]. The liposomes will then remove drug exclusively from vital tissues, which would include the brain and heart. In fact, in such cases, the large organs could act as sinks and remove excess drug from the blood stream as liposomes redistribute the drug from faster equilibrating organs to slower ones. The drug partitioning into the slowly equilibrating organs could actually speed up after liposome administration due to the decrease in the partition coefficient between the organs and the whole blood including liposomes.

Effectively, the liposomes could act as transporters, removing the drug from the rapidly equilibrating organs and redistributing it to the slowly equilibrating ones. This method of redistribution is likely the mechanism for overdose treatment by Fab fragments for digoxin and antidepressants, where the amount of Fab fragments administered is far less than the amount needed to bind the amount of drug present in the entire body [4,113-116]. Evidence for improved pharmacodynamic responses due to redistribution was shown in several animal studies, while human studies revealed an increase in tricyclic antidepressant serum concentrations after protein fragment administration. These pharmacokinetic issues have previously been included in a detailed mathematical model that is applicable to overdose treatment by any type of particles [117], as well as more quantitatively addressed for liposomes in Chapter 7. It is also noted that liposome administration could increase the hepatic drug clearance due to drug concentration increases in the blood, which could in turn lead to additional benefits for overdose treatment.

4.3.6 Comparisons with Prior Studies

Binding measurements in the presence of human serum for 95:5 DOPG/DPPE-mPEG-2000 and 95:5 DOPG/DPPE-mPEG-5000 liposomes demonstrated their

effectiveness at sequestering the weak bases DOS and IMI, and the diprotic drug opipramol. Figure 4-4 summarizes the results from the present and previous chapters by showing the average free drug concentration reductions over the concentration ranges tested for AMI, IMI, DOS, and opipramol. The liposomes were able to reduce the free drug concentration relative to protein samples without liposomes by 84-93% for the charged species and 76% for the partially charged opipramol. In Chapter 2, nortriptyline showed similar uptake results to that of AMI in PBS solutions by similar liposomes, and so its uptake in serum is also expected to be similar to that of AMI. Thus, the liposomes explored in this study have been shown to be effective at sequestering a large fraction of drug under physiological conditions, which includes protein binding. Such results demonstrate the feasibility of using a single detoxification system in a wide variety of circumstances. In Chapter 5, the use of such liposomes is expanded to other classes of drugs as well.

Table 4-4 compares the uptake efficacy of the formulations described here with prior studies on drug sequestration by nanoparticles. Dhanikula et al. [24,25,70] reported significant in vitro uptake of AMI by spherulites composed of soy phosphatidylcholine and cholesterol with a 100 mM citrate buffer internal phase. They reported an AMI sequestration of 97.3 ± 0.4% in the presence of 3% albumin, which is similar to the results obtained with the liposomes tested here. However, only 3% albumin was used, rather than human serum samples containing all serum proteins. Furthermore, their initial drug concentration was only 0.20 μM, which is within the therapeutic range for AMI but far below the toxic level of 1-3 μM. Also, the mass loadings in all of their studies were almost twice as high as those used here. The in

vitro studies of Dhanikula et al. were supplemented with in vivo studies on isolated rat hearts. They showed that infusion of the nanoparticles leads to a significant reduction in toxicity in isolated rat hearts that had been previously injected with relatively high amounts of AMI. Varshney et al. [19] also used nanocarriers in the form of nanoemulsions composed of ethyl butyrate, fatty acids, and poloxamer to sequester bupivacaine from buffer solutions. They reported maximum uptakes of about 90% in PBS, but the effect of serum proteins was not considered and their total mass loadings (surfactants and oil) were fairly high. As summarized in Table 4-4, several types of particles have shown high drug sequestrations. However, pegylated, anionic liposomes seem to have the widest possible spectrum of use and one of the highest binding efficacies for drugs that are mostly positively charged under physiological conditions [21-23].

It should be noted that several factors must be taken into account when evaluating different drug detoxification vehicles. Sequestering high amounts of drug at therapeutically feasible mass loadings, causing minimal toxicity, remaining effective in the presence of serum proteins and the reticuloendothelial system (RES), and remaining in circulation for some period of time after administration are all of utmost importance. Based on the comparisons shown in Table 4-4 and the well-known biocompatibility characteristics of pegylated liposomes, we believe liposomes to be the optimal vehicle for drug overdose treatment. Additional studies on biodetoxification have been reviewed by Leroux [69].

4.4 Conclusions

In this chapter, polymer shielded liposomes composed of 95:5 DOPG/DPPE-mPEG-2000 and 95:5 DOPG/DPPE-mPEG-5000 lipids were tested as nanocarriers for

the treatment of IMI, DOS, and opipramol overdose. The liposomes proved to be capable of sequestering about 98% or more of IMI and DOS and 92.5-95.5% of opipramol. Additionally, the liposomes reduced the free drug concentrations in human plasma by 88-93% in the case of the weak bases IMI and DOS, and 76% for the diprotic drug opipramol (1.44 mg lipid/mL loading). Comparison of the drug binding in PBS with that in human serum showed that the presence of the PEG on the liposome surface reduced protein binding to liposomes, but did not completely eliminate it. These experiments also showed that the length of the PEG chain did not make any detectable difference in uptake. Thus, PEG chain lengths of up to 5000 and possibly higher may be chosen if pharmacokinetic parameters dictate their necessity. Calculations suggested that liposomes are approximately 20 times more effective at binding antidepressants than acidic phospholipids already present in the body. Estimates of the times required for tissues to reach equilibrium also demonstrated that liposomes could significantly alter the drug concentrations in vital organs after a drug overdose. Such free drug reductions and calculations lead to the conclusion that the liposomes tested are prime candidates for treating drug overdoses from a variety of tricyclic antidepressant drugs.

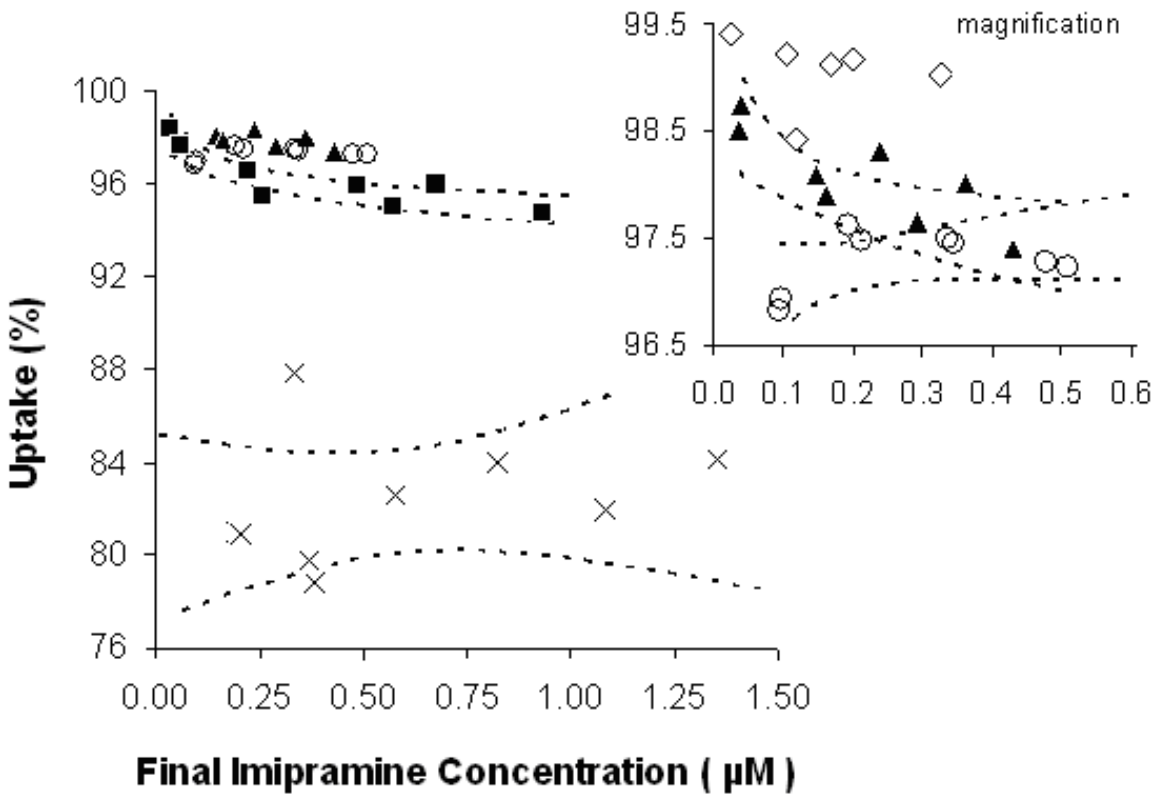

Figure 4-1. Percent imipramine uptake by human serum and by mixtures of human serum and 95:5 DOPG:DPPE-mPEG-2000 liposomes at lipid loadings of 0.72 and 1.44 mg lipid/mL (predicted via Equation 4-1) and mixtures of human serum and 95:5 DOPG:DPPE-mPEG-5000 liposomes at a lipid loading of 1.68 mg lipid/mL versus final imipramine concentration with 95% CI (dashed lines). Key: human serum (X); 95:5 DOPG:DPPE-mPEG-2000 at 0.72 mg lipid/mL (■); 95:5 DOPG:DPPE-mPEG-2000 at 1.44 mg lipid/mL (▲); 95:5 DOPG:DPPE-mPEG-5000 at 1.68 mg lipid/mL (O); prediction for 95:5 DOPG:DPPE-mPEG-2000 at 1.44 mg lipid/mL in human serum via Equation 4-1 (◇).

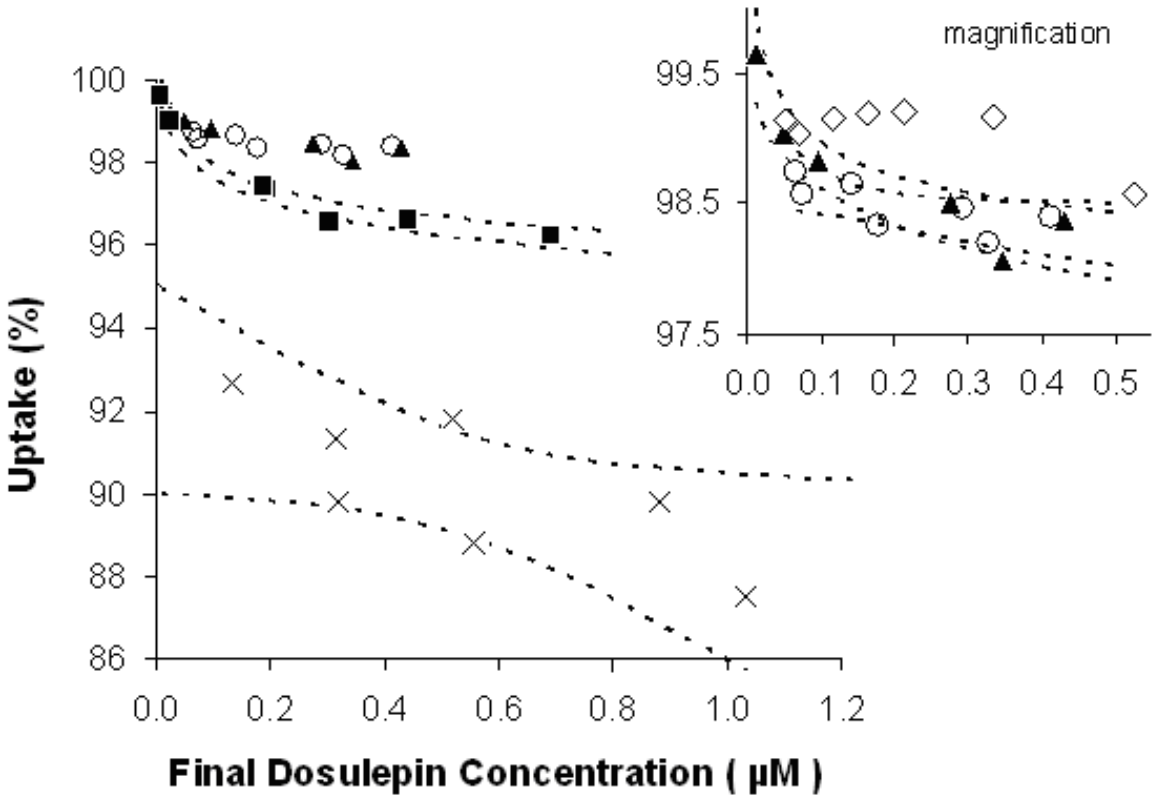

Figure 4-2. Percent dosulepin uptake by human serum and by mixtures of human serum and 95:5 DOPG:DPPE-mPEG-2000 liposomes at lipid loadings of 0.72 and 1.44 mg lipid/mL (predicted via Equation 4-1) and mixtures of human serum and 95:5 DOPG:DPPE-mPEG-5000 liposomes at a lipid loading of 1.68 mg lipid/mL versus final dosulepin concentration with 95% CI (dashed lines). Key: human serum (X); 95:5 DOPG:DPPE-mPEG-2000 at 0.72 mg lipid/mL (■); 95:5 DOPG:DPPE-mPEG-2000 at 1.44 mg lipid/mL (▲); 95:5 DOPG:DPPE-mPEG-5000 at 1.68 mg lipid/mL (O); prediction for 95:5 DOPG:DPPE-mPEG-2000 at 1.44 mg lipid/mL in human serum via Equation 4-1 (◇).

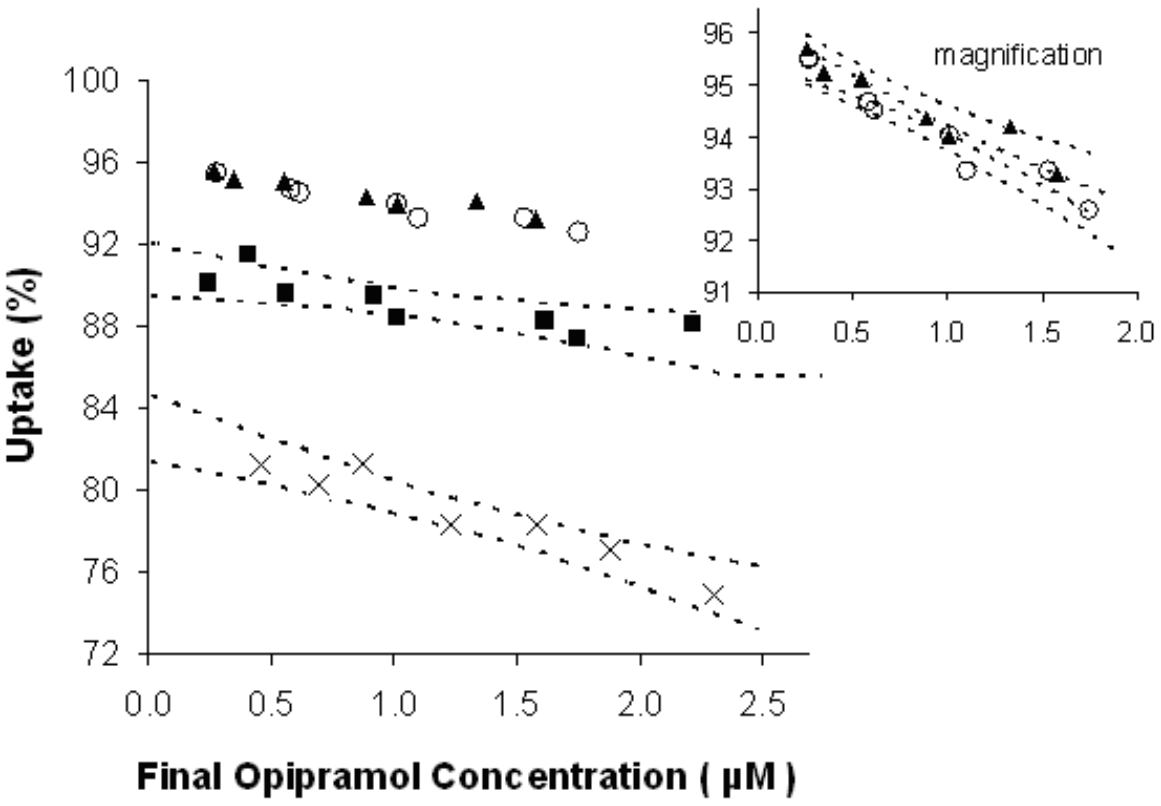

Figure 4-3. Percent opipramol uptake by human serum and by mixtures of human serum and 95:5 DOPG:DPPE-mPEG-2000 liposomes at lipid loadings of 0.72 and 1.44 mg lipid/mL and mixtures of human serum and 95:5 DOPG:DPPE-mPEG-5000 liposomes at a lipid loading of 1.68 mg lipid/mL versus final opipramol concentration with 95% CI (dashed lines). Key: human serum (X); 95:5 DOPG:DPPE-mPEG-2000 at 0.72 mg lipid/mL (■); 95:5 DOPG:DPPE-mPEG-2000 at 1.44 mg lipid/mL (▲); 95:5 DOPG:DPPE-mPEG-5000 at 1.68 mg lipid/mL (O).

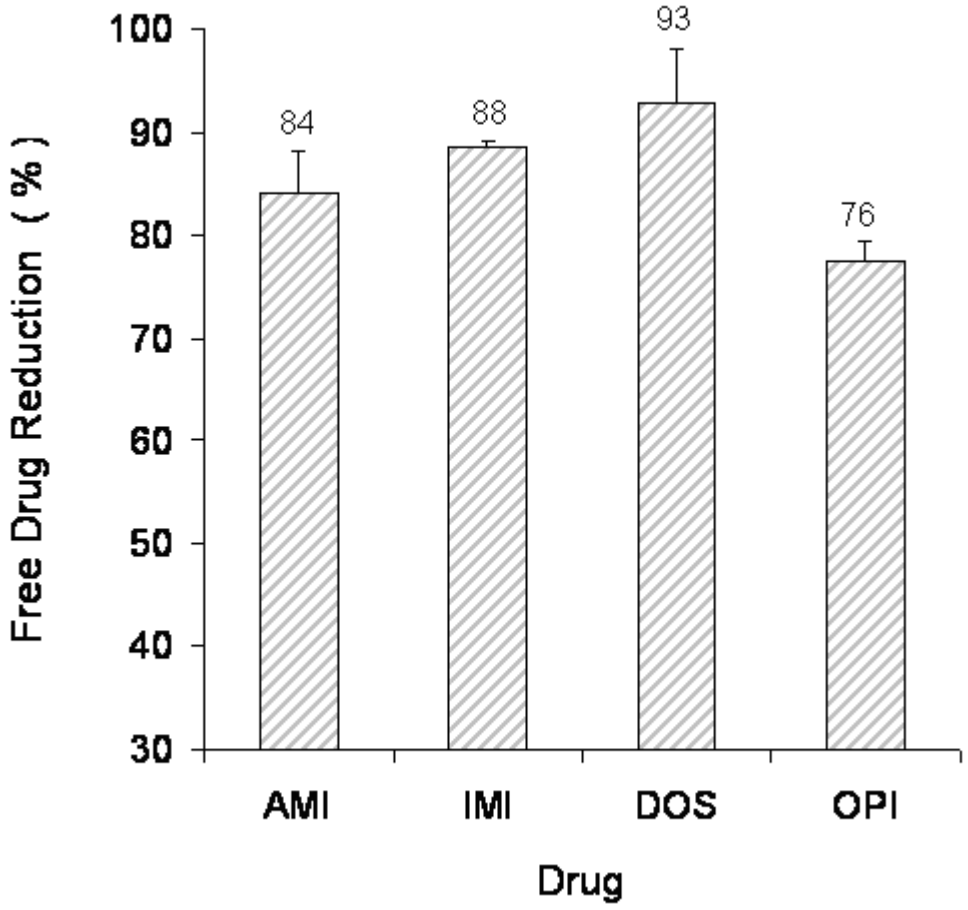

Figure 4-4. Free drug concentration reductions for amitriptyline, imipramine, dosulepin, and opipramol in human serum by 95:5 DOPG:DPPE-mPEG-2000 and 95:5 DOPG:DPPE-mPEG-5000 liposomes at loadings of 1.44 and 1.68 mg lipid/mL, respectively. Free drug reductions were calculated based on the differences between free drug concentrations in human serum samples and free drug concentrations in human serum samples mixed with liposomes.

Table 4-1. Association constant comparison for liposomes and red blood cells

Imipramine Concentration (μM)	K_a
2.0	112.7
3.5	40.2
6.5	85.7
9.3	75.3
11.7	79.5
16.1	67.3
Mean [a]	76.8
K_aRBC [b]	3.9

[a]Association constant for liposomes and imipramine from Equation 4-3. [b]Association constant for red blood cells and imipramine from Equation 4-2.

Table 4-2. Time between ingestion and treatment for antidepressant overdoses

Source	Subjects (N)	Avg Time (h)
[7]	1	4.00
[110]	21	3.05
[111]	3	2.30
[112]	4	4.00

Table 4-3. Pharmacokinetic properties of various organs and imipramine partition coefficients

Organ	V (L) [a]	Q (L/h) [a]	$K_{imipramine}$ [b]	KV / Q (h)	Type
Bone	2.9	41.7	6.6	0.46	Fast
Brain	0.4	6.8	7.8	0.45	Fast
Gut	1.9	44.8	20.8	0.88	Fast
Heart	0.2	16.8	16.9	0.23	Fast
Kidney	0.5	48.2	35.0	0.37	Fast
Liver	2.6	59.9	32.2	1.38	Fast
Lung	0.4	314.6	29.0	0.03	Fast
Spleen	0.1	6.8	22.2	0.45	Fast
Muscle	28.3	95.1	11.7	3.47	Slow
Skin	13.3	19.8	16.0	10.73	Slow
Adipose	5.3	23.9	18.8	4.18	Slow

[a]Organ volume (V) and blood flow rate (Q) from Rodgers et al. [106]. [b]Blood/tissue partition coefficients (K) calculated by Rodgers et al. [106] assuming an imipramine unbound fraction of 0.24.

Table 4-4. Comparison of drug detoxification vehicles

Source	Vehicle	Drug(s)	Mass Loading (mg/mL)	Maximum Uptake (buffer)	Medium	Free Drug Reduction in Medium[a]
Ch. 2, 3, 4	PEG - Liposomes	Amitriptyline Imipramine Dosulepin	1.68	99.50%	Human Serum	88%
Ch. 2, 3, 4	PEG - Liposomes	Opipramol	1.68	96.00%	Human Serum	76%
[24]	Nanocapsules	Haloperidol Docetaxel Paclitaxel	3	46.2% 75% 75%	3% Albumin	0% 60.8% 48.6%
[25]	Spherulites	Amitriptyline	2.5	98.10%	3% Albumin	97.30%
[70]	Spherulites	Haloperidol Docetaxel Paclitaxel	3	75.2% 94.4% 91.5%	Bovine Serum	38.3% No Data No Data
[19]	Nanoemulsions	Bupivacaine	11	90%	No Data	No Data
[21]	Nanocapsules	Quinoline Bupivacaine	14	>97% >99%	No Data	No Data
[22]	Oligochitosans	Amitriptyline	4	90.70%	No Data	No Data
[23]	Nanoparticles	Amitriptyline	1	90%	No Data	No Data

[a]Refers to the difference between the free drug concentration in the presence of proteins and the free drug concentration in the presence of proteins and detoxifying agents.

CHAPTER 5
BUPIVACAINE BINDING TO PEGYLATED LIPOSOMES

5.1 Introduction

In Chapters 2, 3, and 4, pegylated, anionic liposomes were proven capable of sequestering tricyclic antidepressants. Local anesthetics represent another class of charged drugs for which adverse reactions are a major concern. The development of an overdose treatment capable of treating multiple drug classes would greatly increase its utility. We hypothesized that an IV delivery of anionic liposomes after a local anesthetic overdose could reduce the free drug concentration of the drug in the blood stream and lead to the redistribution of the drug from vital organs to the blood compartment and possibly other sink organs as well. Accordingly, the goal of this chapter was to again use in vitro experiments to assess the ability of uni and multilamellar, polymer coated, anionic liposomes to sequester the local anesthetic bupivacaine (BUP) from buffer solutions and human serum. In addition to testing liposome-drug binding within a new drug class, this chapter also includes another strategy for increasing liposome-drug affinity: the use of multilamellar liposomes.

5.2 Methods

5.2.1 Liposome Preparation

Liposomes composed of a molar ratio of 95:5 DOPG:DPPE-mPEG-2000 were prepared via extrusion (Avanti Polar Lipids, Alabaster, AL). Lipids were combined in their respective molar ratios and then dissolved in a 9:1 mixture (by volume) of 99.9% chloroform/99.9% methanol (Sigma-Aldrich, St. Louis, MO) such that a 21 mg/mL concentration of lipids was obtained. The organic solvent was then evaporated under a stream of nitrogen. After an even and uniformly dried lipid film was obtained, the dried

lipid layer was hydrated with PBS (Sigma-Aldrich, St. Louis, MO). The lipid concentration after hydration was 16 or 25 mg lipid/mL PBS, depending on the final lipid loading desired. The lipid suspension was then mixed for 1-2 minutes on level 5 using a Mini Vortexer mixer (Fisher Scientific, Pittsburg, PA). Unilamellar liposomes were then bath sonicated at room temperature for 20 minutes using a G112SP1 Special Ultrasonic Cleaner (Avanti Polar Lipids, Alabaster, AL), whereas multilamellar liposomes were not immediately sonicated. The lipid suspensions were then heated to 30°C and stirred overnight for approximately 20 hours. After stirring, the unilamellar liposomes were extruded through a 100 nm membrane 15 times using an Avanti Mini-Extruder (Avanti Polar Lipids, Alabaster, AL). The size distributions of the extruded liposomes measured by dynamic light scattering are reported in Chapter 3. The liposomes had a mean diameter of 118 ± 15 nm. To make multilamellar liposomes, the lipid dispersion was bath-sonicated for 2 minutes after the overnight stirring. Such short bath sonication times produce multilamellar liposomes [27].

5.2.2 In Vitro Drug Binding Measurements in Buffer or Human Serum

Liposome solutions at loadings of 16 or 25 mg/mL were added to solutions of bupivacaine hydrochloride (Sigma-Aldrich, St. Louis, MO) in PBS or human serum (Fisher Scientific, Pittsburg, PA) such that the volume of the liposome dispersion added was 9% or 11.6% of the final solution volume, giving final lipid loadings of 1.45 or 2.9 mg lipid/mL. These mass loadings were chosen based on results from Chapters 2-4, where similar loadings allowed liposomes to compete with serum proteins for antidepressant binding. Multilamellar liposomes were added at a lipid concentration of 1.45 mg lipid/mL, and a higher binding affinity was observed compared to unilamellar liposomes at the same loading. Based on the increased binding, it would seem logical

to focus on multilamellar liposomes. However, large liposomes will be cleared from systemic circulation into the liver and spleen faster than smaller liposomes, which may not be desirable. Such issues can only be conclusively addressed through in vivo experiments, but, because of the slower clearance, we believe unilamellar liposomes to be more promising for drug overdose treatment. Thus, only unilamellar liposomes were measured at both 1.45 and 2.9 mg lipid/mL. Serum concentrations for BUP during infusion can range from 1 to 15 μM [118,119]. Circulatory collapse in ewes has been observed at concentrations as high as 27.7 μM [120]. Accordingly, the total BUP concentrations tested in our studies ranged from 5 to 50 μM. Control solutions of BUP in PBS and serum without liposomes were also prepared to allow for uptake quantification and comparison. After stirring for 15 minutes, the solutions were ultracentrifuged at 5000 rpm for 15-25 minutes in a 15 mL Centriprep Centrifugal Filter Device (Millipore Corp., Billerica, MA) containing an Ultracel YM10 filter (10,000 molecular weight cutoff). The concentration of BUP in the filtrate (free drug concentration) and the control solution was detected by measuring ultraviolet absorbance at 215 nm after passing the samples through a C18 column (Waters Corp., Milford, MA) using a 99.9% acetonitrile/50 mM KH_2PO_4 solvent mixture in a 25/75 ratio (Sigma-Aldrich, St. Louis, MO). The calibration curves for concentration versus area under the curve were linear with $R^2 > 0.99$. To ensure that all free BUP unbound to liposomes or proteins was accounted for, solutions of BUP at various concentrations were also filtered through YM10 filters and a calibration curve ($R^2 > 0.98$) was made and used to correct for the drug adsorbed to the membranes.

5.2.3 Statistical Analysis

Drug binding results were compared using the Student *t* distribution. Comparisons between drug uptake values or the amount of drug unbound to proteins and/or liposomes were made at each drug concentration because of the presence of interactions between drug concentration and the desired effect of study, which was the liposome loading or the presence or absence of liposomes. In most cases, drug binding was measured for each initial drug concentration at least twice (n = 2). Results were considered significant when $P < 0.05$.

5.3 Results

5.3.1 Bupivacaine Extracted from Buffer

The results for BUP extraction from PBS with 95:5 DOPG:DPPE-mPEG-2000 liposomes are shown in Figure 5-1. The unilamellar liposomes sequestered roughly 60%-65% and 77%-85% of BUP from PBS at 1.45 and 2.9 mg lipid/mL loading, respectively. The increased lipid loading increased the percent BUP uptake substantially at all BUP concentrations measured (P = 0.001, 0.002, <0.001, and <0.003 for 5, 20, 35, and 50 μM, respectively). Also shown in the plot are the drug uptake values measured for multilamellar liposomes at 1.45 mg lipid/mL. As Figure 5-1 shows, the drug binding increased from 60%-65% for unilamellar liposomes to 71%-90% for multilamellar liposomes at the same mass loading (P = 0.002, 0.001, 0.001, and 0.08 for 5, 20, 35, and 50 μM, respectively).

5.3.2 Bupivacaine Extracted from Human Serum

The amount of BUP bound to serum proteins decreased as drug concentration increased (Figure 5-2). At low BUP concentrations, the percentage bound approached 90%, which is consistent with reported values [121]. When liposomes were added to

serum, the total bound fraction increased. The free BUP unbound to liposomes and/or proteins before and after liposome addition is shown in Figure 5-3. The liposomes reduced the free drug in solution by 36% (P = 0.037), 56% (P = 0.022), 47% (P = 0.042), and 50% (P = 0.018) for BUP concentrations of 5, 20, 35, and 50 μM, respectively.

5.4 Discussion

The treatment of local anesthetic-induced toxicity has rapidly evolved over the past 10 years with the emergence of lipid emulsion therapy [41,42,122]. Many case studies continue to provide evidence for the effectiveness of lipid emulsions at toxicity reversal in actual clinical settings [12-14,33-36,40]. However, two major issues surrounding the use of lipid emulsions are currently at the forefront. First, the doses of lipid emulsions required for toxicity reversal are potentially high. The resulting hyperlipidaemia could pose considerable risks to patients, many of which are unknown or not fully understood [43,45]. Second, the mechanism of toxicity reversal remains a major question associated with the use of lipid emulsions. The results from this chapter may offer some insights and potential for exploring these critical issues.

Our results for drug binding support the possibility of achieving significant free drug concentration reductions with liposomes, perhaps with doses lower than those used with lipid emulsions. In vitro BUP binding by lipid emulsions (Intralipid® 20%, Fresenius Kabi, Bad Homburg, Germany) and pluronic microemulsions in buffer was explored by Varshney et al. [19]. They tailored the pluronic microemulsions for maximum drug binding per unit mass by testing several pluronic surfactants, varying the oil to surfactant ratio, and adjusting the fatty acid chain length and concentration. The final concentration of lipid emulsion in the in vitro binding experiments was

approximately 1 mg/mL, which is about 30% lower than the lipid loadings considered in this chapter. At total BUP concentrations similar to those tested here, nearly 30% of BUP was bound to the lipid emulsions, which is about one-third of the drug bound to the liposomes. The total loading of pluronic microemulsions used (surfactant and oil) was 7.7 mg/mL, which is about 5 times the lipid loadings considered here. The maximum drug binding to the microemulsions was 60%, which is substantially less than the drug bound to the liposomes. Thus, comparison of in vitro measurements reported here with the data reported by Varshney et al. [19] suggest that pegylated, anionic liposomes composed of DOPG lipids have more BUP bound per unit mass than lipid emulsions or pluronic microemulsions.

Liposomes sequester such large amounts of BUP and other drugs because of their unique structures and compositions (see Chapters 2,3, and 6). They can be tailored to more specifically target toxins because of surface charge and/or lipophilicity, and can be pharmacokinetically enhanced to circulate for long times through the use of polymers, such as polyethylene glycol. Approximately 83% of BUP, which has a pK_a value of 8.1, is in the charged state at physiological conditions [121,123]. Previous chapters have shown that anionic liposomes preferentially bind to cationic drugs. As drug delivery vehicles, liposomes have also been proven biocompatible. The results in serum confirm that liposomes can effectively compete with serum proteins for drug binding and could rapidly reduce the free drug in the blood compartment. This could, in turn, cause a redistribution of the drug from vital organs to the blood and/or other slowly equilibrating organs. Thus, we propose that liposomes, based primarily on redistribution, could be a more effective detoxification treatment than lipid emulsions

and could be applied to a wider array of drugs, including local anesthetics. The in vitro drug-binding data presented here provide the rationale for in vivo studies to test this hypothesis.

It has been proposed that lipid emulsions may reduce toxicity by either inducing drug redistribution from vital organs to the blood compartment and/or slowly equilibrating organs or the enhancement of oxidative metabolism [44]. The difficulty in discerning between these mechanisms stems from a lack of knowledge as to the destination of lipid emulsions and the time scales for transport to those destinations. Lipid emulsions most likely enter tissues, while polymer-coated liposomes of the type used in this chapter circulate in the bloodstream for some period of time. Our results strongly infer that liposomes bind more BUP per unit mass than lipid emulsions. Therefore, if liposome administration after an overdose reduces BUP toxicity, the mode of reversal will be related to redistribution. Furthermore, if redistribution is the dominant mechanism, then liposomes would be the better detoxification candidate.

5.5 Conclusions

In conclusion, pegylated, anionic liposomes were shown to be highly effective at sequestering the local anesthetic drug BUP from in vitro solutions with a removal efficiency of about 80% in buffer and a free-drug reduction of about 50% in human serum. The promising results present a rationale for further investigation into the treatment of local anesthetic toxicity with liposomes. Such liposomes may offer an alternative therapy to lipid emulsions or microemulsions at treating local anesthetic toxicity. Furthermore, in vivo comparisons of liposomes and lipid emulsions at treating drug toxicity may lead to an improved understanding of the mode of action of lipid emulsions.

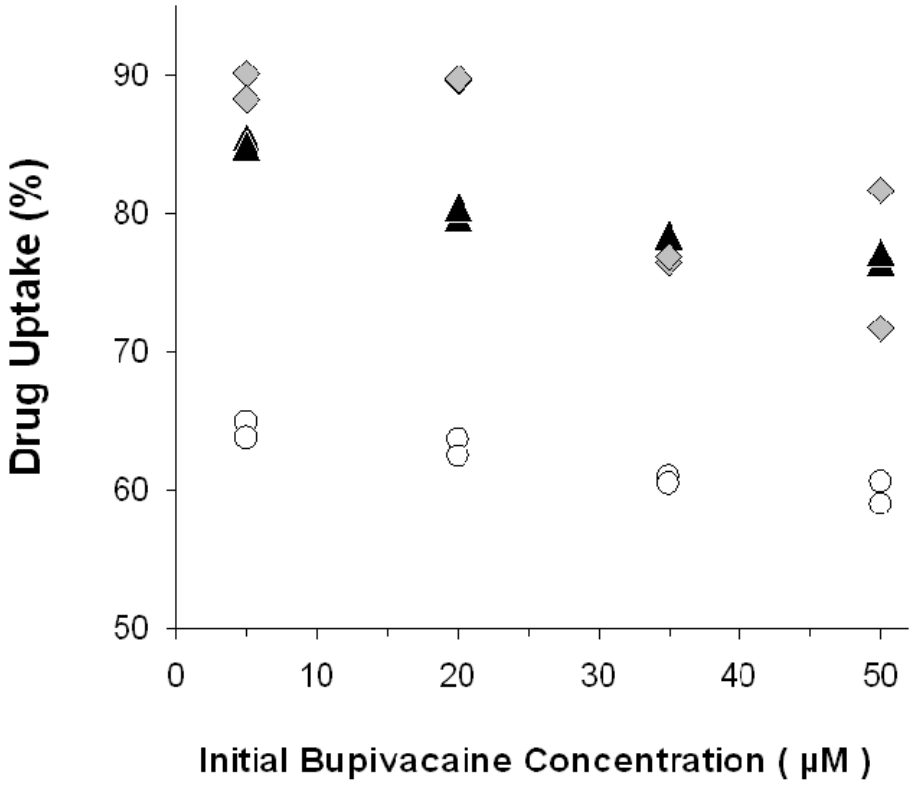

Figure 5-1. Percent of total bupivacaine bound to 95:5 DOPG:DPPE-mPEG-2000 liposomes in buffer solutions for unilamellar liposomes at lipid loadings of 1.45 (O) and 2.9 mg lipid/mL (▲) and multilamellar liposomes at 1.45 mg lipid/mL (◇); n = 2 at all concentrations.

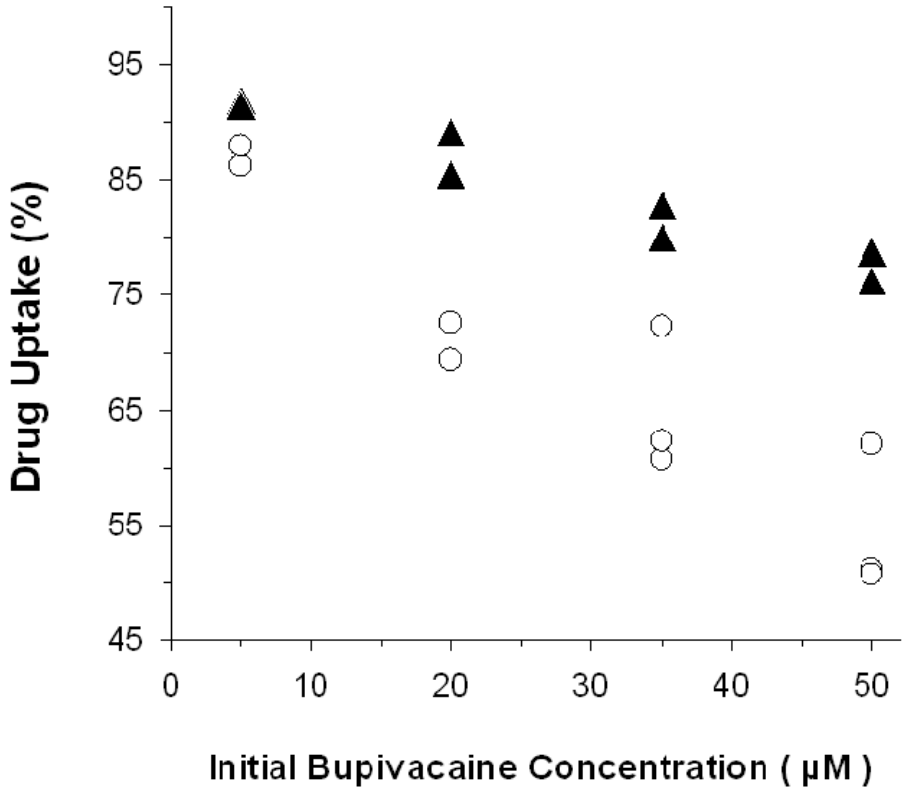

Figure 5-2. Percent of total bupivacaine bound in human serum (O) and in a mixture of human serum and unilamellar liposomes at 2.9 mg lipid/mL (▲); n = 2 for all measurements except serum binding at 35 and 50 µM, where n = 3.

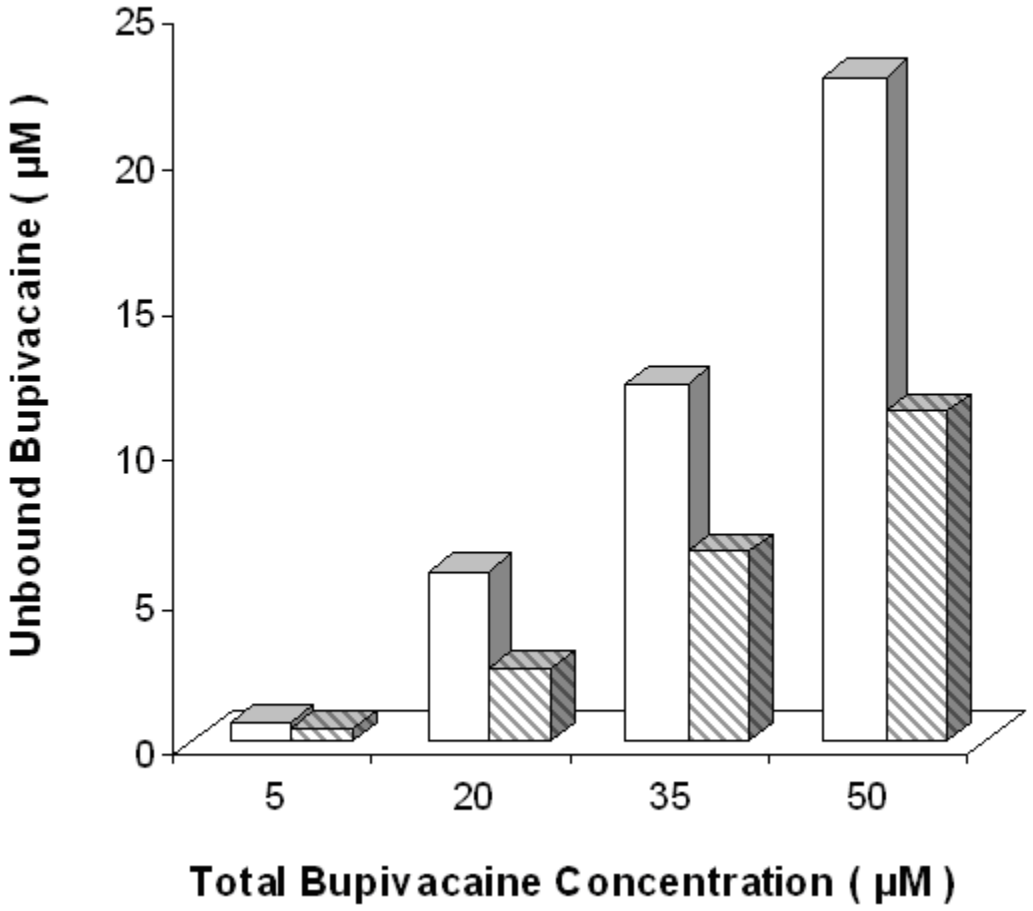

Figure 5-3. Free bupivacaine (unbound to proteins and/or liposomes) versus total bupivacaine concentration in human serum samples in the absence (☐) and presence (▨) of unilamellar, 95:5 DOPG:DPPE-mPEG-2000 liposomes at 2.9 mg lipid/mL calculated from data in Figure 5-2. Differences were significant at all concentrations tested (P = 0.037, 0.022, 0.042 and 0.018 for 5, 20, 35, and 50 µM, respectively).

CHAPTER 6
THE INTERACTION OF CATIONIC DRUGS WITH LIPOSOMES

6.1 Introduction

In the past several chapters, we have shown that anionic liposomes can sequester significant amounts of antidepressant and anesthetic drugs. It is imperative that the interactions responsible for such behaviors are well characterized. Such interactions are important for developing better drug overdose treatments, as well as for many other important membrane related applications related to drug delivery, cell viability, and so on. In this chapter, we focus on characterizing liposome-drug interactions via equilibrium binding and its effect on liposome permeability. Anionic and zwitterionic liposomes were used, along with bupivacaine (BUP), amitriptyline (AMI), and imipramine (IMI). The varying physical properties and structures of the drug molecules allowed a detailed understanding of the effects of these factors on binding and permeability. Additionally, binding was measured to charged poly(methacrylic acid) and poly(acrylic acid) microparticles with total charge comparable to liposomes to investigate the importance of the charge distribution (i.e., surface versus bulk) on binding. To explore the interactions, liposome properties such as surface charge, bilayer fluidity, and number of lamellae were varied, as well as the ionic strength of the bulk medium. The experimental results were supplemented by a continuum model that incorporated electrostatic interactions and a Langmuir binding isotherm. The model was validated by comparing predictions with experiments at high ionic strengths for unilamellar liposomes (ULL).

6.2 Materials and Methods

6.2.1 Materials

Methanol, chloroform, Dulbecco's Phosphate Buffered Saline (PBS) without calcium chloride and magnesium chloride (0.165 M ionic strength), ethylene glycol dimethacrylate (EGDMA), acrylic acid (AA), amitriptyline hydrochloride (AMI), imipramine hydrochloride (IMI), bupivacaine hydrochloride (BUP), and Sephadex G-50 (fine) were purchased from Sigma Aldrich (St. Louis, MO, USA). Dosulepin (dothiepin) hydrochloride (DOS) was purchased from LGC Promochem (Teddington, Middlesex, U.K.). Methacrylic acid (MAA) was purchased from Polysciences, Inc. (Warrington, PA). Ciba Darocur TPO, a photoinitiator, was a gift from Ciba Specialty Chemicals (Tarrytown, NY). Sodium chloride, Centriprep Centrifugal Filter Devices (Millipore Corp., Billerica, MA) containing Ultracel YM10 filters (10 000 molecular weight cutoff), Whatman GF/B glass microfiber filters, and calcein dye (fluorexon) were purchased from Fisher Scientific (Pittsburgh, PA). The lipids DOPG, dissolved in chloroform, DPPE-mPEG-2000, in powder form, DMPG, in powder form, and DMPC, in powder form, as well as a Mini-Extruder kit for liposome preparation, were purchased from Avanti Polar Lipids, Inc. (Alabaster, AL).

6.2.2 Liposome Preparation for Drug Binding and Zeta Potential Measurements

Liposomes composed of pure DOPG, pure DMPG, pure DMPC, and molar ratios of 50:50 DMPC:DOPG, 95:5 DOPG:DPPE-mPEG-2000, and 95:5 DMPG:DPPEmPEG-2000 were prepared via extrusion. Lipids were combined in their respective molar ratios and then dissolved in a 9:1 mixture (by volume) of chloroform:methanol such that a 12-20 mg/mL concentration of lipids was obtained. The organic solvent was then evaporated under a stream of nitrogen. The dried lipid layer was hydrated with PBS or

PBS that had an increased ionic strength of 1.5 M via sodium chloride. The lipid concentration ranged from 8 to 25 mg lipid/mL buffer. The lipid suspension was then bath sonicated for 20 minutes, heated to 30°C, and stirred overnight. After stirring, the liposome solution was extruded through a 100 nm membrane13-15 times to produce liposomes with diameters slightly greater than 100 nm. DOPG liposomes with diameters close to 40 nm were prepared via probe sonication as described in Chapter 2.

To prepare DOPG and 95:5 DOPG:DPPE-mPEG-2000 MLL, a similar procedure to the one described above was followed to obtain a hydrated lipid film. The dispersion was then vortex mixed for 2 minutes at medium speed, heated to 30°C, stirred for 24 hours, and bath sonicated for 2 minutes. Short bath sonication times are well-known to produce MLL [27].

6.2.3 Liposome Preparation for Calcein Leakage Studies

Liposomes composed of pure DOPG and a molar ratio of 95:5 DOPG:DPPE-mPEG-2000 were prepared as described above in Section 6.2.2, except the dried lipid layer was hydrated with 100 mM calcein dye dissolved in PBS such that the lipid concentration was 25 mg lipid/mL solution for pure DOPG and 28 mg/mL for 95:5 DOPG:DPPE-mPEG-2000. The mass loading was slightly higher for the PEG-2000 liposomes so that the number of charged head groups in the liposomes would be identical for both types of liposomes. The lipid suspension was then mixed using a Fisher vortex mixer for 1-2 minutes, followed by bath sonication for 20 minutes. The vesicles were then gently stirred overnight at 30°C for approximately 20 hours to increase the entrapped aqueous volume of liposomes [27]. After stirring, the liposome solution was extruded through a 100 nm membrane 15 times. To remove excess dye

from the bulk, the liposome solution was passed through a mini-column of Sephadex G-50 (fine) using the centrifugation method to ensure that almost all (≈90%) of the lipids added to the Sephadex bed were recovered [124]. The resulting liposome solution was diluted by a factor of 1001 based on the observation that the calcein release at the subsequent liposome loading was in the linear detection range of 0 to 10 μM even upon 100% calcein release after bilayer disruption.

6.2.4 Preparation of Poly(methacrylic acid) and Poly(acrylic acid) Microparticles

Porous poly(methacrylic acid) and poly(acrylic acid) microparticles were studied for their ability to remove AMI from solution. For particle synthesis, MAA or AA was combined with the cross-linker EGDMA. After purging with nitrogen to remove excess oxygen, the photoinitiator Ciba Darocur TPO was added, and 1 mL of the resulting mixture was added to 5 mL of ethyl acetate. The solution was then placed under a UV light source to induce polymerization. After the formation of microparticles, the ethyl acetate was boiled off to yield a gel of microparticles. The microparticles were added to PBS such that the concentration of microparticles was around 9 mg/mL, similar to the concentration of lipids in liposome dispersions previously described. The microparticles were then resuspended in the buffer solution with the use of bath and probe sonicators. The resulting microparticle suspension was then tested for its ability to remove AMI from buffer solutions as described in Section 6.2.6. The final concentration of microparticles was around 0.85 mg/mL and the AMI concentrations measured ranged from 1 to 50 μM.

6.2.5 Liposome Characterization

Mean diameters and size distributions for the liposomes were reported in Chapters 2 and 3 and elsewhere [71]. Briefly, the extruded ULL had diameters of 118 ± 15 nm and the probe sonicated ULL had diameters of 39.2 ± 4.5 nm. The bath sonicated MLL

produced widely varying size distributions with liposomes ranging from roughly 50 nm to 3 μm in size. The zeta potentials of the liposomes are reported in Table 6-1.

6.2.6 Drug Binding to Liposomes in Buffer Solutions

DOPG, DMPG, DMPC, 95:5 DOPG:DPPE-mPEG-2000, and 95:5 DMPG:DPPE-mPEG-2000 liposomes were added to buffer solutions containing drug such that the final lipid concentration ranged from 0.72 to 1.44 mg lipid/mL. Buffer solutions with ionic strengths of 0.165 M, which was the original ionic strength of the buffer, and 1.5 M were used. The increased ionic strength was achieved with the addition of sodium chloride. Control solutions of drug in PBS were also made to allow for uptake quantification and comparison. After being stirred for 15 minutes, the drug-liposome solutions were ultracentrifuged at 5000 rpm for 15 minutes in a vial that contained an Ultracel YM10 filter (10,000 molecular weight cutoff). Experiments were previously done to ensure that the systems were at equilibrium before filtration in Chapter 2. The filters were rinsed with DI water and then with PBS at 5000 rpm for 10 minutes prior to their use in the experiments. The concentration of the drugs in the filtrate (free drug concentration) and the control solution was detected by measuring UV absorbance at 215 nm after passing the samples through a C18 column (Waters Corp., Milford, MA, USA) using an acetonitrile/50 mM $NH_4H_2PO_4$ solvent mixture in a 35/65 ratio for AMI, IMI, and DOS, and an acetonitrile/50 mM KH_2PO_4 solvent mixture in a 25/75 ratio for BUP. The calibration curves for concentration versus area under the curve were linear with $R^2 > 0.99$. To ensure that all of the unbound drug was accounted for, solutions of the drugs at various concentrations were passed through YM10 filters in a separate test. Small amounts of drug were taken up by the filter, and correction curves were made and used to correct for drug adsorbed to the membranes in subsequent tests.

6.2.7 Zeta Potential Measurements

Zeta potential measurements were made for pure DOPG, pure DMPC, and 50:50 DMPC:DOPG liposomes for use in the model developed in Section 6.3.3. The measurements were made in PBS (0.165 M ionic strength) using a Brookhaven Zeta Plus machine with a voltage of 2.5 V at a field frequency of 2 Hz. At least 10 runs were done for each liposome type. Measurements were also done in PBS at AMI and BUP concentrations of 100 μM and 50 μM, respectively. The presence of drug molecules did not change the zeta potential values appreciably. Results are shown in Table 6-1. Measurements could not be made in 1.5 M ionic strength solutions due to extremely high conductance values.

6.2.8 Liposome Leakage Studies

The liposomes prepared by the methods described in Section 6.2.3 contain 100 mM calcein solution in the liposome core. This concentration is sufficiently high so that the fluorescence is quenched, resulting in negligible signal, except from the dye that diffuses out from the liposomes into the bulk [124]. The baseline fluorescence of the liposome solution prior to leakage was first measured using a Quantech Digital Filter Fluorometer with excitation and emission filters at 490 and 515 nm, respectively. A concentrated drug solution or PBS was then added, and the fluorescence was measured after 10 minutes. Drug concentrations of 0 (PBS), 8.6, 38, and 150 μM were studied for 95:5 DOPG:DPPE-mPEG-2000 liposomes. To compute the percent release, the following formula was used,

$$\%\ \text{Release} = \frac{F_t - F_o}{F_{total} - F_o} \text{ x } 100\,, \tag{6-1}$$

where F_t was the fluorescence measurement at time t, F_0 was the fluorescence at time zero, and F_{total} was the total calcein released, which was determined by breaking the liposomes with 100 µL of 20% (v/v) Triton X-100. Corrections were made to account for the dilution upon addition of the drug, PBS, protein, or Triton X-100 solutions. All release experiments were carried out at least twice.

6.2.9 Statistical Analysis

The data was analyzed using R, a free statistical software package developed by the R Project (http://www.r-project.org/). For the drug uptake experiments, ANOVA was used. In such cases, *P* values were reported and a significance level of 0.05 was assumed. When interactions were significant ($P < 0.05$), drug binding was analyzed for each drug concentration independently using the Student's *t* distribution. Error bars are presented in most of the results but are not always evident due to the small standard errors observed in some cases. The data are plotted and reported as mean ± standard error of the mean. Comparisons were made using the Student's *t* distribution. The 95% confidence intervals discussed in Section 6.3.2.2 were computed using JMP (SAS, Cary NC). The standard errors reported for the fitted parameters in Section 6.3.3 (a and K) were computed with R using a nonlinear least-squares (nls) model.

6.3 Results and Discussion

To facilitate the discussion of the results in this chapter, the structures of AMI, BUP, and the lipids used are shown in Figure 6-1. The structure of AMI is similar to all other TCA's. They have two distinct regions, a hydrophilic tail and a lipophilic, aromatic region. Their pK_a values are around 9.5, so that 99% of their molecules are in the charged form at pH 7.4 [106]. BUP has a more centrally located charge, is only 86% protonated at pH 7.4 (pK_a 8.2 at 25°C [123]), and has less surface activity compared to

TCA's. DOPG is anionic and possesses oleic acid carbon chains with cis double bonds at its ninth carbon, causing its gel to fluid phase transition temperature to be very low at -18°C. DMPC is zwitterionic and has saturated myristic acid chains, resulting in a gel to fluid phase transition temperature of 23°C. DMPG is anionic like DOPG but also has saturated myristic acid chains. Thus, the nonpolar interiors of DMPC and DMPG are most likely in the gel phase at room temperature.

6.3.1 Electrostatic Contribution to Drug Binding

To probe the importance of electrostatics in binding between cationic drugs and liposomes, various types of binding experiments were performed. First, anionic DOPG and 95:5 DOPG:DPPE-mPEG-2000 liposomes were tested in solutions of high ionic strength to probe the effect of electrostatics. Next, net neutral DMPC lipids were used to conclusively prove that charge was instrumental in achieving high drug sequestration. Lastly, porous microparticles with negative charge comparable to liposomes but dispersed uniformly throughout the particles were also tested for their drug binding ability to help determine whether or not the charge distribution and lipophilic nature of liposomes were important factors in binding.

6.3.1.1 Effect of ionic strength

If drug binding to liposomes is dominated by electrostatic effects, increasing the ionic strength should reduce drug binding due to shortening of the Debye length and screening of charge-charge interactions. In this case, buffer was used with an ionic strength, I, of 0.165 M, as well as buffer with NaCl added such that the ionic strength was 1.5 M. As described in Section 6.2.2, lipid bilayers were typically hydrated with the 1.5 M ionic strength solution during liposome preparation. In some cases, hydration was carried out with 0.165 M buffer and the ionic strength of the uptake medium was

adjusted to give a final value of 1.5 M. No differences were detected in binding for the two methods with ULL (P = 0.114, data not shown), demonstrating that sodium ions permeated through the bilayers and eliminated ionic strength gradients across the bilayers prior to filtration. The Debye lengths, calculated with the following equation for aqueous solutions at room temperature:

$$l_D = \frac{0.3045}{I^{0.50}}, \tag{6-2}$$

were 0.75 and 0.25 nm for the lower and higher ionic strength solutions, respectively. In addition, Equation 6-12 (see below) predicts the zeta potential change on the liposome surface to be approximately 50 mV for DOPG liposomes when transitioning from 0.165 to 1.5 M ionic strength, in agreement with the experimental results of Egorova [125] and McLaughlin [126].

Results from IMI and BUP uptake studies in both mediums with anionic ULL are shown in Figure 6-2. Clearly, the increased ionic strength reduced the drug uptake for IMI (P = 0.003 for 2.9 μM, P < 0.001 for 24.2 μM) and BUP (P < 0.001). The free fraction of drug was increased by a factor of roughly 2-5 for IMI and 2 for BUP, proving that electrostatics was a significant factor for drug binding in both cases. Furthermore, the amount of BUP bound per unit mass of lipid was less than the amount of IMI bound. This likely resulted from the lower proportion of charged molecules at pH 7.4 for BUP versus IMI, as well as for other reasons discussed later in Section 6.3.4.

6.3.1.2 Drug binding to neutral liposomes

To further explore the importance of electrostatics, drug binding to DMPC liposomes was measured, which have a much less negative surface charge than DOPG. This point is clear from the measured zeta potential values for both liposomes

shown in Table 6-1. The results in Figure 6-2 comparing binding to anionic and DMPC liposomes show that reducing the net negative charge drastically reduces the drug uptake for both IMI ($P < 0.001$) and BUP ($P < 0.001$). This, along with the reduced binding at higher ionic strengths, proves that the binding is dominated by electrostatic interactions between the cationic drug and the negatively charged surface of the liposomes.

6.3.1.3 Drug binding to anionic microparticles

To compare drug binding for microparticles and liposomes, AA and MAA microparticles were prepared and drug binding was measured. Similar experiments have been conducted elsewhere at AMI concentrations greater than 300 μM, which are significantly higher than concentrations explored here and also well beyond the relevant concentrations for drug overdose treatment [23]. At similar mass loadings to liposomes, both the MAA and AA microparticles were unable to sequester any significant amount of AMI from PBS. At 0.85 mg/mL, MAA and AA microparticles possess charges of -0.95 and -1.14 C/mL, respectively, compared to -0.18 C/mL for DOPG liposomes at 1.45 mg/mL. Thus, the ability for liposomes to bind large amounts of drug must be attributed to both their charged surfaces and lipophilic bilayers, as opposed to the charged microparticles, which lack a lipophilic component. Chakraborty and Somasundaran observed relatively large bindings to anionic microparticles at higher drug concentrations but also observed a reduction in binding upon lowering the drug concentration. Upon extrapolation of their results to the low physiological concentrations explored here, the results agree reasonably well [23].

6.3.2 Lipophilic Contribution to Drug Binding

Section 6.3.1 suggests that TCA's and BUP are preferentially attracted to negatively charged liposomes, whereupon they are bound and retained. This observation provides no information about the conformation of the drugs after binding. Drugs could reside in the charged double layer surrounding the liposomes or enter the lipid bilayer to some degree. This issue was investigated through drug binding comparisons between liposomes with contrasting nonpolar, inner bilayers and liposomes with single or multiple concentric bilayers. Additionally, leakage of a water soluble fluorescent dye from the aqueous core of liposomes was monitored while in the presence of AMI, IMI, or BUP. The dye leakage experiments, when viewed in light of the liposome-drug binding results, afforded additional insight into the specific nature of the drug-bilayer interactions.

6.3.2.1 Drug binding with DMPG liposomes: the effect of bilayer fluidity

The difference in bilayer fluidity between DOPG and DMPG is a useful probe for drug-bilayer interactions, since any corresponding change in drug bound would imply that drug-bilayer interactions are important, as opposed to drug-surface interactions alone. Drug binding for both lipid types is plotted as a function of initial drug concentration in Figure 6-2. The DOPG liposomes bound more drug than the DMPG liposomes for IMI ($P < 0.001$) and BUP ($P < 0.001$). The magnitude of the difference was about 2% and 10% of the total IMI and BUP present, respectively. This statistically significant difference in binding leads to the conclusion that both drug types are interacting with the lipid bilayers and suggest that drugs enter fluid bilayers more easily than gel bilayers. Also note the gap in binding for DMPG and DMPC lipids, again confirming the importance of electrostatic interactions.

6.3.2.2 Drug binding with multilamellar liposomes (MLL)

To confirm the hypothesis of drug-bilayer interaction from the bilayer fluidity tests, drug binding was measured with MLL. At equivalent mass loadings, MLL and ULL should bind equal drug amounts if the drugs readily cross lipid bilayers. Figure 6-2 shows the outcomes of AMI and BUP binding experiments using DOPG MLL. MLL bound more drug than ULL at equivalent mass loadings. The disparity is small for AMI due to the high proportion of total drug bound in both cases, but 95% confidence intervals (magnified portion of Figure 6-2) confirm this point. Considerably larger binding increases were observed for BUP at three of the four concentrations measured (P = 0.002, 0.001, 0.001, and 0.08 for 5, 20, 35, and 50 μM, respectively). The results prove that both drug types can cross the bilayers and that MLL bind more drug than ULL for the same lipid loading.

We believe this enhancement to be the result of electrostatic interactions or energy barrier reductions. For MLL without PEG, such as the ones shown in Figure 6-2 for AMI binding, the concentric bilayers were separated by a water layer approximately 1-3 nm thick [127,128]. This proximity allowed adjacent charged layers to interact, thereby increasing the effective potential experienced by the drug bound to the inner layers. BUP binding with PEG coated MLL must have been enhanced in a different way, since adjacent charged layers were separated by about 10 nm, making interaction negligible [129]. In this case, the dielectric constants of the aqueous layers between bilayers were decreased due to the presence of PEG. Aqueous PEG solutions have been shown to have lower dielectric constants than pure water, and this effect is mentioned for liposomes elsewhere as well [130,131]. Lower dielectric constants would reduce the surface potentials of the bilayers [131], which would act to reduce drug

binding based on the results presented thus far. However, there is a competing effect which we believe is overcoming the reduced surface potentials and actually increasing the amount of drug bound. As a result of the reduced dielectric constant, the energy barrier for the cationic drugs to enter the aliphatic bilayers is reduced. The charge-charge interactions are still key, but binding is more energetically favorable. This effect of reduced dielectric constants on ion transport across membranes has been extensively studied [132-134].

To demonstrate that binding was still driven by electrostatics in spite of the reduced energy barrier for membrane interaction, BUP binding to MLL prepared using PBS with salt added to increase the ionic strength to 1.5 M was measured (Figure 6-2). High ionic strength buffer was used to hydrate the liposomes to avoid ionic strength gradients across the bilayers, as such gradients could take long periods of time to disappear due to limited sodium permeability through the multiple layers of the MLL. The BUP binding was much lower than the MLL at the original ionic strength ($P < 0.001$). Additionally, the MLL in 1.5 M ionic strength solutions bound similar amounts of drug to ULL at 1.5 M ionic strength ($P = 0.935$). Thus, while enhanced drug binding stemming from energy barrier reductions for charge transfer across the membrane was important, electrostatic attractions still dominated. The effect of increasing the ionic strength of the medium overcame the lower dielectric constant effect of the aqueous layers.

6.3.2.3 Liposome leakage induced by drugs

In Figure 6-3, the percent of calcein release from pegylated, anionic liposomes 10 minutes after drug application is displayed. For AMI ($P < 0.001$ and $P < 0.001$) and IMI ($P = 0.001$ and $P < 0.001$), leakage at 38 μM and 150 μM was significantly greater than

the control. For BUP, significant leakage was only observed at 150 μM (P = 0.016). Even at 150 μM, BUP provoked less leakage than the TCA's at 38 μM. Despite the higher percentage of drug bound for AMI and IMI compared to BUP, this factor alone cannot account for the differences in leakage because the number of drug molecules bound to the liposomes is larger for BUP at 150 μM compared to TCA's at 38 μM. Results with DMPG and MLL showed that both TCA's and BUP traverse the lipid bilayers easily and likely reside there to some extent. Thus, it is clear that the conformation of TCA's in the bilayer must be such that they enhance the bilayer permeability more than BUP. This seems plausible upon examination of the drug structures. The two contrasting regions of TCA's are structurally separated, which would allow the lipophilic portion to associate with the bilayers and the charged region to extend into the bulk phase. This dual association would disrupt the bilayer significantly. BUP, by contrast, probably remains inside the nonpolar region to a greater degree and alters the bilayer structure to a lesser extent.

6.3.3 Mechanism Validation through Continuum Modeling

6.3.3.1 Model development

All of the experimental findings presented in Chapter 6 thus far point to a combinatorial drug uptake mechanism that includes both electrostatics and drug-bilayer interactions. To further validate that observation, a continuum model was developed and validated by matching model predictions to experiments in solutions of increased ionic strength.

If the Poisson-Boltzmann equation for the potential distribution around spherical surfaces, such as liposomes, is solved under the Debye-Huckel approximation, the following equation is obtained:

$$\psi = \frac{R\zeta}{r} e^{-\kappa (r-R)}, \tag{6-3}$$

where ζ is the zeta potential, r is the radial coordinate with its origin at the center of the liposome, R is the liposome radius, and κ is the inverse of the Debye length [135]. To determine the amount of drug sequestered in the double layer, one can solve the species conservation equation for the drug to obtain

$$C(r) = C_\infty e^{-\frac{e\psi}{kT}}, \tag{6-4}$$

where C(r) is the drug concentration in the double layer as a function of the radial coordinate, C_∞ is the bulk drug concentration far from the liposome surface, *e* is the elementary charge, k is the Boltzmann constant, and T is the temperature. An overall mass balance on the drug gives

$$4\pi N_L \int_0^\infty (C(r) - C_\infty) r^2 dr + C_\infty + S_p \Gamma = C_i, \tag{6-5}$$

where C_i is the total drug concentration, N_L is the number of liposomes per volume, Γ is the concentration of the drug specifically bound to the bilayer surface, and S_p is the surface area of the liposomes per volume, which is given by

$$S_p = \frac{\rho_l N_A f A^0}{(MW)}, \tag{6-6}$$

where MW is the average molecular weight of the lipids present (excluding PEG), N_A is Avogadro's number, ρ_l is the lipid loading in the solution (excluding PEG), f is the fraction of lipid molecules that participate in drug binding, and A^0 is the average area per lipid molecule on the surface. In the limit of double layer thickness (typically a few

nm) much smaller than the liposome radius (>50 nm), the concentration profile simplifies to

$$C = C_\infty e^{\frac{-e\zeta}{kT}(e^{-\kappa y})}, \tag{6-7}$$

where y is the distance from the liposome surface. The overall mass balance also simplifies to

$$C_\infty\left(1 + S_P\int_0^\infty\left(\exp(-\frac{e\zeta}{kT}\exp(-\kappa y)) - 1\right)dy\right) + \Gamma S_P = C_i \tag{6-8}$$

.

The specific drug binding of drugs to lipid bilayers can be modeled as a Langmuir isotherm [57]:

$$\Gamma = \frac{a\,C(r=R)}{K + C(r=R)} = \frac{a\,C_\infty e^{-\frac{e\varsigma}{kT}}}{K + C_\infty e^{-\frac{e\varsigma}{kT}}}, \tag{6-9}$$

where a and K are the parameters of the isotherm. The zeta potentials used for modeling drug binding at 0.165 M ionic strengths were measured, whereas changes due to an increased ionic strength were calculated as detailed below (Table 6-1). Zeta potential values were also measured in the presence of AMI (100 μM) and BUP (50 μM), but the values were relatively unaffected by drug binding. PEG chains have a negligible effect on the surface potential of liposomes but move the slipping plane away from the liposome surface, leading to changes in zeta potential. As a result, zeta potential measurements for pegylated liposomes are less representative of the true surface potential characteristics when compared to unpegylated liposomes.

Measurements were therefore made for unpegylated liposomes and used for pegylated liposomes with similar lipids [136]. In Equation 6-6, the value used for f was 1, since experiments have already shown that all drugs tested can pass through MLL and bind to both sides of the bilayers. Also, the molecular weights and lipid loadings used were corrected to exclude the PEG, as the bulk of the PEG is extended into the aqueous phase on either side of the liposome bilayer and should have little bearing on drug binding. All data used for model fitting or model validation was derived using ULL extruded with 100 nm membranes. The values used for the constants in Equations 6-6 through 6-12 are listed in Table 6-1, along with ranges of previously reported values for similar systems for comparison.

6.3.3.2 Model fits to data for antidepressant drugs

Initially, the amount of AMI bound exclusively within the double layer of DOPG liposomes (1.44 mg/mL) at an AMI concentration of 25 μM was estimated by calculating the first term on the left-hand side of Equation 6-8. The model predicted that a zeta potential value of -50 mV would yield double layer binding of less than 1%. Based on our observations reported in Section 6.3.1 and previous chapters, the drug uptake actually approaches 99% in some cases, providing strong evidence for significant drug-bilayer interactions [71].

Accordingly, Equation 6-8 was used in combination with AMI uptake data by 40 nm, pure DOPG liposomes at a lipid loading of 0.72 mg/mL reported in Chapters 2 and 3 to estimate the parameters a and K under the assumption that the drug molecules were located both in the double layer and the lipid bilayer. The data used ranged from an initial AMI concentration of 1 μM to around 110 μM. Figure 6-4a shows the experimental data and the fitted data based on Equation 6-8. The values of the fitting

parameters, a and K, were 5.36 x 10^{-7} ± 3.3 x 10^{-8} mol/m^2 and 1.88 x 10^{-2} ± 2.1 x 10^{-3} mol/m^3, respectively. The fit was very good, indicating that a combination of electrostatic and lipophilic interactions is a more plausible explanation for the results obtained, rather than simple double layer electrostatics. Based on the value of a obtained from the fit, the area per drug molecule at maximum packing is about 310 $Å^2$, which is about 5 times the area per molecule for the lipid heads.

In Figures 6-4b through 6-4d, the values of a and K for AMI binding to the DOPG liposomes were used to estimate AMI, IMI, and DOS binding by pegylated, anionic liposomes. The fits were all reasonable, suggesting that pegylated and unpegylated liposomes exhibit similar interactions with the drugs, and that the different TCA's exhibit similar interactions with the liposomes due to similarities in their molecular structures.

6.3.3.3 Model fits to data for bupivacaine

The overall mass balance for BUP is

$$C_\infty + \left(C_{p_\infty} S_P \int_0^\infty \left(\exp(-\frac{e\zeta}{kT}\exp(-\kappa y)) - 1 \right) dy \right) + \Gamma S_P = C_i , \qquad (6\text{-}10)$$

where $C_{p\infty} = 0.86C_\infty$ is the bulk concentration of the protonated form of the drug [123]. The specific drug binding of BUP to lipid bilayers can be modeled as a sum of two isotherms, one each for the protonated and the unprotonated forms. The concentration of the protonated form in the bulk, $C_{p\infty}$, is about 6 times that of the unprotonated form, C_∞, and the negative zeta potential further enhances the concentration of the protonated form near the liposome surface by a factor of $e^{-e\varsigma / kT}$. Thus, the binding contribution from the unprotonated form can be neglected, and the specific binding is given by the following equation:

$$\Gamma = \frac{a\, C_p(r = R)}{K + C_p(r = R)} = \frac{a\, C_{p_\infty}\, e^{-\frac{e\zeta}{kT}}}{K + C_{p_\infty}\, e^{-\frac{e\zeta}{kT}}}, \qquad (6\text{-}11)$$

where a and K are the parameters of the isotherms for the protonated form. BUP binding to anionic, pegylated liposomes was significantly lower than for TCA's, and fitting the binding data to the model (Figure 6-4e) yielded an a/K ratio of $3.68 \times 10^{-7} \pm 6.9 \times 10^{-9}$ m. The concentration range tested for BUP was within the linear range, and so determination of individual values of a and K was not possible. The a/K ratio for BUP was about 2 orders of magnitude lower than for TCA's, proving that BUP has a significantly lower affinity for liposomes, likely stemming from the reduced proportion of charged BUP compared to TCA's, and its inability to associate with the charged lipid heads once inside the bilayer. Note that the pK shift for local anesthetics inside lipid bilayers is minimal, leading to a similar proportion of charged drug in the bilayer and the bulk [137].

6.3.3.4 Effect of surface charge on isotherm parameters

The presence of charge on the liposome surface likely contributes to increased drug binding through two mechanisms. First, the negative surface potential leads to an elevated drug concentration near the surface, and thus an increased concentration in the bilayer. This effect is evident in the exponential factor in Equation 6-9. Second, the adsorbed molecules could still interact with the charged surface, resulting in an increased partitioning reflected in the binding isotherm parameters a and K. If the increased binding is purely due to the first effect, i.e., the enhanced surface

concentration, the binding parameters a and K should be relatively similar for both charged and uncharged liposomes.

In Chapter 2, we observed up to 99% of total AMI in solutions bound to liposomes composed of 50:50 DMPC:DOPG. The DOPG liposomes carry a negative zeta potential (-50.9 mV) which is significantly larger in magnitude compared to DMPC liposomes (-6.6 mV) at 0.165 M ionic strength, whereas the 50:50 DMPC:DOPG liposomes more closely resemble the DOPG system (-42.7 mV). The drug uptake data for 50:50 DMPC:DOPG liposomes was fitted with Equation 6-8 (Figure 6-4f) and new values for a and K were obtained ($a = 6.43 \times 10^{-7} \pm 4.2 \times 10^{-8}$ mol/m^2, $K = 5.90 \times 10^{-2} \pm 5.5 \times 10^{-3}$ mol/m^3). The area per molecule for the 50:50 DMPC:DOPG liposomes was assumed to be the mean of the area per molecule of pure DMPC and pure DOPG liposomes. The values of a for both liposome types were similar, whereas K was three times larger for the mixed system, implying that the 50:50 DMPC:DOPG liposomes have a lesser affinity for the drug in the dilute regime. The value of maximum uptake is similar for both systems, but the saturation occurs at a higher concentration for the 50:50 DMPC:DOPG liposomes due to the lower affinity. The value of a was most likely similar due to the fact that DOPG and DMPC lipids are well-mixed in these systems [138], and the maximum drug to lipid ratio observed in these experiments was only 0.12. Additionally, the value of a could be limited by the size of the drug molecules and interactions between bound drug molecules.

The binding of IMI and BUP to DMPC liposomes was simulated using the a and K values obtained with purely anionic liposomes previously mentioned and the measured value of zeta potential (Table 6-1). A good fit to the DMPC data with the same a and K

values would imply that increased drug affinity for anionic liposomes stems purely from increased concentrations near the liposomes, and that bound molecules do not interact with the charged surface. Conversely, if the fitted values failed to accurately predict the drug uptake, it could be viewed as strong evidence for direct interaction between charged drug sites and lipid head groups. The drug uptake results and predicted values for TCA's are compared in Figure 6-5a. Clearly, the predictions were not good, confirming that cationic TCA's interact with DMPC and DOPG differently. In Figure 6-5b, the a/K ratio previously obtained for BUP and anionic liposomes was used to predict BUP binding to DMPC vesicles. Again, the model significantly over predicted the amount of drug bound, and points to interactions between bound BUP molecules and lipid head groups. However, the discrepancy between the model and the data for BUP is slightly less than that for IMI, supporting the previous hypothesis that BUP interacts with the charged lipid head groups to a lesser extent than TCA's.

6.3.3.5 Model validation via salt effects

The model proposed above can be used to predict the effect of increased ionic strength on binding without introducing any new parameter. The fitted a and K values for TCA's and BUP from above were used to predict drug binding with anionic vesicles under such conditions. The liposome zeta potential change (Table 6-1) was estimated via surface potential calculations using the following equation [135]:

$$\zeta = \frac{2kT}{e}\sinh^{-1}[\sigma^{*}(8\varepsilon kT n_{\infty})^{-\frac{1}{2}}], \tag{6-12}$$

where σ* is the surface charge density expressed as a function of A^0, the surface area per charge, in the following way:

$$\sigma^* = \frac{e}{A^o} \quad , \tag{6-13}$$

and n_∞ is the number of ions per cubic meter in the bulk, calculated by the equation below:

$$n_\infty = 1000 N_A I \, , \tag{6-14}$$

where I is the ionic strength of the medium. Based on Equation 6-12 and published experimental results [125,126], the zeta potential of the liposomes decreases by about 50 mV at an ionic strength of 1.5 M. In Figures 6-5c and 6-5d, experimental and predicted binding is compared for IMI and BUP. The calculated values for the amount of each drug bound agreed well with the experimental values. The model demonstrates that increasing the ionic strengths of the solutions reduced the amount of drug bound by reducing the bulk drug concentration in the immediate vicinity of the liposomes.

Fisar et al. also fitted binding data for IMI to both charged and uncharged liposomes and showed that neutral phosphatidylcholine (PC) liposomes were less effective at binding to IMI than anionic phosphatidylserine (PS) vesicles [57]. Somewhat similar values for the parameters denoted herein as a and K ($a = 9.4 \times 10^{-7}$ mol/m^2, K = 0.12 mol/m^3) were reported for PS vesicles and IMI in their study. They attributed high IMI binding to electrostatic interactions in concurrence with van der Waals and hydrophobic interactions. Despite these similarities, our systematic variance of lipid charge and bilayer fluidity and structure, in combination with the inclusion of PEG-modified lipids, as well as our direct comparison between BUP and TCA's and the use of dye leakage to augment the binding and modeling results, allowed us to gain a deeper understanding of the drug-liposome interaction details.

6.3.4 Summary of the Proposed Mechanism of Drug Sequestration

To summarize the findings from this chapter, TCA's are attracted to anionic liposomes by electrostatic interactions and associate with lipid bilayers so that their charged regions interact with the charged phospholipid head groups, while their lipophilic, aromatic regions associate with the lipid bilayers. This is illustrated in Figure 6-6a (bilayer thickness and drug size is exaggerated for clarity). Because of their structures, which include distinct hydrophilic and lipophilic regions, they are able to associate with the bulk aqueous phase, the charged phospholipid head groups, and the lipid bilayers. BUP, however, with a more centrally located charge, sits within the lipid bilayers as depicted in Figure 6-6b. It is again attracted to the vesicle through electrostatics and is also positioned so that charge-charge interactions are maximized, but interacts with the bulk phase and the phospholipid head groups to a lesser extent. The increased drug-liposome affinity for TCA's over BUP stems from two factors. First, the lower pK_a of BUP when compared to TCA's results in a lower proportion of BUP molecules in the charged state. Second, the unique structures of TCA's afford them very distinct lipophilic and hydrophilic regions, allowing them to reach a lower energy state than BUP within lipid bilayers.

Austin et al. and Deo et al. proposed similar mechanisms for cationic drug uptake by liposomes [55,72]. In both cases, charge was identified as a key aspect for high affinity binding. Sanganahalli et al. completed fluorescence spectroscopic studies using phosphatidylcholine liposomes and confirmed that both IMI and AMI penetrate lipid bilayers [58]. While studying the effect of BUP on model membranes composed of PC and phosphatidylethanolamine (PE), Suwalsky et al. [59] found that BUP interacted with the membranes to a significant degree and proposed that BUP partitioned into lipid

bilayers. More recently, Mizogami et al. studied the effects of BUP enantiomers on PC membranes and found that BUP disorders lipid bilayers in cholesterol free membranes and selectively associates with membranes when cholesterol is present [60]. These results clearly support the drug-liposome interaction details put forth in this chapter for both TCA's and BUP. In addition, our use of a common drug binding model and liposome leakage experiments allowed for a direct comparison of the drugs' bilayer conformations. Also, the use of MLL and ULL also provided new insight into the effect of PEG aqueous layers on inner bilayer surface charge.

6.4 Conclusions

In this chapter, drug binding experiments performed using filtration and centrifugation, calcein leakage from liposomes, and a Langmuir binding model were utilized to explore the mechanisms of drug binding to liposomes and anionic microgels. In spite of higher charge densities, anionic microgel particles bound significantly less drug than liposomes. The binding of tricyclic antidepressants such as AMI, IMI, and DOS was compared to each other and to the binding by the local amide anesthetic bupivacaine. The mechanisms, as validated with binding isotherm parameters, are similar for all TCA's but are significantly different for BUP.

The experiments and modeling indicate that the amount of drug molecules in the electrical double layer is negligible but the electrostatic effects play a major role in binding. The electrostatic interactions are responsible for the initial association between antidepressants and liposomes, whereupon the drug enters the bilayer with its charged region closely associated with the charged lipid head groups and its lipophilic region closely associated with the lipid bilayers. BUP, which is predominantly in the protonated state at pH 7.4 and 25°C as well (86%), is also preferentially attracted to the charged

vesicle [123]. Once bound, it appears to be located within the bilayer to a greater extent than the antidepressants with minimal interactions with the charged surface. The structure of BUP makes it less able to access the bulk aqueous phase surrounding or encompassed by the lipid bilayers. The conclusions regarding the differences in conformations between antidepressants and the anesthetic bupivacaine are supported by the fact that bupivacaine binding leads to a much lower increase in liposome permeability compared to antidepressant binding.

Drug binding is similar for both pegylated and unpegylated liposomes because the PEG layer is sufficiently porous to allow rapid drug diffusion. For both the pegylated and unpegylated cases, as well as both drug types, more drug is bound to multilamellar rather than unilamellar liposomes. This difference vanishes at high ionic strengths. We attribute the increased binding for multilamellar liposomes without PEG to enhanced electrostatic interactions between adjacent charged layers. For pegylated liposomes, the reduced dielectric constant in the aqueous-PEG layer between adjacent bilayers results in a lower energy barrier for cationic drug transport across the aliphatic tail region [130,132-134].

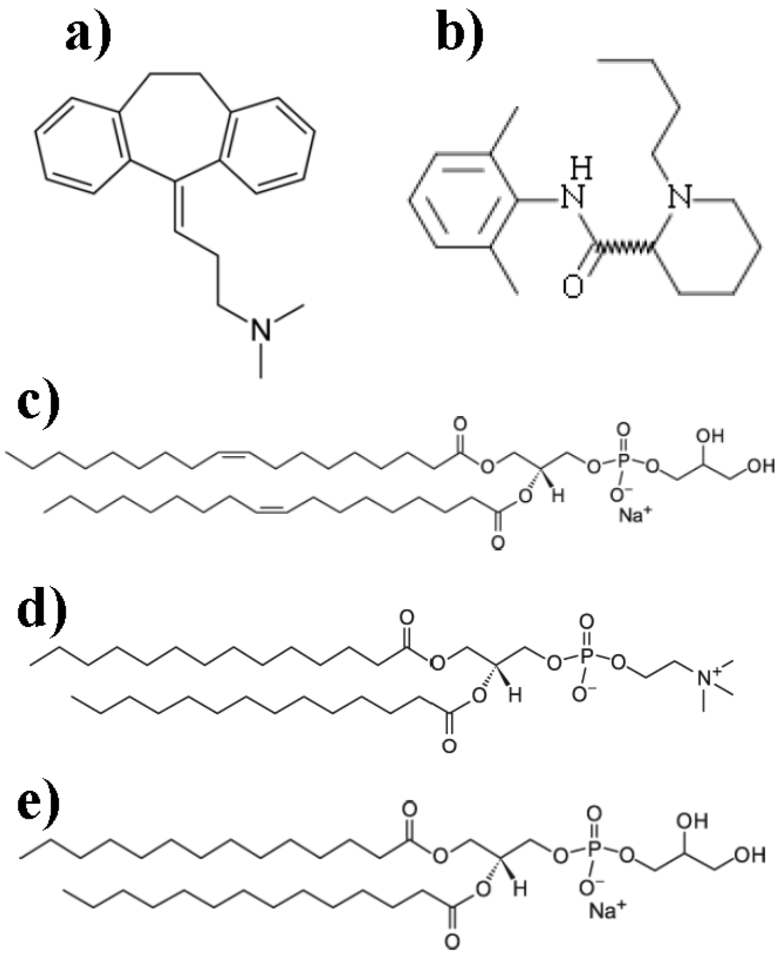

Figure 6-1. Structures of the drugs a) amitriptyline and b) bupivacaine and the phospholipids c) DOPG, d) DMPC, and e) DMPG used for studying drug-liposome interactions.

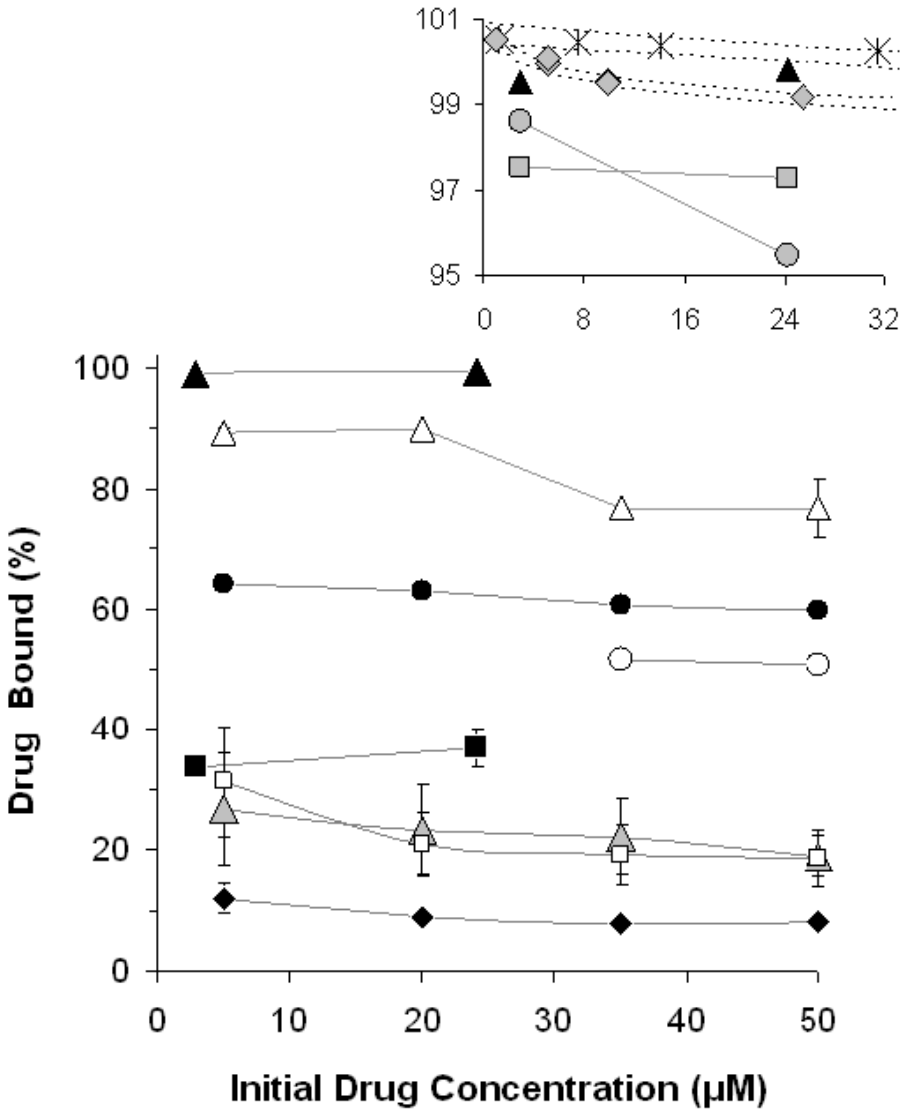

Figure 6-2. Percent of IMI bound to DOPG (anionic) ULL at 1.44 mg lipid/mL in solutions of 0.165 M (▲) and 1.5 M (●) ionic strength and to DMPG (anionic) ULL at 1.44 mg lipid/mL in solutions of 0.165 M ionic strength (■). Percent of AMI bound to DOPG (anionic) ULL (◇) and MLL (✳) at 0.72 mg lipid/mL in PBS with 95% confidence intervals shown. Percent of BUP bound to 95:5 DOPG:DPPE-mPEG-2000 (anionic) ULL at 1.44 mg lipid/mL in solutions of 0.165 M (●) and 1.5 M (△) ionic strength. Percent of IMI bound to DMPC ULL at 1.44 mg lipid/mL in PBS (■). Percent of BUP bound to DMPC ULL at 1.44 mg lipid/mL in PBS (◆). Percent of BUP bound to 95:5 DMPG:DPPE-mPEG-2000 (anionic) ULL at 1.44 mg lipid/mL in PBS (○). Percent of BUP bound to 95:5 DOPG:DPPE-mPEG-2000 (anionic) MLL at 1.44 mg lipid/mL in solutions of 0.165 M ionic strength (△) and 1.5 M ionic strength (□). Data are reported as mean ± standard error of the mean with n = 2, except for AMI binding data where all data points are shown and 95% CI displayed.

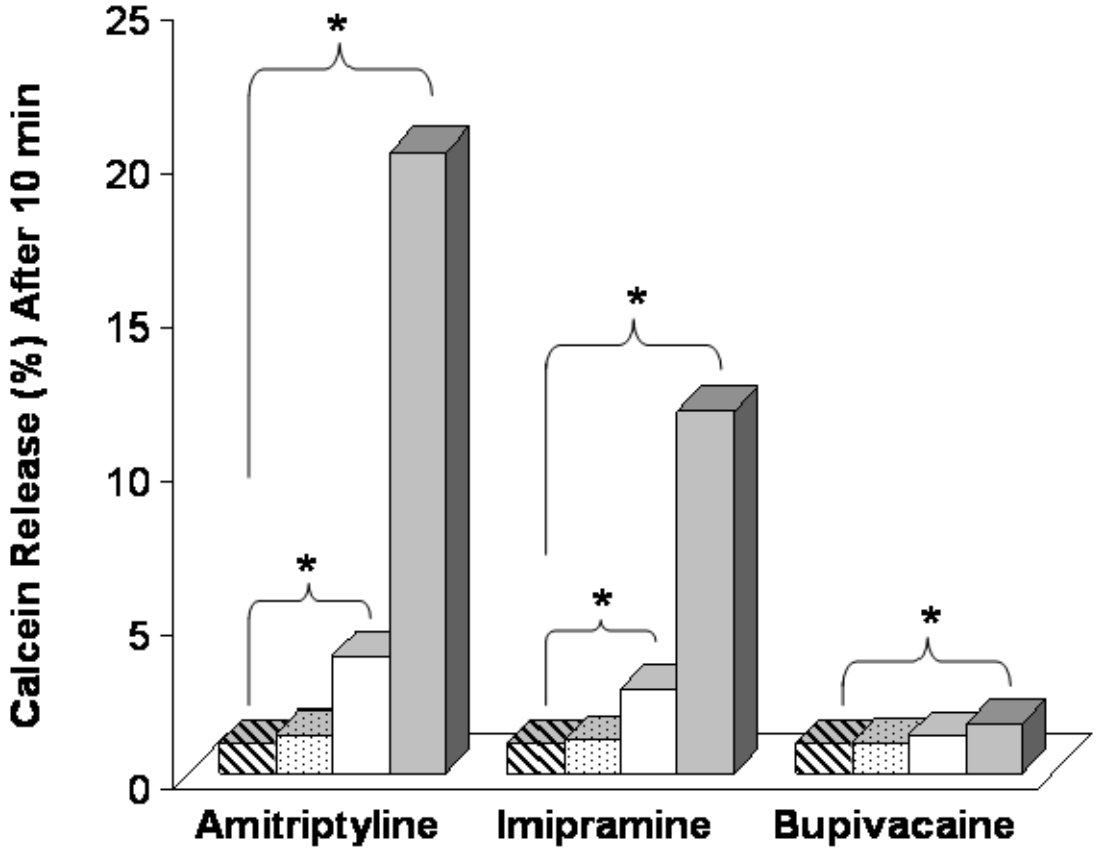

Figure 6-3. Percent of entrapped calcein released by 95:5 DOPG:DPPE-mPEG-2000 ULL 10 minutes after exposure to AMI, IMI, or BUP at drug concentrations of 0 (▨), 8.6 (⬚), 38 (□), and 150 (▭) μM. Means are shown with n = 2-4. Marker (*) denotes $P < 0.05$.

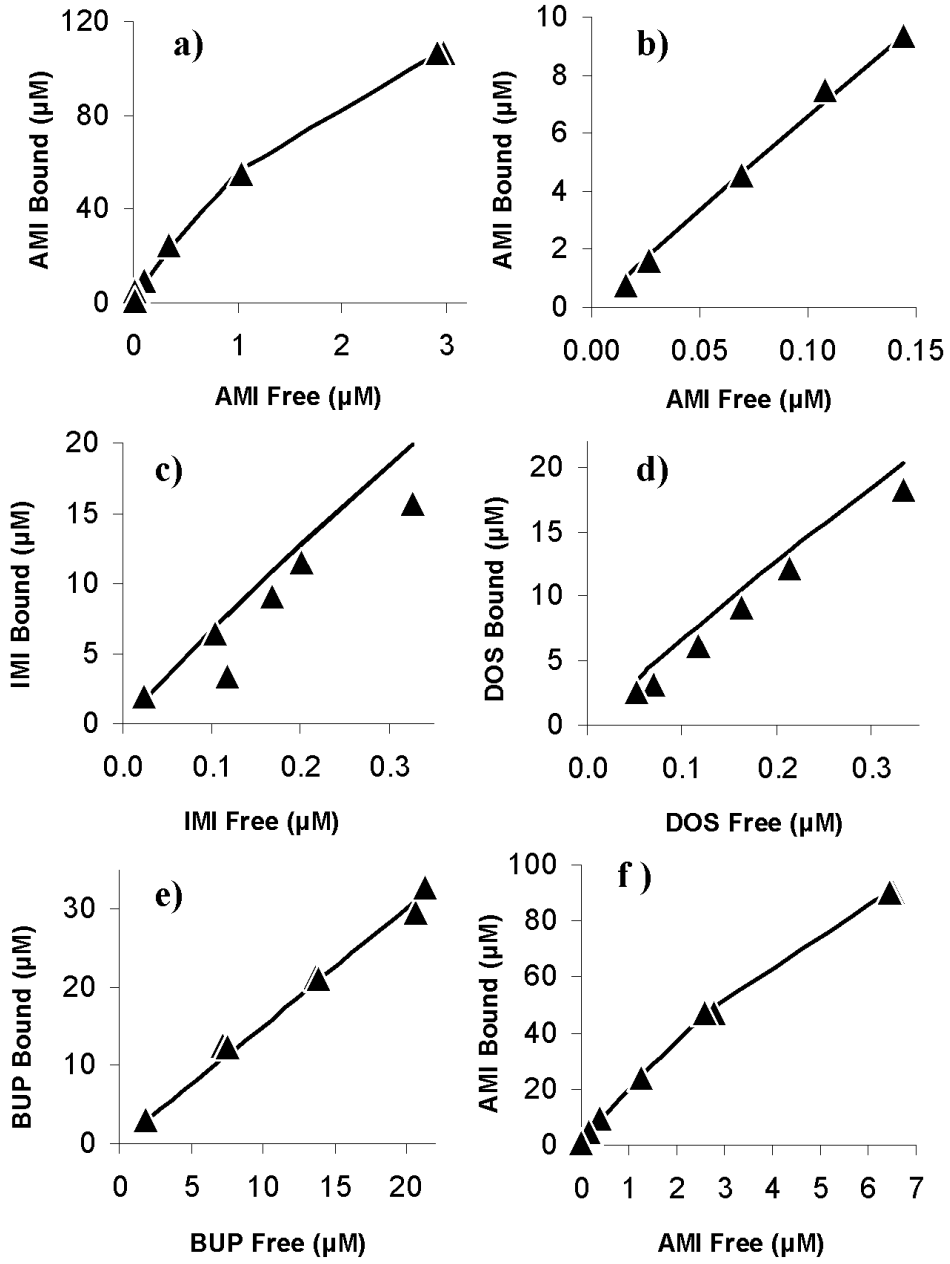

Figure 6-4. Concentration of a) AMI bound to DOPG ULL at 0.72 mg lipid/mL versus unbound AMI, b) AMI, c) IMI, and d) DOS bound to 95:5 DOPG:DPPE-mPEG-2000 ULL at 0.72 mg lipid/mL versus unbound drug determined experimentally (▲) or estimated from Equation 6-8 (—) with a = 5.36 x 10^{-7} moles/m^2 and K = 1.88 x 10^{-2} moles/m^3, e) BUP bound to 95:5 DOPG:DPPE-mPEG-2000 ULL at 1.44 mg lipid/mL versus unbound BUP determined experimentally (▲) or estimated from Equation 6-8 (—) with a/K = 3.68 x 10^{-7} m, f) AMI bound to 50:50 DOPG:DMPC ULL at 0.72 mg lipid/mL versus unbound AMI determined experimentally (▲) or estimated from Equation 6-8 (—) with a = 6.43 x 10^{-7} moles/m^2 and K = 5.90 x 10^{-2} moles/m^3.

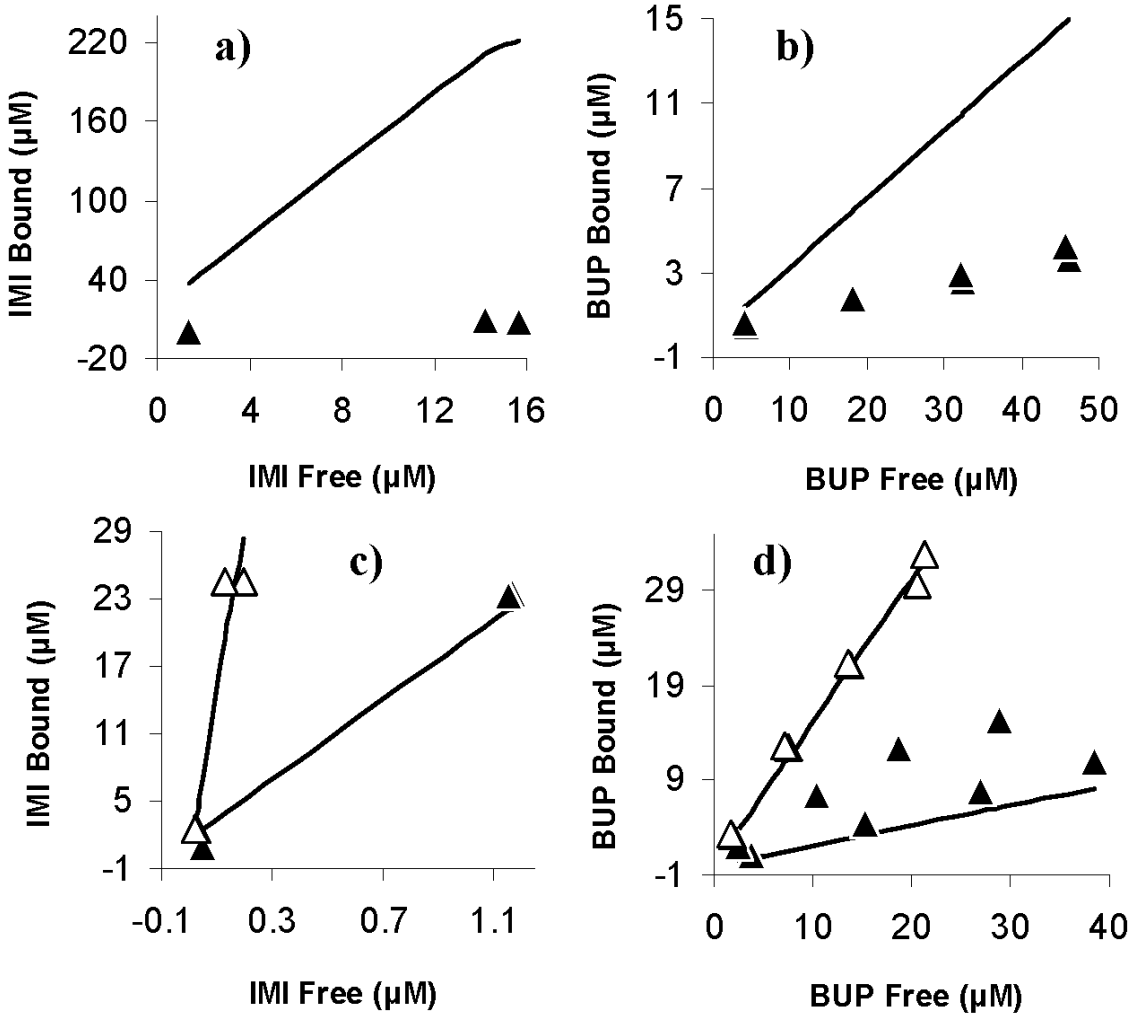

Figure 6-5. Concentration of a) IMI or b) BUP bound to DMPC ULL at 1.44 mg lipid/mL in 0.165 M (▲) ionic strength solutions determined experimentally and c) IMI or d) BUP bound to DOPG ULL at 1.44 mg lipid/mL determined experimentally in 0.165 M (△) or 1.5 M (▲) ionic strength solutions. Predictions were made using Equation 6-8 (—) with $a = 5.36 \times 10^{-7}$ moles/m^2 and $K = 1.88 \times 10^{-2}$ moles/m^3 for IMI and $a/K = 3.68 \times 10^{-7}$ m for BUP. See Table 6-1 for corresponding changes in zeta potential.

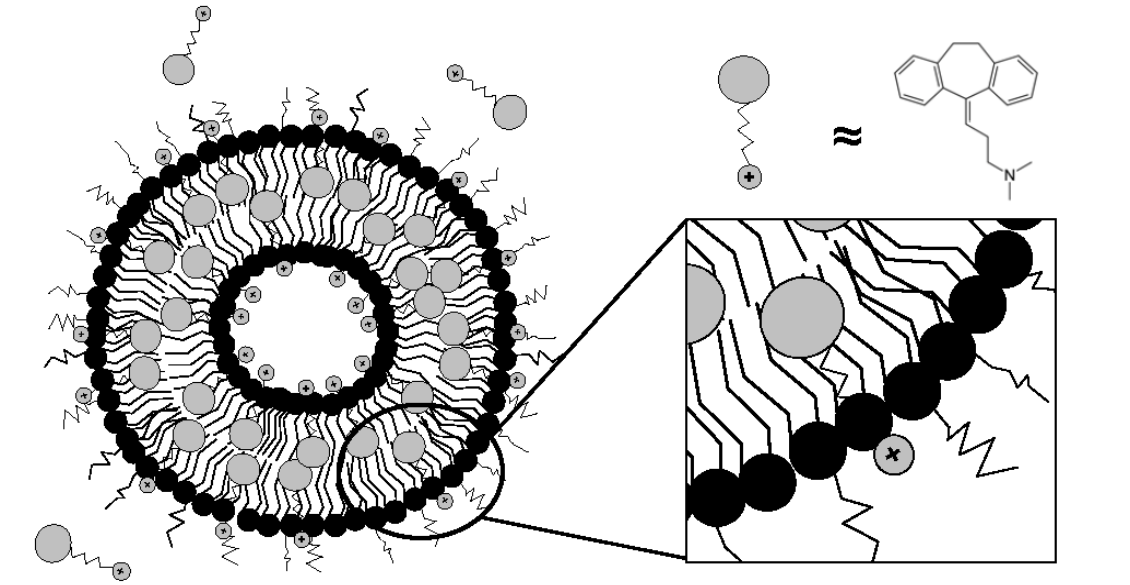

A

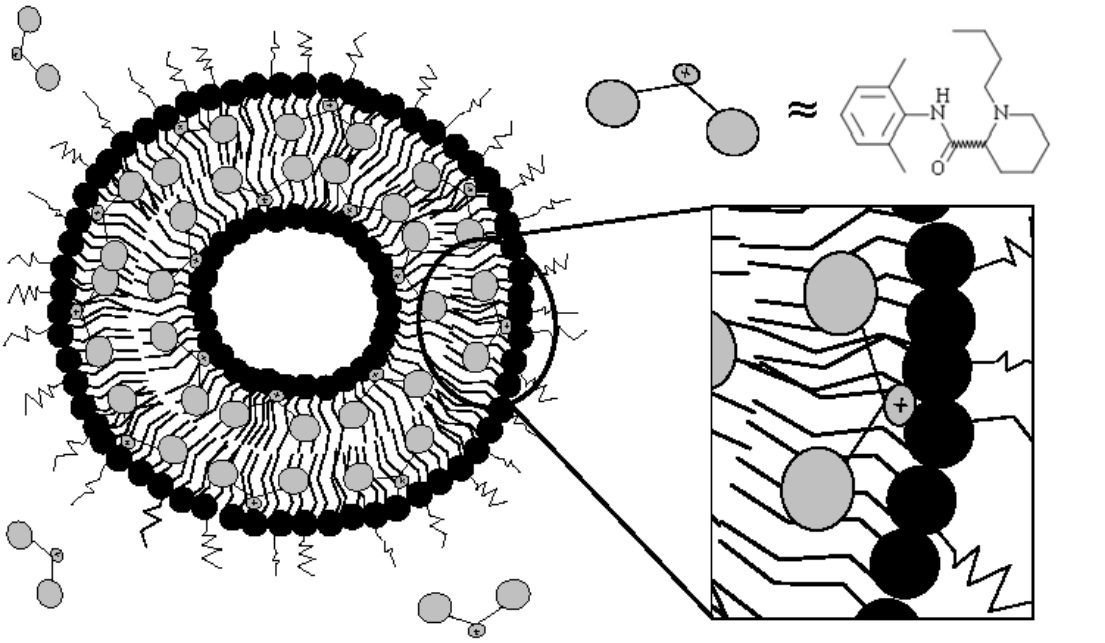

B

Figure 6-6. Plausible mechanism for a) TCA and b) BUP binding to pegylated, anionic liposomes. For TCA's, charged lipid head groups associate with the protonated portion of the drug (depicted in gray, molecular structure also shown) and the bulk aqueous phase, while the uncharged portion of the drug associates with the hydrophobic lipid bilayer. For BUP, the drug is predominantly located within the lipid bilayer with its charged region oriented towards the charged lipid head groups.

Table 6-1. Values for constants and parameters used for drug binding predictions from Equations 6-6 through 6-12 (lipid loadings are specified in figure legends)

Constant	Value	Range of Observed Values	Units
$A°$ [a]	6.86×10^{-19}		m^2 / lipid
$A°$ [b]	6.22×10^{-19}	$5.96 - 6.52 \times 10^{-19}$	m^2 / lipid
$A°$ [c]	6.54×10^{-19}		m^2 / lipid
MW (DOPG)	797.04		g / mole
MW (95:5 DOPG:DPPE-mPEG-2000) [d]	794.66		g / mole
MW (DMPC)	677.94		g / mole
MW (50:50 DMPC:DOPG)	737.49		g / mole
κ (0.165 M) [e]	1.33×10^{9}		1/m
κ (1.5 M) [e]	3.33×10^{9}		1/m
e	1.6×10^{-19}		C
k	1.38×10^{-23}		m^2 kg s^{-2} K^{-1}
T	298		K
ε [f]	6.951×10^{-10}		C / (V • m)
ζ (DOPG - 0.165 M) [g]	-50.9 ± 2.63	-60 to -65	mV
ζ (DOPG - 1.5 M) [h]	0		mV
ζ (50:50 DMPC:DOPG - 0.165 M) [i]	-42.7 ± 4.82	-40	mV
ζ (DMPC - 0.165 M) [j]	-6.6 ± 7.56	0 to -20	mV

[a]Average area per DOPG lipid molecule on the liposome surface at 30°C. The same value was used for 95:5 DOPG:DPPE-mPEG-2000 liposomes [139]. [b]Average area per DMPC lipid molecule on the liposome surface at 27-30°C [127,128,140]. [c]Average area per lipid molecule on the liposome surface for 50:50 DMPC:DOPG liposomes at nearly 30°C, calculated as the average of the pure values for DMPC and DOPG. [d]The molecular weight of pegylated liposomes was calculated excluding the PEG chains. [e]Inverse of the Debye length at 0.165 M and 1.5 M ionic strengths [135]. [f]Product of the dielectric constant and the relative static permittivity of water (78.54) used for surface potential calculations for ULL. [g]Measured zeta potential (mean ± standard error) of DOPG liposomes in PBS (0.165 M ionic strength). Observed values were measured at ionic strengths of 0.1 M [126] and 0.165 M [125]. [h]The zeta potential change from about -50 mV to 0 mV when increasing the ionic strength to 1.5 M was estimated from the surface potential change calculated with Equation 6-12 and has also been noted in literature [125,126]. [i]Measured zeta potential (mean ± standard error) of 50:50 DMPC:DOPG liposomes in PBS (0.165 M ionic strength). The observed value was measured at an ionic strength of 0.1 M [126]. [j]Measured zeta potential (mean ± standard error) of DMPC liposomes in PBS (0.165 M ionic strength). Observed values were measured at ionic strengths of 0.1 M [126] and 0.165 M [95].

CHAPTER 7
PREDICTING THE EFFICACY OF AMITRIPTYLINE AND BUPIVACAINE OVERDOSE TREATMENT WITH LIPOSOMES IN MAN WITH PHYSIOLOGICALLY BASED PHARMACOKINETIC MODELS

7.1 Introduction

Chapters 1-6 focused on developing and understanding high affinity binding between liposomes and drugs. In this chapter, physiologically based pharmacokinetic (PBPK) models were constructed to simulate the treatment of AMI and BUP overdoses with liposomes to assess the effect of liposome administration on drug redistribution and possible toxicity reversal. A preliminary model framework and discussion concerning requirements for nanoparticles capable of treating overdoses was formerly published, but lacked the details or in vitro data required to extract specific information [117]. To develop our PBPK models, mechanistically based equations for tissue to blood partition coefficients developed by Rodgers et al. [106] were combined with in vitro drug binding data from previous chapters and drug specific input parameters from literature. The partition coefficients were validated by comparing model predictions to intravenous (IV) data, followed by best fits to non-IV data to obtain first-order absorption rate constants. AMI and BUP overdoses and the efficacy of liposomes at reversing the overdoses were then simulated by including liposomes into the mass balances of the PBPK models and utilizing the in vitro drug-liposome binding data. Simulations were also conducted to evaluate the model sensitivity. Finally, published in vitro data on the function of cardiac ion channels [9,16,141] and atrial contractility [10] was utilized to estimate, to a first approximation, the molecular level pharmacodynamic effects in the heart resulting from liposome therapy.

7.2 Methods

7.2.1 Obtaining Tissue Partition Coefficients

A precursor to developing a useful PBPK model is obtaining reasonable values for the organ to blood partition coefficients for the drugs or compounds of interest. This is often done experimentally using animal or post-mortem data. However, the values reported in such studies can vary widely from study to study and/or species to species, and many organs are typically omitted due to practical limitations. Furthermore, in cases of new compounds, studies to measure the partition coefficients could be prohibitively expensive. Poulin et al. began the process of overcoming this problem by developing methods for predicting partition coefficients based on compound properties [73,142-144]. Rodgers et al. subsequently developed additional mechanistic equations for acidic and basic compounds [106,145]. Their equations for moderate-to-strong bases were utilized here to predict the partition coefficients for AMI, IMI, and BUP [106]. The mechanistic equations were developed for partition coefficient predictions in rats [106], and we have assumed the values are reasonably transferrable from rats to humans.

The drug partition coefficients between the tissues and the concentrations unbound in plasma, Kpu, were calculated utilizing the association constant for blood cells, K_{aBC}, as detailed by Rodgers et al. [106]. The compound specific parameters necessary for the calculations are shown in Table 7-1 [106-108,119,121,123,146-158]. Table 7-2 [85,150,151,158,159] shows the calculated Kpu values for the drugs modeled. Note that TCA's are highly lipophilic and thus very likely to partition into organs. The integration of Kpu values into our model is outlined below. However, for a

detailed review of the equations and parameters necessary for the Kpu calculations, the reader is directed to the work of Rodgers et al. [106].

For the PBPK model developed herein, we have assumed steady state conditions between tissue and blood concentrations (i.e. blood-flow limited transport). Kpu values can be related to C_f, the free concentration in the blood, and H, the hematocrit, in the following way:

$$\mathrm{Kpu} = \frac{C_t}{C_{u,p}} = \frac{C_t(1-H)}{C_f}, \tag{7-1}$$

where C_t is the concentration in the tissues and $C_{u,p}$ is the concentration unbound in the plasma. The (1-H) factor is added to correct for the discrepancy in volume between blood and plasma [160]. The PBPK equations described in the next section require the partition coefficients between the tissue and the whole blood, including proteins and red blood cells (RBC). Additionally, if the blood contains any other component that can bind substantial amounts of drug such as liposomes, the effect on the partition coefficient also needs to be accounted for. To describe the binding between drugs and proteins, liposomes, and red blood cells (RBC), we define the partition coefficients K_1, K_2, and K_3 as

$$K_1 = \frac{C_{b,p}}{C_f}, \quad K_2 = \frac{C_{b,lip}}{C_f}, \quad K_3 = \frac{C_{b,RBC}}{C_f}, \tag{7-2}$$

where $C_{b,p}$, $C_{b,lip}$, and $C_{b,RBC}$ are effective drug concentrations in blood bound to proteins, liposomes, and RBC's, respectively, based on the blood volume. A new parameter, Keff, is defined as follows:

$$\mathrm{Keff} = \frac{\text{drug concentration in tissues}}{\text{drug concentration in whole blood}} = \frac{C_t}{C_f + C_f K_1 + C_f K_2 + C_f K_3}. \tag{7-3}$$

By examining Equations 7-1 and 7-3, Keff can also be defined as

$$\mathrm{Keff} = \frac{\mathrm{Kpu}}{(1-\mathrm{H})(1+\mathrm{K_1}+\mathrm{K_2}+\mathrm{K_3})}. \qquad (7\text{-}4)$$

The values of K_1 and K_2 shown in Table 7-3 were obtained using experimentally measured drug binding to liposomes and proteins reported in Chapters 2-5. The values of K_1 and K_2 depend linearly on the amount of protein and liposomes, respectively, in the blood. The concentration of protein in the blood is relatively constant, and so a constant K_1 that corresponds to physiological concentrations of protein can be used in the simulations. However, liposomes introduced into the blood through IV administration are cleared, and so the concentration of liposomes in blood is time dependent. Accordingly, the dependence of K_2 on the liposome concentration must be included in the simulations. Experimental data on drug binding to liposomes shows that K_2 depends linearly on the liposome concentration, which is expected based on mass balance considerations. Accordingly, a linear dependence of K_2 on the liposome concentration is utilized (Table 7-3). The drug binding to RBC's that is needed to determine K_3 was not directly measured, but was obtained by utilizing reported values of blood-to-plasma drug concentration ratios (B:P), which can be related to the various partition coefficients through a mass balance to yield the following equation:

$$\mathrm{B{:}P} = \frac{\mathrm{C_f} + \mathrm{K_1C_f} + \mathrm{K_2C_f} + \mathrm{K_3C_f}}{\frac{\mathrm{C_f} + \mathrm{K_1C_f}}{(1-\mathrm{H})}}. \qquad (7\text{-}5)$$

The K_3 values shown in Table 7-3 were calculated by solving Equation 7-5 using reported B:P ratios (Table 7-1) with K_2 going to zero, since no liposomes were present in the cited studies in which B:P was measured. Table 7-3 shows that K_1 was taken to

be independent of drug concentrations for TCA's and BUP. This is a reasonable assumption for TCA's across a fairly broad range of drug concentrations (see Chapters 2-4) and for BUP (Chapter 5) within the low concentration range observed during adverse reactions (< 1 μg/mL). BUP concentrations are often low because overdose is not intentional, as it occurs in a clinical setting.

To validate the Keff values obtained from the methods illustrated above, K_1 and K_3 values for AMI and BUP were used to calculate Keff values in the absence of liposomes. Comparisons were then made to tissue to blood partition coefficients reported from various animal or post-mortem human studies [161-167]. Comparisons were only made for the organs for which data was available in literature. Figure 7-1 compares the experimental and calculated values for AMI and BUP, the two drugs used for the overdose simulations. The partition coefficients agree reasonably well for most of the organs. Experimental error is not shown due to the lack of error estimation in some of the studies with small sample sizes. However, when taking into consideration the large inter- and intra-species variations associated with tissue to blood partition coefficients, as well as the level of difficulty of such experiments, the experimental values clearly support the validity of the mechanistic equations developed by Rodgers et al. [106] for AMI and BUP. Moreover, the larger than predicted values observed in the experimental studies for organs such as the lungs and liver could have arisen from post-mortem drug redistribution, an occurrence cited in several published reports [163,168].

7.2.2 PBPK Model Structure

The PBPK model included venous and arterial blood compartments and 13 additional organs (Figure 7-2). A local equilibrium between tissue and blood

concentrations (i.e. blood-flow limited transport) was assumed for all organs. All equations were solved using MATLAB™ software (The Mathworks, Natick, MA, USA). Q_i, V_i, and C_i refer to blood flow rates to organs (denoted by i), organ volumes, and drug concentrations of organs, respectively. Subscripts denote organs as follows: venous whole blood (vb), arterial whole blood (ab), lungs (l), adipose (ad), brain (br), heart (ht), pancreas (p), gut (g), spleen (sp), liver (h), thymus (th), bone (bo), skin (sk), muscle (m), and kidneys (k). Hepatic and renal clearance values are denoted as CL_h and CL_r, respectively. The arterial blood flow directly to the liver (ha) is denoted as Q_{ha}. The mass balance equation for non-eliminating tissue (i = ad, br, ht, p, g, sp, th, bo, sk, mu) was as follows:

$$\frac{dC_i}{dt} = \frac{Q_i}{V_i}\left(C_{ab} - \frac{C_i}{Keff_i}\right) . \quad (7\text{-}6)$$

Liver concentrations were obtained from

$$\frac{dC_h}{dt} = \frac{\left(Q_{ha}C_{ab} + Q_p\frac{C_p}{Keff_p} + Q_g\frac{C_g}{Keff_g} + Q_{sp}\frac{C_{sp}}{Keff_{sp}}\right)(1-E_h) - Q_h\frac{C_h}{Keff_h}}{V_h} , \quad (7\text{-}7)$$

where the hepatic extraction ratio, E_h, was defined as [73,108,169]

$$E_h = \frac{CL_h}{Q_h + CL_h} . \quad (7\text{-}8)$$

For the kidneys, Equation 7-9 was solved:

$$\frac{dC_k}{dt} = \frac{Q_k}{V_k}\left(C_{ab} - \frac{C_k}{Keff_k}\right) - \frac{CL_r C_k}{V_k Keff_k} . \quad (7\text{-}9)$$

For the lungs, Equation 7-10 was solved:

$$\frac{dC_l}{dt} = \frac{Q_l}{V_l}\left(C_{vb} - \frac{C_l}{Keff_l}\right) . \quad (7\text{-}10)$$

The venous blood compartment was represented by Equation 7-11:

$$\frac{dC_{vb}}{dt} = \frac{\sum_{ad,br,ht,h,th,bo,sk,m,k} Q_i \frac{C_i}{Keff_i} - Q_l C_{vb}}{V_{vb}}, \quad (7\text{-}11)$$

while the arterial blood was represented by Equation 7-12:

$$\frac{dC_{ab}}{dt} = \frac{Q_l}{V_{ab}}\left(\frac{C_l}{Keff_l} - C_{ab}\right). \quad (7\text{-}12)$$

7.2.3 Model Input Parameters

Organ blood flow rates, organ volumes, and total cardiac output for humans were obtained from various sources [78,79,144,170-172] and are shown in Table 7-4. Renal and hepatic clearance values used in Equations 7-7 through 7-9 and bioavailable drug fractions after oral dosages (F) were obtained from human studies and are shown in Table 7-5 [73,108,148-150,169,173-185]. Hematocrit values were taken to be 0.45 for all simulations [181]. Averages were weighted according to the number of subjects for parameter values pooled from multiple studies.

7.2.4 Validation of Model Parameters by Predicting Intravenous Data

To prove the reliability of the parameters utilized here, PBPK simulations were conducted to simulate various experimental studies where AMI [149,175,176], IMI [173,174], or BUP [151,177-179,186] was given intravenously. IMI was used for model validation but was omitted from drug overdose simulations due to the very similar nature of AMI and IMI. Reported subject weights, drug doses, and dosage protocols (i.e. infusion time, etc.) were utilized in the simulations, and drug concentrations were then predicted using the PBPK model described above. The PBPK model results were then compared to the corresponding data sets. Note that no fitting parameters were utilized

for model validation, as all PBPK parameters were obtained by procedures described above.

7.2.5 Determining Absorption Rate Constants by Fitting to non-Intravenous Data

IV data afforded PBPK model and human data comparisons in the absence of fitting parameters. TCA's are, however, almost exclusively prescribed and overdosed on orally. To account for oral administration, an additional compartment was added to the PBPK model which fed into the venous blood compartment to simulate drug absorption from the gut [169,187]. The mass of drug remaining in this additional compartment X(t) is given by

$$X(t) = De^{-k_a t}, \tag{7-13}$$

where D is the drug dose. The rate of drug absorption from this additional compartment into the IV compartment was calculated as k_aFX, where F is the bioavailability and k_a is the first-order absorption rate constant. To obtain values for k_a, least squares fits were done for several oral data sets for AMI [149,188-191] and IMI [109,173]. IMI oral data sets were used solely for model validation, since IMI overdose simulations were not conducted. The average of the k_a values obtained from the AMI fits was used for the AMI overdose simulations.

Unlike TCA's, BUP is typically given through non-oral, non-IV routes that include injections or infusions into the dural**,** intraperitoneal, or intercostal spaces, among others [192-198]. In many cases, short infusions are administered that can be modeled as bolus doses into an additional compartment that feeds into the venous blood, as described by Equation 7-13. This was done for several cases to obtain k_a values for BUP [192-196]. The value of F was assumed to be 1 for all BUP models, since first

pass elimination is largely circumvented with non-oral dosage procedures. More lengthy or complex infusion procedures [197,198] were also simulated for least squares fits using a single absorption rate constant, k_a, where an additional compartment was again added that released drug into the venous blood. The following mass balance was integrated from time zero (t_o) to the end of the first infusion (t_1) for an infusion rate I_1 into a non-IV compartment containing mass X at time t,

$$\frac{dX}{dt} = I_1 - k_a X \quad , \tag{7-14}$$

to yield Equation 7-15, the amount of drug remaining in the compartment between t_o and t_1:

$$X(t) = \frac{I_1}{k_a}(1 - e^{-k_a t}) \quad . \tag{7-15}$$

For the i^{th} additional infusion rate given after I_1, the mass balance was solved to produce

$$X(t) = \frac{I_i}{k_a} + e^{k_a(t_{i-1} - t)}(X(t_{i-1}) - \frac{I_i}{k_a}) \quad , \tag{7-16}$$

for t_{i-1} to t_i, where t_{i-1} and t_i represent the time points at which the previous and i^{th} infusions stop, respectively. Finally, the amount of drug in this compartment after the final i^{th} infusion was obtained from Equation 7-17 for t_i to t_∞:

$$X(t) = X(t_i)\, e^{k_a(t_i - t)} \quad . \tag{7-17}$$

The above equations were solved to obtain X(t), and the rate of drug absorption into the IV compartment was again calculated as k_aX. Although many BUP data sets were used for least squares fits to demonstrate the model's ability to predict non-oral, non-IV data with a single absorption rate constant (k_a), the dosage methods varied widely

throughout the non-oral data sets used, making an overall average k_a value meaningless. Consequently, k_a values obtained from fits to three studies with dural space dosages [192,194,197] were averaged to simulate BUP overdose treatment.

7.2.6 Drug Overdose Treatment Simulations

AMI [7,110,111,115] and BUP [192-196] doses for simulating overdoses were based on values reported in literature for overdoses and/or adverse reactions. AMI overdose was modeled as an oral dose and BUP administration was modeled as a bolus injection into the dural space. Liposome doses were based on in vitro data of drug binding to liposomes (Chapters 2-6) and were modeled as bolus IV doses. Bolus administration is a reasonable approximation because the lipid concentrations in liposome formulations [199] can be as high as 50 mg/mL, allowing rapid delivery of the required amount of lipids in small fluid volumes [12,14,15,40]. The total liposome doses simulated were deemed clinically safe based on reported studies [25,200,201]. The amount of time expiring between drug ingestion or administration and liposome dosing (t_{lag}) was based on the time required for TCA patients to reach the hospital [7,110-112,202] after ingestion for AMI, and the time required to administer lipid emulsion therapy during adverse reactions for BUP [12-15]. Drug doses, liposome doses, and t_{lag} values are given in Table 7-6. The cardiac output and organ volumes for overdose simulations were based on a patient weight of 70 kg. Note that several t_{lag} values and drug doses were simulated for AMI due to the large variability in lag times and drug ingested during TCA overdoses.

7.2.7 Liposome and Drug Clearance

As explained earlier, the value of K_2 depends linearly on the liposome concentration in the blood (Table 7-3). It is thus necessary to determine the liposome

concentration in the blood, which decreases with time due to clearance. Several important assumptions were made about the liposome fate in the body. First, the size and pegylated nature of the liposomes studied in previous chapters and simulated here make them stable and unlikely to traverse capillaries [26,90]. Therefore, the liposomes are assumed to remain well-mixed in the venous and arterial blood compartments until elimination. Finally, the elimination of the liposomes has been assumed to be similar to the elimination of pegylated, anionic liposomes observed in rabbits [30]. The following equation specifying the percent of liposomes remaining in the blood compartments as a function of time (in hours) over a 22 hour period was fit from data by Awasthi et al. [30],

$$\%\ \text{Liposomes Remaining} = 0.2354t^2 - 7.8865t + 100 . \qquad (7\text{-}18)$$

The time dependent value of K_2 was calculated by multiplying the percent of liposomes remaining at time t from Equation 7-18 by the initial liposome concentration in the blood stream from Table 7-6 and plugging the corresponding liposome concentration into the equation for K_2 shown in Table 7-3. Note that prior to the liposome administration, i.e., for $t < t_{lag}$, the value of K_2 is zero and increases suddenly upon liposome administration at $t = t_{lag}$. Rather than assuming a step increase in K_2, we have assumed a linear increase in K_2 over 1 minute from zero at $t = t_{lag}$ to the value corresponding to the equation shown in Table 7-3 for K_2. Practically speaking, this assumes that the liposomes become well-mixed and reach equilibrium drug binding within the blood compartments after 1 minute. The 1 minute duration is sufficient to achieve equilibrium between liposome and free drug based on in vitro studies [71].

Liposomes cause the drug concentrations in the venous and arterial blood compartments to increase, which causes hepatic extraction of the drug to increase. The

presence of liposomes in the blood could potentially alter the hepatic extraction ratio, but since no data is available for this effect, we assumed that the hepatic extraction ratio is unaltered by the liposome addition. Effectively, hepatic extraction in the model is based on the total drug concentration in the blood including drug bound to liposomes, as opposed to the free drug concentration. This assumption could potentially overestimate the hepatic drug clearance. On the other hand, estimating the clearance of the liposomes as described above (Equation 7-18) implicitly assumes that the liposomes simply disappear from the blood stream and release the drug bound to them over time. A large portion of the liposomes actually end up in the liver [30], thereby potentially accelerating drug metabolism due to metabolism of the bound drug. Neglecting this increased metabolism leads to an underestimation of the drug clearance, which partially offsets the overestimation caused due to the neglect of changes in hepatic extraction ratio upon liposome addition. Although no quantitative analysis to prove the effects roughly offset one another is possible, the error associated with neglecting such competing effects is at least reduced. While including these effects in the PBPK model is theoretically possible, it would require details about hepatic metabolism of drug bound to liposomes, which is not available in literature.

7.2.8 Metabolites

Both AMI and BUP are converted to active metabolites in the body. Inclusion of metabolites in the model is in principal straightforward, but requires details regarding transformation and clearance rates, tissue partition coefficients, and protein and liposome binding, which are not available. Additionally, the extent to which AMI [150,182,188] or BUP [178,185,203] is converted to one particular metabolite versus many others varies from individual to individual [178,185,203,204]. Furthermore, many

metabolites, such hydroxymetabolites for AMI [150,182,188] and pipecolyxylidine (PPX) for BUP [185], are much less lipophilic than their parent drugs, making their effects on the body, their organ partitioning and elimination, and their liposome binding significantly different from the parent molecules. Due to the reasons listed above, metabolism is not included in the model. Neglecting metabolism may not be critical because metabolism is the body's natural way of preparing drugs for renal elimination, making metabolites almost exclusively less dangerous than their parent drugs. Also, the large volume of distribution for AMI dictates that most of the drug is partitioned into tissues over the first 5 to 10 hours of overdose, which makes metabolite tracking less important during the most critical moments for treatment. Additionally, the protein and liposome binding of AMI and BUP in the PBPK model are drug and liposome concentration independent, which makes the model valid even as metabolites are present. Finally, BUP adverse reactions are treated within 5-15 minutes of drug administration. The short time lapse between drug and liposome dosing reduces the amount of time available for metabolite formation, making it less significant in this case.

7.2.9 Drug Dose in Overdose Simulations

The doses simulated varied from 100 mg to 2500 mg. 2500 mg is clearly outside of the therapeutic dose range for AMI. The parameters obtained from clinical studies for AMI, such as clearance and bioavailability, are perhaps less accurate at drastically increased AMI concentrations. Ideally, data taken from patients undergoing AMI or TCA overdoses would be compared to model predictions to refute this position. This was practically impossible due to the inexact nature of reported drug doses ingested and time lapses occurring between ingestion and drug concentration measurements in overdosed patients. While this issue could introduce some errors into the model, it is

likely not critical for the following reasons. First, Venkatakrishnan et al. [204] have reported in vitro data supporting linear AMI metabolism below AMI concentrations of around 200 μM or 55 μg/mL, well below all concentrations reached in the AMI overdose simulations. Next, reduced F values owing to self-inhibited AMI absorption, gastric lavage, or charcoal administration would not reduce the efficacy of the treatment, as evidenced by the effectiveness of the treatment at both high and low drug concentrations (see below). Finally, the effect of changing parameters like k_a, F, and others has been directly addressed in Section 7.2.11.

7.2.10 Validation of the Numerical Calculations

As a check for numerical accuracy, a conservation of mass calculation was done for the overdose simulations. The drug concentrations in each organ at a final time point were multiplied by organ volumes to obtain the drug retained within the organs. The total drug metabolized was calculated as shown below,

$$\text{Drug Metabolized} = E_h \int_{t_o}^{t_f} \left(Q_{ha} C_{ab} + \sum Q_i \frac{C_i}{Keff_i} \right) dt \quad , \tag{7-19}$$

with C_i representing the drug concentrations in the gut (g), pancreas (p), and spleen (sp). Renal elimination was obtained from Equation 7-20:

$$\text{Renal Elimination} = Cl_r \int_{t_o}^{t_f} \frac{C_k}{Keff_k} dt \, . \tag{7-20}$$

AMI lost to first pass metabolism and drug not absorbed from the stomach or the dural space by the final time point was also included in the mass balance. The total mass in the system was at least 99.99% of the original mass at all times in all simulations, proving the numerical accuracy of the calculations.

7.2.11 Sensitivity Analysis

The model predictions for the effect of liposomes during an overdose obviously depend on the various model parameters, which are uncertain due to variability in the studies from which they were obtained and the inherent intra and inter-subject variation in humans. While a detailed population PK model is beyond the scope of this work, the effect of parameter variations on treatment efficacy was explored by varying the chosen parameter in a range and exploring its effect on the results of the simulations. Hepatic extraction variation was based on maximum [149,178] and minimum [176,179] average values observed from single studies. Maximum and minimum k_a values for AMI and BUP were based on the standard deviation of the average k_a value calculated from best fits from oral AMI data [149,188-191] and non-IV BUP data [192,194,197]. Liposome-drug binding was reduced by reducing K_2 values. K_2 values were not increased since this would only increase the efficacy of the treatment. Standard deviations for K_2 values from data reported in previous chapters were low and would not have afforded a meaningful sensitivity analysis. Therefore, K_2 values at each liposome concentration were reduced by 20% and new curves for K_2 as a function of liposome concentration were generated. The percent of liposomes remaining in the blood stream reported by Awasthi et al. [30] for pegylated, anionic liposomes in rabbits was reduced by 30% at each time point and a new curve generated. Once more, the standard deviations reported in their study were much lower than 30%, but a higher value was used to allow for a meaningful examination of how enhanced liposome elimination would affect overdose treatment with liposomes. Slower liposome elimination was not studied, since it would only improve the treatment. A detailed list of the values and equations used for the sensitivity analysis for hepatic extraction, absorption, liposome-drug binding, and

liposome elimination is presented in Table 7-7. Finally, the sensitivity of the model to Keff was examined by varying B:P [150,151] and f_u [85,158,159] within clinically feasible ranges and computing Kpu and Keff with the modified values. To be consistent, the modified values of B:P and f_u were also utilized to compute K_1 and K_3. Refer to Table 7-2 for the exact B:P, f_u, and Kpu values used for the analysis.

7.3 Results

7.3.1 Tricyclic Antidepressant Model Validation and Fits for Absorption Coefficients

Model predictions and human data sets for IV TCA administration are compared in Figures 7-3a through 7-3j. No model parameters were allowed to vary to match the predictions. The PBPK models predicted the drug concentrations accurately. Error bars are shown for all studies for which they were originally reported but were unavailable in many cases. Figures 7-4a through 7-4k show TCA oral data sets and PBPK best fits using k_a as a fitting parameter. Some predictions such as Figures 4c and 4d did not match the data well, but overall the model fitted the data successfully. The k_a value obtained for AMI overdose simulations from Figures 7-4d through 7-4k was $0.0930 \pm 0.0394\ h^{-1}$ (mean ± standard deviation).

7.3.2 Bupivacaine Model Validation and Fits for Absorption Coefficients

Model predictions and human data sets for IV BUP administration are compared in Figures 7-3k through 7-3o. No model parameters were allowed to vary to match the predictions. The PBPK models predicted the BUP concentrations very well except at high BUP concentrations in Figures 7-3k and 7-3o. This discrepancy likely arose from reduced protein-BUP binding at high BUP concentrations, as has been observed (Chapter 5, [158]). Over-predictions at high BUP concentrations during BUP infusions

have also been observed elsewhere [179]. Figures 7-4l through 7-4s show BUP non-IV, non-oral data sets and PBPK best fits using k_a as a fitting parameter. The fits were reasonably good. The average k_a value obtained for BUP from Figures 7-4l, 7-4r, and 7-4s (dural spaces) was 0.1794 ± 0.0790 h^{-1} (mean ± standard deviation). This value was used in the overdose simulations reported below.

7.3.3 Tricyclic Antidepressant Overdose Simulations

AMI overdoses were simulated according to the conditions specified in Table 7-6 and an average k_a value of 0.0930 h^{-1}. Note that all four liposome loadings and all three lag times were simulated for the 2500 mg drug dose, whereas only one liposome dose and lag time was simulated for the other two drug doses. Table 7-8 shows the areas under the concentration versus time curves (AUC) and peak drug concentrations for AMI for several key organs under a variety of different conditions. The percent reductions were calculated relative to overdose simulations without liposomes at the same drug doses. AMI AUC reductions in free venous blood, the heart, and the brain varied from 63.3% to 20.9%, 64.0% to 21.2%, and 64.0% to 21.2%, respectively. AMI peak concentration reductions in free venous blood, the heart, and the brain were 15.6%, 20.1% , and 20.0%, respectively, for t_{lag} = 2 hours and insignificant for t_{lag} > 2 hours since AMI peaks had basically been reached prior to liposome dosing. The reductions of AUC and peak concentration in the brain and heart were similar because both of these tissues are in equilibrium with the venous blood because of the high perfusion rates. Figure 7-5 shows AUC or peak AMI concentration values as a function of liposome dose or t_{lag}. Note that the liposome efficacy saturates as the liposome dose increases. Figure 7-5d displays the effect of t_{lag} on AUC at a set liposome dosing of 1.44 g/L.

Figure 7-6 shows AMI concentrations versus time for several key organs at a liposome dose of 1.44 g/L. In Figure 7-6, the control curve should be followed until the desired t_{lag} is reached. The first alternate curve should then be followed for t_{lag} = 2 hours, the second for t_{lag} = 4 hours, and so on. Note that peak C_{vb} values increased due to liposome administration by three to four fold for all time lags. The muscle is included in Figure 7-6e to illustrate the effect of sink organs. Sink organs require such long periods of time to reach their peak drug concentrations that liposome doses within about 4 hours actually cause their drug concentrations to momentarily increase above the control value before enhanced elimination reduces the blood and therefore the organ concentration as well. Although this effect is clear in Figure 7-6e, its magnitude suggests it to be fairly insignificant compared to the amount of AMI held in the blood compartment by the liposomes.

7.3.4 Bupivacaine Overdose Simulations

BUP overdoses were simulated according to the conditions specified in Table 7-6 and an average k_a value of 0.1794 h^{-1}. Table 7-9 shows the AUC values and peak drug concentrations for BUP. BUP AUC reductions in free venous blood, the heart, and the brain varied from 15.5% to 8.5%, 15.4% to 8.5% , and 15.3% to 8.3%, respectively. BUP peak concentration reductions in free venous blood, the heart, and the brain were 17.3% for the maximum liposome dose of 2.88 g/L.

Figure 7-7 shows BUP concentrations versus time for several key organs at a liposome dose of 2.88 g/L. Owing to the much shorter t_{lag} value of 15 minutes for BUP, the plots appear much different from those in Figure 7-6. C_{vb} increases and organ concentration decreases are much lower than those for AMI, but could still be clinically

significant. The muscle (Figure 7-7e) is again relatively unaffected by the liposomes within the first few hours due to the long equilibration times.

7.3.5 Sensitivity Analysis Results

Tables 7-10 and 7-11 show the percent AUC and peak drug concentration reductions as a function of altered sensitivity analysis parameters for AMI and BUP, respectively. The values from simulations with the original parameters are also shown for comparison at the top of the tables.

7.4 Discussion

7.4.1 Model Validation

The close correlations between IV data and PBPK model predictions in Figure 7-3 demonstrate the validity of the model parameters. Experiments for obtaining partition coefficients are often very difficult, expensive, and require sacrificing large numbers of animals to ensure accuracy. Figures 7-1 and 7-3 stand as direct evidence to both the reliability of the equations developed by Rodgers et al. [106] and the significant opportunities for using PBPK modeling in the drug development process [73-76]. Best fits to non-IV data in Figure 7-4 confirm that using a single first-order absorption rate constant for non-IV dosing was an acceptable approach for the cases considered here.

7.4.2 Evidence for Drug Redistribution with Liposomes

Simulated liposome treatments greatly altered AMI concentrations. Table 7-8 and Figure 7-6 show C_{vb} increases of up to four fold, immediate concentration drops upon liposome dosing in C_{vbf} and critical organs, and enhanced elimination resulting in reduced drug concentrations over the entire 24 hour period. The prolonged concentration reductions led to much lower AUC values, as Figure 7-5 suggests. Peak reductions were lower for t_{lag} = 2 hours and nonexistent otherwise. Peak reductions are

not the primary concern for TCA's since most patients spend several hours receiving treatment in the hospital, with the mean time spent reported as 8.5 hours in one study [3]. Patients often face complications after prolonged drug exposure, making the AUC reductions and the reduced time spent at elevated concentrations most important.

An interesting clinical study was done by Heard et al. [4] where patients suffering moderate but not severe TCA overdoses were treated with Fab fragments. Fab fragments are isolated, concentrated protein fragments that preferentially bind to a targeted drug, and are thus similar in principle to liposomes. This is an attractive strategy since TCA's are naturally highly protein bound. The study showed that using redistribution methods such as the liposome treatment examined herein is a safe practice, and that elevated serum TCA concentrations pose no obvious, additional dangers. The patients were treated with protein fragments three times after hospital admittance. Final serum concentrations increased an average of six fold compared to the initial serum concentrations. The study mentioned that all patients fully recovered but the researchers were unable to fully attribute patient recoveries to the treatment since overdoses were less than severe.

Although drug binding to Fab fragments is different than binding to liposomes, the PBPK modeling results for C_{vb} are validated qualitatively by the fact that drug concentrations increased as much or more in their study, supporting the hypothesis of drug redistribution through liposomes. Heard et al. were unable to comment on whether or not their protein fragments had any direct effect on specific organs such as the heart, brain, etc. Since C_{vb} values are remarkably similar for both studies, our model results could be used to gauge the effectiveness of the Fab fragments on tissue concentration

reductions. Figure 7-6 suggests that the C_{vb} reductions observed by Heard et al. [4] are strong evidence for significant TCA concentration reductions in the heart, brain, and C_{vbf}. This is an excellent example of how PBPK modeling and clinical studies can work in tandem to provide clarity and improved understanding.

In contrast to AMI, BUP results shown in Figure 7-7 and Table 7-9 show less drastic drug redistribution upon liposome dosing, even with a four fold increase in the lipid loading. Obviously, treating TCA overdose with liposomes is more likely to be successful than treating an adverse reaction to BUP, due to stronger TCA-liposome binding. However, with AUC and BUP peak reductions in key organs of roughly 15% and 17%, respectively, liposome administration, with single or multiple doses, could still reduce adverse effects and speed recovery times for patients with BUP overdose.

7.4.3 Pharmacodynamics

Both AMI and BUP can bind to fast Na^+ channels [9,16] and lethally impair cardiac function. Na^+ channel binding alters the cardiac conduction system through slowed action potential propagation, often leading to elongated QRS intervals [2,17]. Hypotension resulting from reduced cardiac contractility is a major cause of death [2]. Compromised cardiac myocyte contractility arises from both Na^+ channel blockage and other effects. AMI has been shown to directly interfere with the calcium-induced-calcium-release mechanism of myocyte contraction [141]. The open probability of ryanodine receptor (RyR) channels connecting the myocyte plasma membrane to the sarcoplasmic reticulum (SR) increases in the presence of AMI in a dose dependent fashion [141]. This leads to depleted Ca^{2+} levels in the SR, which in turn reduces binding between actin and myosin filaments. AMI also inhibits SR Ca^{2+} ATPase pumps (SERCA) from pumping Ca^{2+} back into the SR [141]. Effectively, the cardiac system

works by constantly creating ion gradients that drive energy intensive processes, and AMI disturbs this cycle.

BUP also impairs contractility, possibly through direct Ca^{2+} related effects or interference with mitochondrial activity, which starves ATPase pumps of ATP molecules needed to create ion gradients [17]. Both AMI and BUP can disrupt the central nervous system (CNS) and cause seizures, delirium, and disorientation [2,17]. This is more of a primary concern for BUP.

Many ex-vivo studies involving isolated hearts have attempted to observe drug-induced cardiac toxicity. The PBPK models developed herein predict the drug concentration in human heart tissue as a function of time. Many factors determine the state of the heart at any given moment. Indicators such as the QRS interval, beats per minute, and blood pressure show changes resulting from local drug-induced effects mentioned above and the sympathetic and parasympathetic nervous systems. As a result, it is impractical to attempt to predict heart function on the macro-scale as a function of time. However, published studies directly linking localized or molecular level cardiac function with drug concentrations do offer opportunities to approximate the local effects that liposomes may have on the cardiac system.

Accordingly, in vitro published data relating localized cardiac function to drug concentrations was utilized to project local cardiac function improvements following liposome administration. Several investigators have measured and reported various cardiac parameters as a function of drug concentration. Correlation curves were fit to those data points over the concentration ranges encountered in the PBPK models. Drug concentration predictions as a function of time from the PBPK models were then

inserted into the correlation equations, resulting in time dependent predictions of local cardiac changes during drug overdose. Human cardiac cell (Hh1) Na^+ channel function in the presence of AMI and BUP was studied by Nau et al. [9,16]. Changes in baseline contractility of human atrial tissue versus AMI concentration were reported by Heard et al. [10]. AMI effects on RyR channels were published by Zima et al. [141]. The drug concentrations measured in the in vitro experiments in these three cases would most accurately correspond to the unbound drug concentration in the extracellular water in the heart, $C_{u,EW,ht}$, which is equivalent to the unbound drug concentration in the plasma in the heart, $C_{u,p,ht}$ [106]. This concentration was calculated using C_{ht} from our model as follows:

$$C_{u,p,ht} = C_{u,EW,ht} = \frac{C_{ht}}{Keff_{ht}\,(1-H)\,(1+K_1+K_2+K_3)}. \tag{7-21}$$

AMI effects on calcium movement by SERCA were also published by Zima et al. [141]. Because the SERCA are located within the myocyte plasma membranes on the surface of the SR, they are exposed to the unbound drug in the intracellular water in the heart, $C_{u,IW,ht}$. Intracellular and extracellular water concentrations can be related via their pH values and drug pKa values by the following equation [106],

$$C_{u,IW,ht} = C_{u,EW,ht}\left(\frac{1+10^{pKa-pH_{IW}}}{1+10^{pKa-pH_{EW}}}\right). \tag{7-22}$$

Equation 7-22 was utilized to predict $C_{u,IW,ht}$ and thus predict SERCA function versus time during an AMI overdose. Figures 7-8a through 7-8d show that Na+ channels, baseline contractility, SERCA velocity, and RyR channels rapidly recover from an AMI overdose with liposomes. Figure 7-8e shows that Na+ channel current more closely

resembles normal levels for BUP reaction when liposomes are administered. The necessary data for predicting additional BUP effects was unavailable.

Figure 7-8 provides evidence for cardiac toxicity reversal from liposome therapy after AMI or BUP overdose. The data suggests that the effect on contractility is as important as the effect on conduction disturbances. This is evident for AMI, where percent baseline contractility and Na^+ channel recovery are both significant and rapid. The dual nature of the recovery is of special significance when comparing liposome therapy to the administration of sodium bicarbonate or lipid emulsions. Sodium bicarbonate has traditionally been used to treat TCA overdose as a means of counteracting conduction disturbances [2]. This does not treat reduced contractility from direct drug-cell interaction, the main cause of hypotension. On the other hand, the mode of action of lipid emulsion therapy used to treat local anesthetic overdoses [12-15] has been hypothesized as counteracting the inhibition of fatty acid transport at the inner mitochondrial membrane [44,205]. This method represents a direct effect on contractility, but in vitro BUP binding data [19] with lipid emulsions composed of mostly soy bean oil suggests that redistribution is unlikely to be accomplished. Thus, conduction disturbances caused by Na^+ channel blockage would be largely unaffected. Based on this reasoning, a combination of liposomes designed to sequester high amounts of TCA's and sodium bicarbonate would optimally treat conduction disturbances and contractility reductions during TCA overdoses. In the case of BUP, the conduction disturbance improvements induced with liposomes would have to be more thoroughly compared with the contractility recovery caused by lipid emulsions.

7.4.4 Sensitivity Analysis

The sensitivity of the PBPK model to key parameters was probed by varying the parameters as stipulated in Table 7-7. This analysis is valuable for identifying future pitfalls for treatment development. Although increasing E_h resulted in slightly higher AUC reductions due to faster clearance, neither AMI nor BUP simulations were especially sensitive to clinically relevant changes in E_h. Increased organ to blood partition coefficients (Keff), B:P, and f_u had the biggest effect on liposome efficacy. The tissues were more able to compete with the liposomes for drug binding, causing the treatment to be about 50% less effective at reducing the AUC for BUP. AUC reductions of slightly less than 50% were still achieved for AMI due to the extremely high binding affinity between AMI and liposomes. 20% K_2 reductions representing less effective liposome-drug binding caused AUC and peak reductions to drop by a few percentage points in both cases. This was less noteworthy for AMI as the overall change was still very large. The change for BUP represented a much larger portion of the AUC and peak reductions and may be important. A reduction in k_a increases t_{max}, i.e., the time at which the peak is reached. Accordingly, for a fixed t_{lag} (=2 hours), a reduction in k_a results in a reduction in the blood concentration at the time of liposome administration, leading to a larger reduction in the peak concentration. No effect of changing k_a was seen for BUP since liposome dosing occurs shortly after drug dosing. More rapid liposome clearance altered AMI AUC reductions by about 9% compared to 30% for BUP, again illustrating the reduced room for error for BUP.

Overall, the model results were not particularly sensitive to any one parameter and the liposomes would probably redistribute a considerable amount of AMI and a smaller but potentially significant amount of BUP in most patients. Kpu values have the

potential to modify the results the most. The reduced liposome affinity for BUP makes the parameter changes more significant for the anesthetic compared to AMI. A more thorough analysis of threshold drug concentration changes needed for effective toxicity reversal is required for drawing more concrete conclusions.

7.4.5 Liposome Dose Optimization

Dose optimization is a difficult challenge when developing new therapies. Besides ensuring a low level of toxicity, it is practically very difficult to predict what concentrations are optimal for therapeutic effectiveness while also avoiding unnecessary patient risk and material waste. Even arriving at the correct doses for animal experiments can be time consuming and expensive. PBPK models can improve dose optimization by identifying effective dose ranges early [74]. In Figures 7-5a and 7-5b, heart, brain, and C_{vbf} AUC values for AMI rapidly decrease as liposome dose increases, but this effect subsides as the liposome dose increases. Figure 7-5c demonstrates that AMI peak reductions level off prior to reaching 0.72 g/L. The benefit to dose ratio for AMI decreases as major changes in the distribution of AMI become harder to achieve at higher C_{vb} concentrations. This is a direct result of the large proportion of AMI being extracted from the tissues at liposome doses of 0.72 g lipid/L. Essentially, loading much more than 0.72 g lipid/L into the body to further increase C_{vb} and decrease C_{ht} and C_{br} may not be worth the potential side effects of increased lipid dosing. Conversely, liposome-BUP binding is much lower and a large proportion of BUP still remains inside tissues at 2.88 g lipid/L. As displayed in Table 7-9, lipid doses for BUP treatment should be as large as possible, limited solely by the maximum safe dose of phospholipids.

7.4.6 Time Lapse Between Drug Administration and Liposome Treatment

AMI overdose treatment and BUP adverse reaction treatment represent two very different scenarios in terms of the amount of time elapsing between drug and liposome dosing. This difference is quantitatively evident in the PBPK model results. The therapeutic effect for AMI patients diminishes as the time between ingestion and treatment increases (Figure 7-5d). Regardless, the model points to large AUC reductions even with t_{lag} = 8 hours. Therapeutic benefits even for large t_{lag} are possible because of high affinity binding between AMI and the liposomes, resulting in rapid concentration reductions upon dosing. The absorption rate constant is also a factor for AMI since rapid absorption coupled with large t_{lag} values increases the patient's exposure to the drug. These effects are altogether avoided in the case of BUP, where patients are already at a medical facility and available for immediate treatment.

7.4.7 Limitations

The central goal of the PBPK model developed here is to serve as a tool for evaluating the potential of liposome based therapy for overdose treatment in an average patient, and to aid the design of animal and human studies. While the model predictions are encouraging, several issues related to the assumptions and parameters utilized in the model must be considered. Uncertainties in Kpu calculations, drug and liposome specific input parameters, and the data used for validation and fitting added inherent variability to the modeling results. Equations used to estimate hepatic extraction and non-IV absorption ignored possible non-linearities at elevated drug concentrations. Drug metabolites, which could independently contribute to toxicity, were not accounted for. Finally, differences between the in vitro environment in which liposome-drug binding and protein-drug binding were measured and the physiological

environment (i.e. shear forces on liposomes, presence of enzymes and other trace molecular entities, immune system response) could alter the ultimate effect of the therapy. These issues represent opportunities for further investigation in the future.

7.5 Conclusions

A physiologically based pharmacokinetic (PBPK) model consisting of 15 compartments was developed by employing published [106] equations for tissue to blood partition coefficients and parameters pooled from numerous clinical studies. IV data affirmed the ability of the models to predict drug concentrations in the blood compartments with reasonable accuracy. Least squares fits of model results to non-IV data were utilized to obtain first-order absorption rate constants.

Drug overdose simulations for AMI revealed that liposomes are capable of reducing brain and heart AUC values by over 60% and peak AMI concentrations by 20% if treatments are provided within 2 hours of ingestion. AMI concentration increases in venous blood for the PBPK simulations and clinical overdose treatments with protein fragments were similar [4]. BUP AUC and peak reductions were much lower at around 15-17%. First approximations of localized cardiac pharmacodynamics suggested improved ion channel function and myocyte contractility with liposome therapy, especially for AMI. Although the models suggested between 0.72 and 1.44 g lipid/L as an optimal starting dose for treating AMI overdoses, the maximum safe dose of liposomes should be given for adverse reactions to BUP. The modeling results were relatively insensitive to reasonable variations in model parameters. The modeling predictions agree, at least qualitatively, with reports on overdose treatments by Fab fragments, which like liposome administration, is an approach based on high affinity binding between fragments and the drug.

In conclusion, the PBPK models developed in this chapter suggests that liposomes are capable of redistributing both AMI and BUP into the blood compartments to significant degrees and may be effective at treating AMI overdoses and adverse reactions to BUP. Liposomes will, in general, be more effective at treating overdoses of drugs with high volumes of distribution and slow elimination characteristics, such as TCA's.

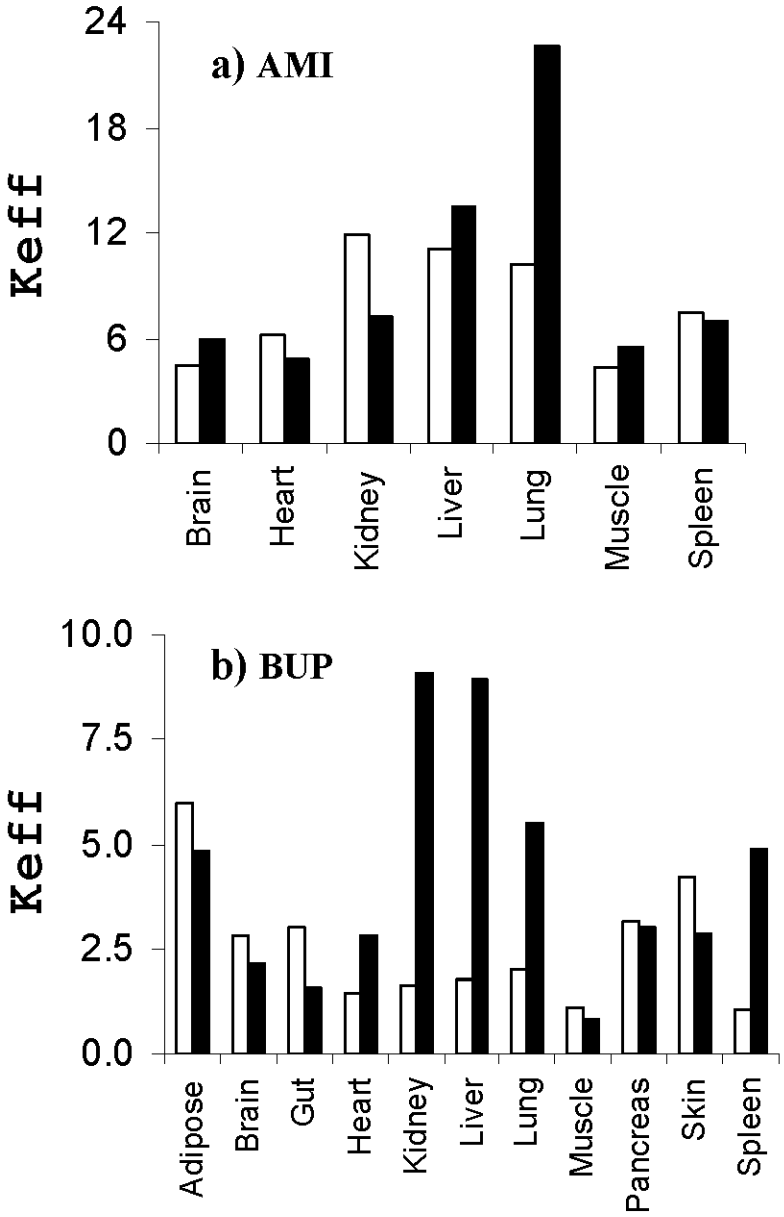

Figure 7-1. Organ to blood partition coefficients (Keff) calculated using Equation 7-4 (□) or determined experimentally (■) for a) AMI [161-163] or b) BUP [164-167].

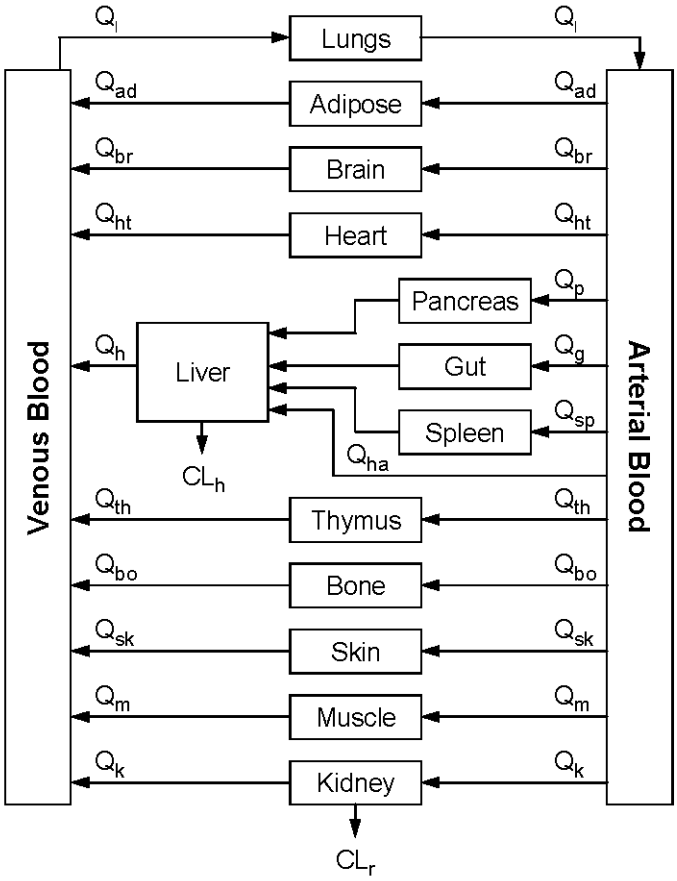

Figure 7-2. PBPK model structure used for AMI and BUP overdose simulations.

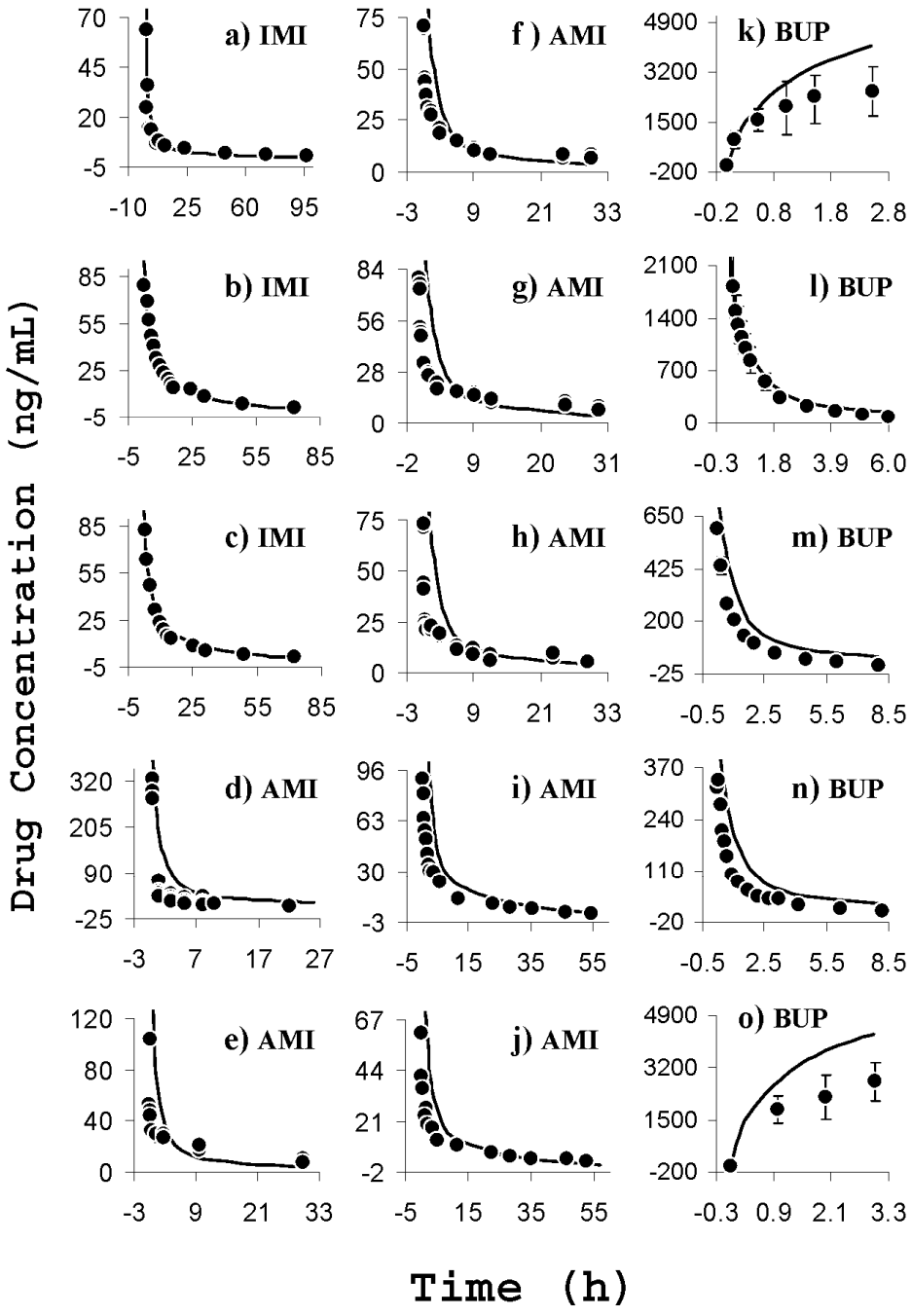

Figure 7-3. Drug concentrations versus time predicted using PBPK models (—) or measured (●) after IV dosage for a) IMI [173] in venous plasma, b-c) IMI [174] in venous plasma, d) AMI [175] in venous plasma, e-h) AMI [176] in venous plasma, i-j) AMI [149] in venous whole blood, k) BUP [179] in arterial plasma, l) BUP [151] in arterial plasma, m) BUP [178] in venous whole blood, n) BUP [177] in venous plasma, and o) BUP [186] in arterial plasma. Error bars are shown for experimental results when reported.

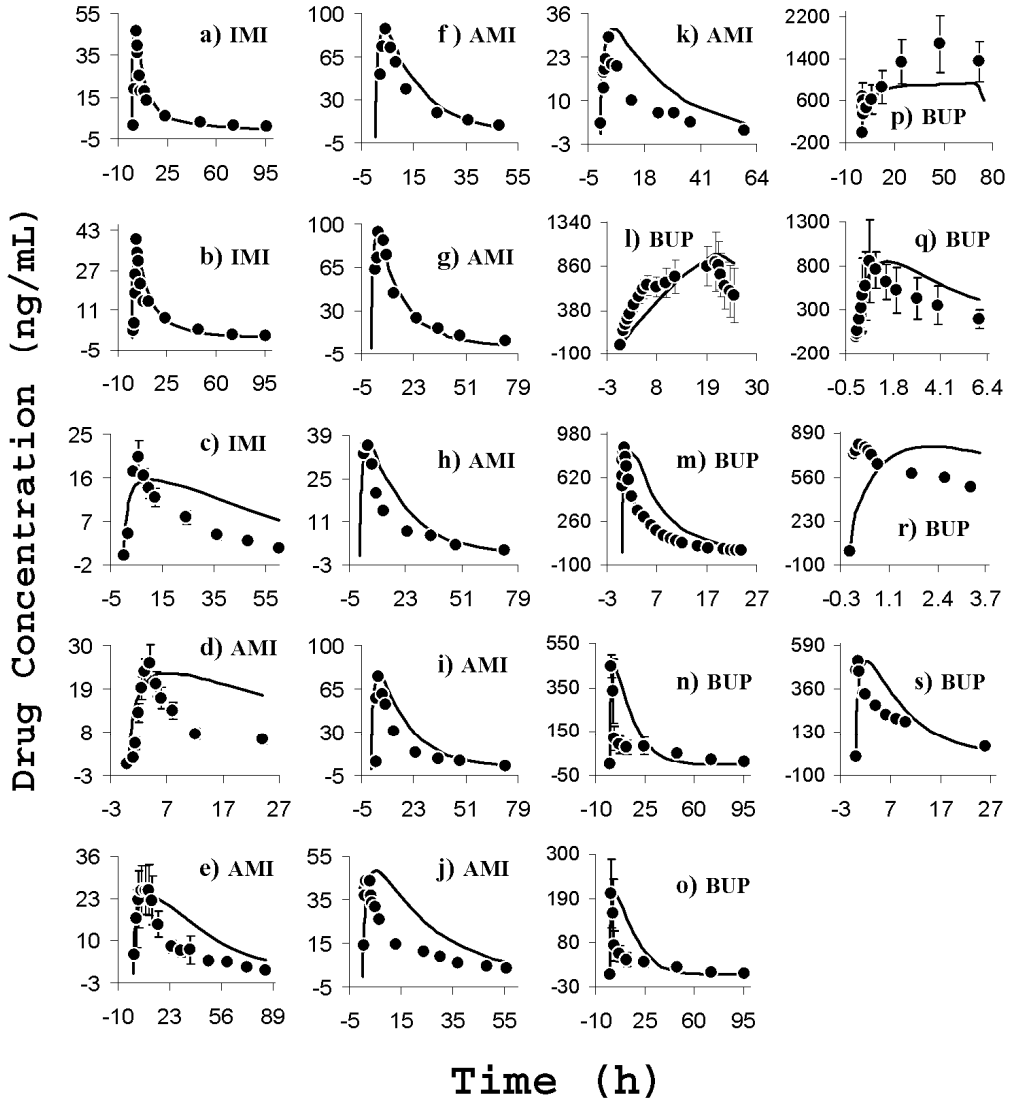

Figure 7-4. Drug concentrations versus time for PBPK models (—) where k_a was allowed to vary to obtain best fits to measured non-IV dosage data (●) for a-b) IMI [173], c) IMI [109], d) AMI [191], e) AMI [190], f-h) AMI [188], i) AMI [189], j-k) AMI [149], l) BUP [197] into the epidural space, m) BUP [195] into the intercostal space, n-o) BUP [196] into the leg, p) BUP [198] into the intercostal space, q) BUP [193] into the intraperitoneal space, r) BUP [192] into the epidural space, and s) BUP [194] into the epidural space. TCA dosages (a-k) were all oral. Error bars are shown for experimental results when reported.

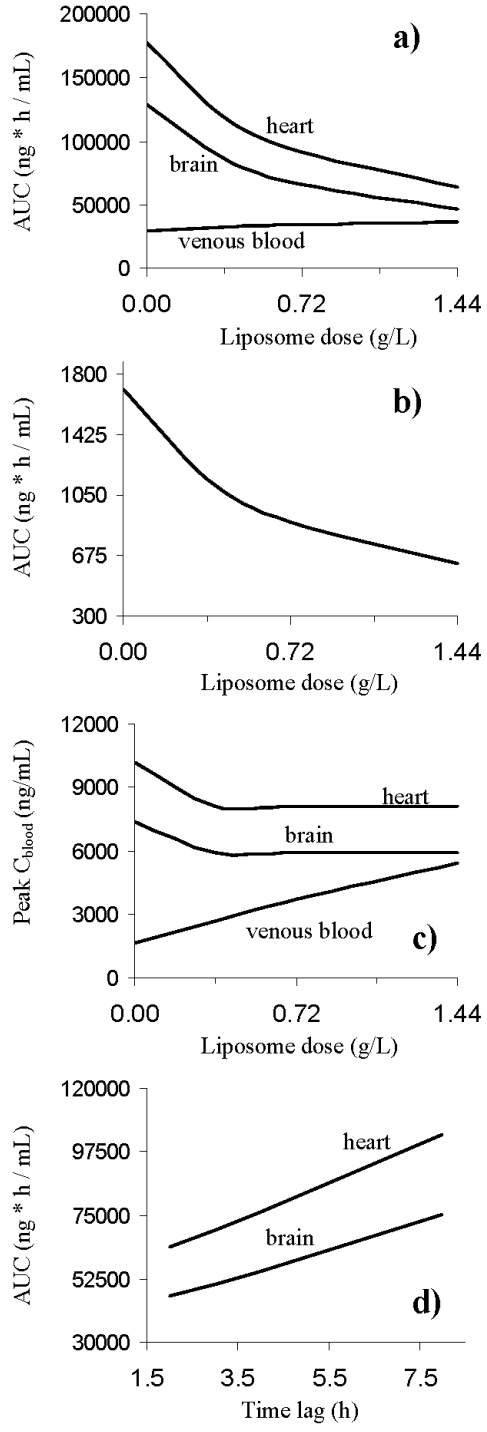

Figure 7-5. Summary of AMI overdose (2500 mg) simulation results. AMI AUC values versus liposome dose for a) venous blood and key organs with t_{lag} = 2 hours; b) free AMI in venous blood (C_{vbf}) with t_{lag} = 2 hours; c) peak AMI concentrations versus liposome dose with t_{lag} = 2 hours; d) AMI AUC values versus t_{lag}, the time between drug ingestion and liposome treatment, with C_{lip} = 1.44 g/L.

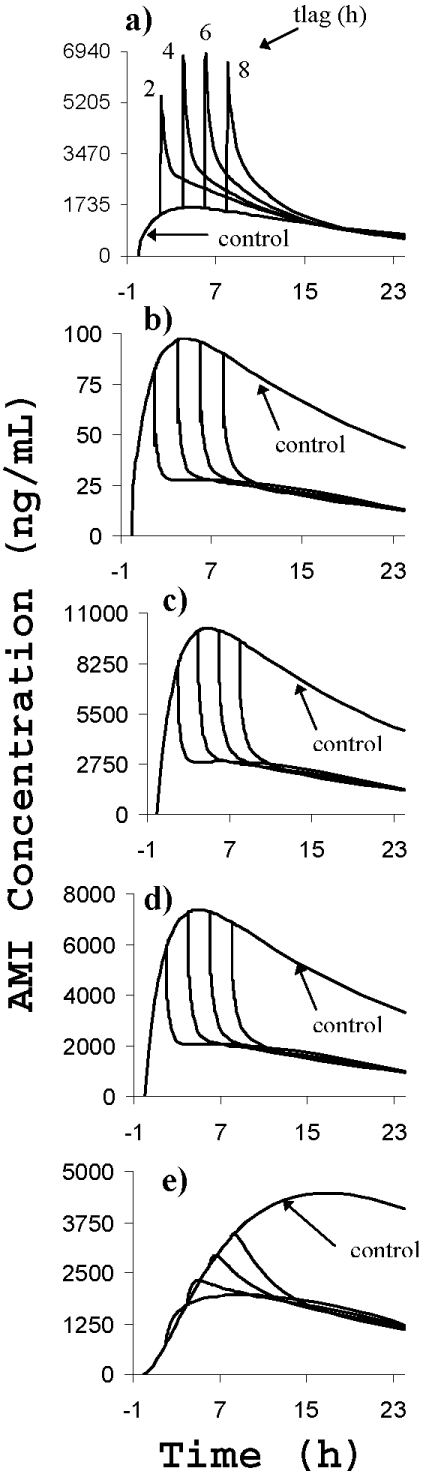

Figure 7-6. AMI concentrations versus time for simulated overdose cases (2500 mg) without liposomes and with liposomes at 1.44 g/L for t_{lag} = 2, 4, 6, and 8 hours for a) venous whole blood, b) free AMI in venous blood, c) heart, d) brain, and e) muscle.

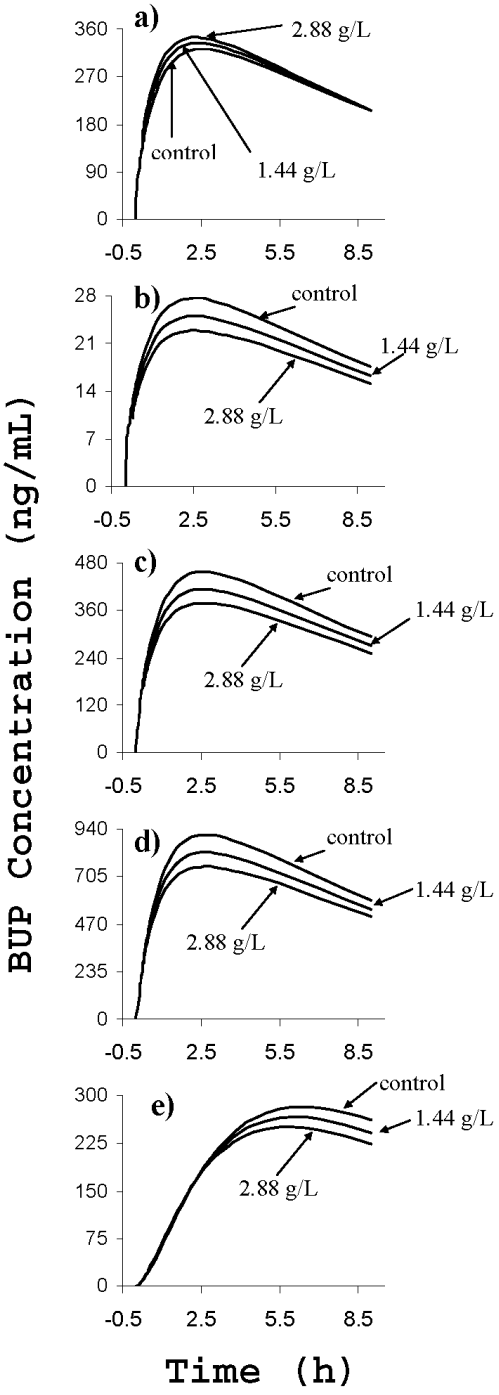

Figure 7-7. BUP concentrations versus time for simulated adverse reactions (100 mg) without liposomes and with liposomes at 1.44 or 2.88 g/L for t_{lag} = 0.25 hours for a) venous whole blood, b) free BUP in venous blood, c) heart, d) brain, and e) muscle.

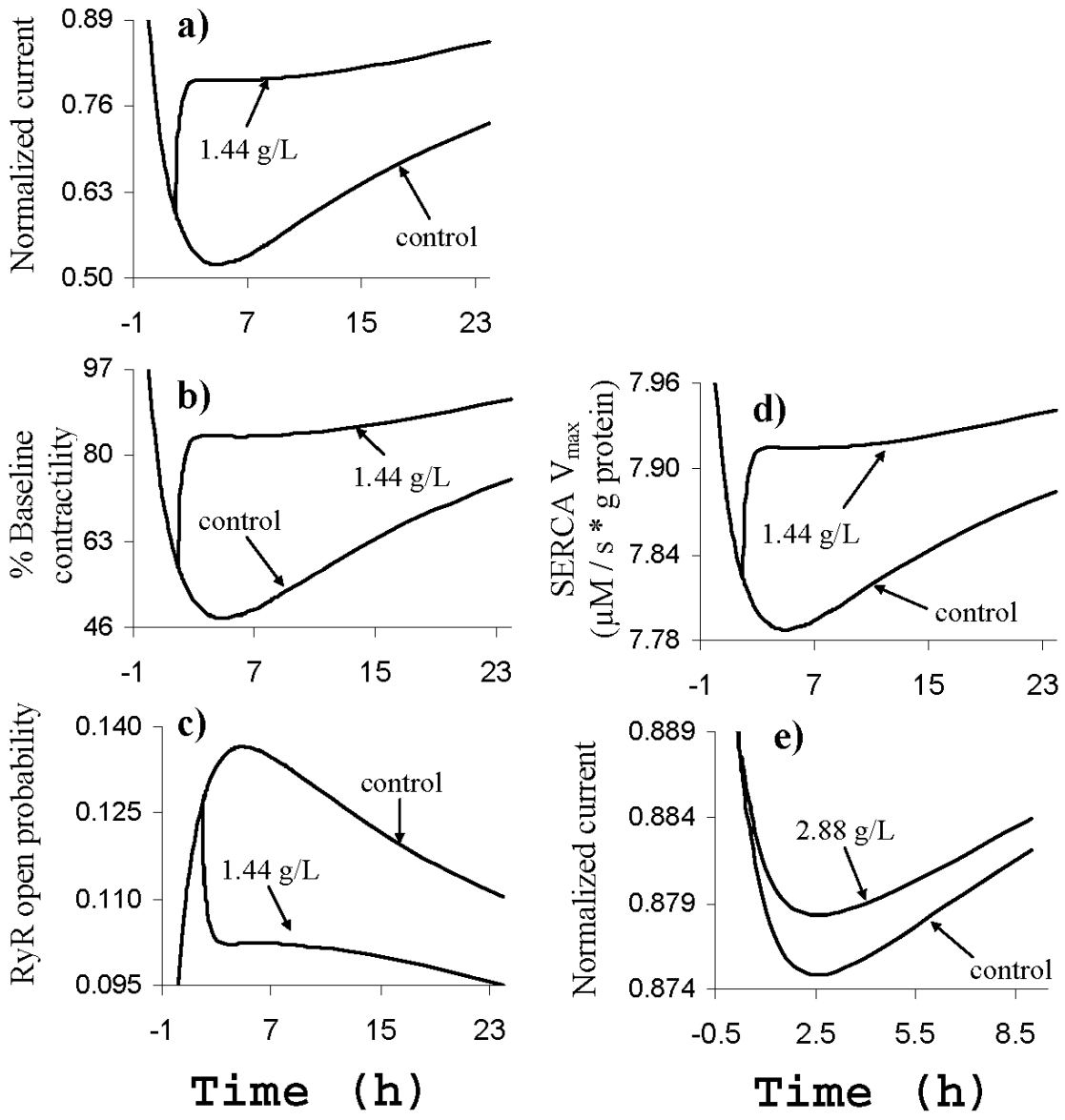

Figure 7-8. Pharmacodynamics in the heart as a function of time. Correlations from drug concentrations in the heart predicted by our PBPK models to local pharmacodynamic effects were estimated through the use of published data. Controls were simulated overdoses with no liposomes; lipid loadings are specified for simulated overdoses with liposomes. The plots show a) normalized current through cardiac (hH1) Na^+ channels [9] for AMI overdose, b) % baseline contractility of atrial tissue [10] for AMI overdose, c) the open probability of type 2 ryanodine receptors (RyR) [141] for AMI overdose, d) maximum Ca^{2+} uptake by sarcoplasmic reticulum (SR) Ca^{2+} ATPase pumps (SERCA) [141] for AMI overdose, e) normalized current through cardiac (hH1) Na^+ channels [16] for BUP adverse reaction. T_{lag} was 2 hours for AMI and 0.25 hours for BUP; AMI and BUP doses were 2500 mg and 100 mg, respectively.

Table 7-1. Drug specific parameters for Kpu calculations

	Imipramine		Amitriptyline		Bupivacaine	
	Value	Refs.	Value	Refs.	Value	Refs.
pK_a	9.5	[106]	9.4	[146]	8.1	[123]
B:P	1.1	[147,148]	0.86 [a]	[149,150]	0.64 [a]	[151,152]
f_u	0.18 [b]	Ch. 4	0.08 [c]	Ch. 3	0.10 [d]	Ch. 5
$LogP_{vo:w}$	4	[106]	4.1 [e]	[153]	2.4 [e]	[153]
$LogP_{oc:w}$	4.8	[106]	4.92	[154]	3.4	[155]
Kpu_{BC}	6.8 [f]	[106]	8.6 [f]	[106]	2.0 [f]	[106]
K_{aBC}	6.13 [g]	[106]	7.45 [g]	[106]	0.10 [g]	[106]

Key: pK_a - acid dissociation constant; B:P - blood to plasma concentration ratio; f_u - fraction of drug unbound in plasma; $LogP_{vo:w}$ - log of the vegetable oil to water partition coefficient; $LogP_{oc:w}$ - log of the octanol to water partition coefficient; Kpu_{BC} - affinity for blood cells [106]; K_{aBC} - association constant of drugs to blood cells [106]. [a]Weighted average from two studies. [b]Our value originated from experimental data at physiological IMI concentrations (Chapter 4) and 0.1 [108,156], 0.12 [157], and 0.11 [107] have been reported in literature. An f_u of 0.24 was used for Kpu calculations by Rodgers et al. [106]. [c]Our value originated from experimental data at physiological AMI concentrations (Chapter 3) and 0.08 [157], 0.05 [108], and 0.06 [156] have been reported in literature. [d]Our value originated from experimental data at physiological BUP concentrations (Chapter 5) and 0.10 [121], 0.06 [119], and 0.05 [158] have been reported in literature. [e]$LogP_{vo:w}$ values were calculated from published methods [153] from reported $LogP_{oc:w}$ values. [f]Kpu_{BC} values were calculated [106] using f_u and B:P values with H = 0.45. [g]K_{aBC} values were calculated using drug specific parameters reported here and published equations [106].

Table 7-2. Calculated drug to tissue partition coefficient (Kpu) values

Organ	IMI	AMI	AMI [a]	BUP	BUP [b]
Adipose (ad)	73.5	114.0	131.5	38.2	46.1
Bone (bo)	19.9	27.8	57.1	8.3	21.7
Brain (br)	27.4	41.6	59.1	18.1	26.1
Gut (g)	59.0	80.5	185.8	19.3	67.3
Heart (ht)	44.4	57.4	155.8	9.1	53.9
Kidney (k)	87.9	110.6	330.4	10.5	110.7
Liver (h)	81.8	103.6	302.9	11.3	102.1
Lung (l)	74.0	95.2	266.1	13.0	90.8
Muscle (m)	31.1	40.1	106.9	7.0	37.4
Pancreas (p)	49.1	68.8	141.8	20.3	53.5
Skin (sk)	51.8	76.1	133.8	26.9	53.2
Spleen (sp)	55.7	69.7	208.7	6.8	70.2
Thymus (th)	46.7	60.6	161.1	10.3	56.1

[a]These Kpu values were used for the AMI sensitivity analysis. To estimate the upper Kpu bounds for AMI, an f_u of 0.05 [85,159] and a B:P ratio of 1.04 [150], the weighted B:P average from 1 of 2 studies used for the overall AMI B:P average, were used.
[b]These Kpu values were used for the BUP sensitivity analysis. To estimate the upper Kpu bounds for BUP, an f_u of 0.05 [158] and a B:P ratio of 0.73 [151], the weighted B:P average from 1 of 2 studies used for the overall BUP B:P average, were used.

Table 7-3. Partition coefficients for drug binding to proteins, liposomes, and red blood cells

	K_1 [a]	K_2 [b]	K_3 [c]
IMI	4.8 ± 1.1	-	5.803
AMI	9.8 ± 1.3	$64.15C_{lip}$	6.106
BUP	9.0 ± 0.75	$1.39C_{lip}$	1.64

Key: K_1 - Concentration ratio for drug bound to proteins to free drug; K_2 - concentration ratio for drug bound to liposomes to free drug; K_3 - concentration ratio for drug bound to RBC's to free drug; C_f - free drug concentration in ng/mL; C_{lip} - liposome concentration in venous blood in g/L. [a]Based on measured fractions bound to serum proteins of 0.83 (IMI - Chapter 4) and 0.91 (AMI - Chapters 2,3) at drug concentrations from 1 to 10 μM (mean ± standard deviation) and BUP protein binding at low BUP concentrations extrapolated from our data (Chapter 5). [b]IMI overdose simulations were not done. AMI and BUP equations are based on measured, concentration dependent drug binding to liposomes (Chapters 2,3,5). The equations are valid from C_{lip} = 0 to 1.44 mg/mL for AMI and 0 to 2.88 mg/mL for BUP. [c]K_3 values for IMI, AMI, and BUP were based on B:P ratios of 1.1, 0.86, and 0.64, respectively, and solved for as shown in the text.

Table 7-4. Organ blood flow and volume fractions for humans

Organ	Fraction of Cardiac Output [a]	Fraction of Body Volume [b]
Adipose (ad)	0.0342	0.1196
Bone (bo)	0.1665	0.0856
Brain (br)	0.1001	0.0200
Gut (g)	0.1368	0.0171
Heart (ht)	0.0316	0.0047
Kidney (k)	0.1632	0.0044
Liver (h)	0.2080	0.0260
Lung (l)	1.0000	0.0076
Muscle (m)	0.0395	0.4000
Pancreas (p)	0.0313	0.0014
Skin (sk)	0.2567	0.0371
Spleen (sp)	0.0351	0.0026
Thymus (th)	0.0014	0.0004

[a]Total cardiac output in L/min was calculated from the allometric ($CO = 0.235 Weight^{0.71}$) with weight in kg [170]. Blood flow was scaled to match the reported weights of patients in studies when reported (70 kg otherwise). Fractions of cardiac output were calculated from values reported by Igari et al. [78] for a 70 kg man for all organs except the thymus and bone. The proportion of liver blood supply coming from the pancreas, spleen, gut, and arterial blood were calculated from data reported by Benowitz et al. [171] for rhesus monkeys. Thymus and bone blood supplies were scaled by organ weight from blood supplies to rat thymus and bone reported by Meno-Tetang et al. [79]. The fractions of cardiac output were scaled so they added to exactly 1 after all were combined.
[b]Fractions of total body volume were taken from Poulin et al. [144] except for the pancreas and thymus. Pancreas and thymus volumes were estimated from weights of 100 g and 25 g, respectively [172]. Total body volume was estimated from body weight at a density of 1 L/kg. Body volumes were scaled to match reported weights or average weights of patients studied when reported (70 kg otherwise). Venous and arterial blood volumes were taken as 3.6 and 1.8 L [78], respectively, for a 70 kg subject and scaled linearly with weight.

Table 7-5. Input parameters for PBPK model

	Imipramine		Amitriptyline		Bupivacaine	
	Value	Refs.	Value	Refs.	Value	Refs.
Cl_h	709.4 [a]	[173,174]	579.6 [a]	[149,150,175,176]	498.4 [b]	[177-180]
Cl_r	12.3 [c]	[173,174]	10.0 [c]	[149,150,175,176]	10.7 [d]	[177-180]
H	0.45	[181]	0.45	[181]	0.45	[181]
F	0.42 [e]	[148,173,174]	0.45 [e]	[149,150,182,183]	1 [f]	-

Key: Cl_h - hepatic clearance in mL/(h*kg); Cl_r - renal clearance in mL/(h*kg); H - hematocrit; F - bioavailability. [a]Weighted average from cited studies used to calculate E_h as shown in the text [73,108,169] assuming 98.3% of elimination is hepatic for TCA's [184]. [b]Weighted average from cited studies used to calculate E_h as shown in the text [73,108,169] assuming 97.9% of elimination is hepatic for BUP [178,185]. [c]Weighted average from cited studies assuming 1.7% of elimination is renal for TCA's [184]. [d]Weighted average from cited studies assuming 2.1% of elimination is renal for BUP [178,185]. [e]Weighted average from cited studies. [f]Bioavailability was assumed to be 1 for BUP since non-oral routes of administration were used.

Table 7-6. Drug specific inputs for overdose simulations

	Amitriptyline		Bupivacaine	
	Value	Refs.	Value	Refs.
D_{drug}	100, 500, 2500 [a]	[7,110,111,115]	100 [b]	[192-196]
D_{lip}	0.36, 0.72, 1.44 [c]	Ch. 2,3	1.44, 2.88 [c]	Ch. 5
t_{lag}	2, 4, 6, 8 [d]	[7,110-112,202]	0.25 [e]	[12-15]

Key: D_{drug} - drug dose(s) simulated with PBPK models in mg; D_{lip} - liposome doses simulated with PBPK models in g lipid/L blood; t_{lag} - elapsed time between drug administration or ingestion and liposome treatment in hours. [a]Doses of 300 mg [7], 1-2 g [110], and 3.7-9.2 g [111] were clinically observed in AMI overdose cases and 1.4-2.8 g has been suggested as common for AMI overdoses [115]. [b]BUP Doses of 150 mg [192,196], 100 mg [193,194], and 140 mg [195] have been clinically administered. [c]Corresponds to 27.8-111 mg/kg or 1.9-7.8 g of total phospholipids for AMI and 111-222 mg/kg or 7.8-15.6 g of total phospholipids for BUP. Liposome doses were modeled as bolus doses based on maximum possible lipid concentrations of about 50 mg/mL in liposome formulations [199] and fluid volumes given as bolus doses or rapid infusions in clinical studies [12,14,15,40]. Dhanikula et al. [25] suggest that at least 10 g of liposomes could be administered safely; up to 250 g of lipids (phospholipids and oil) have been suggested as safe for anesthetic overdose treatment (http://lipidrescue.squarespace.com/), and 100 g has been used in a clinical overdose case [200]. Up to 190 mg/kg of liposomes have been given to mice in animal studies [201]. [d]Time lags between overdose and treatment have been observed clinically from 2-8 hours for TCA's. [e]Time between drug administration and lipid emulsion treatment have been observed clinically from 0.1-0.25 hours for anesthetics.

Table 7-7. Sensitivity analysis setup

	Amitriptyline		Bupivacaine	
	Simulation	Sensitivity	Simulation	Sensitivity
E_h	0.41	0.33, 0.45 [a]	0.37	0.33, 0.45 [a]
k_a	0.093	0.054, 0.132 [b]	0.179	0.100, 0.258 [c]
K_2	63.0 - 84.0 [d]	50.4 - 67.2 [d]	1.64 - 4.19 [d]	1.31 - 3.35 [d]
Cl_{lip}	$0.24t^2$ - 7.89t + 100 [e]	-9.1ln(t +0.01) + 59.4	$0.24t^2$ - 7.89t + 100 [e]	-9.1ln(t + 0.01) + 59.4

Key: E_h - hepatic extraction factor (Equation 7-8); k_a - first-order absorption rate constant in h^{-1}, K_2 - concentration ratio for drug bound to liposomes to free drug; Cl_{lip} - equation defining the percent of the initial liposome dose remaining in the blood stream as a function of time, used to simulate liposome clearance. [a]Upper [149,178] and lower [176,179] bounds were taken from maximum and minimum average values observed in single studies that were part of the studies used to obtain hepatic drug clearance (see Table 7-5). [b]Upper and lower bounds were calculated using the standard deviations of the averaged k_a value which was averaged from best fits to data from oral AMI studies [149,188-191]. [c]Upper and lower bounds were calculated using the standard deviations of the averaged k_a value which was averaged from best fits to data from non-IV BUP studies [192,194,197]. [d]Range of liposome concentration dependent K_2 values used to calculate the equation for K_2 as a function of C_{lip}. The values were reduced by 20%, although this was larger than the observed standard deviations, to investigate significantly reduced binding. The equations became ($51.32C_{lip}$) for AMI and ($1.11C_{lip}$) for BUP. See Table 7-3 for comparison. [e]A new liposome elimination curve as a function of time was generated by reducing the percent of liposomes left at each time point by 30%. This was much larger than the error bars shown for the data [30] but was done to investigate large variation in elimination. Extended liposome circulation times were not investigated as they only increase the efficacy of the treatment. Note that 0.01 was added to t to avoid values greater than 100% when logarithms were used.

Table 7-8. AMI overdose simulation results

AMI	D_{lip}	t_{lag}	AUC_{vb}	$Peak_{vb}$	AUC_{ht}	$Peak_{ht}$	AUC_{br}	$Peak_{br}$	AUC_{vbf}	$Peak_{vbf}$
2500	0.00	0	28985	1652	177560	10175	128650	7372	1711	97.5
2500	0.36	2	32325	2665	118390	8131	85792	5900	1146	82.3
2500	0.72	2	34344	3721	91187	8131	66086	5900	887	82.3
2500	1.44	2	36483	5445	63874	8131	46302	5900	628	82.2
2500	0.36	4	32389	3229	124790	10039	90430	7275	1210	96.9
2500	0.72	4	34427	4574	100460	10040	72814	7275	980	97.0
2500	1.44	4	36546	6782	75998	10038	55093	7274	747	97.0
2500	0.36	6	32448	3239	132360	10175	95920	7372	1283	97.5
2500	0.72	6	34519	4616	111300	10175	80668	7372	1084	97.5
2500	1.44	6	36649	6886	89930	10175	65187	7372	881	97.5
2500	0.36	8	32486	3071	139860	10175	101350	7372	1354	97.5
2500	0.72	8	34594	4393	122060	10175	88458	7372	1186	97.5
2500	1.44	8	36761	6584	103750	10175	75194	7372	1012	97.5
500[a]	0.00	0	5797	330.3	35512	2035	25731	1474	342	19.5
500	1.44	2	7297	1089	12775	1626	9260	1180	125.5	16.4
100 [a]	0.00	0	1159	66.1	7102	407	5146	294.9	68.4	3.9
100	1.44	2	1459	217.8	2555	325.3	1852	236	25.1	3.3

Key: D_{lip} - liposome doses simulated with PBPK models in g lipid/L blood; t_{lag} - elapsed time between drug administration or ingestion and liposome treatment in hours; AUC - area under the AMI concentration versus time curve in (ng*h)/mL; Peak - maximum AMI concentration reached in the specified organ in ng/mL; vb - venous blood; ht - heart; br - brain; vbf - free AMI in venous blood. [a]Drug doses of 500 and 100 mg are only shown for the most effective liposome dose of 1.44 mg/mL.

Table 7-8 Continued. AMI overdose simulation results

AMI	D_{lip}	t_{lag}	% AUC_{vbf}	% $Peak_{vbf}$	% AUC_{ht}	% $Peak_{ht}$	% AUC_{br}	% $Peak_{br}$
2500	0.00	0	-	-	-	-	-	-
2500	0.36	2	33.0 [a]	15.6	33.3	20.1	33.3	20.0
2500	0.72	2	48.1	15.6	48.6	20.1	48.6	20.0
2500	1.44	2	63.3	15.6	64.0	20.1	64.0	20.0
2500	0.36	4	29.3	0.6	29.7	1.3	29.7	1.3
2500	0.72	4	42.8	0.5	43.4	1.3	43.4	1.3
2500	1.44	4	56.3	0.5	57.2	1.3	57.2	1.3
2500	0.36	6	25.0	0.0	25.5	0.0	25.4	0.0
2500	0.72	6	36.7	0.0	37.3	0.0	37.3	0.0
2500	1.44	6	48.5	0.0	49.4	0.0	49.3	0.0
2500	0.36	8	20.9	0.0	21.2	0.0	21.2	0.0
2500	0.72	8	30.7	0.0	31.3	0.0	31.2	0.0
2500	1.44	8	40.8	0.0	41.6	0.0	41.6	0.0
500	0.00	0	-	-	-	-	-	-
500	1.44	2	63.3 [a]	15.7	64.0	20.1	64.0	20.0
100	0.00	0	-	-	-	-	-	-
100	1.44	2	63.3 [a]	15.7	64.0	20.1	64.0	19.9

Key: D_{lip} - liposome doses simulated with PBPK models in g lipid/L blood; t_{lag} - elapsed time between drug administration or ingestion and liposome treatment in hours; AUC - area under the AMI concentration versus time curve in (ng*h)/mL; Peak - maximum AMI concentration reached in the specified organ in ng/mL; % AUC - percent reduction in AUC compared to case without liposomes; % Peak - percent reduction in drug concentration peak compared to case without liposomes; vb - venous blood; ht - heart; br - brain; vbf - free AMI in venous blood. [a]Blanks are cases with no liposomes and % AUC and peak changes with liposomes are calculated based on the no liposome cases at equivalent AMI doses.

Table 7-9. BUP overdose simulation results

D_{lip}[a]	AUC_{vb}	$Peak_{vb}$	AUC_{ht}	$Peak_{ht}$	AUC_{br}	$Peak_{br}$	AUC_{vbf}	$Peak_{vbf}$
0	2399	323	3391	458	6695	911	206.1	27.7
1.44	2465	334	3105	414	6134	824	188.6	25.1
2.88	2526	344	2868	379	5669	754	174.2	22.9

Table 7-9 Continued. BUP overdose simulation results

D_{lip}[a]	% AUC_{vbf}	% $Peak_{vbf}$	% AUC_{ht}	% $Peak_{ht}$	% AUC_{br}	% $Peak_{br}$
0	-	-	-	-	-	-
1.44	8.5 [b]	9.6	8.5	9.6	8.4	9.6
2.88	15.5	17.3	15.4	17.3	15.3	17.3

Key: D_{lip} - liposome doses simulated with PBPK models in g lipid/L blood; AUC - area under the BUP concentration versus time curve in (ng*h)/mL; Peak - maximum BUP concentration reached in the specified organ in ng/mL; % AUC - percent reduction in AUC compared to case without liposomes; % Peak - percent reduction in drug concentration peak compared to case without liposomes; vb - venous blood; ht - heart; br - brain; vbf - free BUP in venous blood. [a]The BUP dose was 100 mg and t_{lag} = 0.25 hours. [b]Blanks are cases with no liposomes and % AUC and peak changes with liposomes are calculated based on the no liposome cases at equivalent BUP doses.

Table 7-10. AMI sensitivity analysis results

Change in Model	AMI	D_{lip}	t_{lag}	% AUC_{vbf}	% $Peak_{vbf}$	% AUC_{ht}	% $Peak_{ht}$	% AUC_{br}	% $Peak_{br}$
None	2500	1.44	2	63.3 [a]	15.6	64.0	20.1	64.0	20.0
E_h (0.45) [b]	2500	1.44	2	63.8	13.9	64.6	18.2	64.5	18.1
E_h (0.33)	2500	1.44	2	61.9	19.6	62.5	24.2	62.5	24.1
Kpu [c]	2500	1.44	2	46.6	16.5	47.1	21.9	46.9	19.2
K_2 [d]	2500	1.44	2	58.6	15.6	59.3	20.1	59.2	20.0
k_a (0.132) [e]	2500	1.44	2	63.6	10.6	64.5	14.7	64.5	14.6
k_a (0.054)	2500	1.44	2	62.7	23.4	63.2	27.8	63.1	27.7
Cl_{lip} [f]	2500	1.44	2	57.7	15.6	58.4	20.1	58.4	20.0

Key: E_h - hepatic extraction factor (Equation 7-8); Kpu - organ to plasma partition coefficient with respect to the free drug concentration in plasma; K_2 - concentration ratio for drug bound to liposomes to free drug; k_a - first-order absorption rate constant in h^{-1}; Cl_{lip} - equation defining the percent of the initial liposome dose remaining in the blood stream as a function of time, used to simulate liposome clearance; AMI - AMI dose in mg; D_{lip} - liposome doses simulated with PBPK models in g lipid/L blood; t_{lag} - elapsed time between drug administration or ingestion and liposome treatment in hours; % AUC - percent reduction in AUC compared to case without liposomes; % Peak - percent reduction in drug concentration peak compared to case without liposomes; ht - heart; br - brain; vbf - free AMI in venous blood. [a]All % changes were calculated from the case of no liposomes with the same sensitivity analysis parameter altered as specified for that particular row. [b]The value of E_h used for the overdose simulations was 0.41. [c]An f_u value of 0.05 and a B:P ratio of 1.04 was used to estimate the increased Kpu values; see Table 7-2 for values and details. [d]Values were decreased by 20% at each liposome concentration; see Table 7-7 for details. [e]The absorption constant used for the AMI overdose simulations was 0.093. [f]Liposome clearance was increased by 30% at each time point to generate a new elimination function; see Table 7-7 for details.

Table 7-11. BUP sensitivity analysis results

Change in Model	BUP	D_{lip}	t_{lag}	% AUC_{vbf}	% $Peak_{vbf}$	% AUC_{ht}	% $Peak_{ht}$	% AUC_{br}	% $Peak_{br}$
None	100	2.88	0.25	15.5 [a]	17.3	15.4	17.3	15.3	17.3
E_h (0.45) [b]	100	2.88	0.25	16.2	18.2	16.2	18.1	16.1	18.1
E_h (0.33)	100	2.88	0.25	15.0	16.8	15.0	16.8	14.9	16.7
Kpu [c]	100	2.88	0.25	8.2	8.9	8.0	8.9	8.1	8.9
K_2 [d]	100	2.88	0.25	12.8	14.4	12.8	14.4	12.7	14.4
k_a (0.258) [e]	100	2.88	0.25	15.8	17.4	15.8	17.4	15.7	17.3
k_a (0.100)	100	2.88	0.25	15.1	15.9	15.0	15.9	14.9	15.9
Cl_{lip} [f]	100	2.88	0.25	10.9	11.7	10.9	11.7	10.8	11.7

Key: E_h - hepatic extraction factor (Equation 7-8); K_2 - concentration ratio for drug bound to liposomes to free drug; k_a - first-order absorption rate constant; Cl_{lip} - equation defining the percent of the initial liposome dose remaining in the blood stream as a function of time, used to simulate liposome clearance; BUP - BUP dose in mg; D_{lip} - liposome doses simulated with PBPK models in g lipid/L blood; t_{lag} - elapsed time between drug administration or ingestion and liposome treatment in hours; % AUC - percent reduction in AUC compared to case without liposomes; % Peak - percent reduction in drug concentration peak compared to case without liposomes; ht - heart; br - brain; vbf - free BUP in venous blood. [a]All % changes were calculated from the case of no liposomes with the same sensitivity analysis parameter altered as specified for that particular row. [b]The value of E_h used for the overdose simulations was 0.37. [c]An f_u value of 0.05 and a B:P ratio of 0.73 was used to estimate the increased Kpu values; see Table 7-2 for values and details. [d]Values were decreased by 20% at each liposome concentration; see Table 7-7 for details. [e]The absorption constant used for the BUP overdose simulations was 0.1794. [f]Liposome clearance was increased by 30% at each time point to generate a new elimination function; see Table 7-7 for details.

CHAPTER 8
CONCLUSIONS

Treatments capable of reversing toxicity resulting from prescription drug overdose or adverse reaction are needed. While several therapies are in development elsewhere, including protein fragments, lipid emulsions, polymeric particles, and microemulsions, no widely effective treatment has been introduced into the market. This work was aimed at developing a drug overdose treatment using liposomes. The primary drugs targeted for treatment included TCA's, such as AMI, IMI, and DOS, as well as the local anesthetic BUP.

In Chapter 2, we demonstrated that DOPG liposomes and 50:50 DMPC:DOPG liposomes sequestered at least 99% of AMI at low drug concentrations. In the presence of albumin, pure DOPG liposomes were shown to be greatly inhibited by the proteins. In the presence of 7% proteins (w/w) composed of 4% albumin, 2% fibrinogen, and 1% globulins, the 50:50 DMPC:DOPG liposomes at a lipid loading of 0.72 mg lipid/mL sequestered 95-96% of the free drug, as opposed to a predicted 99%. The free AMI concentration was still reduced by 50-60%, however. In human serum, the 50:50 DMPC:DOPG liposomes took up about 94-98% of the drug and reduced the free drug concentration by 35-70%. Liposome-protein interactions were likely responsible for the reduced effectiveness of 50:50 DMPC:DOPG liposomes at sequestering AMI in serum versus PBS. We also proved that AMI binding to liposomes in the presence of proteins is quick and reversible. Uptake studies conducted with nortriptyline suggested that systems developed for AMI overdose treatment may also be useful for reducing the free concentration of nortriptyline.

Chapter 3 revealed that AMI uptake by 50:50 DMPC:DOPG liposomes was not enhanced by increased lipid loading in the presence of serum proteins. Drug binding was also shown to be independent of liposome size. Predominantly anionic lipids with a small amount of PEG-modified lipids were shown to sequester AMI from human serum most effectively. The optimal amount of PEG-modified lipid to be incorporated into liposomes to effectively shield proteins while also allowing diffusion and binding of the drug to the charged lipid membrane appeared to be 5%. Increasing the lipid loading of the polymer shielded liposomes by a factor of 2 resulted in a reduced free AMI concentration in human serum by nearly 90% across a wide range of initial drug concentrations. Liposomes were effective at drug binding after storage for about one month.

The primary goal of Chapter 4 was to extend the use of pegylated, anionic liposomes from AMI binding to other TCA's and opipramol. In PBS, the liposomes proved capable of sequestering about 98% or more of IMI and DOS and 92.5-95.5% of opipramol. Additionally, the liposomes reduced the free drug concentrations in human plasma by 88-93% in the case of the weak bases IMI and DOS, and 76% for the diprotic drug opipramol (1.44 mg lipid/mL loading). The data supports liposome therapy as effective for a variety of TCA's. The length of the PEG chain did not make any detectable difference in uptake. Calculations suggested that liposomes are approximately 20 times more effective at binding antidepressants than acidic phospholipids already present in the body. Estimates of the times required for tissues to reach equilibrium also demonstrated that liposomes could significantly alter the drug concentrations in vital organs after a drug overdose.

While Chapters 2-4 focused on optimizing pegylated, anionic liposomes for TCA binding, BUP binding was the subject of Chapter 5. Local anesthetics such as BUP are extremely useful clinically, but some patients suffer unexpected adverse reactions. Pegylated, anionic liposomes were shown to be highly effective at sequestering BUP from in vitro solutions, with a removal efficiency of about 80% in buffer and a free-drug reduction of about 50% in human serum. Comparisons to published data for lipid emulsions and microemulsions suggested that liposomes are better binding agents than either of the two. The results of Chapter 5 are especially encouraging, since a drug overdose therapy capable of successfully treating patients for a variety of drug classes would be more clinically acceptable and easier to administer.

Chapter 6 was intended to explore the detailed interactions between drug molecules and liposomes. Binding of TCA's such as AMI, IMI, and DOS was compared to binding of the local amide anesthetic BUP. The experiments and modeling indicated that the amount of drug molecules in the electrical double layer is negligible but the electrostatic effects play a major role in binding. The electrostatic interactions are responsible for the initial association between antidepressants and liposomes, whereupon the drug enters the bilayer with its charged region closely associated with the charged lipid head groups and its lipophilic region closely associated with the lipid bilayers. BUP, which is predominantly in the protonated state at pH 7.4 and 25°C as well (86%), is also preferentially attracted to the charged vesicle [123]. Once bound, it appears to be located within the bilayer to a greater extent than the antidepressants with minimal interactions with the charged surface. The structure of BUP makes it less able to access the bulk aqueous phase surrounding or encompassed by the lipid

bilayers. The conclusions regarding the differences in conformations between antidepressants and the anesthetic bupivacaine were supported by the fact that bupivacaine binding leads to a much lower increase in liposome permeability compared to antidepressant binding.

Assuming all other variables were held constant, multilamellar liposomes bound more drug molecules than unilamellar liposomes. The difference vanished at high ionic strengths. We attributed the increased binding for multilamellar liposomes without PEG to enhanced electrostatic interactions between adjacent charged layers. For pegylated liposomes, the reduced dielectric constant in the aqueous-PEG layer between adjacent bilayers results in a lower energy barrier for cationic drug transport across the aliphatic tail region [130,132-134]. Overall, Chapter 6 afforded a better understanding of the molecular level interactions responsible for the high affinity binding between the liposomes and the drugs.

While in vitro experiments allow for deeper understanding and the control of extraneous variables, estimates of in vivo efficacy are also extremely important during the early development phase. In Chapter 7, PBPK models were developed for this purpose. IV data affirmed the ability of the models to predict drug concentrations in the blood compartments with reasonable accuracy. Least squares fits of model results to non-IV data were utilized to obtain first-order absorption rate constants.

Drug overdose simulations for AMI revealed that liposomes are capable of reducing brain and heart AUC values by over 60% and peak AMI concentrations by 20% if treatments are provided within 2 hours of ingestion. AMI concentration increases in venous blood for the PBPK simulations and clinical overdose treatments with protein

fragments were similar [4]. BUP AUC and peak reductions were much lower at around 15-17%. First approximations of localized cardiac pharmacodynamics suggested improved ion channel function and myocyte contractility with liposome therapy, especially for AMI. The PBPK models developed suggested that liposomes are capable of redistributing both AMI and BUP into the blood compartments to significant degrees and may be effective at treating AMI overdoses and adverse reactions to BUP. The models also suggested that liposomes will, in general, be more effective at treating overdoses of drugs with high volumes of distribution and slow elimination characteristics, such as TCA's.

The work comprised herein shows that pegylated, anionic liposomes composed of DOPG and PEG-modified phospholipids exhibit high affinity binding to TCA's and BUP. The time scales for binding, feasible liposome doses, and typical drug doses all point to a very strong likelihood of treatment efficacy in critical care situations. However, several additional concerns should be addressed in future work. Liposome-drug binding should be measured in whole blood to ensure that RBC's and other whole blood components do not negatively impact liposome-drug affinity. A detailed understanding of the fate of liposome-drug complexes in the liver and spleen should also be explored. This could be done with in vitro and in vivo experiments, along with a detailed hepatic model including the distinctive nature of liver tissue, genetic factors, and disease states. Results from the hepatic model would hopefully allow for a better estimate of the clearance characteristics of the exact liposomes used. Of course, in vivo experiments examining liposome clearance, liposome toxicity, and treatment effectiveness in animal models would also be tremendously informative.

Related but broader work in this area could also be done. Molecular dynamics simulations could be performed to study the drug-bilayer interactions in even greater detail. Liposome-drug binding could be measured for non-prescription drugs or molecules, such as drugs of abuse or toxic compounds encountered in military applications. Liposomes could be loaded with antidotes or specific neutralizers, so that a combination of specific and non-specific treatment could be achieved. Finally, liposome surfaces could be designed to direct the liposome-drug complexes to one tissue over another to achieve the slowest and safest elimination route possible. Each of the above mentioned research topics represents an excellent opportunity to utilize liposomes in the context of drug overdose treatment to improve treatment options or uncover stirring scientific findings.

LIST OF REFERENCES

[1] Wysowski DK. Surveillance of Prescription Drug-Related Mortality Using Death Certificate Data. Drug Safety 2007;30(6):533-40.

[2] Liebelt EL, Francis PD. Cyclic Antidepressants. In: Goldfrank LR, Flomenbaum NE, Lewin NA, Howland MA, Hoffman RS, Nelson LS, editors. Goldfrank's Toxicologic Emergencies, 7th ed. New York: McGraw-Hill, 2002. p. 847-64.

[3] Unverir P, Atilla R, Karcioglu O, Topacoglu H, Demiral Y, Tuncok Y. A retrospective analysis of antidepressant poisonings in the emergency department: 11-year experience. Hum Exp Toxicol 2006;25:605-12.

[4] Heard K, Dart RC, Bogdan G, O'Malley GF, Burkhart KK, Donovan JW, Ward SB. A Preliminary Study of Tricyclic Antidepressant (TCA) Ovine FAB for TCA Toxicity. Clin Toxicol 2006;44:275-81.

[5] Henry JA, Alexander CA, Sener EK. Relative mortality from overdose of antidepressants. Brit Med J 1995;310:221-4.

[6] Morgan O, Griffiths C, Baker A, Majeed A. Fatal toxicity of antidepressants in England and Wales, 1993–2002. Health Statistics Quarterly 2004;23:18-24.

[7] Kiyan S, Aksay E, Yanturali S, Atilla R, Ersel M. Acute Myocardial Infarction Associated with Amitriptyline Overdose. Basic Clin Pharmacol 2006;98:462-66.

[8] Kerr GW, McGuffie AC, Wilkie S. Tricyclic antidepressant overdose: a review. Emerg Med J 2001;18:236-41.

[9] Nau C, Seaver M, Wang S, Wang GK. Block of Human Heart hH1 Sodium Channels by Amitriptyline. J Pharmacol Exp Ther 2000;292:1015-23.

[10] Heard K, Cain BS, Dart RC, Cairns CB. Tricyclic Antidepressants Directly Depress Human Myocardial Mechanical Function Independent of Effects on the Conduction System. Acad Emerg Med 2001;8(12):1122-7.

[11] Olson KR. Poisoning & Drug Overdose. New York: McGraw–Hill, 2007.

[12] Ludot H, Tharin JY, Belooudah M, Mazoit JX, Malinovsky JM. Successful resuscitation after ropivacaine and lidocaine-induced ventricular arrhythmia following posterior lumbar plexus block in a child. Anesth Analg 2008;106:1572-4.

[13] Warren J, Brian T, Georgescu A, Shah S. Intravenous lipid infusion in the successful resuscitation of local anesthetic-induced cardiovascular collapse after supraclavicular brachial plexus block. Anesth Analg 2008;106:1578-80.

[14] Litz RJ, Roessel T, Heller AR, Stehr SN. Reversal of central nervous system and cardiac toxicity after local anesthetic intoxication by lipid emulsion injection. Anesth Analg 2008;106:1575-7.

[15] Whiteside J. Reversal of local anaesthetic induced CNS toxicity with lipid emulsion. Anaesthesia 2008;63:202-13.

[16] Nau C, Wang S, Strichartz GR, Wang GK. Block of Human Heart hH1 Sodium Channels by the Enantiomers of Bupivacaine. Anesthesiology 2000;93:1022-33.

[17] Kaufman B, Wahlander S. Local Anesthetics. In: Goldfrank LR, Flomenbaum NE, Lewin NA, Howland MA, Hoffman RS, Nelson LS, editors. Goldfrank's Toxicologic Emergencies, 7th ed. New York: McGraw-Hill, 2002. p. 824-34.

[18] Rahman YE, Rosenthal MW, Cerny EA. Intracellular plutonium: Removal by liposome encapsulated chelating agent. Science 1973;180:300-2.

[19] Varshney M, Morey TE, Shah DO, Flint JA, Moudgil BM, Seubert CN, Dennis DM. Pluronic Microemulsions as Nanoreservoirs for Extraction of Bupivacaine from Normal Saline. J Am Chem Soc 2004;126:5108-12.

[20] James-Smith MA, Shekhawat D, Moudgil BM, Shah DO. Determination of Drug and Fatty Acid Binding Capacity to Pluronic F127 in Microemulsions. Langmuir 2007;23:1640-4.

[21] Underhill RS, Jovanovic AV, Carino SR, Varshney M, Shah DO, Dennis DM, Morey TE, Duran RS. Oil-Filled Silica Nanocapsules for Lipophilic Drug Uptake: Implications for Drug Detoxification Therapy. Chem Mater 2002;14:4919-25.

[22] Lee D, Baney R. Detoxification of amitriptyline by oligochitosan derivatives. Biotechnol Lett 2004;26:713-6.

[23] Chakraborty S, Somasundaran P. Sequestration of drugs using poly(acrylic acid) and alkyl modified poly(acrylic acid) nanoparticles. Soft Matter 2006;2:850-4.

[24] Dhanikula AB, Khalid NM, Lee SD, Yeung R, Risovic V, Wasan KM, Leroux J. Long circulating lipid nanocapsules for drug detoxification. Biomaterials 2007;28:1248-57.

[25] Dhanikula AB, Lamontagne D, Leroux J. Rescue of amitriptyline-intoxicated hearts with nanosized vesicles. Cardiovasc Res 2007;74:480-86.

[26] Lasic DD. Novel applications of liposomes. Trends Biotechnol 1998;16:307-21.

[27] Szoka F, Papahadjopoulos D. Comparative Properties and Methods of Preparation of Lipid Vesicles (Liposomes). Ann Rev Biophys Bioeng 1980;9:467-508.

[28] MacDonald RC, MacDonald RI, Menco BP, Takeshita K, Subbarao NK, Hu LR. Small-volume extrusion apparatus for preparation of large, unilamellar vesicles. Biochim Biophys Acta 1991;1061:297-303.

[29] Woodle MC. Controlling liposome blood clearance by surface-grafted polymers. Adv Drug Delivery Rev 1998;32:139-52.

[30] Awasthi VD, Garcia D, Klipper R, Goins BA, Phillips WT. Neutral and Anionic Liposome-Encapsulated Hemoglobin: Effect of Postinserted Poly(ethylene glycol)-distearoylphosphatidylethanolamine on Distribution and Circulation Kinetics. J Pharmacol Exp Ther 2004;309:241-8.

[31] Hoarau D, Delmas P, David S, Roux E, Leroux JC. Novel Long-Circulating Lipid Nanocapsules. Pharm Res 2004;21:1783-89.

[32] Lee CM, Choi Y, Huh EJ, Lee KY, Song HC, Sun MJ, Jeong HJ, Cho CS, Bom HS. Polyethylene Glycol (PEG) Modified 99mTcHMPAO Liposome for Improving Blood Circulation and Biodistribution: The Effect of the Extent of PEGylation. Cancer Biother Radio 2005;20(6):620-8.

[33] Rosenblatt MA, Abel M, Fischer GW, Itzkovich CJ, Eisenkraft JB. Successful Use of a 20% Lipid Emulsion to Resuscitate a Patient after a Presumed Bupivacaine-related Cardiac Arrest. Anesthesiology 2006;105:217-8.

[34] Litz RJ, Popp M, Stehr SN, Koch T. Successful resuscitation of a patient with ropivacaine induced asystole after axillary plexus block using lipid infusion. Anaesthesia 2006;61:800-1.

[35] Foxall G, McCahon R, Lamb J, Hardman JG, Bedforth NM. Levobupivacaine-induced seizures and cardiovascular collapse treated with Intralipid. Anaesthesia 2007;62:516-8.

[36] Zimmer C, Piepenbrink K, Riest G, Peters J. Cardiotoxic and neurotoxic effects after accidental intravascular bupivacaine administration: therapy with lidocaine propofol and lipid emulsion. Anaesthesist 2007;56:449-53.

[37] Harvey M, Cave G. Intralipid outperforms sodium bicarbonate in a rabbit model of clomipramine toxicity. Ann Emerg Med 2007;49:178-85.

[38] Tebbutt S, Harvey M, Nicholson T, Cave G. Intralipid prolongs survival in a rat model of verapamil toxicity. Acad Emerg Med 2006;13:134-9.

[39] Harvey M, Cave G. Intralipid infusion ameliorates propranolol induced hypotension in rabbits. J Med Toxicol 2008;4:71-6.

[40] Sirianni AJ, Osterhoudt KC, Calello DP, Muller AA, Waterhouse MR, Goodkin MB, Weinberg GL, Henretig FM. Use of Lipid Emulsion in the Resuscitation of a Patient With Prolonged Cardiovascular Collapse After Overdose of Bupropion and Lamotrigine. Ann Emerg Med 2008;51:412-5.

[41] Weinberg GL, VadeBoncouer T, Ramaraju GA, Garcia-Amaro MF, Cwik MJ. Pretreatment or Resuscitation with a Lipid Infusion Shifts the Dose Response to Bupivacaine-induced Asystole in Rats. Anesthesiology 1998;88:1071-5.

[42] Weinberg G, Ripper R, Feinstein DL, Hoffman W. Lipid Emulsion Infusion Rescues Dogs From Bupivacaine-Induced Cardiac Toxicity. Reg Anesth Pain Med 2003;28:198-202.

[43] Rowlingson JC. Lipid Rescue: A Step Forward in Patient Safety? Likely So! Anesth Analg 2008;106:1333-6.

[44] Weinberg GL. Lipid Infusion Therapy: Translation to Clinical Practice. Anesth Analg 2008;106:1340-2.

[45] Mathieu S, Cranshaw J. Treatment of severe local anaesthetic toxicity. Anaesthesia 2008;63:202-3.

[46] Wildsmith JAW. Treatment of severe local anaesthetic toxicity. Anaethesia 2008;63:778-89.

[47] Boogaerts J, Declercq A, Lafont N, Benameur H, Akodad EM, Dupont JC, Legros FJ. Toxicity of bupivacaine encapsulated into liposomes and injected intravenously: comparison with plain solutions. Anesth Analg 1993;76:553-5.

[48] Boogaerts JG, Lafont ND, Declercq AG, Luo HC, Gravet ET, Bianchi JA, Legros FJ. Epidural administration of liposome associated bupivacaine for the management of postsurgical pain: a first study. J Clin Anesth 1994;6:315-20.

[49] Singh R, Vyas SP. Topical liposomal system for localized and controlled drug delivery. J Dermatol Sci 1996;13:107-11.

[50] Fisher R, Hung O, Mezei M, Stewart R. Topical anaesthesia of intact skin: liposome-encapsulated tetracaine vs EMLA. Br J Anaesth 1998;81:972-3.

[51] Eichenfield LF, Funk A, Fallon-Friedlander S, Cunningham BB. A clinical study to evaluate the efficacy of ELA-Max (4% liposomal lidocaine) as compared with eutectic mixture of local anesthetics cream for pain reduction of venipuncture in children. Pediatrics 2002;109:1093-9.

[52] Taddio A, Soin HK, Schuh S, Koren G, Scolnik D. Liposomal lidocaine to improve procedural success rates and reduce procedural pain among children: a randomized controlled trial. Can Med Assoc J 2005;172:1691-5.

[53] Franz-Montan M, Silva ALR, Cogo K, Bergamaschi CC, Volpato MC, Ranali J, Paula E, Groppo FC. Liposome-Encapsulated Ropivacaine for Topical Anesthesia of Human Oral Mucosa. Anesth Analg 2007;104:1528-31.

[54] Casarotto MG, Craik DJ. Solution Dynamics of Imipramine and Amitriptyline in Phospholipid Vesicles as Studied by ^{1}H and ^{13}C NMR. J Colloid Interf Sci 1993;158:326-32.

[55] Austin RP, Barton P, Davis AM, Fessey RE, Wenlock MC. The Thermodynamics of the Partitioning of Ionizing Molecules Between Aqueous Buffers and Phospholipid Membranes. Pharm Res 2005;22:1649-57.

[56] Ahyayauch H, Goni FM, Bennouna M. Interaction of electrically neutral and cationic forms of imipramine with liposome and erythrocyte membranes. Int J Pharm 2004;279:51-8.

[57] Fisar Z, Fuksova K, Velenovska M. Binding of Imipramine to Phospholipid Bilayers Using Radioligand Binding Assay. Gen Physiol Biophys 2004;23:77-99.

[58] Sanganahalli BG, Joshi PG, Joshi NB. Differential effects of tricyclic antidepressant drugs on membrane dynamics-a fluorescence spectroscopic study. Life Sci 2000;68:81-90.

[59] Suwalsky M, Schneider C, Villena F, Norris B, Cardenas H, Cuevas F, Sotomayor CP. Structural Effects of the Local Anesthetic Bupivacaine Hydrochloride on the Human Erythrocyte Membrane and Molecular Models. Blood Cell Mol Dis 2002;29:14-23.

[60] Mizogami M, Tsuchiya H, Ueno T, Kashimata M, Takakura K. Stereospecific Interaction of Bupivacaine Enantiomers with Lipid Membranes. Region Anesth Pain M 2008;33:304-11.

[61] Bryl K, Kedzierska S, Taylor A. Mechanism of the Leakage Induced on Lipid Model Membranes by Rz1 Lipoprotein, the Bacteriophage λ Rz1 Gene Product: A Fluorescence Study. J Fluoresc 200;10:209-16.

[62] Nikolova AN, Jones MN. Effect of grafted PEG-2000 on the size and permeability of vesicles. Biochim Biophys Acta 1996;1304:120-8.

[63] Hashizaki K, Taguchi H, Sakai H, Abe M, Saito Y, Ogawa N. Carboxyfluorescein Leakage from Poly(ethylene glycol)-Grafted Liposomes Induced by the Interaction with Serum. Chem Pharm Bull 2006;54:80-4.

[64] Yokouchi Y, Tsunoda T, Imura T, Yamauchi H, Yokoyama S, Sakai H, Abe M. Effect of adsorption of bovine serum albumin on liposomal membrane characteristics. Colloid Surface B 2001;20:95-103.

[65] Yokoyama S, Takeda T, Tsunoda T, Ohta Y, Imura T, Abe M. Membrane properties of mixed dipalmitoylphosphatidylglycerol/ganglioside GM3 liposomes in the presence of bovine serum albumin. Colloid Surface B 2002;27:141-6.

[66] Sadzuka Y, Nakade A, Tsuruda T, Sonobe T. Study on the characterization of mixed polyethyleneglycol modified liposomes containing doxorubicin. J Control Release 2003;91:271-80.

[67] Monkkonen J, Liukkonen J, Taskinen M, Heath TD, Urtti A. Studies on liposome formulations for intra-articular delivery of clodronate. J Control Release 1995;35:145-54.

[68] Soni V, Kohli DV, Jain SK. Transferrin coupled liposomes as drug delivery carriers for brain targeting of 5-florouracil. J Drug Target 2005;13:245-50.

[69] Leroux JC. Injectable nanocarriers for biodetoxification. Nat Nanotechnol 2007;2:679-84.

[70] Dhanikula AB, Lafleur M, Leroux J. Characterization and in vitro evaluation of spherulites as sequestering vesicles with potential application in drug detoxification. Biochim Biophys Acta 2006;1758:1787-96.

[71] Fallon M, Chauhan A. Sequestration of amitriptyline by liposomes. J Colloid Interf Sci 2006;300:7-19.

[72] Deo N, Somasundaran T, Somasundaran P. Solution properties of amitriptyline and its partitioning into lipid bilayers. Colloids Surf B 2004;34:155-9.

[73] Poulin P, Theil FP. Prediction of Pharmacokinetics prior to In Vivo Studies. II. Generic Physiologically Based Pharmacokinetic Models of Drug Disposition. J Pharm Sci 2002;91:1358-70.

[74] Lavé T, Parrott N, Grimm HP, Fleury A, Reddy M. Challenges and opportunities with modelling and simulation in drug discovery and drug development. Xenobiotica 2007;37(10):1295-310.

[75] Parrott N, Lave T. Applications of Physiologically Based Absorption Models in Drug Discovery and Development. Mol Pharm 2008;5(5):760-75.

[76] Thomas S. Clinical relevance of predictive physiologically based pharmacokinetic methods. Expert Opin Drug Dis 2008;3(7):725-32.

[77] Nestorov I. Whole Body Pharmacokinetic Models. Clin Pharmacokinet 2003;42(10):883-908.

[78] Igari Y, Sugiyama Y, Sawada Y, Iga T, Hanano M. Prediction of diazepam disposition in the rat and man by a physiologically based pharmacokinetic model. J Pharmacokinet Biopharm 1983;11:577-93.

[79] Meno-Tetang GML, Li H, Mis S, Pyszczynski N, Heining P, Lowe P, Jusko WJ. 2006. Physiologically Based Pharmacokinetic Modeling of FTY720 (2-Amino-2[2-(-4-octylphenyl)ethyl]propane-1,3-diol hydrochloride) in Rats After Oral and Intravenous Doses. Drug Metab Dispos 2006;34:1480-7.

[80] Garg A, Balthasar JP. Physiologically-based pharmacokinetic (PBPK) model to predict IgG tissue kinetics in wild-type and FcRn-knockout mice. J Pharmacokinet Phar 2007;34:687-709.

[81] Bonate PL, Swann A, Silverman PB. Preliminary Physiologically Based Pharmacokinetic Model for Cocaine in the Rat: Model Development and Scale-Up to Humans. J Pharm Sci 1996;85(8):878-83.

[82] Peters SA. Identification of Intestinal Loss of a Drug through Physiologically Based Pharmacokinetic Simulation of Plasma Concentration-Time Profiles. Clin Pharmacokinet 2008;47(4):245-59.

[83] Guyton AC. Textbook of Medical Physiology. Philadelphia: Saunders, 1986.

[84] Franssen EJF, Kunst PWA, Bet PM, Strack van Schijndel RJM, van Loenen AC. Toxicokinetics of Nortriptyline and Amitriptyline: Two Case Reports. Ther Drug Monit 2003;25:248-51.

[85] Benet LZ, Hoener B. Changes in plasma protein binding have little clinical relevance. Clin Pharmacol Ther 2002;71:115-21.

[86] Chonn A, Semple SC, Cullis PR. Association of Blood Proteins with Large Unilamellar Liposomes in Vivo. J Biol Chem 1992;267:18759-65.

[87] Semple SC, Chonn A, Cullis PR. Interactions of liposomes and lipid-based carrier systems with blood proteins: Relation to clearance behavior in vivo. Adv Drug Deliver Rev 1998;32:3-17.

[88] Levitt MA, Sullivan JB, Owens SM, Burnham L, Finley PR. Amitriptyline plasma protein binding: Effect of plasma pH and relevance to clinical overdose. Am J Emerg Med 1986;4:121-5.

[89] Franssen EJF, Kunst PWA, Bet PM, Strack van Schijndel RJM, van Loenen AC. Toxicokinetics of Nortriptyline and Amitriptyline: Two Case Reports. Ther Drug Monit 2003;25:248-51.

[90] Awasthi VD, Garcia D, Goins BA, Phillips WT. Circulation and biodistribution profiles of long-circulating PEG-liposomes of various sizes in rabbits. Int J Pharm 2003;253:121-32.

[91] Coune A, Sculier JP, Fruhling J, Stryckmans P, Brassinne C, Ghanem G, Laduron C, Atassi G, Ruysschaert JM, Hildebrand J. IV Administration of a Water-Insoluble Anti-Mitotic Compund Entrapped in Liposomes - Preliminary Report on Infusion of Large Volumes of Liposomes To Man. Cancer Treat Rep 1983;67:1031-33.

[92] Sculier JP, Coune A, Brassinne C, Laduron C, Atassi G, Ruysschaert JM, Fruhling J. Intravenous Infusion of High Doses of Liposomes Containing NSC-251635, A Water-Insoluble Cytostatic Agent - A Pilot Study with Pharmacokinetic Data. J Clin Oncol 1986;4:789-97.

[93] Weissig V, Babich J, Torchilin V. Long-circulating gadolinium-loaded liposomes: potential use for magnetic resonance imaging of the blood pool. Colloids Surf B 2000;18:293-99.

[94] Lapinski MM, Castro-Forero A, Greiner AJ, Ofoli RY, Blanchard GJ. Comparison of Liposomes Formed by Sonication and Extrusion: Rotational and Translational Diffusion of an Embedded Chromophore. Langmuir 2007;23:11677-83.

[95] Yoshida A, Hashizaki K, Yamauchi H, Sakai H, Yokoyama S, Abe M. Effect of Lipid with Covalently Attached Poly(ethylene glycol) on the Surface Properties of Liposomal Bilayer Membranes. Langmuir 1999;15:2333-7.

[96] Newman MS, Colbern GT, Working PK, Engbers C, Amantea MA. Comparative pharmacokinetics, tissue distribution, and therapeutic effectiveness of cisplatin encapsulated in long-circulating, pegylated liposomes (SPI-077) in tumor-bearing mice. Cancer Chemoth Pharm 1999;43:1-7.

[97] Nicolazzi C, Mignet N, Figuera N, Cadet M, Ibad RT, Seguin J, Scherman D, Bessodes M. Anionic polyethyleneglycol lipids added to cationic lipoplexes increase their plasmatic circulation time. J Control Release 2003;88:429-43.

[98] Zhigaltsev IV, Maurer N, Wong KF, Cullis PR. Triggered release of doxorubicin following mixing of cationic and anionic liposomes. Biochim Biophys Acta 2002;1565:129-35.

[99] Rex S, Zuckermann MJ, Lafleur M, Silvius JR. Experimental and Monte Carlo Simulation Studies of the Thermodynamics of Polyethyleneglycol Chains Grafted to Lipid Bilayers. Biophys J 1998;75:2900-14.

[100] Moghimi SM, Szebeni J. Stealth liposomes and long circulating nanoparticles: critical issues in pharmacokinetics, opsonization and protein-binding properties. Prog Lipid Res 2003;42:463-78.

[101] Gbadamosi JK, Hunter AC, Moghimi SM. PEGylation of microspheres generates a heterogeneous population of particles with differential surface characteristics and biological performance. FEBS Lett 2002;532:338-44.

[102] Attwood D, Natarajan R. Effect of pH on the micellar properties of amphiphilic drugs in aqueous solution. J Pharm Pharmacol 1981;33:136-40.

[103] Wiczling P, Markuszewski MJ, Kaliszan M, Galer K, Kaliszan R. Combined pH/organic solvent gradient HPLC in analysis of forensic material. J Pharmaceut Biomed 2005;37:871-75.

[104] Brittain H, Prankerd RJ. Profiles of Drug Substances, Excipients, and Related Methodology, Volume 33: Critical Compilation of Pka Values for Pharmaceutical Substances. London: Academic Press, 2007. p. 155.

[105] Musshoff F, Padosch S, Steinborn S, Madea B. Fatal blood and tissue concentrations of more than 200 drugs. Forensic Sci Int 2004;142:161-210.

[106] Rodgers T, Leahy D, Rowland M. Physiologically Based Pharmacokinetic Modeling 1: Predicting the Tissue Distribution of Moderate-to-Strong Bases. J Pharm Sci 2005;94:1259-76.

[107] Kristensen CB. Imipramine serum protein binding in healthy subjects. Clin Pharmacol Ther 1983;34:689-94.

[108] Obach RS. Prediction of Human Clearance of Twenty-nine Drugs from Hepatic Microsomal Intrinsic Clearance Data: An Examination of In Vitro Half-Life Approach and Nonspecific Binding to Microsomes. Drug Metab Dispos 1999;27:1350-59.

[109] Callaghan JT, Cerimele BJ, Kassahun KJ, Nyhart Jr EH, Hoyes-Beehler PJ, Kondraske GV. Olanzapine: interaction study with imipramine. J Clin Pharmacol 1997;37:971-78.

[110] Pedersen OL, Gram LF, Kristensen CB, Moller M, Thayssen P, Bjerre M, Kragh-Sorensen P, Klitgaard NA, Sindrup E, Hole P, Brinklov M. Overdosage of Antidepressants: Clinical and Pharmacokinetic Aspects. Eur J Clin Pharmacol 1982;23:513-21.

[111] Swartz CM, Sherman A. The Treatment of Tricyclic Antidepressant Overdose with Repeated Charcoal. J Clin Psychopharmacol 1984;4:336-40.

[112] Ilett KF, Hackett LP, Dusci LJ, Paterson JW. Disposition of Dothiepin After Overdose: Effects of Repeated-Dose Activated Charcoal. Ther Drug Monit 1991;13:485-9.

[113] Ragusi C, Boschi G, Risede P, Rips R, Harrison K, Scherrmann J. Influence of various combinations of specific antibody dose and affinity on tissue imipramine redistribution. Brit J Pharmacol 1998;125:35-40.

[114] Ragusi C, Scherrmann J, Harrison K, Smith DS, Rips R, Boschi G. Redistribution of Imipramine from Regions of the Brain Under the Influence of Circulating Specific Antibodies. J Neurochem 1998;70:2099-105.

[115] Pentel PR, Scarlett W, Ross CA, Landon J, Sidki A, Keyler DE. Reduction of Desipramine Cardiotoxicity and Prolongation of Survival in Rats With the Use of Polyclonal Drug-Specific Antibody Fab Fragments. Ann Emerg Med 1995;26:334-41.

[116] Shelver WL, Keyler DE, Lin G, Murtaugh MP, Flickinger MC, Ross CA, Pentel PR. Effects of Recombinant Drug-Specific Single Chain Antibody Fv Fragment on [3H]-Desipramine Distribution in Rats. Biochem Pharmacol 1996;51:531-7.

[117] Fallon MS, Varshney M, Dennis DM, Chauhan A. A Physiologically-Based Pharmacokinetic Model of Drug Detoxification by Nanoparticles. J Pharmacokinet Phar 2004;31:381-400.

[118] Dauphin A, Gupta RN, Young JEM, Morton WD. Serum bupivacaine concentrations during continuous extrapleural infusion. Can J Anaesth 1997;44:367-70.

[119] Mazoit JX, Cao LS, Samii K. Binding of Bupivacaine to Human Serum Proteins, Isolated Albumin and Isolated Alpha-1-Acid Glycoprotein. Differences between the Two Enantiomers are Partly Due to Cooperativity. J Pharmacol Exp Ther 1996;276:109-15.

[120] Morishima HO, Pedersen H, Finster M, Hiraoka H, Tsuji A, Feldman HS, Arthur GR, Covino BG. Bupivacaine Toxicity in Pregnant and Nonpregnant Ewes. Anesthesiology 1985;63:134-9.

[121] Martinez-Gomez MA, Villanueva-Camanas RS, Sagrado S, Medina-Hernandez MJ. Evaluation of enantioselective binding of basic drugs to plasma by ACE. Electrophoresis 2007;28:3056-63.

[122] Weinberg GL, Ripper R, Murphy P, Edelman LB, Hoffman W, Strichartz G, Feinstein DL. Lipid infusion accelerates removal of bupivacaine and recovery from bupivacaine toxicity in the isolated rat heart. Reg Anesth Pain Med 2006;31:296-303.

[123] Strichartz GR, Sanchez V, Arthur GR, Chafetz R, Martin D. Fundamental Properties of Local Anesthetics. II. Measured Octanol:Buffer Partition Coefficients and pKa Values of Clinically Used Drugs. Anesth Analg 1990;71:158-70.

[124] Zuidam NJ, Vrueh R, Crommelin DJA. Characterization of Liposomes. In: Torchilin VP, Weissig V, editors. Liposomes, 2nd ed. New York: Oxford University Press, 2003. p. 31-61.

[125] Egorova EM. Dissociation constants of lipid ionizable groups II. Changes in surface pK at low ionic strengths. Colloid Surface A 1998;131:19-31.

[126] McLaughlin S. The Electrostatic Properties of Membranes. Annu Rev Biophys Bio 1989;18:113-36.

[127] Lis LJ, McAlister M, Fuller N, Rand RP, Parsegian VA. Interactions Between Neutral Phospholipid Bilayer Membranes. Biophys J 1982;37:657-65.

[128] Rand RP, Parsegian VA. Hydration forces between phospholipid bilayers. Biochim Biophys Acta 1989;988:351-76.

[129] Kenworthy AK, Hristova K, Needham D, McIntosh TJ. Range and Magnitude of the Steric Pressure Between Bilayers Containing Phospholipids with Covalently Attached Poly(ethylene glycol). Biophys J 1995;68:1921-36.

[130] Arnold K, Herrmann A, Pratsch L, Gawrisch K. The dielectric properties of aqueous solutions of poly(ethylene glycol) and their influence on membrane structure. Biochim Biophys Acta 1985;815: 515-8.

[131] Kuhl TL, Leckband DE, Lasic DD, Israelachvili JN. Modulation of interaction forces between bilayers exposing short-chained ethylene oxide headgroups. Biophys J 1994;66:1479-88.

[132] Blow AMJ, Botham GM, Lucy JA. Calcium ions and cell fusion. Effects of chemical fusogens on the permeability of erythrocytes to calcium and other ions. Biochem J 1979;182:555-63.

[133] Elworthy PH, McIntosh DS. The effect of solvent dielectric constant on micellisation by lecithin. Colloid Polym Sci 1964;195:27-34.

[134] Parsegian A. Energy of an Ion crossing a Low Dielectric Membrane: Solutions to Four Relevant Electrostatic Problems. Nature 1969;221:844-6.

[135] Hiemenz PC, Rajagopalan R. Principles of Colloid and Surface Chemistry, 3rd ed. New York: Marcel Dekker, 1997. p. 499-533.

[136] Silvander M, Hansson P, Edwards K. Liposomal Surface Potential and Bilayer Packing As Affected by PEG-Lipid Inclusion. Langmuir 2000;16:3696-702.

[137] Malheiros SVP, Pinto LMA, Gottardo L, Yokaichiya DK, Fraceto LF, Meirelles NC, de Paula E. A new look at the hemolytic effect of local anesthetics, considering their real membrane/water partitioning at pH 7.4. Biophys Chem 2004;110:213-21.

[138] Balali-Mood KT, Harroun A, Bradshaw JP. Molecular dynamics simulations of a mixed DOPC/DOPG bilayer. Eur Phys J E 2003;12:S135-40.

[139] Kim JH, Kim MW. Temperature effect on the transport dynamics of a small molecule through a liposome bilayer. Eur Phys J E 2007;23:313-7.

[140] Balgavy P, Dubnickova M, Kucerka N, Kiselev MA, Yaradaikin SP, Uhrikova D. Bilayer thickness and lipid interface area in unilamellar extruded 1,2-diacylphosphatidylcholine liposomes: a small-angle neutron scattering study. Biochim Biophys Acta 2001;1512:40-52.

[141] Zima AV, Qin J, Fill M, Blatter LA. Tricyclic antidepressant amitriptyline alters sarcoplasmic reticulum calcium handling in ventricular myocytes. Am J Physiol-Heart 2008;295:H2008-H2016.

[142] Poulin P, Theil FP. A priori prediction of tissue: plasma partition coefficients of drugs to facilitate the use of physiologically-based pharmacokinetic models in drug discovery. J Pharm Sci 2000;89(1):16-35.

[143] Poulin P, Schoenlein K, Theil FP. Prediction of adipose tissue: plasma partition coefficients for structurally unrelated drugs. J Pharm Sci 2001;90(4):436-47.

[144] Poulin P, Theil FP. Prediction of pharmacokinetics prior to in vivo studies. I. Mechanism-based prediction of volume of distribution. J Pharm Sci 2002;91(1):129-56.

[145] Rodgers T, Rowland M. Physiologically Based Pharmacokinetic Modelling 2: Predicting the Tissue Distribution of Acids, Very Weak Bases, Neutrals and Zwitterions. J Pharm Sci 2006;95(6):1238-57.

[146] Banerjee T, Singh SK, Kishore N. Binding of Naproxen and Amitriptyline to Bovine Serum Albumin: Biophysical Aspects. J Phys Chem B 2006;110:24147-56.

[147] Sallee FR, Pollack BG. Clinical pharmacokinetics of imipramine and desipramine. Clin Pharmacokinet 1990;18:346-64.

[148] Abernathy DR, Greenblatt DJ, Shader RI. Imipramine and desipramine disposition in the elderly. J Pharmacol Exp Ther 1985;232:183-8.

[149] Schulz P, Turner-Tamiyasu K, Smith G, Giacomini KM, Blaschke TF. Amitriptyline disposition in young and elderly normal men. Clin Pharmacol Ther 1983;33:360-6.

[150] Rollins DE, Alvan G, Bertilsson L, Gillette JR, Mellstrom B, Sjoqvist F, Traskman L. Interindividual differences in amitriptyline demethylation. Clin Pharmacol Ther 1980;28:121-9.

[151] Tucker GT, Mather LE. Pharmacokinetics of Local Anaesthetic Agents. Brit J Anaesth 1975;47:213-24.

[152] Tucker GT, Boyes RN, Bridenbaugh PO, Moore DC. Binding of Anilide-type Local Anesthetics in Human Plasma: II. Implications In Vivo, with Special Reference to Transplacental Distribution. Anesthesiology 1970;33:304-13.

[153] Leo A, Hansch C, Elkins D. Partition Coefficients and Their Uses. Chem Rev 1971;71:525-616.

[154] Verschueren K. Handbook of Environmental Data on Organic Chemicals, 4th ed. New York: John Wiley and Sons, 2001.

[155] Nava-Ocampo AA, Bello-Ramirez AM. Lipophilicity Affects the Pharmacokinetics and Toxicity of Local Anaesthetic Agents Administered by Caudal Block. Clin Exp Pharmacol P 2004;31:116-8.

[156] Martensson E, Axelsson R, Nyberg G, Svensson C. Pharmacokinetic properties of the antidepressant drugs amitriptyline, clomipramine, and imipramine: a clinical study. Curr Ther Res 1984;36:228-38.

[157] Brinkschulte M, Breyer-Pfaff U. Binding of tricyclic antidepressants and perazine to human plasma. Methodology and findings in normals. Naunyn-Schmiedeberg's Archives of Pharmacology 1979;308:1-7.

[158] Tucker GT, Boyes RN, Bridenbaugh PO, Moore DC. Binding of Anilide-type Local Anesthetics in Human Plasma: I. Relationships between Binding, Physiochemical Properties, and Anesthetic Activity. Anesthesiology 1970;33:287-303.

[159] Baumann P, Jonzier-Perey M, Koeb L, Le PK, Tinguely D, Schopf J. Amitriptyline Pharmacokinetics and Clinical Response: I. Free and Total Plasma Amitriptyline and Nortriptyline. Int Clin Psychopharm 1986;1:89-101.

[160] Rowland M, Tozer TN. Clinical pharmacokinetics: concepts and applications, 3rd ed. New York: Lippincott Williams & Wilkins, 1995. p. 502.

[161] Bynum ND, Poklis JL, Gaffney-Kraft M, Garside D, Ropero-Miller JD. Postmortem Distribution of Tramadol, Amitriptyline, and Their Metabolites in a Suicidal Overdose. J Anal Toxicol 2005;29:401-6.

[162] Tracqui A, Kintz P, Ritter-Lohner S, Mangin P, Lugnier A, Chaumont A. Toxicological findings after fatal amitriptyline selfpoisoning. Hum Exp Toxicol 1990;9:257-61.

[163] Hilberg T, Ripel A, Smith AJ, Slordal L, Morland J, Bjorneboe A. Postmortem Amitriptyline Pharmacokinetics in Pigs after Oral and Intravenous Routes of Administration. J Forensic Sci 1998;43(2):380-7.

[164] Shi B, Heavner JE. Nitric Oxide Modulation Affects the Tissue Distribution and Toxicity of Bupivacaine. Pharmacol Biochem Be 2000;66(3):623-9.

[165] Feldman HS, Hartvig P, Wiklund L, Doucette AM, Antoni G, Gee A, Ulin J, Langstrom B. Regional Distribution of ^{11}C-Labeled Lidocaine, Bupivacaine, and Ropivacaine in the Heart, Lungs, and Skeletal Muscle of Pigs Studied with Positron Emission Tomography. Biopharm Drug Dispos 1997;18(2):151-64.

[166] Sjostrand U, Widman B. Distribution of Bupivacaine in the Rabbit under Normal and Acidotic Conditions. Acta Anaesth Scand 1973;17(s50):5-24.

[167] Goehl TJ, Davenport JB, Stanley MJ. Distribution, Biotransformation and Excretion of Bupivacaine in the Rat and the Monkey. Xenobiotica 1973;3(12):761-72.

[168] Pounder DJ, Jones GR. Postmortem drug redistribution-a toxico-logical nightmare. Forensic Sci Int 1990;45:253-63.

[169] Shargel L, Wu-Pong S, Yu ABC. Applied Biopharmaceutics and Pharmacokinetics, 5th ed. New York: McGraw-Hill, 2005. p. 164,339.

[170] Simone de G, Devereux RB, Daniels SR, Mureddu G, Roman MJ, Kimball TR, Greco R, Witt S, Contaldo F. Stroke Volume and Cardiac Output in Normotensive Children and Adults - Assessment of Relations With Body Size and Impact of Overweight. Circulation 1997;95:1837-43.

[171] Benowitz N, Forsyth RP, Melmon KL, Rowland M. Lidocaine disposition kinetics in monkey and man I: Prediction by a perfusion model. Clin Pharamcol Ther 1974;16:87-98.

[172] Gray H. Anatomy of The Human Body, 20th ed. New York: Lea and Febiger, 1918. p. 1199-273.

[173] Abernethyl DR, Divoll M, Greenblatt DJ, Harmatz JS, Shader RI. Absolute bioavailability of imipramine: Influence of food. Psychopharmacology 1984;83:104-6.

[174] Brosen K, Gram LF. First-pass metabolism of imipramine and desipramine: Impact of the sparteine oxidation phenotype. Clin Pharmacol Ther 1988;43:400-6.

[175] Filser JG, Kaumeier S, Brand T, Schanz H, Terlinden R, Muller WE. Pharmacokinetics of Amitriptyline and Amitriptylineoxide after Intravenous or Oral Administration in Humans. Pharmacopsychiatry 1988;21:381-93.

[176] Jorgensen A, Hansen V. Pharmacokinetics of Amitriptyline Infused Intravenously in Man. Eur J Clin Pharmacol 1976;10:337-41.

[177] Burm AGL, De Boer AG, Van Kleef JW, Vermeulen NPE, De Leede LGJ, Spierdijk J, Breimer DD. Pharmacokinetics of Lidocaine and Bupivacaine and Stable Isotope Labelled Analogues: A Study In Healthy Volunteers. Biopharm Drug Dispos 1988;9:85-95.

[178] Reynolds F. Metabolism and Excretion of Bupivacaine in Man: A Comparison with Mepivacaine. Brit J Anaesth 1971;43:33-6.

[179] Tucker GT, Wiklund L, Berlin-Wahlen A, Mather LE. Hepatic Clearance of Local Anesthetics in Man. J Pharmacokinet Biop 1977;5:111-21.

[180] Wiklund L. Human Hepatic Blood Flow and its Relation to Systemic Circulation during Intravenous Infusion of Bupivacaine or Etidocaine. Acta Anaesth Scand 1976;21:189-99.

[181] Fox SI. Human Physiology, 9th ed. New York: McGraw-Hill, 2006. p. 383.

[182] Burch JE, Herries DG. The Demethylation of Amitriptyline Administered by Oral and Intramuscular Routes. Psychopharmacology 1983;80:249-53.

[183] Wong SL, Cavanaugh J, Shi H, Awni WM, Granneman GR. Effects of divalproex sodium on amitriptyline and nortriptyline pharmacokinetics. Clin Pharmacol Ther 1996;60:48-53.

[184] Sjoqvist F, Berglund F, Borga O, Hammer W, Andersson S, Thorstrand C. The pH-dependent excretion of monomethylated tricyclic antidepressants. Clin Pharmacol Ther 1969;10:826-33.

[185] Friedman GA, Rowlingson JC, DiFazio CA, Donegan MF. Evaluation of the Analgesic Effect and Urinary Excretion of Systemic Bupivacaine in Man. Anesth Analg 1982;61:23-7.

[186] Tucker GT. Pharmacokinetics of Local Anaesthetics. Brit J Anaesth 1986;58:717-31.

[187] Welling PG. Pharmacokinetics – Processes, Mathematics, and Applications, 2nd ed. Washington DC: American Chemical Society, 1997. p. 224.

[188] Burch JE, Hullin RP. Amitriptyline Pharmacokinetics A Crossover Study with Single Doses of Amitriptyline and Nortriptyline. Psychopharmacology 1981;74:35-42.

[189] Burch JE, Hullin RP. Amitriptyline Pharmacokinetics Single Doses of Lentizol Compared with Ordinary Amitriptyline Tablets. Psychopharmacology 1981;74:43-50.

[190] Gupta SK, Shah JC, Hwang SS. Pharmacokinetic and pharmacodynamic characterization of OROS® and immediate-release amitriptyline. J Clin Pharmacol 1999;48:71-8.

[191] Venkatakrishnan K, Schmider J, Harmatz JS, Ehrenberg BL, von Moltke LL, Graf JA, Mertzanis P, Corbett KE, Rodriguez MC, Shader RI, Greenblatt DJ. Relative contribution of CYP3A to amitriptyline clearance in humans: in vitro and in vivo studies. J Clin Pharmacol 2001;41:1043-54.

[192] Tucker GT. Determination of Bupivacaine (Marcaine) and Other Anilide-type Local Anesthetics in Human Blood and Plasma by Gas Chromatography. Anesthesiology 1970;32:255-60.

[193] Narchi P, Benhamou D, Bouaziz H, Fernandez H, Mazoit JX. Serum concentrations of local anaesthetics following intraperitoneal administration during laparoscopy. Eur J Clin Pharmacol 1992;42:223-5.

[194] Morrison LMM, Emanuelsson BM, McClure JH, Pollok AJ, McKeown DW, Brockway M, Jozwiak H, Wildsmith JAW. Efficacy and kinetics of extradural ropivacaine: comparison with bupivacaine. Brit J Anaesth 1994;72:164-9.

[195] Kopacz DJ, Emanuelsson BM, Thompson GE, Carpenter RL, Stephenson CA. Pharmacokinetics of Ropivacaine and Bupivacaine for Bilateral Intercostal Blockade in Healthy Male Volunteers. Anesthesiology 1994;81:1139-48.

[196] Kopacz DJ, Bernards CM, Allen HW, Landau C, Nandy P, Wu D, Lacouture PG. A Model to Evaluate the Pharmacokinetic and Pharmacodynamic Variables of Extended-Release Products Using In Vivo Tissue Microdialysis in Humans: Bupivacaine-Loaded Microcapsules. Anesth Analg 2003;97:124-31.

[197] Emanuelsson BMK, Zaric D, Nydahl PA, Axelsson KH. Pharmacokinetics of Ropivacaine and Bupivacaine During 21 Hours of Continuous Epidural Infusion in Healthy Male Volunteers. Anesth Analg 1995;81:1163-8.

[198] Schug SA, Payne JP, Baker P, Holford NHG. Non-stationary pharmacokinetics of bupivacaine during continuous interpleural infusion. Acute Pain 1997;1:15-20.

[199] New RRC. Liposomes: a practical approach. New York: Oxford University Press, 1990. p. 55.

[200] Finn SDH, Uncles DR, Willers J, Sable N. Early treatment of a quetiapine and sertraline overdose with Intralipid. Anaesthesia 2009;64:191-4.

[201] Gabizon A, Horowitz AT, Goren D, Tzemach D, Shmeeda H, Zalipsky S. In Vivo Fate of Folate-Targeted Polyethylene-Glycol Liposomes in Tumor-Bearing Mice. Clin Cancer Res 2003;9:6551-9.

[202] Spina E, Henthorn TK, Eleborg L, Nordin C, Sawe J. Desmethylimipramine Overdose: Nonlinear Kinetics in a Slow Hydroxylator. Ther Drug Monit 1985;7:239-41.

[203] Tucker GT, Mather LE. Clinical Pharmacokinetics of Local Anaesthetics. Clin Pharmacokinet 1979;4:241-78.

[204] Venkatakrishnan K, Grenblatt DJ, von Moltke LL, Schmider J, Harmatz JS, Shader RI. Five Distinct Human Cytochromes Mediate Amitriptyline N-Demethylation In Vitro: Dominance of CYP 2C19 and 3A4. J Clin Pharmacol 1998;38:112-21.

[205] Tetzlaff JE. Clinical Pharmacology of Local Anesthetics. Boston: Butterworth-Heinemann, 2000. p. 41-5, 115-23.

BIOGRAPHICAL SKETCH

Brett A. Howell was born in Salisbury, North Carolina in 1983. After graduating from South Rowan High School (China Grove, North Carolina) in May of 2002, he began his undergraduate studies at North Carolina State University in Raleigh, North Carolina in August of 2002. He received his Bachelor of Science degrees in both chemical and textile engineering in May of 2006, and joined the Department of Chemical Engineering at the University of Florida in the Fall of 2006. Shortly thereafter, in January of 2007, he joined Dr. Anuj Chauhan's research group, where he has since worked to complete his doctoral research on drug overdose treatment with liposomes.